



universität  
wien

# DISSERTATION

Titel der Dissertation

MAP1B and S-nitrosylation in axon guidance, glial cell function and  
neurodegeneration

angestrebter akademischer Grad

Doktorin der Naturwissenschaften (Dr. rer. nat.)

Verfasserin

Mag. Luise Descovich

Matrikel-Nummer:

9840357

Dissertationsgebiet

A 091 490, Molekulare Biologie

Betreuer:

Univ.-Prof. Dr. Friedrich Propst

Wien, Oktober 2009



## **ACKNOWLEDGEMENTS**

*This work was funded by the FWF, Wings of Life, the Medical University of Vienna and the University of Vienna*

*I especially thank Univ. Prof. Dr. Friedrich Propst who gave me the opportunity to work in his lab on this exciting project, for continuous support and supervision and for critical discussions*

*I am grateful to the members of my PhD committee Univ. Prof. Dr. Manuela Baccarini and Univ. Prof. Dr. Barry Dickson for their comments and suggestions*

*Many thanks go to all my colleagues from the department of molecular cell biology, especially Lilli, Ilse, Ewa, Christina, Marianne, Waltraud, Alzbeta and Nevena for their friendship, support, discussions and very nice working atmosphere*

*Special thanks go to my parents, my brothers, Friedl, Claudias, Eva and Michi for continuous support and encouragement*



## TABLE OF CONTENTS

ABSTRACT.....	9
ZUSAMMENFASSUNG .....	11
INTRODUCTION .....	15
Regulatory elements of the neuronal cytoskeleton .....	15
The cytoskeleton in neuronal cells.....	15
Microtubule associated proteins .....	16
MAP1B .....	18
Regulation of cytoskeletal dynamics in neuritogenesis .....	21
Axon retraction .....	22
Axonal transport of mitochondria and peroxisomes .....	23
Axon guidance .....	24
The growth cone .....	24
Axon guidance cues .....	27
The role of calcium, cyclic AMP, and cyclic GMP in guidance responses.....	29
The axon guidance cue netrin-1 .....	31
The netrin-1-signaling pathway .....	34
Semaphorins and their signaling .....	37
Semaphorin 3A .....	39
Nitric oxide production and its effects.....	40
Nitric oxide synthases .....	40
NO.....	42
S-nitrosylation.....	44
MAP1B, NO and netrin-1 .....	45
NO and MAP1B in oligodendrocytes .....	46
MAP1B in oligodendrocytes .....	48
NO and neurodegenerative diseases .....	49
PART I RESULTS: .....	53
NO in netrin-1 and Sema3A mediated axon guidance .....	53
The role of NO in the netrin-1 axon guidance signaling pathway.....	55
Netrin-1 induces retraction in wild-type and MAP1B <sup>-/-</sup> DRG neurons .....	55
The role of laminin in NO-induced axon retraction .....	57
Netrin-1 induced retraction involves production of intracellular NO.....	60

Inhibition of nNOS reduces netrin-1 induced axon retraction in wild-type DRG neurons .....	61
nNOS and eNOS expression and localization in wild-type and MAP1B <sup>-/-</sup> DRG neurons .....	66
Inhibition of eNOS reduces netrin-1 induced retraction in MAP1B <sup>-/-</sup> DRG neurons .....	71
Soluble guanylyl cyclase as downstream target of netrin-1 induced NO synthesis .....	76
The role of NOS in the Sema3A signaling pathway .....	83
PART I DISCUSSION .....	89
PART II RESULTS:.....	99
The role of MAP1B and nitric oxide in oligodendrocytes .....	99
Morphology and differentiation of oligodendrocytes .....	101
Expression of MAP1B in oligodendrocytes and OLN93 cells .....	101
Expression of nitric oxide synthases in oligodendrocytes .....	104
Localization of peroxisomes and mitochondria in oligodendrocytes.....	107
Expression and localization of EF1 $\alpha$ in OPCs .....	109
Differentiation of wild-type and MAP1B <sup>-/-</sup> oligodendrocytes.....	110
Effect of increased NO concentration on OPCs and oligodendrocytes .....	113
Reaction of undifferentiated wild-type and MAP1B <sup>-/-</sup> OPCs to the NO-donor SNAP .....	113
Reaction of differentiated wild-type and MAP1B <sup>-/-</sup> oligodendrocytes to the NO-donor SNAP .....	117
Effect of calcium influx and subsequent NOS activation in oligodendrocytes.....	119
Inhibition of NOS leads to process elongation.....	126
Presence of MAP1B reduces the effect of a microtubule destabilizing reagent on oligodendrocytes .....	127
PART II DISCUSSION .....	129
MATERIALS AND METHODS .....	135
Tissue culture .....	135
Culture of cell lines .....	135
Preparation of glass coverslips.....	135
Cultivation of dissociated adult DRG neurons.....	135
Cultivation of dissociated embryonic DRG neurons.....	136
Cultivation of adult and embryonic DRG explants.....	137

Cultivation of hippocampal neurons from newborn mice .....	137
Cultivation and staining of hippocampal explants.....	138
Cultivation of oligodendrocytes from newborn mice .....	138
Time lapse microscopy and local application of reagents .....	139
Treatment of cells with different inhibitors or other reagents .....	140
Immunological Assays.....	140
Immunofluorescence of primary neurons and glia cells.....	140
Incubation of DRG neurons with the fluorescent NO indicator DAF-FM DA ....	141
Immunohistochemistry on cryosections .....	141
Western blot analysis .....	143
Solutions: .....	143
ANNEX .....	145
Table of figures and tables.....	145
References.....	149
Curriculum Vitae .....	167
Publications.....	169





## ABSTRACT

Activation of neuronal nitric oxide synthase (nNOS) in dorsal root ganglia (DRG) neurons leads to axon retraction dependent on S-nitrosylation of microtubule associated protein 1B (MAP1B)<sup>1</sup>. These findings raised the question whether this mechanism is involved in classical axon guidance signaling, for example in response to the guidance cues netrin-1 and semaphorin3A. Netrin-1 is expressed at the midline of the developing central nervous system and can act as attractive or repulsive cue, depending on the environmental context. The absence or presence of laminin in the extracellular matrix determines whether netrin-1 triggers attraction or repulsion, respectively<sup>2</sup>. On the other hand, it has been shown that MAP1B is necessary for the proper transduction of the attractive netrin-1 signal<sup>3</sup> and for axon guidance across the midline in the murine forebrain<sup>4</sup>. Netrin-1 guidance involves calcium influx and could lead to nNOS activation.

In the first part of my PhD thesis, I investigated the role of nNOS, NO and MAP1B in netrin-1 guidance. I analyzed growth cone behaviour of wild-type and MAP1B<sup>-/-</sup> DRG neurons on laminin and monitored the morphological changes upon netrin-1 treatment and intracellular NO synthesis. The analysis of the response of wild-type and MAP1B<sup>-/-</sup> DRG neurons to netrin-1 revealed a significant increase of retracted neurons after the incubation with netrin-1 in both cell types suggesting that MAP1B is not relevant for repulsive netrin-1 signaling in DRG neurons. Moreover, after netrin-1 treatment, a striking increase in the production of intracellular NO could be observed in wild-type and MAP1B<sup>-/-</sup> DRG neurons. The highest concentration of NO was seen in the collapsed growth cones of retracted axons. This result suggests that the Ca<sup>2+</sup> influx induced by netrin-1 activates a NOS. With the help of specific NOS inhibitors I could show that in wild-type DRG neurons nNOS was activated downstream of netrin-1, whereas in MAP1B<sup>-/-</sup> DRG neurons it was endothelial NOS (eNOS). This difference in the downstream target of netrin-1 was due to a greatly reduced expression of nNOS in MAP1B<sup>-/-</sup> DRG neurons. These results demonstrate a novel role for nNOS and NO in netrin-1 mediated axon guidance. The production of NO following netrin-1 treatment can affect two possible downstream effectors: protein-S-nitrosylation or the cGMP pathway. Since my results indicate that S-nitrosylation of MAP1B is probably not essential for netrin-1 repulsion, the cGMP pathway was investigated in more detail. For

this purpose the specific inhibitors for soluble guanylyl cyclase (sGC), ODQ and LY83583 were used. However, the inhibition of sGC did not prevent netrin-1 induced retraction. Instead, inhibitions of sGC *per se* lead to rapid, MAP1B-dependent axon retraction and an increase in NO synthesis. This indicates that a negative feedback mechanism, which was previously suggested by results obtained *in vitro*<sup>5</sup>, is indeed at work in DRG neurons. According to this model, NO triggers cGMP synthesis, which in turn will activate PKG to phosphorylate and thereby inactivate nNOS. By inhibiting sGC, this negative feedback mechanism is shut down and nNOS continues to produce NO which will finally lead to MAP1B dependent axon retraction. Consistent with this model, I could show that sGC inhibitor induced axon retraction is not observed in MAP1B<sup>-/-</sup> Neurons and can be prevented in wild-type neurons by NPA, which mimicked inhibition of nNOS by PKG.

In order to analyze whether NO might also play a role in the semaphorin3A pathway, I grew explants from hippocampus and DRGs in media supplemented with semaphorin3A in the presence of NOS inhibitors. I obtained strong evidence that NO production might indeed be involved in repulsive semaphorin3A signaling.

In the second part of my PhD thesis I was interested in the role of MAP1B in oligodendrocytes. MAP1B expression precedes terminal differentiation of and was observed in oligodendrocytes that initiate ensheathment of axons<sup>6</sup>. NO has been postulated to play a role in oligodendrocyte damage and myelin loss in multiple sclerosis<sup>7</sup>. This raised the question whether MAP1B might be a mediator of the highly toxic effect of NO to oligodendrocytes. Moreover, it was suggested that MAP1B plays a role in the transport of mRNA in DRG neurons. As the transport of mRNAs to the cell periphery is essential for the establishment of myelin bearing sheaths during terminal oligodendrocyte differentiation, I investigated the role of MAP1B in these cells.

Surprisingly, *in vitro* oligodendrocyte differentiation was normal in MAP1B<sup>-/-</sup> cells. Moreover, oligodendrocytes did not show any reaction when treated with NO donors at high concentrations suggesting a lower susceptibility to NO than expected. In contrast, stimulation of calcium influx in oligodendrocytes triggered a NOS-dependent collapse of the cytoskeleton. This collapse could be partially prevented by inhibition of nNOS in wild-type and eNOS in MAP1B<sup>-/-</sup> cells suggesting that in oligodendrocytes, as in neurons, lack of MAP1B changes the NOS expression pattern. These results show that NOS and NO can indeed be toxic to oligodendrocytes, affecting their cytoskeleton.

## **ZUSAMMENFASSUNG**

Die Aktivierung der neuronalen Stickoxidsynthase (nNOS) in dorsalen Wurzelganglion (DRG) Neuronen führt zu Axonretraktion die abhängig von MAP1B S-Nitrosylierung ist<sup>1</sup>. Um zu untersuchen ob dieser Mechanismus auch in klassischen Signaltransduktionswegen der Axonführung wichtig ist, erforschte ich die Rolle von MAP1B und NO in den Netrin-1- und Semaphorin3A-Signaltransduktionswegen. Netrin-1 wird an der Mittellinie des sich entwickelnden zentralen Nervensystems exprimiert und kann, je nach extrazellulärer Umgebung, entweder anziehend oder abstossend auf Nervenzellen wirken. Zum Beispiel wurde gezeigt, dass die Verfügbarkeit von Laminin bestimmt ob Netrin-1 attraktiv oder repulsiv agiert<sup>2</sup>. Ausserdem scheint MAP1B wichtig für die korrekte Interpretierung des attraktiven Netrin-1 Signals<sup>3</sup> und die Axonführung über die Mittellinie im Mausvorderhirn<sup>4</sup>. Bindung von Netrin-1 an seinen Rezeptor induziert einen Kalziumeinstrom welcher eventuell nNOS aktivieren könnte.

Im ersten Teil meiner Dissertation erforschte ich die Rolle von nNOS, NO und MAP1B in Netrin-1-Axonführung. Ich analysierte das Verhalten von neuronalen Wachstumskegeln von Wildtyp und MAP1B<sup>-/-</sup> DRG Neuronen auf Laminin und die morphologischen Veränderungen, sowie die Bildung von intrazellulärem NO nach einer Behandlung mit Netrin-1. Die quantitative Analyse zeigte, dass Netrin-1 in Wildtyp sowie in MAP1B<sup>-/-</sup> DRG Neuronen einen signifikanten Anstieg in Axonretraktion hervorruft, was wiederum annehmen lässt, dass MAP1B im repulsiven Netrin-1 Signalweg keine Rolle spielen dürfte. Nach der Behandlung mit Netrin-1 wurde in Wildtyp und MAP1B<sup>-/-</sup> DRG Neuronen ein starker Anstieg in der Produktion von NO beobachtet. Die stärkste Konzentration an NO war in kollapierten Wachstumskegeln und zurückgezogenen Axonen zu sehen. Das weist darauf hin, dass durch den Netrin-1 induzierten Kalziumeinstrom eine NOS aktiviert wird. Mithilfe spezifischer NOS-Inhibitoren konnte ich zeigen, dass in Wildtyp DRG Neuronen nNOS und in MAP1B<sup>-/-</sup> DRG Neuronen endotheliale NOS (eNOS) durch Netrin-1 aktiviert werden. Dieser Unterschied kommt daher, dass in MAP1B<sup>-/-</sup> DRG Neuronen nNOS-Expression stark herunterreguliert ist. Diese Resultate deuten auf eine neue Rolle von nNOS und NO in Netrin-1 Axonführung hin. Die NO-Synthese kann zwei Effekte bewirken: zum Ersten die S-Nitrosylierung von Protein oder die Aktivierung des sGMP Signalweges. Da

meine Resultate zeigen, dass die S-Nitrosylierung von MAP1B nicht essenziell im repulsiven Netrin-1 Signalweg ist, untersuchte ich den cGMP Signalweg etwas genauer. Dafür verwendete ich spezifische Inhibitoren für soluble Guanylyl Cyclase (sGC), ODQ und LY83583. Die Inhibierung von sGC verhinderte nicht die Netrin-1 induzierte Axonretraktion. Stattdessen führte die Inhibierung von sGC *per se* zu einer rapiden, MAP1B-abhängigen Axonretraktion. Dieses Resultat weist darauf hin, dass ein negativer Feedbackmechanismus, der zuvor beschrieben wurde<sup>5</sup>, in der Tat in DRG Neuronen auftritt. Demnach bewirkt NO die cGMP-Synthese, diese aktiviert PKG welche nNOS phosphoryliert und deaktiviert. Durch die Inhibierung der sGC wird dieser negative Feedbackmechanismus ausgeschaltet und nNOS bleibt aktiv und synthetisiert weiterhin NO, welches letztendlich zu MAP1B-abhängiger Axonretraktion führte. Übereinstimmend damit konnte ich zeigen, dass sGC Inhibitor-induzierte Axonretraktion nicht in MAP1B<sup>-/-</sup> Neuronen auftritt und, dass die Retraktion in Wildtypneuronen durch NPA verhindert werden kann, welche die Inhibierung von nNOS durch PKG nachahmt.

Um herauszufinden, ob NO Synthese auch im Semaphorin3A Signalweg eine Rolle spielt, kultivierte ich Explantate von Hippocampus und DRGs in Wachstumsmedium welches Semaphorin3A und/oder NOS Inhibitoren enthielt. Diese Experimente gaben einen klaren Hinweis darauf, dass NO in der Tat wichtig für den repulsiven Semaphorin3A Mechanismus ist.

Im zweiten Teil meiner Dissertation interessierte ich mich für die Rolle von MAP1B in Oligodendrozyten. MAP1B Expression geht der terminalen Differenzierung dieser Zellen voran und wurde in Oligodendrozyten beobachtet, die kurz davor stehen, Axone zu myelinisieren<sup>6</sup>. Es wurde mehrmals postuliert, dass NO in Oligodendrozytenschädigungen und in der Demyelinisierung im Laufe von Krankheiten wie Multipler Sklerose involviert ist<sup>7</sup>. Daher stellt sich die Frage, ob MAP1B als Mediator der NO-Toxizität in diesen Zellen dienen könnte. Ausserdem wurde gezeigt, dass MAP1B für den Transport von mRNA in DRG Neuronen wichtig ist. Da der mRNA-Transport zur Zellperipherie essenziell für die Etablierung einer Myelinschicht ist, wollte ich die Wichtigkeit von MAP1B in diesen Zellen untersuchen.

Überraschenderweise differenzierten MAP1B<sup>-/-</sup> Zellen *in vitro* normal. Oligodendrozyten zeigten auch keine Reaktion auf eine Behandlung mit hochkonzentrierten NO-Donoren. Andererseits bewirkte die Stimulierung eines Kalziumeinstroms, welcher NOS aktiviert, einen Kollaps des Zytoskeletts. Dieser

Kollaps konnte teilweise durch die Inhibierung von nNOS in Wildtyp und eNOS in MAP1B<sup>-/-</sup> Zellen verhindert werden. Ich nehme daher an, dass in Oligodendrozyten, wie in Neuronen, ein Unterschied im NOS Expressionsschema zu finden ist. Ausserdem zeigen die Resultate, dass NOS und NO in der Tat toxisch auf Oligodendrozyten wirken und das Zytoskelett beeinflussen.



## **INTRODUCTION**

### **Regulatory elements of the neuronal cytoskeleton**

The nervous system is a highly complex network of billions of neurons supported by glial cells. Neurons have an elaborate morphology. They possess structural and functional polarity with short dendrites conveying information towards the cell body and a long axon conveying information away from the cell body. Glial cells provide nutrition and form myelin insulating neuronal processes in order to facilitate signal transmission. During development of the nervous system, neurons and glial cells have to migrate from the place of birth to their final destination. For migration and axon guidance, neurons bear at the end of each axon the growth cone, a motile terminal structure that explores the environment and translates guidance information into movement<sup>8</sup>. This requires an accurate coordination and regulation of cytoskeletal components in response to extracellular guidance cues. Thus, proteins interacting with the cytoskeleton, such as microtubule-associated proteins, actin-binding proteins, and motor proteins, play important roles in the establishment and maintenance of neuronal morphology and functionality.

### **The cytoskeleton in neuronal cells**

As in other motile cells, the cytoskeleton of developing neurons consists of microtubules, actin filaments and intermediate filaments, called neurofilaments.

Microtubules are polar structures composed of tubulin dimers assembled into linear arrays forming stable, cross-linked bundles in the axon shaft. Tubulin dimers are assembled from one  $\alpha$ -tubulin subunit and one  $\beta$ -tubulin subunit<sup>9</sup>. Microtubules lend structural support to the neuronal cytoskeleton and are involved in many cellular processes including intracellular transport mechanisms and growth cone steering. In axons, all microtubules are oriented with their plus end towards the distal tip of the axon, whereas in dendrites they exhibit both orientations. Single microtubules also emerge into the growth cone. These filaments display the classic properties of dynamic

instability, polymerizing and shrinking as they explore the peripheral region of the growth cone<sup>10</sup>.

Actin filaments play an essential role in driving motility and guidance of growth cones<sup>11</sup>. They are helical polymers composed of actin monomers, often referred to as globular actin. It can exist as ATP-actin and ADP-actin. ATP- and ADP-actin can associate and dissociate from both the rapidly growing barbed and the slower growing pointed ends *in vitro*<sup>12</sup>. G-actin polymerizes into actin filament as ATP-actin and is converted to ADP-actin through its intrinsic ATPase activity. Several actin-associated proteins have been found to bind preferentially to these different forms of actin<sup>13</sup>. The actin filaments connect to the extracellular substrate via interactions with integral membrane proteins such as cadherins, integrins and neural cell adhesion molecules<sup>14</sup>.

Neurofilaments are present in the axon and the central domain of the growth cone but their function in growth cone motility and axon guidance is unknown<sup>15</sup>. Since my work focuses on the interplay between signaling molecules, microtubules, and actin, neurofilaments will not be dealt with.

## **Microtubule associated proteins**

Classical microtubule associated proteins, such as MAP1A, MAP1B, MAP2 and tau, were among the first identified microtubule regulators<sup>16</sup>. MAPs were suggested to play a role in the establishment and regulation of neuronal morphology because of their specific associations with the three structural compartments of neurons – the axon, the soma and the dendrites. MAP2 shows a preferential subcellular expression in dendrites and somata but not in axons *in vivo*. In contrast to MAP2, tau is enriched in the axons. The MAP1 family has been found to be prominent in axons as well as in somata and dendrites.

MAP1B and MAP2 are among the most abundant neuronal MAPs but they do not show all the same developmental expression pattern. Early MAPs that are expressed during fetal and neonatal stages are the 48 kDa isoform of tau, MAP2, MAP2 and MAP1B. Later expressed MAPs include the heavier isoforms of tau and MAP1A<sup>17</sup>. MAP2 is present at both early and late stages and has three isoforms, MAP2A, B and C<sup>18</sup>. MAP2-deficient mice develop without any apparent abnormalities suggesting a functional redundancy among MAPs.



MAP1B and MAP2 have overlapping functions in neuronal migration and neurite outgrowth by organizing microtubules in developing neurons. *MAP1B*<sup>-/-</sup>*MAP2*<sup>-/-</sup> double knockout mice die in their perinatal period. They show fiber tract malformations and disrupted cortical patterning caused by retarded neuronal migration. Hippocampal neurons of these mice reveal inhibition of microtubule bundling and neurite elongation<sup>19, 20</sup>. Similarly, the phenotypes of *tau*<sup>-/-</sup>*MAP1B*<sup>-/-</sup> double mutants are markedly more severe than the single mutants of those proteins. They show hypoplastic commissural axon tracts and disorganization of neuronal layering in the brain. Moreover, in neurons from double knockout mice inhibited axonal elongation and delayed neuronal migration were observed<sup>21</sup>.

Although structural differences among the MAPs exist, all of them can interact with tubulin, stabilize microtubules and link them with other components of the cytoskeleton<sup>22</sup>. This function is dependent on posttranslational modifications of the MAPs. Dependent on the kinase and the phosphorylation site, phosphorylation of MAP1B can lead to an increased association with microtubules, whereas phosphorylation of MAP2/tau generally results in their dissociation from microtubules<sup>23</sup>. Studies suggest that MAPs can restrict access to the microtubule for certain molecular motors. Thus, there is the potential for tight regulation by signaling cues relevant to neuronal development and degeneration. Overexpression of tau can inhibit the attachment of both motor proteins kinesin and dynein, MAP4 and MAP2c similarly inhibit motor-based transport<sup>24</sup>. The current view is that MAPs generally diminish the frequency by which a motor can interact with the microtubule and thereby move along it<sup>25</sup>.

Microtubule associated proteins have also been suggested to contribute to the regulation of axonal transport of mitochondria. In comparison with wild-type neurons, the highest velocities of mitochondrial movement in the anterograde fashion are reached in tau-deficient neurons<sup>26</sup> whereas the highest rates of mitochondrial retrograde movement are attained in MAP1B-deficient neurons. This suggests that MAP1B and tau could compete with kinesin and/or dynein motors, respectively, for binding or positioning on the microtubule tracks<sup>27</sup>.

## MAP1B

MAP1B is one of the three members of the structurally related family of MAP1 proteins comprising MAP1A, MAP1B and MAP1S (Figure 1). MAP1B is translated as a polyprotein containing the heavy chain and one of the two light chains, LC1, which is cleaved from the C-terminus of the precursor after translation. MAP1A and MAP1S are also posttranslationally cleaved into a heavy and a light chain<sup>28, 29</sup>. Futsch is the homologue of MAP1B in flies; it is also cleaved into a heavy chain and a light chain after translation<sup>30</sup>. MAP1A, MAP1B and MAP1S share homology domains (MH1-3); futsch bears the homology domains MH1 and MH3. The activity of the light chains is inhibited by the heavy chain, whereby the interaction takes place between the MH1 domain of the heavy chain and the MH3 domain of the LC1 or LC2<sup>20</sup>. LC1 and LC2 are able to interact with the heavy chains of either MAP1A or MAP1B<sup>31</sup>.

MAP1B is expressed in neuronal and non-neuronal cells in the nervous system. MAP1B protein and mRNA for MAP1B are expressed at high levels during development and while they are down-regulated at the end of axonogenesis in most regions of the CNS they remain at relatively high levels in adult PNS<sup>32</sup>, including some of the developmentally regulated phosphorylated isoforms<sup>22</sup>. In contrast to MAP1B, MAP1A is expressed in mature neurons only. MAP1S is expressed in a wide range of tissues and represents a nonneuronal counterpart of this cytolinker family<sup>29</sup>. Futsch is expressed in many neurons in the fly CNS and was also shown to bind microtubules.

Binding of the MAP1B LC1 to microtubules induces formation of stable but flexible microtubules with increased resistance to nocodazole and taxol but it was not found to promote microtubule bundling, like MAP2 and tau<sup>22</sup>. The LC2 of MAP1B interacts with PDZ-Rho-GEF, a member of a Rho-GEF subfamily. Mutants of PDZ-Rho-GEF alter the activation of Rho-GTPases, thus, modulation of the guanine nucleotide exchange activity of PDZ-Rho-GEF through interaction with MAP1B LC2 may coordinate microtubule integrity and the reorganization of actin cytoskeleton<sup>33</sup>. Futsch is required to regulate microtubule architecture, thereby controlling growth cone function and synapse formation<sup>25</sup>.

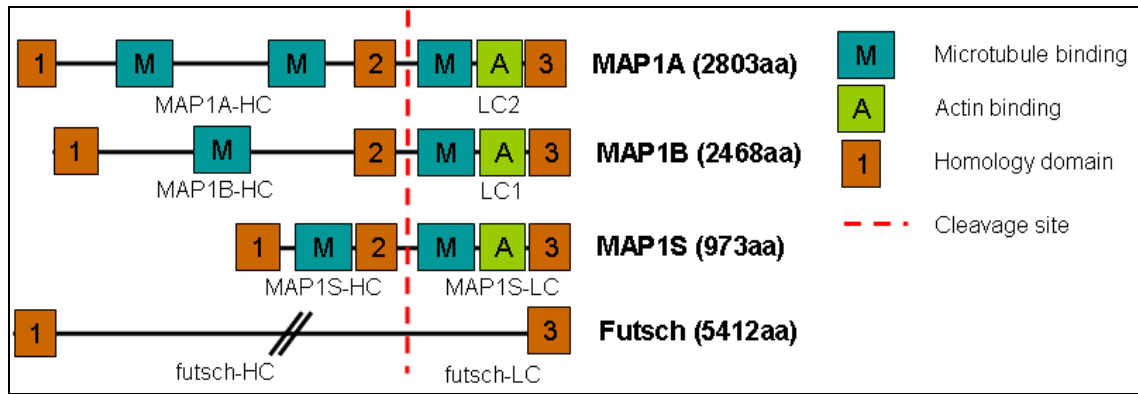


**Figure 1: The family of microtubule associated proteins 1 with its members MAP1A, MAP1B, MAP1S, and Futsch.**

MAP1A, MAP1B, MAP1S and futsch, the fly homologue of MAP1B, are posttranslationally cleaved into a heavy chain and a light chain bearing microtubule and actin binding domains<sup>34</sup>. The blue boxes indicate microtubule binding sites and the green boxes show actin binding sites. The three MAP1s share 3 homology domains (MH1-3) indicated by the brown boxes. Futsch shares 2 homology domains with the MAP1 family.

MAP1B can be phosphorylated at more than 33 serine and threonine sites via two modes: mode I sites are generated by the proline-directed serine/threonine kinases cdk5 and GSK-3 $\beta$ , and mode II sites are generated by casein kinase II<sup>35</sup>. GSK-3 $\beta$  is expressed in two isoforms: a short form GSK-3 $\beta$ 1 and a long form GSK-3 $\beta$ 2. GSK-3 $\beta$ 1 is more efficient in phosphorylating MAP1B than GSK-3 $\beta$ 2. Despite much work that has been performed on different phosphorylation sites of MAP1B, it is difficult to know exactly which particular phosphorylation site is examined. Thus the effects of the different kinds of MAP1B phosphorylation remain elusive. So far it is known that mode I phosphorylated MAP1B concentrates at distal regions of regenerating nerves, whereas mode II phosphorylation undergoes an overall decrease in regenerating axons<sup>36</sup>. In the developing nervous system, the expression of GSK-3 $\beta$  phosphorylated MAP1B is spatially restricted to growing axons, despite the expression of MAP1B and GSK-3 $\beta$  throughout the entire neuron. This suggests a mechanism which is spatially regulating the phosphorylation of MAP1B by GSK-3 $\beta$ <sup>37</sup>. Moreover, mode I phosphorylated MAP1B is present only in stable regions of a growth cone and absent from unstable regions of a turning growth cone. Additionally, the activator of Cdk5, p35, is also restricted to the stable parts of the growth cone. Inhibition of Cdk5 results in loss of mode I phosphorylated MAP1B and growth cone collapse, axon retraction and prevents axonal outgrowth<sup>38</sup>.

Another function of the phosphorylation of MAP1B is the regulation of the interaction between MAP1B and another MAP, the lissencephaly-related protein 1 (LIS1). This interaction interferes with the association between LIS1 and the microtubule dependent molecular motor dynein, thereby regulating the functions attributed to the LIS1-dynein complex, including those related to extension of the neural processes necessary for neuronal migration<sup>39</sup>.

Studies of cultured primary neurons showed that MAP1B is constitutively highly expressed in adult dorsal root ganglia (DRG) and is associated with central sprouting and peripheral regeneration of these neurons. MAP1B negative neurites grow often in a curled manner and exhibit higher terminal and collateral branching<sup>40</sup>. During synaptogenesis *in vitro*, MAP1B was observed to be translocated to the plasma membrane of rat cortical neurons and seems to contribute to the maturation of neurites after an initial phase of neurite elongation<sup>41</sup>. Moreover, it has been reported that a significant fraction of MAP1B is expressed as an integral membrane glycoprotein in vesicles and the plasma membrane of neurons<sup>42</sup>.

Four groups generated mice bearing a mutated product of MAP1B. They showed either embryonic lethality<sup>43</sup>, perinatal lethality when smaller isoforms of the protein were overexpressed<sup>44</sup>, only a weak influence on nervous system development<sup>45</sup>. The complete deletion of the MAP1B gene leads to an agenesis of the corpus callosum. Commissural nerve fibers that should cross the midline at the regions of the corpus callosum and the hippocampal commissure form thick bundle of fibers that run in the longitudinal direction of the brain, the so called Probst bundles. Moreover, axonal myelination defects were observed, resulting in reduced motor nerve conduction velocity. The discrepancies concerning the severity of the MAP1B phenotype might be due to different strategies for inactivation of the gene and for differences in the genetic background of the four MAP1B mutant lines. However, this demonstrates that MAP1B is required for correct axon guidance during brain development<sup>4</sup>.

A loss of function *futsch* allele produces defects in axonal and dendritic growth in the embryonic nervous system<sup>46, 47</sup>. Moreover, it was shown to play a critical role in the maintenance of the CNS throughout adult life and is involved in progressive neurodegeneration<sup>48</sup>.

The phenotype of the complete MAP1B knock-out shares similarities with the phenotype of mice lacking netrin-1, DCC or Mena. All of them have severe defects in generation of the corpus callosum<sup>49-51</sup>. However, one has to keep in mind that netrin-1,

DCC and Mena mutant mice show much stronger phenotypes than MAP1B mutants. Callosal axon guidance defects are also observed in mice lacking the cdk5 activator p35<sup>52</sup> which is implicated in regulation of laminin-induced MAP1B phosphorylation<sup>53</sup>. Thus, MAP1B might also be involved in laminin-mediated cell signaling and regulation of actin polymerization in the growth cone involved in corpus callosum formation<sup>4, 49</sup>.

## **Regulation of cytoskeletal dynamics in neuritogenesis**

In neuritogenesis, behaviors such as advancing, retracting, turning and branching are driven by the dynamics and reorganization of the actin and microtubule cytoskeleton regulated through signaling pathways downstream of guidance cue receptors located at the growth cone<sup>54</sup>. Enzymes essential for directed motility during neurite extension, axon guidance and neuronal migration are the Rho family of GTPases, including Cdc42 (cell division cycle 42), Rac (Ras-related C3 botulinum toxin substrate) and Rho (Ras homologous)<sup>55</sup>. There are three isoforms of Rho: RhoA, RhoB and RhoC; in neurons RhoA is expressed at higher levels than the other isoforms<sup>56</sup>. In fibroblasts, RhoA, Rac and Cdc42 induce the formation of stress fibers, lamellipodia, and filopodia, respectively<sup>57, 58</sup>. There is evidence that Rho is involved in growth cone collapse and repulsion whereas Rac and Cdc42 participate in growth cone attraction and advance<sup>59</sup>. The balance of these opposing activities of the different Rho GTPases is crucial for the morphology of the neurons<sup>60</sup>.

Other important signaling molecules are cAMP/cGMP and calcium. Levels of intracellular calcium have a profound influence on growth cone behavior, neurite sprouting, elongation and motility of axons and dendrites<sup>61, 62</sup>, either by directly acting on cytoskeletal proteins or by activating various calcium-binding proteins<sup>63</sup>. Small or relatively large local  $\text{Ca}^{2+}$  elevations trigger growth cone repulsion, whereas a moderate local elevations induce growth cone motility and extension<sup>64</sup>. Recent evidence indicates that  $\text{Ca}^{2+}$  can regulate Rho GTPases through  $\text{Ca}^{2+}$ -regulated GTPases-activating proteins and  $\text{Ca}^{2+}$ -regulated guanine nucleotide exchange factors<sup>65</sup>.

## Axon retraction

The selective elimination of axons, dendrites and synaptic connections without death of the parent neurons is a crucial common theme in many biological processes and central to normal neuritogenesis and neural function. The mode of axon elimination occurs through one of two distinct phenomena: small-scale elimination typically occurs by retraction, whereas large-scale elimination appears to occur primarily by degeneration. A retracting neuron shows three characteristics: sinusoidal bundles along the axon shaft, a collapsed growth cone and a trailing remnant (Figure 2).

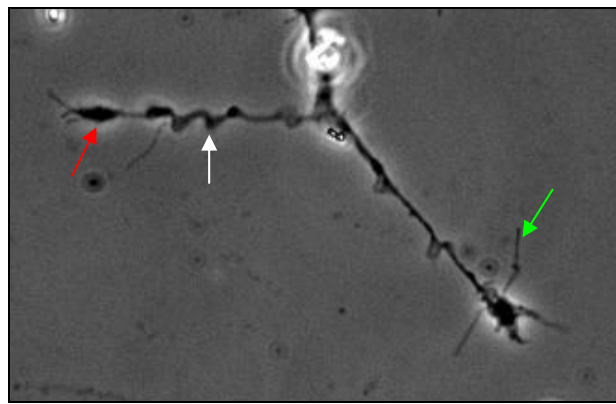


**Figure 2: A retracting axon.**

The figure shows phase contrast picture of a retracting DRG neuron with collapsed growth cone (red arrow), sinusoidal bundles (white arrow) and a trailing remnant (green arrow).

Axon retraction entails major rearrangements of both the axonal and growth cone cytoskeleton and can be triggered by changes in the activity of microtubule or actin motors. For example, inhibition of microtubule motor dynein causes axon retraction in the presence of intact microtubules; this effect is reversed by depletion of the actin cytoskeleton or inhibition of myosin motors. Thus, myosin-actin and dynein-microtubule cytoskeletons were proposed to contribute opposing and counter-balanced forces regulating axon stability<sup>66</sup>. Moreover, cytoplasmic dynein and dynactin are essential for the transport of microtubules from the centrosome into the axon, thereby serving to align them with one another and permit them to invade filopodia<sup>67, 68</sup>.

RhoA plays an important role in axon retraction. Its activation results in changes in actin dynamics and activation of myosin which further lead for instance to prevention of axon initiation in primary neurons<sup>69</sup>, neurite retraction in cultured neuroblastoma cell lines<sup>70</sup> and retraction of dendritic processes in maturing neurons *in vivo*<sup>71</sup>. Moreover,

activation of RhoA is also implicated in mediating the activity of myelin-associated inhibitors in blocking axon regeneration<sup>72</sup>. Given the potential similarities between repulsive axon guidance and axon retraction, repulsive guidance molecules such as ephrins, slits or semaphorins, all of which signal through RhoA, could also signal axon retraction<sup>11</sup>. Moreover, outgrowth of one axonal process is often accompanied by simultaneous retraction of another process belonging to the same axon, suggesting a competitive mechanism for differential process outgrowth<sup>73</sup>.

### **Axonal transport of mitochondria and peroxisomes**

Organelle transport is essential for the axonal development and maintenance. In neurons and glia cells, the distances between the sites of organelle biogenesis, function and degradation can be vast. Long-range transport along microtubules provides delivery of biosynthetic products and organelles produced in the cell body to the neurite<sup>74</sup>. Defects in axonal transport such as transport blockade of nutrients, survival factors, or any other proteins lead to neuronal dysfunction and degeneration<sup>66</sup> and eventually to neurological disorders including Alzheimer's, Huntington's, and motor neuron diseases<sup>75</sup>.

Mitochondria are essential for the function of all aerobic cells; they produce ATP, buffer cytosolic calcium and sequester apoptotic factors<sup>76</sup>. Mitochondria were also suggested to play a pivotal role in organizing neuronal polarity, possibly by controlling local calcium and/or energy gradients<sup>77</sup>. Nevertheless, mitochondria are often involved in pathologies of the nervous system due to alterations in their migratory behavior or localization<sup>78</sup>. Movement of mitochondria in axons can serve as a general model for how organelles generally move. They move along both microtubules and actin filaments, they pause and change direction, and their transport is modulated in response to physiological signals. Mitochondria can quickly switch between anterograde and retrograde movement and shift between moving and stationary states<sup>79</sup>. Anterograde organelle transport implicates motor proteins of the kinesin superfamily and retrograde transport involves proteins of the dynein family<sup>80</sup>. Mitochondria can also move along actin filaments in axons implicating myosin motors<sup>81</sup>. Kinesins, cytoplasmic dynein and myosins cooperate to give rise to the complex movement of mitochondria but possible control mechanisms remain largely speculative<sup>76</sup>.

For peroxisomes, although the interaction with microtubules has been demonstrated<sup>82</sup>, little is known about the nature of involved proteins. Two types of peroxisome movement can be distinguished: a relatively slow, random, vibration-like movement displayed by the majority of the peroxisomes, and a saltatory, fast directional movement exhibited by only a small fraction of the peroxisomes, possibly being energy dependent<sup>83</sup>. Addition of ATP or motor proteins kinesin and dynein increases the binding capacity of peroxisomes to microtubules, while ATP-depletion or microtubule associated proteins such as MAP2 and tau decrease it<sup>84</sup> and inhibition of cytoplasmic dynein based motility inhibits the movement of peroxisomes. Microtubule-destabilizing agents disturb proper localization and directional movement of peroxisomes. In contrast, microtubule-stabilizing compounds do not exert effects<sup>85</sup>.

The lack of MAP1B was shown to influence the motility of mitochondria<sup>27</sup>, whereas the role of MAP1B in peroxisomal movement has never been investigated. This subject will be outlined in the second part of this thesis.

## **Axon guidance**

### **The growth cone**

Growth cones, the highly motile tips of growing axons, are guided through their environment in response to multiple sources of spatial information to reach the appropriate region in the brain. Besides cell adhesion molecules and the extracellular matrix (ECM) molecules, diffusible chemotropic cues direct the traveling growth cone<sup>86</sup>. The two main structures of the growth cone are actin-based fingerlike protrusions called filopodia and flattened extensions called lamellipodia (Figure 3). The filopodia are thought to be particularly sensitive to extrinsic signals because of their small intracellular volume<sup>87</sup>. The major changes that occur in the cytoskeleton of growing neurites are rapid rearrangements of actin filaments in the filopodia and lamellipodia of growth cones and polymerization of microtubules<sup>61</sup>. The shape and the size of the growth cone change according to the rate of neurite extension. Large, splayed growth cones are typical during prolonged pauses, as the neurite explores the local microenvironment, whereas rapidly extending neurites have small and streamlined growth cones<sup>16</sup>.



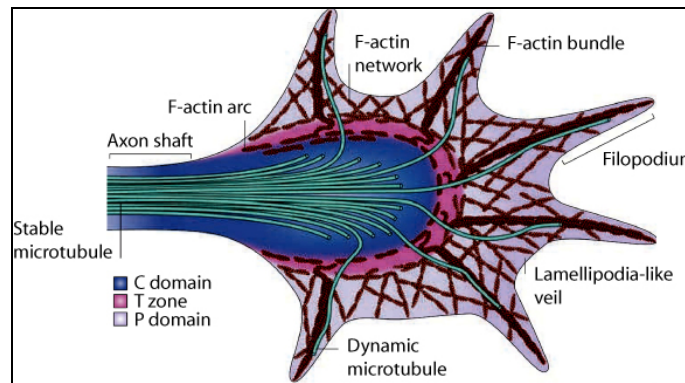


**Figure 3: The structure of the growth cone.**

The peripheral (P) domain of a growth cone comprises filopodia, fine extensions of F-actin bundles and dynamic microtubules that explore the environment, and lamellipodia, veil-like structures consisting of F-actin meshwork. The central (C) domain of the growth cone is dominated by stable microtubules<sup>86</sup>.

In growth cones, microtubules predominate in the central region whereas actin filaments prevail in the periphery. However, there are extensive regulatory and structural interactions between these two cytoskeletal elements in the growth cone transitional domain containing the actin arcs<sup>88</sup> required for functions such as cell motility and growth cone guidance<sup>89</sup>. Actin arcs are thought to mediate the microtubule alignment from the growth cone to the neurite shaft<sup>90</sup>. The neurite shaft is generated by a process called consolidation, which results from the collapse of the proximal part of the growth cone and the suppression of protrusive activity along the neurite<sup>8</sup>. This dynamic interaction is believed to be made possible through shared regulatory proteins such as MAP1B, MAP2 and spectraplakins, which can bind to both actin and microtubules<sup>16</sup>.

Microtubules were found to extend along actin filament bundles that served to guide their anterograde and retrograde transport. Although many stable microtubules remain in the center of the growth cone, a population of dynamic microtubules can actively explore the periphery and penetrate filopodia<sup>54</sup>. The cytoplasmic motor protein dynein transports short microtubules anterogradely along the axon in part by pushing against the actin cytoskeleton. These dynein-driven forces overcome myosin-II-driven counterforces, oppose the tendency of the axon to retract, and thereby, permit microtubules to advance into the peripheral zone of the growth cone<sup>91</sup>.

The prevailing view is that axonal growth involves the assembly of new cytoskeleton components and axonal retraction involves the disassembly of existing

cytoskeletal components<sup>92</sup>. Guidance cue receptors located at filopodia and lamellipodia and their downstream signaling pathways regulate those cytoskeletal dynamics. When microtubule dynamics are inhibited by nocodazole or taxol the growth cone is not capable to respond in a proper manner to signaling molecules. Otherwise, local stabilization of microtubules is an important mechanism to guide a growth cone. Microtubule stabilization in one side of the growth cone induces attractive steering in this direction. This can be abolished by inhibition of actin polymerization. In contrast, local microtubule depolymerization causes growth cones to steer away. Thus, inhibition of microtubule dynamics and localized stabilization and de-stabilization of microtubules are sufficient to induce attractive and repulsive turning<sup>93</sup>.

Another important feature of growth cones is that they contain mRNAs, a translation machinery, and a protein degradation machinery. Thus, the protein synthesis is not confined to the perikaryon<sup>94</sup>. Guidance molecules can activate translation initiation factors and stimulate a marked rise in protein synthesis within minutes. This suggests that they can steer axon growth by triggering rapid local changes in protein levels in growth cones<sup>95</sup>. Local translation and upregulation of expression of specific receptors might also be used to completely switch the growth cone's responsiveness to specific cues once it reaches an intermediate target<sup>96</sup>. The best described intermediate target is the central nervous system midline<sup>97</sup>. First, commissural axons grow toward the midline, and after crossing, they are prevented from recrossing and are guided along longitudinal tracts even though they were ignoring the same tracts before crossing. This involves for instance local upregulation of specific receptors.

Nevertheless, protein synthesis is not strictly required in the mechanisms for growth cone responses to many guidance cues. In the presence of cycloheximide or anisomycin, some guidance cues still induce growth cone collapse and loss of actin filaments. In contrast, NGF and neurotrophin-3 still induce growth cone protrusion and increase filamentous actin while sensory growth cones turn toward the NGF source<sup>98</sup>.

In addition, interactions between neurons and ECM components are fundamental. The most prominent promoters of neurite growth are the laminins which are an important family of ECM glycoproteins<sup>99</sup>. A typical laminin molecule consists of three polypeptide chains linked via disulfide bonds forming the asymmetric cross-structure<sup>100</sup>. Laminin is also required for normal CNS myelination although the exact mechanisms remain unknown<sup>101</sup>. Adult mouse DRG neurons have been shown to express different receptors for laminins, such as integrin  $\alpha 3$ ,  $\alpha 6$ ,  $\alpha 7$  and  $\beta 1$ <sup>102</sup>. As it is

the case in many other signaling pathways, laminin mediated growth cone turning requires an influx of extracellular  $\text{Ca}^{2+}$ <sup>103</sup>.

## Axon guidance cues

Classically, guidance cues have been divided into attractive and repulsive signals. The cues can be substrate bound or cell-membrane bound and act on nearby axons<sup>97</sup>. Alternatively, cues secreted from far away sources diffuse and form gradients, this mechanism is called chemotropism<sup>104, 105</sup>.

Guidance cues are grouped into four classes, the netrins/Unc6<sup>106</sup>, the slits<sup>107</sup>, the semaphorins<sup>108</sup> and the ephrins<sup>109</sup>. More recent reports also identified the Wnt family<sup>110</sup>, sonic hedgehog<sup>111</sup> and FGFs<sup>112</sup> as axon guidance molecules. Slits, semaphorins and netrins are widely expressed outside the nervous system and they may also play important roles in cancers. They were denoted to act as tumor suppressors and appear to control the vascularization of tumors. Moreover, many axon guidance cues regulate cell migration and apoptosis in normal and tumorigenic tissues<sup>113</sup>. How a growth cone responds to those cues, being attracted or repelled, depends on the receptors present on its surface, on their downstream targets that become activated and on the extracellular matrix on which the axon grows. These factors finally lead to the decision whether the axon extends along the dorsal-ventral or the anterior-posterior axes or if they cross the midline.

Disturbed responses to axon guidance cues during development can result in defects in the formation of commissures. Furthermore, major brain or motor dysfunctions might be the consequences<sup>114</sup>. Growth cone migration in the dorsal-ventral region is mainly controlled by netrins with their receptors, Unc-40/DCC/Frazzled and Unc-5, and the slits with their receptors, Robo/SAX-3. Axon guidance in the anterior-posterior axis is mainly controlled by Wnts and their receptors, the Frizzleds. There is evidence that the axes of growth cone migration are determined by the manner in which netrin, slit and Wnt receptors are localized within the neuron prior to axon outgrowth<sup>115</sup>.

Targets for the signaling pathways downstream of guidance receptors are molecules such as the actin nucleator Arp2/3, proteins to promote filament elongation, adhesion molecules to couple actin filaments to the substrate and motorproteins to regulate the transport of actin filaments. Molecules that capture microtubule ends or

suppress microtubule instability, such as MAP1B, are also potential targets for guidance signals<sup>116</sup>.

Guidance cues such as netrins have been shown to induce actin polymerization in case of attractive signaling, thereby promoting rapid axon branching. Netrin-1 rapidly increases axon branching and growth cone filopodia in cortical neurons with a concomitant increase in actin filaments<sup>117</sup>.

In contrast, inhibitory guidance cues such as semaphorins collapse growth cones by depolymerizing actin filaments<sup>118</sup>. For instance, semaphorin3A (referred to hereafter as Sema3A) induces depolymerization of actin filaments, attenuates microtubule dynamics and collapses microtubule arrays. Additionally to its repellent effect, Sema3A also inhibits branching of cortical axons without affecting axon length significantly. Netrins and semaphorins are especially interesting for this thesis and will be discussed in a separate chapter.

Other repellent factors are the slits. Mice lacking slit1 and slit2 are deficient in all three major forebrain commissures<sup>119</sup>. Slits are large secreted proteins that signal through Roundabout (Robo) family receptors and control midline crossing of axons in *Drosophila*<sup>120</sup> and in regions of the mammalian CNS<sup>121</sup>. In *Drosophila*, slits are expressed at the ventral midline, where they act as a short-range repellents to prevent ipsilateral axons from crossing the midline and commissural axons from recrossing<sup>120</sup>. Moreover, an intracellular signaling pathway has emerged linking slit2/Robo to actin regulation. Slit2 was shown to stimulate the binding of a Rho GTPase activating protein with the intracellular domain of Robo, leading to the inactivation of Cdc42<sup>122</sup>. The current working model is that Robo3 interferes with slit-mediated repulsion, thereby allowing Robo1/2-expressing axons to reach and cross the midline<sup>123</sup>. Commissural neurons that grow towards the midline are first attracted by netrins but insensitive to midline repellents slit and semaphorins. After an axon has been guided successfully to the midline, attraction by netrin is turned off and repulsion is turned on. Once midline crossing has occurred, the axons are guided along either rostral or caudal on the contralateral side in tracts parallel to the midline<sup>120</sup>.

There are several theories how an axon loses the responsiveness to a special guidance cue once it has reached its destination. It was shown that netrin-1 induces for instance the ubiquitination and proteolytic cleavage of DCC in dissociated cortical neurons<sup>124</sup>. Another hypothesis is that there is one hierarchical silencing mechanism, which involves the suppression of the attractive effect of netrin by the repulsive

guidance cue slit. Slit activates Robo which silences the attractive effect of netrin-1 through direct binding of its cytoplasmic domain to the cytoplasmic domain of DCC<sup>125</sup>. Mutations in *robo* lead to a phenotype, in which too many axons cross the midline<sup>126</sup>, perhaps because recrossing is not impeded. In addition, slit was identified as a factor that stimulates sensory axon branching and elongation. Thus, slits, like netrins, are multifunctional<sup>127</sup>.

Another family of guidance cues are the Wnts. Wnts are well-studied morphogens involved in asymmetric cell divisions in many organisms. They were also found to play a role in neurite outgrowth, midline crossing and anterior-posterior guidance<sup>110</sup>.

Matrix and membrane bound molecules also directly instruct neuronal growth and migration. The classical members of this family include EphB2, its ligand EphrinB2 and heparin sulfate glycosaminoglycans<sup>128</sup>. The ephrins are membrane-bound ligands for the Eph family of receptor tyrosine kinases. Ephrins belong to either of two classes: ephrin-As are anchored to the membrane by a glycosylphosphatidylinositol linkage and bind EphA receptors, and ephrin-Bs have a transmembrane domain and bind EphB receptors<sup>129</sup>. The functional link between EphA receptors, Rho GTPases and the cytoskeleton<sup>130</sup> suggests that the ephrin signaling pathway also influences actin cytoskeletal dynamics in the growth cone<sup>131, 132</sup>.

Recently, a new axon guidance cue, draxin, has been identified. It does not show any homology with known axon guidance cues and inhibits neurite outgrowth from dorsal spinal cord and cortical explants in vitro. Draxin-knockout mice show defasciculation of spinal cord commissural axons and absence of all forebrain commissures<sup>133</sup>.

## **The role of calcium, cyclic AMP, and cyclic GMP in guidance responses**

The internal state of the growth cone is extremely important in deciding how a guidance cue is interpreted by the developing axon. The intracellular calcium concentration, cyclic nucleotide levels, and membrane potential are all reported to modulate the transduction of guidance cues<sup>134</sup> and play an essential role in axon growth, survival and regeneration. Neurons maintain a baseline intracellular  $\text{Ca}^{2+}$  concentration at the resting state, termed the resting  $\text{Ca}^{2+}$  concentration<sup>64</sup>. Cytoplasmic

$\text{Ca}^{2+}$  levels determine whether a growth cone responds by turning away from or toward a guidance cue. One proposed mechanism how calcium signaling brings about growth cone turning is the creation of cytoplasmic  $\text{Ca}^{2+}$  gradients downstream of the action of guidance cues<sup>135</sup>. Netrin-1 signaling involves for example increases in  $\text{Ca}^{2+}$  that are highest on the side of the growth cone facing the source of the factor<sup>136</sup>. It has been suggested that netrin-1 acts on its receptor to ultimately open plasma membrane  $\text{Ca}^{2+}$  channels.  $\text{Ca}^{2+}$  influx then activates  $\text{Ca}^{2+}$  induced  $\text{Ca}^{2+}$  release from internal stores and these sources contribute to local amplifications of  $\text{Ca}^{2+}$  levels<sup>137</sup>. Reduction of  $\text{Ca}^{2+}$  signals by blocking either of these two sources can convert an induced attractive response into repulsion<sup>136</sup>.

Localized spontaneous  $\text{Ca}^{2+}$  transients of different frequencies occur in restricted regions of axons and their branches. Higher frequencies occur in more rapidly extending processes whereas lower frequencies occur in processes that stall or retract. Global  $\text{Ca}^{2+}$  transients inhibit extension of the primary axon, whereas localized  $\text{Ca}^{2+}$  transients evoked by netrin-1 signaling could promote branching of the axon in regions of high-frequency  $\text{Ca}^{2+}$  transients<sup>138</sup>.

Calmodulin, CaM, is an abundant intracellular  $\text{Ca}^{2+}$  receptor in filopodia and growth cones<sup>139</sup>. Upon  $\text{Ca}^{2+}$  binding,  $\text{Ca}^{2+}$ /CaM can associate with a wide range of targets, including kinases, such as  $\text{Ca}^{2+}$ /CaM dependent protein kinases (CaMK) I, II and IV<sup>140</sup>, and phosphatases, such as calcineurin (CaN)<sup>141</sup>. Moreover, CaMKII, and protein kinase C (PKC), which can both be activated by  $\text{Ca}^{2+}$ , can activate Rho GTPases<sup>142</sup>.

Because membrane potential has the ability to influence the levels of second messengers like cAMP<sup>143</sup> and to determine the amount of extracellular  $\text{Ca}^{2+}$  that enters the cell<sup>144</sup> it is possible that its tight regulation is critical in ensuring that cues are correctly interpreted by the growth cone<sup>145</sup>.  $\text{Ca}^{2+}$  can regulate the production of cAMP and cGMP via its action on adenylyl cyclases and nitric oxide synthase, NOS, respectively. Moreover, cyclic nucleotides can act by modulating  $\text{Ca}^{2+}$  channels<sup>146</sup> resulting in distinct patterns of  $\text{Ca}^{2+}$  signals that underlie attractive or repulsive growth cone steering. Thus,  $\text{Ca}^{2+}$  regulation of growth cone motility depends on both the spatiotemporal patterns of  $\text{Ca}^{2+}$  signals and the internal state of the neuron<sup>147</sup>.

Second messengers such as cAMP and cGMP are also known to regulate attractive and repulsive axonal guidance by ligands like the netrins and semaphorins. In case of the netrin signaling pathway, a high cAMP:cGMP ratio favors attraction,

whereas a low ratio favors repulsion. cAMP signaling modulates both DCC- mediated attraction and DCC-Unc5-mediated repulsion<sup>146</sup>. During local application of normally attractive neurotrophin BDNF the reduction of cAMP level also leads to repulsive turning of the growth cones<sup>148</sup>. Moreover, cyclic nucleotide signaling directly modulates the activity of L-type  $\text{Ca}^{2+}$  channels, LCC, in axonal growth cones<sup>146</sup>. Furthermore, cGMP signaling suppresses LCC activity and is required for growth-cone repulsion mediated by the DCC-Unc5 receptor complex<sup>149</sup>.

Likewise, *Sema3A/NRP1* repulsive signaling can be switched into chemoattraction by the distribution of sGC<sup>150</sup> and an increase in intracellular cGMP concentration<sup>151</sup>. cAMP analogs have no significant effect on the repulsion induced by semaphorin3 but convert the repulsion induced by myelin associated glycoprotein (MAG) into attraction<sup>151</sup>. Thus, the dependence on cyclic nucleotide signaling pathways might differ among different types of repulsive signals<sup>146</sup>.

### **The axon guidance cue netrin-1**

As already mentioned, netrins (the “one who guides” in Sanskrit) are extracellular molecules that play an important role in neuronal migration and axon guidance. They are laminin-related molecules that function by interacting with the transmembrane receptor of the immunoglobulin superfamily deleted in colorectal cancer, DCC<sup>152</sup>/Frazzled, and Unc5<sup>153</sup> in several neuronal populations. The first identified member of the netrin family was Unc-6, characterized in *C. elegans*<sup>154</sup>. Soon after, homologues of the product of the *unc-6* gene in *C. elegans*, netrin-A and netrin-B were described in *Drosophila*<sup>155</sup>, and in Zebrafish. In chicken netrin-1 and netrin-2 have been reported to be diffusible factors secreted by floor plate cells that promote the outgrowth of commissural neurons<sup>156, 157</sup>. In mice, humans and rats, netrin-1, -2, -3/NTL2, -4/ $\beta$  and G-netrins have been cloned, of which netrin-1, -2, -3/NTL2 and -G are closely related to the laminin- $\gamma$  chains<sup>158</sup>. The homology between the murine netrin-1 protein and chick netrin-1 is 89%<sup>50</sup>. The greatest identity between the netrins and Unc-6 is found in the domain V which is rich in epidermal growth factor repeat structures<sup>157</sup> (Figure 4).

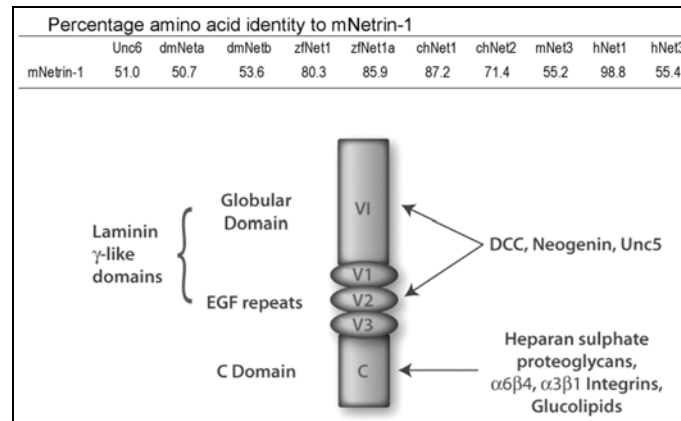


**Figure 4: The homology between different netrins and the structure of netrin.**

The table shows the percentage of identity between mouse netrin and netrins of other organisms. The netrin gene is thought to have derived from the laminin- $\gamma$  gene. The protein bears a globular domain, three EGF repeats and the positively charged C domain<sup>159</sup>. The arrows indicate the binding sites for different receptors.

Netrin-1 is widely expressed both in the developing nervous system and in mesodermal tissues<sup>160</sup>. It is expressed by floor plate cells and its gradient extends many cell diameters dorsal to the floor plate<sup>161</sup>. Floor plate cells have been shown to attract commissural axons coming from dorsal parts of the neural tube<sup>162, 163</sup>.

The first indication that netrin-1 is involved in neuronal migration and axon guidance came from the observation that in *netrin-1* null mice, the ventral commissure of the spinal cord was reduced and the basilar pontine nuclei are completely missing. Netrin-1 was then shown to attract the tangential migration of DCC-expressing pontine neurons from the rhombic lip to the midline and the hindbrain<sup>164,165</sup>. Additionally, in the mutant mice, commissural axons do not cross the midline; instead they show misorientation of fiber tracts and pathfinding errors. Both the corpus callosum and the hippocampal commissure are completely absent in homozygous mutants and the anterior commissure shows variances. However, two dorsal commissures appear intact in the mutant animals<sup>49, 166</sup>.

Mice deficient in netrin-1 die within a few days; they cannot move their forelimbs independently of one another and do not suckle milk. Mice that are DCC-deficient show a phenotype similar to netrin-1-deficient mice and lack the main commissures of the CNS<sup>50</sup>. In *Drosophila*, mutation in *frazzled* results in reduced or absent axon commissures, however, many axons still cross the midline normally<sup>167</sup>.

In the hippocampus at E14-E18, netrin-1 is highly expressed in the fimbria, which is the route followed by developing hippocampal axons to reach the hippocampal



commissure. High expression was detected just above the emerging corpus callosum and below the hippocampal commissure.

Netrin-1 expression levels in embryonic and adult striatum or spinal cord do not differ, suggesting that it not only influences the development of striatal circuitry but may also participate in the maintenance and plasticity of connections in the adult CNS<sup>168</sup>. At early postnatal stages, overall netrin-1 expression decreased but is still noticeable in the septum, dentate gyrus and in some hippocampal interneurons<sup>63</sup>. In the adult, netrin-1 is also expressed on spinal interneurons and motoneurons, cells of the central canal, the meninges and on mature oligodendrocytes but not astrocytes. Netrin-1 protein in white matter is enriched adjacent to paranodal loops of myelin in nodes of Ranvier. The majority of the protein is not freely soluble but is associated with membranes or the extracellular matrix. Thus, netrin-1 may also contribute to the maintenance of appropriate axon-glial interactions in the mature nervous system<sup>169</sup>. Outside the nervous system, netrin-1 is expressed in the limb-primordium, somatic mesoderm, mammary gland, pancreas, dorsal aorta and cardiac muscle<sup>158</sup>.

In the developing mouse spinal cord, netrin-1 is expressed in the floor plate from E10.5 until E11.5 and the netrin-1 receptor *Unc5c* is expressed in DRG neurons. Netrin-1 acts additionally as an early ventral spinal cord-derived chemorepellent for DRG axons but may not act as a repellent at later stages, as the expression levels of netrin receptor *Unc5c* is downregulated in the DRG neurons of late stage embryos<sup>170, 171</sup>. The central projections of DRG neuron axons in the spinal cord are tightly regulated spatially and temporally. During development, DRG neurons enter the spinal cord at the dorsal root entry zone (DREZ) and then grow to the marginal zone of the spinal cord longitudinally to form the dorsal funiculus. Netrin-1 is transiently expressed or upregulated in the dorsolateral region, adjacent to the DREZ, during the waiting period, from day E11.5 to E13.5, and the loss of netrin-1 results in a delay between the formation of the dorsal funiculus and the extension of collaterals into the dorsal mantle layer<sup>172</sup>. Moreover, netrin-1 and DCC might play a role in promoting outgrowth and guidance of pioneering olfactory axons toward the olfactory bulb primordium<sup>173</sup>. In addition, netrin-1 attracts retinal ganglion cell axons toward the optic disc<sup>174</sup> and all precerebellar neurons toward the midline<sup>165, 175, 176</sup>. Netrin-1 also increases cortical branching, which is essential for establishing CNS connectivity, without affecting outgrowth of the primary axon<sup>117</sup>.

Conversely, netrin-1 and DCC mediate the repulsion of the cerebellar neurons from the external granule layer and the striatal neurons from the subventricular zone<sup>177</sup>. Netrin-1 also repels migrating granule cells exiting explants taken from external granular layer from postnatal cerebellum<sup>178</sup>. Netrin was also shown to be crucial for the initial dispersal of spinal cord oligodendrocyte precursors, allowing polarization and directional migration, and their subsequent development in the white matter. In the spinal cord of netrin-1 mutant mice, oligodendrocyte precursors fail to disperse from the ventral midline<sup>179</sup>.

### **The netrin-1-signaling pathway**

The translation of the netrin-1 signal is dependent on which receptor is involved in the signal transduction pathway, DCC or Unc5. Signaling by netrin-1 binding to DCC results in attraction whereas intracellular signaling by Unc5 leads to repulsion. Upon netrin binding, the receptors form homodimers or heterodimers but only DCC homodimers transmit attraction. Apparently, netrin-1 induced formation of a DCC/Unc5 heterodimer converts DCC-mediated attraction to DCC/Unc5-mediated repulsion. The dimers become phosphorylated and, via  $\text{Ca}^{2+}$  influx and diverse signaling molecules, influence the ratio between cAMP and cGMP which controls the response of the growth cone (Figure 5). DCC further activates the mitogen-activated protein kinase (MAPK) which leads to the recruitment of ERK-1/2 to a DCC receptor complex<sup>180</sup>.

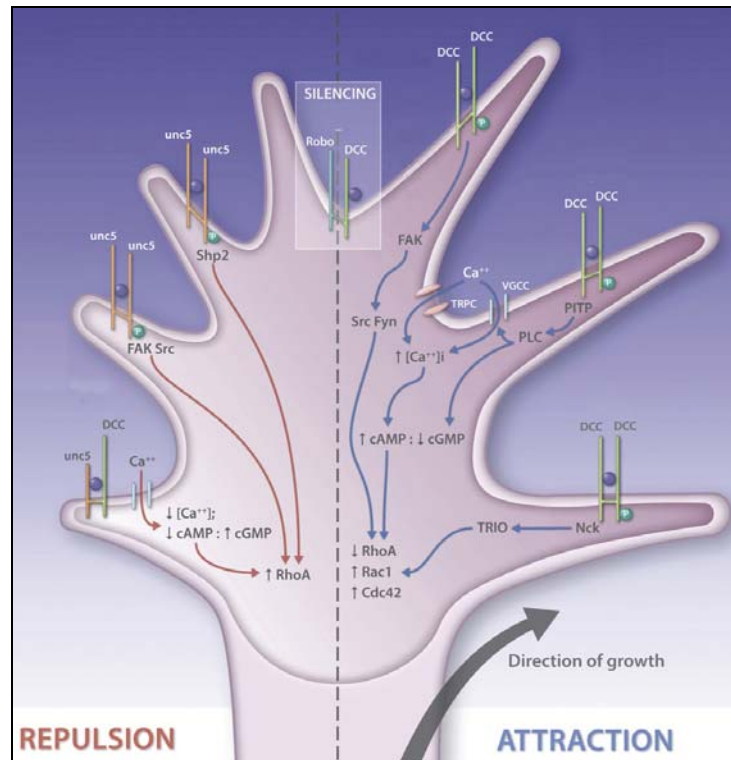


**Figure 5: Attractive or repulsive signaling by netrin-1.**

Depending on the receptor bound by netrin-1, attractive or repulsive signaling pathways can be activated. Binding of netrin-1 to DCC or Unc5 induces homodimerization or heterodimerization of the receptors and activation of downstream signaling pathways. These activate actin and microtubule machineries and eventually result in a turning of the growth cone<sup>159</sup>.

DCC is distributed both on the cell surface and in an intracellular vesicular pool in embryonic spinal commissural neurons. Membrane depolarization and increasing the intracellular concentration of cAMP or activating cAMP dependent protein kinase (PKA) in these cells produces a netrin-1-dependent increase in plasma membrane bound DCC. This further increases commissural axon outgrowth and chemoattractive turning in response to netrin-1<sup>181, 182</sup>.

Besides DCC and Unc5, netrins also bind to integrins<sup>183</sup>. Integrins could have complementary functions in the response of neurons to netrin migration signaling. Further evidence for the cooperative roles of integrins and DCC/Unc5 is that the integrin ligand laminin-1 is able to convert netrin-mediated attraction into repulsion in neurons from *Xenopus*.

A major downstream target of the  $\text{Ca}^{2+}$  influx induced by netrin is the Calcium/calmodulin-dependent protein kinase II, CaMKII, which is required for axon branching and axon outgrowth<sup>138</sup>. CaMKII, CaN, and protein-phosphatase-1 (PP1)

provide a mechanism to control the direction of  $\text{Ca}^{2+}$ -dependent growth cone turning. When the  $\text{Ca}^{2+}$  elevation is large enough, it leads to activation of CaMKII resulting in netrin-1 induced attraction, while a modest local  $\text{Ca}^{2+}$  signal acting through CaN and PP-1 produces repulsion. This repulsion can be inhibited by activation of soluble adenylyl cyclase (sAC), producing cAMP which negatively regulates CaN-PP1<sup>184</sup>. Studies on the role of  $\text{Ca}^{2+}$  and cyclic nucleotides in regulating growth cone turning behaviors of *Xenopus* spinal neurons have shown that the examined guidance cues can be classified into two groups. In group I, which includes netrin-1, BDNF, acetylcholine, NGF and MAG, the turning responses are abolished by depleting extracellular  $\text{Ca}^{2+}$ , and the level of cytosolic cAMP or the activity of PKA is critical in determining whether the turning response is attractive or repulsive<sup>148, 185, 186</sup>. Low cAMP levels lead to the conversion of attraction into repulsion and in the presence of laminin-1 the amount of cAMP decreases in the growth cones. Thus, repulsion takes place in regions in which laminin and netrin are coexpressed, which may help to drive axons to sites where only netrin is present<sup>2, 185</sup>. In group II, which includes semaphorin3 and NT-3, the turning responses are independent of extracellular  $\text{Ca}^{2+}$  and are regulated by cGMP or cGMP dependent protein kinase (PKG)<sup>151</sup>.

Another mechanism by which netrin signaling occurs is the stimulation of tyrosine phosphorylation of DCC by PTK2 and recruitment of Src to the receptor which is essential for axon outgrowth and turning<sup>106</sup>. Moreover, tyrosine phosphorylation of DCC causes N-WASP, Pak1 and FAK to associate with the intracellular domain of DCC and induces activation of phospholipase C (PLC) and the Rho GTPases Rac and Cdc42. These effectors collaborate to alter the axonal cytoskeleton<sup>187</sup>. For instance, attractive netrin-1 signaling promotes the formation of a protein complex including DOCK180, a member of GEFs for Rho GTPases and DCC, leading to activation of Rac1<sup>188</sup>. Rac1, a member of the Rho family of small GTPases, coordinates dynamic instability of microtubules and actin polymerization during lamellipodial protrusion in epithelial cells<sup>189</sup>. Interestingly, Rac1 has been implicated in netrin signaling. After netrin-1 binding to DCC, Rac1 is activated by the Rho-GEF Trio or by high cAMP levels<sup>190, 191</sup>.

Contrary, RhoA signaling decreases the amount of plasma membrane bound DCC, thereby reducing the netrin-1-mediated axonal outgrowth and chemoattractive axon turning. In spinal commissural neurons netrin-1 was shown to inhibit RhoA,

leading to a recruitment of DCC to the plasma membrane and to a positive feedback mechanism<sup>192</sup>.

Concerning filopodial formation on hippocampal neurons, netrin-1 promotes phosphorylation of Ena/VASP proteins through activation of PKA<sup>193</sup>. Ena/VASP proteins regulate elongation at the growing end of actin filaments by antagonizing actin capping proteins that normally terminate actin filament elongation<sup>194</sup>.

Another study has shown that netrin-1 may execute its guidance action also through the regulation of a newly identified microtubule-plus end binding protein neuron navigator-1, NAV1, a mouse homolog of Unc-53, which regulates directional cell migration in *C. elegans*<sup>195</sup>.

Similar to other guidance cues, netrin has been implicated in cancer mechanisms too. DCC, whose expression is lost in numerous cancers, was suggested to be a putative tumour suppressor which appears to be dependent on its ability to trigger apoptosis when disengaged from its ligand netrin-1. Netrin-1 was shown to inhibit the proapoptotic activity of DCC in developing spinal cord commissural neurons<sup>196</sup>.

Additionally, netrin plays a role in angiogenesis, the induction of which is mediated by an increase in endothelial nitric oxide production. Netrin-1 induces a time-dependent phosphorylation of eNOS<sub>s1179, s116</sub> and a rapid dephosphorylation of eNOS<sub>t497</sub><sup>197</sup>.

## Semaphorins and their signaling

Semaphorins are a large family of guidance molecules comprising secreted, or transmembrane or GPI-linked proteins which can be grouped into eight classes on the basis of their structure<sup>198</sup> (Figure 6). Their expression was best described in the nervous system but they are also expressed in many other tissues, giving the semaphorins a wide range of functions. They are involved in generation of neural connectivity, angiogenesis, immunoregulation and cancer. In the nervous system many pathologic conditions, such as multiple sclerosis<sup>199</sup>, epilepsy<sup>200</sup> or Alzheimer's disease<sup>201</sup> are in part due to misregulation of Sema3A or 3F expression.

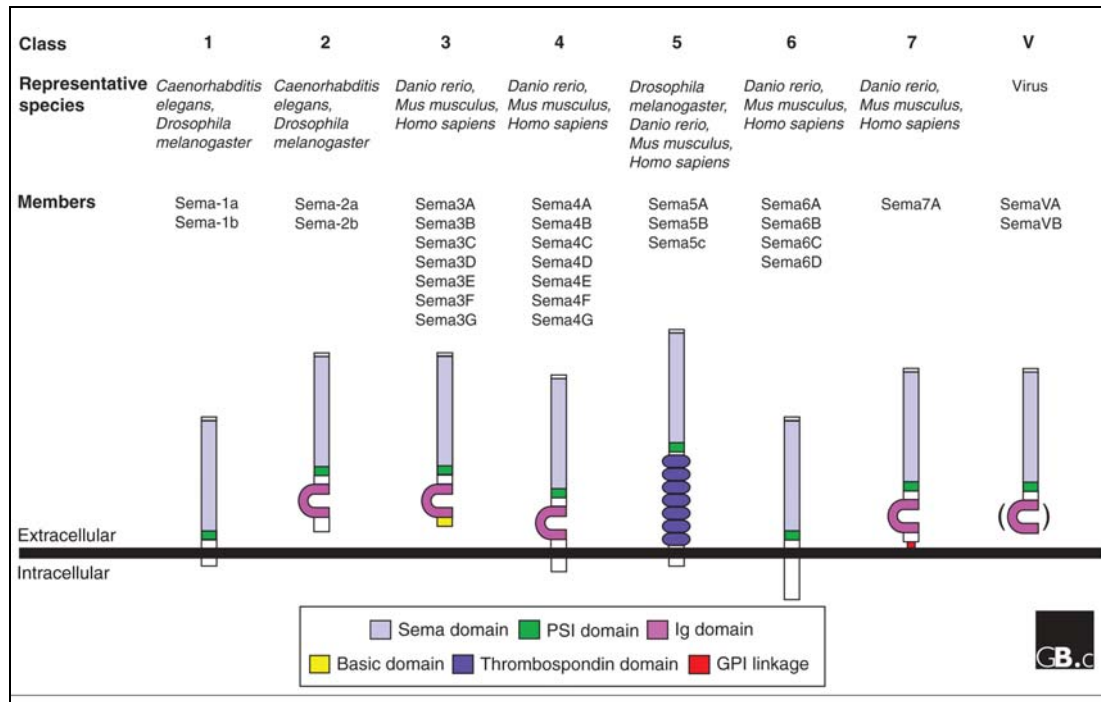


**Figure 6: Protein structures of the semaphorin family.**

Semaphorins are grouped into eight classes, class 1, 4, 5 and 6 are transmembrane proteins, class 2, 3 and V are secreted forms and class 7 semaphorin contains a GPI moiety at its carboxy terminus<sup>202</sup>.

In the nervous tissue of vertebrates semaphorins of the classes 4-7 were found to be expressed<sup>202</sup>. All classes of semaphorins except class 2 bind the plexin family of transmembrane receptors. Several other proteins have been identified to act as semaphorin receptors, such as CD72 and  $\beta$ 1-integrin. Class 3 semaphorins especially bind neuropilin (NRP) which allows indirect binding to plexins<sup>203</sup>. The intracellular domain of plexin is responsible for initiating the signal transduction cascade leading to growth cone collapse, axon repulsion or growth cone turning<sup>204</sup>. The cytoplasmic domains of plexins bind and activate GTPases or their regulators, act on MAP Kinases and other kinases<sup>205</sup> and thereby lead to cytoskeletal rearrangement and repulsive axon guidance<sup>206</sup>. Semaphorin3 and semaphorin4 and their receptors neuropilin-1 and -2 are expressed in the hippocampus. Hence, the hippocampal axons can be repelled by two distinct semaphorins via two different receptors<sup>207</sup>.

Genetic analyses of semaphorin function in flies and in mice suggest that they primarily act as short-range inhibitory cues that repel axons away from inappropriate regions, or guide them through repulsive corridors<sup>208, 209</sup>. Repellent guidance cues induce growth cone collapse and promote axon retraction. Their signaling results in depolymerization of growth cone F-actin characterized by the loss of protrusive

lamellipodia and filopodia, which is of fundamental importance during refinement of axonal projections<sup>66, 210</sup>. One plexin signaling pathway even leads to Rac1 induced inhibition of integrin-mediated adhesion allowing detachment from the substratum and retraction<sup>211</sup>. Semaphorins may also limit the regrowth of axons after an injury<sup>212</sup> as several class 3 secreted semaphorins are highly expressed after CNS lesions<sup>213</sup> and expression of the transmembrane semaphorin 4D is upregulated by oligodendrocytes after spinal cord lesion<sup>214</sup>.

Interestingly, semaphorins may also act as attractive cues for certain axons, signaling at least in part via NRP1<sup>150, 209</sup>.

### Semaphorin 3A

Class 3 semaphorins bind NRP1 and NRP2 which can complex at the surface of growth cones with plexins and semaphorins to form a holoreceptor essential for mediating repulsive semaphorin signaling in neurogenesis<sup>215</sup>. The prototypic member of this class is *Sema3A*, previously designated collapsin-1 or *semD/III*. It acts as a diffusible repulsive guidance cue *in vivo* for the peripheral projections of embryonic DRG neurons.

*Drosophila* mutants in the gene encoding a related semaphorin gene die after eclosion<sup>216</sup>. In *Sema3A* null mice many axonal errors are detected and the mice die soon after birth. The initial trajectory of neurons in the DRG is abnormal, suggesting that *Sema3A* instructs neuronal polarity, in addition to its classic repellent role<sup>217</sup>. The cerebral cortex of mutant mice shows abnormally oriented neuronal processes, especially of the large pyramidal neurons<sup>218</sup>.

Cdk5 and GSK-3 $\beta$  play a critical role in *Sema3A* signaling. Cdk5 and GSK-3 $\beta$  phosphorylate collapsing response mediating protein-2 (CRMP2) causing reduction of its affinity to tubulin. *Sema3A* stimulation enhances the levels of the phosphorylated form of CRMP2. This phosphorylation is essential for *Sema3A*-induced growth cone collapse in DRG neurons<sup>219, 220</sup>. Pharmacological blocking of GSK-3 prevents *Sema3A*-induced growth cone collapse, but activation of GSK-3 alone does not induce growth cone collapse<sup>221</sup>.

*Sema3A*, similar to semaphorin3F, inhibits the activity of phosphatidylinositol 3-kinase (PI3K) and contributes to growth cone collapse and axon retraction. The

suppression of PI3K-signaling occurs concomitant with the activation of GSK-3, which depends on the phosphatase activity of the tyrosine phosphatase PTEN. The main substrate of PTEN is PIP3 which is produced by PI3-Kinase, which in turn regulates the activity of numerous downstream signaling proteins including GEFs, Akt and PDKs<sup>222</sup>. PTEN is highly enriched in the axonal compartment of the central domain of sensory growth cones during axonal extension, where it co-localizes with microtubules and accumulates rapidly at the growth cone membrane following exposure to Sema3A. Neuronal PTEN associates with microtubules and functions as an essential mediator of PI3K and GSK-3 signaling in response to Sema3A<sup>223</sup>. Specifically, inhibition of PI3K activates the actin-myosin II system for generating cellular contractile forces, while also blocking the formation of F-actin structures that serve as precursors to the protrusion of filopodia<sup>224</sup>.

When guidance cues induce growth cone collapse and axon retraction the upstream regulators of myosin II, RhoA and the RhoA-kinase ROCK have been shown to be signaling intermediates<sup>225</sup>. ROCK positively regulates the activity of myosin II by increasing the phosphorylation of myosin II regulatory light chains<sup>226</sup> and it is required for Sema3A-induced activation of myosin II in axons<sup>227</sup>.

In *Xenopus* spinal neurons and rat DRG explants, the repellent effect of Sema3A can be switched into attraction by increasing the concentration of intracellular cGMP levels. Interestingly, also elevation of NO-levels in these cells has the same effect<sup>151</sup>.

## **Nitric oxide production and its effects**

### **Nitric oxide synthases**

The nitric oxide synthases, NOS, were first identified in 1989. There have been identified three distinct isoforms of NOS, products of different genes, with different localization, regulation, catalytic properties and inhibitor sensitivity. In the neuronal tissue, the predominating form is the neuronal NOS (nNOS) also known as NOS-1. The inducible form of NOS is iNOS which is found in a wide range of tissues, it is also known as NOS-2. The third isoform is the endothelial NOS (eNOS or NOS-3) which is found mainly in vascular endothelial cells but it is also expressed in neurons and glia cells. The isoforms differ in being constitutively (nNOS and eNOS) or inducibly



expressed (iNOS) and in their calcium-dependence (nNOS and eNOS) or -independence (iNOS) (Figure 7).

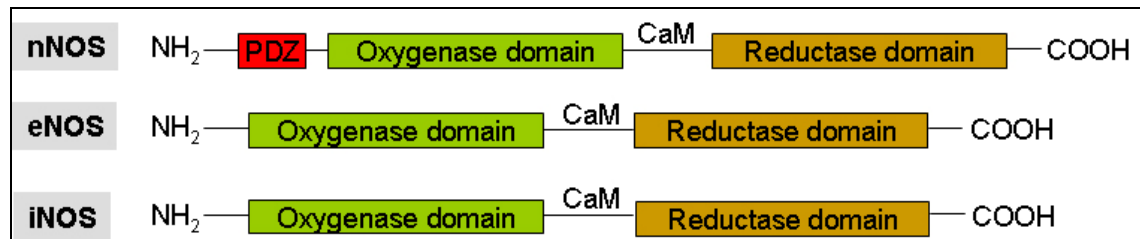


**Figure 7: The three nitric oxide synthases.**

All three nitric oxide synthases bear an oxygenase and a reductase domain and binding sites for FMN. nNOS is the only one with a PDZ domain at its N-terminus that targets nNOS to synaptic sites in brain and skeletal muscle. The NOSs have all recognition sites for CaM and the reductase domains include binding sites for FAD and NADPH<sup>228</sup>.

The enzymes are usually referred to as dimeric in their active form, where each NOS monomer is associated with calmodulin. The NOS enzymes catalyze a reaction of L-arginine, NADPH, and oxygen to the free radical NO, citrulline and NADP. The cellular and tissue specific localization of NOSs can be regulated by transcriptional regulation, protein-protein interactions, and alternative mRNA splicing or covalent modifications. CaM is known to be necessary for the enzymatic activity of all three isoforms and for activation of CaMKII. Also phosphorylation has an effect on nNOS and eNOS activity. The protein kinase Akt phosphorylates eNOS at Ser<sup>1179</sup> which results in an increase in NO production<sup>229</sup>. In contrast, the phosphorylation of nNOS at Ser<sup>847</sup> by CaMKII leads to a decrease in synthase activity<sup>230</sup>. Conversely, CaMKII is known to be regulated by autophosphorylation which increases its Ca<sup>2+</sup>-independent activity and NO reversibly inhibits CaMKII by S-nitrosylating it at Cys<sup>6</sup>. This inactivation may contribute to NO-induced neurotoxicity in brain<sup>231</sup>. On the other hand, phosphorylation by PKC increases nNOS activity<sup>232</sup> and dephosphorylation by CaN activates nNOS. Moreover, PKG and PKA phosphorylate nNOS thereby inhibiting its catalytic activity<sup>5</sup>. In contrast, eNOS is rapidly and strongly activated and phosphorylated in the presence of PKGII and PKA. This activation is independent of Ca<sup>2+</sup>/CaM. Since NO activates sGC and cGMP activates PKGII, this suggests a positive feedback mechanism for NO/cGMP<sup>233</sup>.

Mice lacking nNOS show slowed Wallerian degeneration, a delay in regeneration and a disturbed pruning of uncontrolled axon sprouts. A lack of eNOS is

well tolerated, although a delay in nerve revascularization is observed. Thus, after peripheral nerve lesion, regular NOS activity is essential for cell survival and recovery<sup>234</sup>.

nNOS appears to be targeted to membranes by binding to PSD-95 that associates with N-methyl-D-aspartate receptors (NMDAR) at synapses<sup>235</sup>. NO has been implicated in hippocampal long term potentiation (LTP) but mutant mice for either nNOS or eNOS do not show a significant reduction in LTP. Only mice double mutant for nNOS and eNOS show significant reduction in LTP in stratum oriens, suggesting that neuronal and endothelial NOS forms can compensate for each other in mice with a single mutation<sup>236</sup>.

In PC12 cells NO production is a part of the mechanism of laminin-induced neurite outgrowth. Inhibition of nNOS prevents the formation of NO and prevents neurite outgrowth<sup>237</sup>. DRG neurons express nNOS during early development, while in the adult the enzyme expression decreases<sup>238</sup>. Following peripheral nerve injury, DRG neurons reexpress nNOS and in all three isoforms of NOS are upregulated in the affected nerve. At the same time cGMP synthesis is increased in satellite glia cells<sup>239</sup>, suggesting that NOS play an essential role in regeneration<sup>240</sup>.

## **NO**

NO is a gaseous freely diffusible intercellular messenger molecule that regulates a wide variety of physiological processes in the cardiovascular and immune system, central and peripheral nervous system, including neurotransmitter release, plasticity and apoptosis, and elsewhere<sup>241-244</sup>. How NO signals are decoded and translated into downstream physiological effects is poorly understood. The best known NO receptor is the enzyme sGC the activity of which results in cGMP accumulation in target cells. It is known that NO binds to a haem prosthetic group on the receptor and triggers a conformational change that increases the catalysis of cGMP synthesis by several hundred-fold<sup>245</sup>. Thus,  $\text{Ca}^{2+}$  signals which activate NOS may either upregulate the activity of cGMP-dependent pathways<sup>246</sup>.

NO has the capacity to interact with and modify a wide variety of molecules: free radicals such as the superoxide anion, key redox regulators such as glutathione, and macromolecules like DNA or proteins. Binding of a NO group to a free thiol of an amino acid is called S-nitrosylation. NO can influence protein function by S-

nitrosylation of specific cysteines. S-nitrosylation is a reversible and specific modification and, in contrast to phosphorylation, enzyme-independent. S-nitrosylation has emerged as a potent protein modification. Proteins like hemoglobin, NMDAR, p21<sup>ras</sup> and I- $\kappa$ B have been found to undergo S-nitrosylation resulting in changes of their activities<sup>247-251</sup>. Over the past decade, the number of reported protein substrates for S-nitrosylation has grown to well over a hundred<sup>252</sup>. NO is generated by NOS after NMDAR stimulation and feedback S-nitrosylation of NMDAR and of NOS is inhibitory<sup>253</sup> (Figure 8).

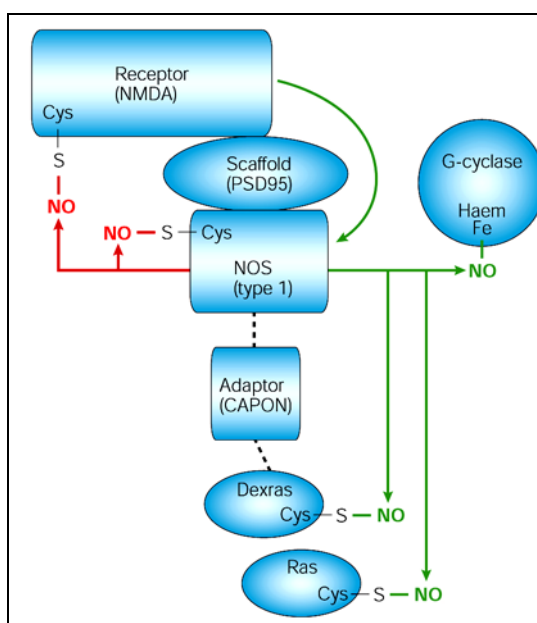


**Figure 8: Activation of nNOS and downstream targets of NO.**

In neurons NMDAR serves as  $\text{Ca}^{2+}$  channel regulating nNOS (NOS type 1) activity and is at the same time a substrate for nNOS-dependent S-nitrosylation within a negative feedback-loop (red arrows). nNOS is linked to NMDAR via the scaffold protein PSD95 and to the small G-protein Dexras via the adaptor protein Capon. Dexras is activated by S-nitrosylation (green arrows). Another important target of NO is the sGC which starts cGMP synthesis upon activation by  $\text{NO}^{253}$ .

In the central nervous system, NO has an array of functions, such as the regulation of synaptic plasticity, the sleep-wake cycle, hormone secretion, and neurotransmission. NO production is associated with cognitive function, control of appetite, body temperature and neurosecretion<sup>254, 255</sup>. In the peripheral nervous system, NO regulates the non-adrenergic, non-cholinergic relaxation of smooth muscle cells<sup>256</sup>. It acts as neurotransmitter in both the CNS and PNS by mechanisms that are dependent

on cGMP<sup>257</sup>. Important downstream effectors of cGMP are PKG, PIP3-kinase, the antiapoptotic Akt serine/threonine kinase and cyclic nucleotide-gated channels<sup>258</sup>.

On the one hand, NO acts neuroprotective. For instance, in the NMDA-mediated neurotoxicity by S-nitrosylation of the NR1 and NR2 subunits of the NMDAR<sup>259</sup>. NO can also confer cytoprotection through the inhibition of caspase activity by S-nitrosylating cysteines of the catalytic site<sup>260</sup>.

On the other hand, NO is harmful under pathological conditions that involve the production of reactive oxygen species, such as superoxide anions, and the formation of peroxynitrite<sup>254</sup> whose prolonged stimulation of NMDAR causes excitotoxic cell death<sup>254</sup>. NO and peroxynitrite may also kill neurons by indirect activation of caspases or by caspase-independent disruption of mitochondrial function<sup>7</sup> since NO can reversibly inhibit brain mitochondrial ATP synthesis<sup>261</sup>. For instance cortical NO production increases during hypoxia in the immature brain and is associated with neurotoxicity, mitochondrial dysfunction and decrease in mitochondrial size. The effects of hypoxia on mitochondrial movement and morphology can be partially prevented by NOS inhibitors<sup>262</sup>.

In cerebrospinal fluid (CSF) nitrite is a reliable indicator of NO production. Physiological concentrations in brain under normal conditions are around 1nM NO and 1μM nitrite. During pathological conditions, NO level can reach up to 1μM while nitrite levels are around 100μM. An increase in nitrite level in CSF is considered an indicator of intrathecal NO production and a sign of brain inflammation<sup>7</sup>.

## **S-nitrosylation**

The crucial difference between S-nitrosylation and phosphorylation is that phosphorylation is enzyme driven, whereas S-nitrosylation is achieved through the non-catalysed chemical modification of a protein residue<sup>263</sup>. It is regulated precisely in time and space<sup>264</sup>. Only a fraction of cysteine residues present in proteins in the free-thiol state become nitrosylated. However, the molecular mechanisms underlying this specificity are not understood. For example common structural motif that might determine the reactivity of individual cysteines are present only in a subset of proteins amenable to S-nitrosylation<sup>265</sup>.

S-nitrosylation is a light sensitive and very labile covalent modification which is hard to detect and the cleavage of the S-NO bond can occur without the help of specific enzymes<sup>266</sup>. Hence, whether or not nitrosylation occurs depends on the concentration of the nitrosylating agent and the proximity of the target proteins and NO synthases<sup>267</sup>. A method called biotin-switch has been developed to identify S-nitrosylated proteins. In this assay S-nitrosylated cysteines are converted to biotinylated cysteines and these can then be detected by immunoblotting or chromatography<sup>268</sup>.

In diverse cell types a portion of basal level of S-nitrosylated cysteines is stable in the presence of NOS inhibitors<sup>247</sup>. A well-characterized example of such modularity is provided by the multiprotein complex that incorporates nNOS, PSD93/95 and NMDAR. S-nitrosylation of caspase-3, caspase-9, apoptosis-signal-regulating kinase 1 (ASK1) and c-Jun-N-terminal kinase (JNK) blocks their activity and inhibits apoptosis, whereas S-nitrosylation of matrix metalloproteinase-9 (MMP9) and nuclear factor B promotes cell death<sup>253</sup>. In addition, the hypoxia-inducible factors HIF that respond to low oxygen concentrations is a well characterized example of S-nitrosylation<sup>269</sup>.

### **MAP1B, NO and netrin-1**

When the intracellular NO-levels increase, axons from different types of neurons, such as chick sensory neurons or mouse DRG neurons, retract dramatically. In retracting neurons the mass of microtubules is not decreasing during retraction suggesting a backward retreat of cytoskeletal elements rather than their wholesale depolymerisation<sup>270</sup>. MAP1B was found to play a critical role in this process. Nitrosylation of the MAP1B LC1 leads to its enhanced interaction with microtubules and subsequently, MAP1B dependent growth cone collapse and axon retraction occurs<sup>1</sup>.

Moreover, MAP1B was suggested to be involved in netrin-1 signal transduction. Netrin-1 stimulates the GSK-3 $\beta$  and Cdk5-dependent mode I phosphorylation of MAP1B, thereby it is potentially regulating microtubule and actin dynamics. Furthermore, the chemoattractive effect of netrin-1 of *MAP1B*-deficient neurons is compromised, suggesting that MAP1B may be an essential downstream effector in the chemoattractive netrin-1 signaling pathway. Another evidence for MAP1B requirement for correct transduction of the netrin-1 signal is that *MAP1B* null mice display a similar

migration defect of pontine nuclei as *netrin-1* mutants and both lack commissural structures in the brain<sup>3</sup>.

Since netrin-1 signaling involves changes in  $\text{Ca}^{2+}$  levels and  $\text{Ca}^{2+}$  is known to activate nNOS, this raises the question whether nNOS is part of the signal transduction pathway downstream of netrin-1. NO production regulates the activity of sGC which further influences the ratio between cAMP and cGMP. This proportion eventually controls whether a growth cone turns towards or away from a netrin-1 source. Considering that the S-nitrosylation of MAP1B is necessary for NO-induced retraction, I would like to address the question whether S-nitrosylated MAP1B is important in the interpretation of axon guidance cues like netrin-1 or Sema3A.

## NO and MAP1B in oligodendrocytes

During myelination, the process of a myelinating cell wraps around an axon to elaborate a myelin sheath. The myelin sheath is a fatty insulation composed of modified plasma membrane that surrounds axons and promotes the rapid and efficient conduction of electrical impulses along myelinated axons (Figure 9). The majority of CNS myelination occurs postnatally<sup>271</sup>. The myelin sheath itself can be divided into two domains, compact and non-compact myelin, each of which contains a non-overlapping set of proteins. Compact myelin forms the bulk of the myelin sheath; non-compact myelin is found in paranodes and in Schmidt-Lantermann incisures<sup>272</sup>.

In the CNS, oligodendrocytes are the glial cells responsible for the formation and maintenance of myelin. In the peripheral nervous system Schwann cells are the myelin forming cells. They elaborate a myelin sheath around a single axonal segment, whereas an oligodendrocyte is able to myelinate up to 60 axons<sup>273</sup>. Oligodendrocytes derive from stem cell precursors which arise in the subventricular zone of the developing CNS. Growth, differentiation and survival of CNS glial progenitors and their progeny are influenced by PDGF, bFGF, IGF-1 and 2, NT-3, CNTF, retinoic acid, glial growth factors, sonic hedgehog, interleukin-6 and LIF<sup>274</sup>. In the spinal cord, oligodendrocyte precursors appear to share a developmental lineage with motor neurons, although they may also develop from restricted glial precursors. Immature oligodendrocyte precursors are highly migratory. They migrate from their site of origin to developing white matter tracts using a variety of guidance cues. The final match of

oligodendrocyte and axon number is accomplished through a combination of local regulation of cell proliferation, differentiation and cell death. Not all oligodendrocyte precursors differentiate during development, and the adult CNS contains a significant population of precursors<sup>271</sup>.

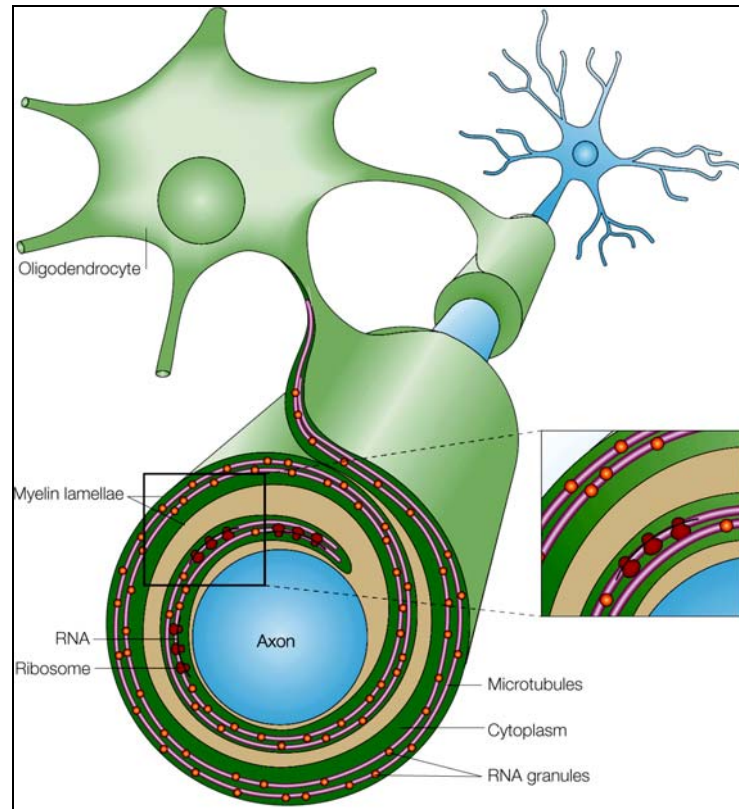


**Figure 9: Ensheathment of an axon by an oligodendrocyte.**

Myelinating glia cells wrap around an axon in order to allow saltatory conduction of action potentials along the axon and to provide protection. Microtubules and local protein translation play an essential role in maintenance of the myelin sheath.

Myelin contains a high percentage of lipids, such as cholesterol and galactocerebroside, GalC, and special proteins like myelin basic protein, MBP, myelin associated glycoprotein, MAG, proteolipid-protein, PLP and others. Oligodendrocytes express two proteins that are not expressed by Schwann cells, myelin-oligodendrocyte glycoprotein, MOG, on their outer cell membrane<sup>275</sup> and myelin-oligodendrocyte basic protein, MOBP<sup>276</sup>.

Because the development of neuronal morphology is known to depend on the presence of highly organized microtubule arrays, it may be hypothesized that the properties of microtubules influence the form and function of oligodendrocytes as well.

The oligodendrocyte have polarized microtubules oriented with their plus-end towards the distal part of the processes<sup>277</sup>. Morphogenesis of and myelination by oligodendrocytes depends on export of RNA from the nucleus to the perikaryon, assembly of the RNA into RNA granules, transport of RNA granules along microtubules, and localization and translational activation in the myelin compartment. mRNAs of MBP and MOBP have been localized to the myelin compartment in oligodendrocytes. Furthermore, several membrane components, including PLP and sulfatide, are transported through the Golgi to the plasma membrane or myelin. The maintenance of membrane sheets by oligodendrocytes in culture is a dynamic process, requiring ongoing microtubule turnover and transport of molecules through the Golgi<sup>278</sup>. Concerning the retrograde movement of RNA granules in oligodendrocytes, it is possible that the minus-end motor, cytoplasmic dynein is also involved, given the plus-end-distal polarity of the microtubules in oligodendrocyte processes<sup>279</sup>.

Neuronal electrical activity has been shown to be critical for the proliferation of the progenitors of oligodendrocytes. Moreover, adhesion molecules, which bring the axon and glial cell into close apposition and transduce signals between these cells, are essential for correct myelination. Demyelination-induced disruption of these axonal signals and axoglial interaction is likely to inhibit myelin repair<sup>273</sup>.

## **MAP1B in oligodendrocytes**

Oligodendrocytes differentiate from a bipolar A2B5-positive progenitor to an O4-positive preoligodendrocyte and further into a complex process-bearing GalC-positive oligodendrocyte. These processes are rich in microtubules and their development requires reorganization of the cytoskeleton. MAP1B is first detectable in O4<sup>+</sup> preoligodendrocytes prior to terminally differentiated myelin-forming oligodendrocyte, but not in astrocytes. The expression of MAP1B is limited to the cell body and the processes, whereas flattened membranes are not MAP1B positive<sup>280</sup>. The timing of MAP1B expression implies a possible role of MAP1B microtubule interactions in the formation and stabilization of myelin-forming processes<sup>6</sup>. The distinct subcellular localizations and patterns of developmental expression of MAP1B, MAP4 and MAP2c suggest that these MAPs have different roles in the regulation of the microtubule network during the differentiation of oligodendrocytes<sup>281</sup>. MAP1B



deficiency causes delayed myelin development, suggesting the functional importance of MAP1B in oligodendroglia<sup>282</sup>.

The transition from premyelinating oligodendrocytes into myelin-bearing cells is accompanied by a dramatic upregulation in expression of the RNA binding QKI proteins which facilitate movement of mRNAs to myelin via the cytoskeleton. MAP1B mRNA was found to be posttranscriptionally regulated by the selective RNA-binding protein QKI<sup>283</sup>.

MAG, which is expressed in periaxonal membranes of myelinating glia where it is believed to function in glia-axon interactions, binds to a phosphorylated neuronal isoform of MAP1B expressed as a membrane glycoprotein on the surface of DRG neurons but not to the isoform expressed in glial cells. This interaction of MAG and MAP1B also suggests its requirement for normal long term maintenance of myelinated axons<sup>284</sup>.

In Schwann cells the expression of MAP1B is induced following sciatic nerve lesion and regeneration and in cultured primary Schwann cells. The isoform expressed in Schwann cells is similar to MAP1B expressed in neurons but shows a different phosphorylation state<sup>32</sup>.

## **NO and neurodegenerative diseases**

The presence of nNOS has never been found in oligodendrocytes whereas eNOS has been detected in primary cultures of oligodendrocytes. It was present at all stages of maturation from bipolar to membrane-bearing oligodendrocytes expressing MBP and MOG. Oligodendrocytes grown for several days in the general NOS inhibitor L-NMMA show marked changes in arborization. The cells show flattened cell bodies and thinner, less ramified processes suggesting that NO might play a role in the organization of the oligodendrocyte cytoskeleton and differentiation<sup>7</sup>.

Nitric oxide production seems to play a role in diverse neurodegenerative diseases like Alzheimer's disease, Parkinson's disease or multiple sclerosis (MS). MS is the most common cause of chronic neurologic disability resulting from interruption of myelinated tracts in the central nervous system. The autoimmune disease experimental allergic (or autoimmune) encephalomyelitis, EAE, and MS share common clinical, histologic, immunologic and genetic features; hence EAE is widely considered to be a

relevant animal model for the human disease. It can be induced in a variety of animal species by immunization with myelin proteins or peptide derivatives<sup>285</sup>.

For many years MS was considered an immune-mediated disorder. Investigations revealed that a neurodegenerative process, unresponsive to immunosuppression, was responsible for progressive neurological impairment<sup>286</sup>. Even though myelin loss is the key event of MS, substantial axonal damage in active lesions has already been described too<sup>287</sup>. This axonal destruction in plaques leads to Wallerian degeneration<sup>288</sup>. Macrophages and activated microglia have also been reported to be in close contact with degenerating axons. These cells produce inflammatory mediators such as NO. It is suggested that NO injures axons by inhibiting mitochondrial respiration<sup>289</sup>. Both physiological and pathological actions of NO are mediated by its targets that become structurally modified by reactive NO or its derivatives peroxynitrite, formed after the reaction with superoxide, and S-nitroso-L-glutathione (GSNO)<sup>290</sup>.

*In vitro*, NO induces ATP depletion and loss of mitochondrial membrane potential, DNA damage, morphological changes and necrotic cell death in rat oligodendrocytes<sup>7</sup>. The vulnerability of developing oligodendrocytes to NO also involves translocation of the apoptosis-inducing factor from mitochondria to nuclei<sup>291</sup>. Peroxynitrite induces strong primary axonal damage with characteristics of primary acute axonopathy, together with severe myelin alteration, demyelination and nitrotyrosine formation. It damages cells by modifying cellular compounds by peroxidation of lipids, DNA and proteins. Nitrotyrosine has been detected in MS demyelinating lesions associated with lipid-laden macrophages, cell debris, myelinated axons<sup>292</sup> and in EAE lesions<sup>293</sup>. Moreover, high levels of NO lead to irreversible decompaction of CNS myelin, but not PNS myelin<sup>294</sup>.

Oligodendrocytes can be stimulated to express iNOS by inflammatory cytokines, which are known to accumulate in the MS brain. Tumor necrosis factor- $\alpha$  and IFN $\gamma$  cause elevated NO production by iNOS in primary cultures of rat oligodendrocytes. Simultaneously, NO-mediated mtDNA damage occurs<sup>295</sup>. Both macrophages and astrocytes are considered to be the main cellular sources of iNOS expression in MS lesions<sup>296</sup>. In EAE, iNOS mRNA expression within the CNS is enhanced both at onset and peak of clinical signs<sup>297</sup> and nitrotyrosine has been detected in lesions<sup>292</sup>. Moreover, antibodies reactive with nitroso-S-cysteine coupled to serum albumin are elevated in sera from MS patients<sup>298</sup>. Anti-SNO-cysteine antibodies are also increased at times of MS attacks and in progressive disease, suggesting a potential relevance of these

antibodies as biological markers for clinical activity<sup>299</sup>. Interestingly, the NOS inhibitor L-NAME has a protective effect in MOG induced EAE, the extent of CNS inflammation and demyelination<sup>300</sup>.

Referring to *in vitro* experiments, developing oligodendrocytes are more sensitive to high NO concentrations than mature ones in particular with regard to the maintenance of their mitochondrial transmembrane potential<sup>301</sup>. Thus, also the remyelination, involving immature oligodendrocytes generated from precursors could be affected by high NO-levels.

In consideration of the facts that MAP1B is expressed in glial cells and these cells are sensitive to NO, the question arises if S-nitrosylation of MAP1B LC1 might affect the functionality of oligodendrocytes.



**PART I RESULTS:**

**NO in netrin-1 and Sema3A mediated axon guidance**



## The role of NO in the netrin-1 axon guidance signaling pathway

### Netrin-1 induces retraction in wild-type and MAP1B<sup>-/-</sup> DRG neurons

Different groups showed that the guidance cue netrin-1 is essential for proper development of the nervous system in mice where it can act either as attractive or repulsive cue dependent on the receptor through which it signals. Some analogies in the phenotypes of mice lacking netrin-1<sup>49</sup>, DCC<sup>50</sup>, or MAP1B<sup>4</sup> were observed and MAP1B was shown to be necessary for the correct transduction of attractive netrin-1 signaling<sup>3</sup>. This prompted me to explore the role of MAP1B in netrin-1 signaling in more detail. Dorsal root ganglia (DRG) neurons isolated from adult mice are a well established model for the investigation of axon guidance signaling pathways. Thus, wild-type and MAP1B<sup>-/-</sup> DRG neurons were cultured on poly-L-lysine (PLL) and laminin coated glass coverslips for 24hrs (Figure 10A). Since the presence of laminin was shown to switch the attractive netrin-1 signaling to a repulsive one<sup>2</sup>, DRG neurons cultured on laminin were expected to be repelled by netrin-1. Whether neurites are attracted or repelled by a guidance cue can be assessed by observing the growth cone turning toward or away from the source of the cue. In case of bath application, the appraisal of retracted neurons is the only way to analyse the nature of the response. Hence, in the case of DRG neurons grown on laminin and treated with 250ng/ml netrin-1, repulsion would be seen at the retraction of their axons. Indeed, after a treatment with netrin-1, axons of DRG neurons exhibited typical features of retraction. In wild-type and MAP1B<sup>-/-</sup> DRG neurons, netrin-1 treatment induced collapse of growth cones, formation of sinusoidal microtubule bundles along the axon shaft and trailing remnants (Figure 10B). No difference in the phenotype and no delay in the response to the treatment could be observed between wild-type and MAP1B<sup>-/-</sup> DRG neurons. The quantitative analysis of the response of wild-type and MAP1B<sup>-/-</sup> DRG neurons to netrin-1 revealed a significant increase of retracted neurons after the incubation for 21hrs with netrin-1 (Figure 10C). In untreated samples, the percentage of retracted wild-type DRG neurons was 10% and for MAP1B<sup>-/-</sup> DRG neurons it was 11%. This amount of retracted neurons might be due to changes in temperature or due to the stress cells undergo during fixation. However, after the treatment with netrin-1, 34% of wild-type DRG neurons and 40% of MAP1B<sup>-/-</sup> DRG neurons showed retraction. The similarity in the reaction of wild-type and MAP1B<sup>-/-</sup> DRG neurons to the axon guidance cue suggests that MAP1B does not play

an essential role in the repulsive netrin-1 signaling pathway, in contrast to the results observed for attractive netrin-1 signaling<sup>3</sup>.

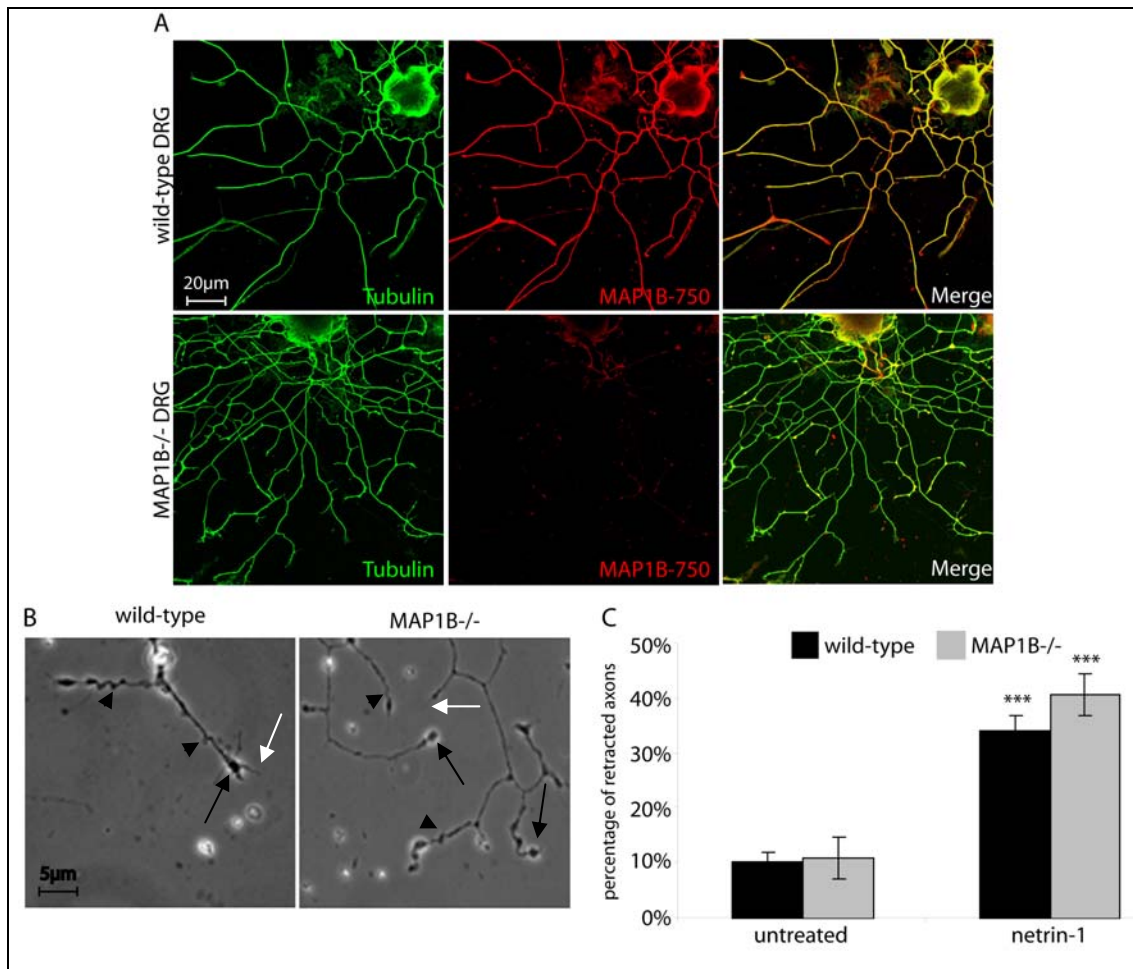


**Figure 10: Expression of MAP1B in mouse DRG neurons and netrin-1 induced retraction.**

Mouse DRG neurons were isolated from wild-type and MAP1B<sup>-/-</sup> mice and cultured for 24hrs on PLL-laminin coated coverslips. A) Neurons were fixed and stained for MAP1B-750 and tubulin. In wild-type DRG neurons MAP1B was expressed in the cell body and in all axons and co-localized with tubulin. In MAP1B<sup>-/-</sup> DRG neurons only background staining of MAP1B was visible. Many of these neurons showed increased branching of axons. B) Neurons were treated with 250ng/ml netrin-1 for 4-5hrs. Cells were visualized *in vivo* by phase contrast microscopy (Zeiss). Both wild-type and MAP1B<sup>-/-</sup> DRG neurons showed axon retraction. Typical retraction included the collapse of the growth cone (black arrows), sinusoidal bends along the axon shaft (arrowheads) and a trailing remnant (white arrows). There was no difference in the morphology of the nerve cells after netrin-1 treatment between wild-type and MAP1B<sup>-/-</sup> DRG neurons. C) The graph shows the quantitative analysis of the retracted neurons in culture after netrin-1 treatment. Wild-type and MAP1B<sup>-/-</sup> DRG neurons, were left untreated or treated for 21hrs with 250ng/ml netrin-1, as indicated, fixed, stained for tubulin and analysed by confocal microscopy. For quantitative analysis, approximately 100 cells in each of 6 independent experiments were assessed for microtubule configuration. DRG neurons with one axon exhibiting features of retraction were considered as retracted. In untreated samples the amount of retracting neurons was in the range of 10 to 11%. After



netrin-1 treatment, wild-type cultures showed 34% and MAP1B<sup>-/-</sup> cultures showed 40% of retracted DRG neurons. Error bars represent standard errors of the mean. Asterisks indicate that the values for cells treated with netrin-1 were significantly different from corresponding values of untreated cells (\*\*\*,  $p < 0.001$ ).

### **The role of laminin in NO-induced axon retraction**

The presence of the extracellular matrix component laminin was shown to be responsible for at least one phenotypic difference between wild-type and MAP1B<sup>-/-</sup> DRG neurons. Grown on PLL-laminin coated coverslips, MAP1B<sup>-/-</sup> DRG neurons exhibit a more branched phenotype than wild-type DRG neurons. This morphological distinction was never observed when DRG neurons were grown on PLL or PDL only (Krupa, PhD Thesis 2009). This raised the question whether laminin also plays a role in the signal transduction of MAP1B-S-nitrosylation. Therefore, DRG neurons from wild-type and MAP1B<sup>-/-</sup> mice were cultured on PLL-laminin and on PDL for 24hrs. Then, cells were treated either with 1 $\mu$ M calcimycin for 15min or with 100 $\mu$ M SNAP for 1h. In case of calcimycin treatment, intracellular NO production was visualized with DAF-FM DA. This cell permeable dye is cleaved in the cell by esterases and reacts in the presence of oxygen with NO yielding the photostable fluorescent product DAF-FM T. Since SNAP is a NO-donor, DAF-FM DA was not used for these samples. In wild-type DRG neurons, a clear increase in DAF-FM T fluorescence was observed following calcimycin treatment, independent of the substrate on which DRG neurons grew (Figure 11A). Calcimycin and SNAP treatment led to significant increase in axon retraction in wild-type DRG neurons grown on PLL-laminin. In contrast, irrespective to NO production, wild-type DRG neurons did not exhibit an increase of retracted neurons when cultured on PDL (Figure 11B). In MAP1B<sup>-/-</sup> DRG neurons, DAF-FM DA staining did not reveal any change in intracellular NO production (Figure 12A). Moreover, the calcimycin and SNAP induced axon retraction did not occur, independent of the substrate (Figure 12B). This suggests that laminin might be necessary to mediate NO-induced axon retraction in wild-type DRG neurons.

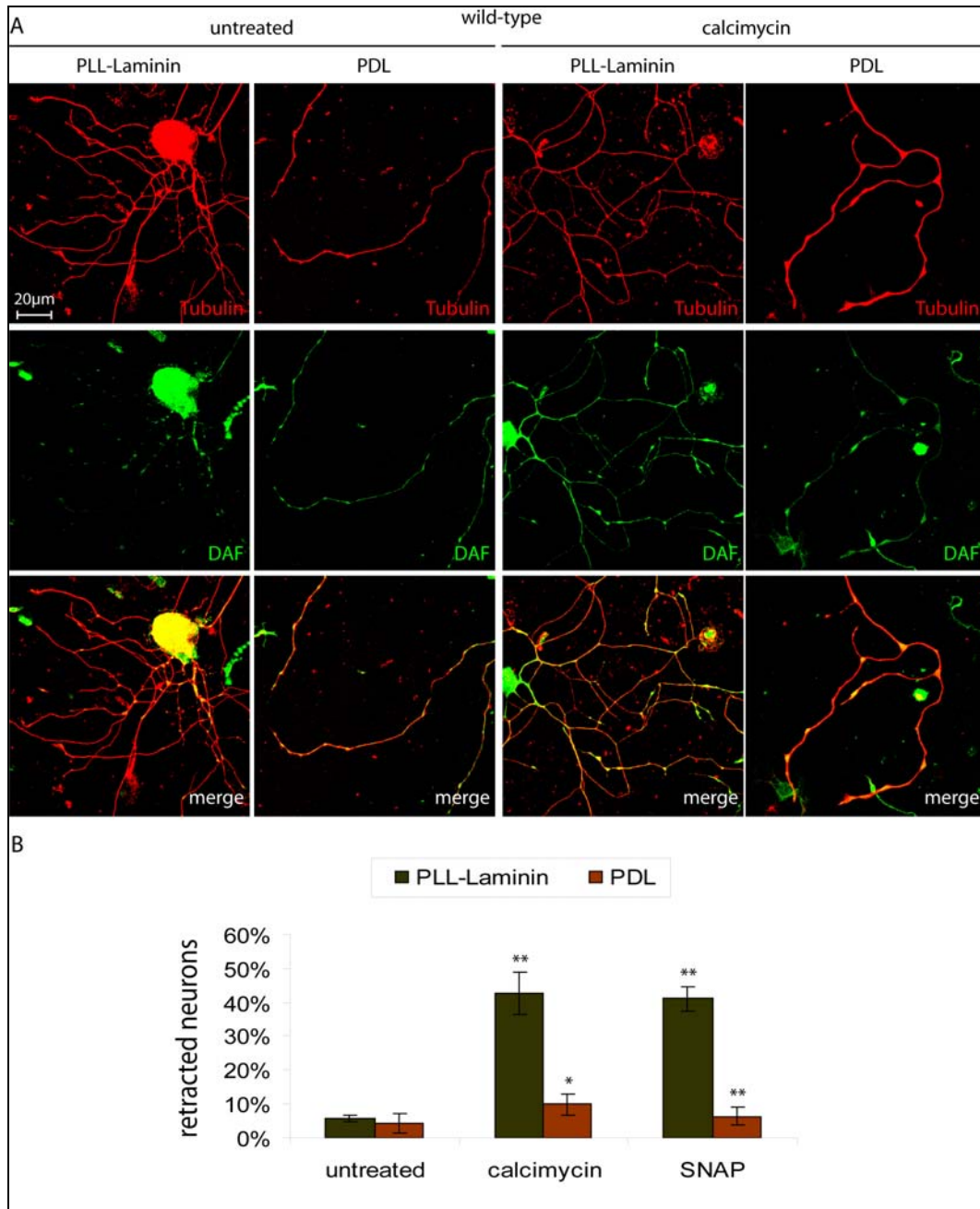


**Figure 11: Calcimycin and SNAP induce axon retraction only in wild-type DRG neurons in the presence of laminin**

Mouse DRG neurons were isolated from wild-type mice, cultured for 24hrs on PLL-laminin or PDL coated coverslips and were left untreated or were treated with 1 $\mu$ M calcimycin for 15min or 100 $\mu$ M SNAP for 1h, as indicated. A) Before fixation, cells were incubated with the cell permeable, photo-stable fluorescent indicator for intracellular NO-levels DAF-FM DA (5 $\mu$ M) for 1h. Then cells were fixed and stained for tubulin. Untreated wild-type DRG neurons showed basic NO-levels revealed by the very weak DAF-FM T fluorescent signal on both coatings. Calcimycin treatment led to an increase in NO production, independent of the coating. B) For the quantitative analysis, approximately 100 cells in each of 3 independent experiments were assessed for microtubule configuration. DRG neurons with one axon exhibiting features of retraction were considered as retracted. In untreated samples the amount of retracting neurons was in the range of 6 to 8%. After treatment with calcimycin or SNAP, wild-type

cultures showed 36% and 39% of retracted neurons, respectively. Error bars represent standard errors of the mean. Asterisks indicate that the values for cells treated with calcimycin or SNAP were significantly different from corresponding values of untreated cells and the values for cells treated with calcimycin or SNAP on PLL-laminin were significantly different from corresponding values of cells treated with calcimycin or SNAP on PDL (\*,  $p < 0.05$ ; \*\*,  $p < 0.005$ ).

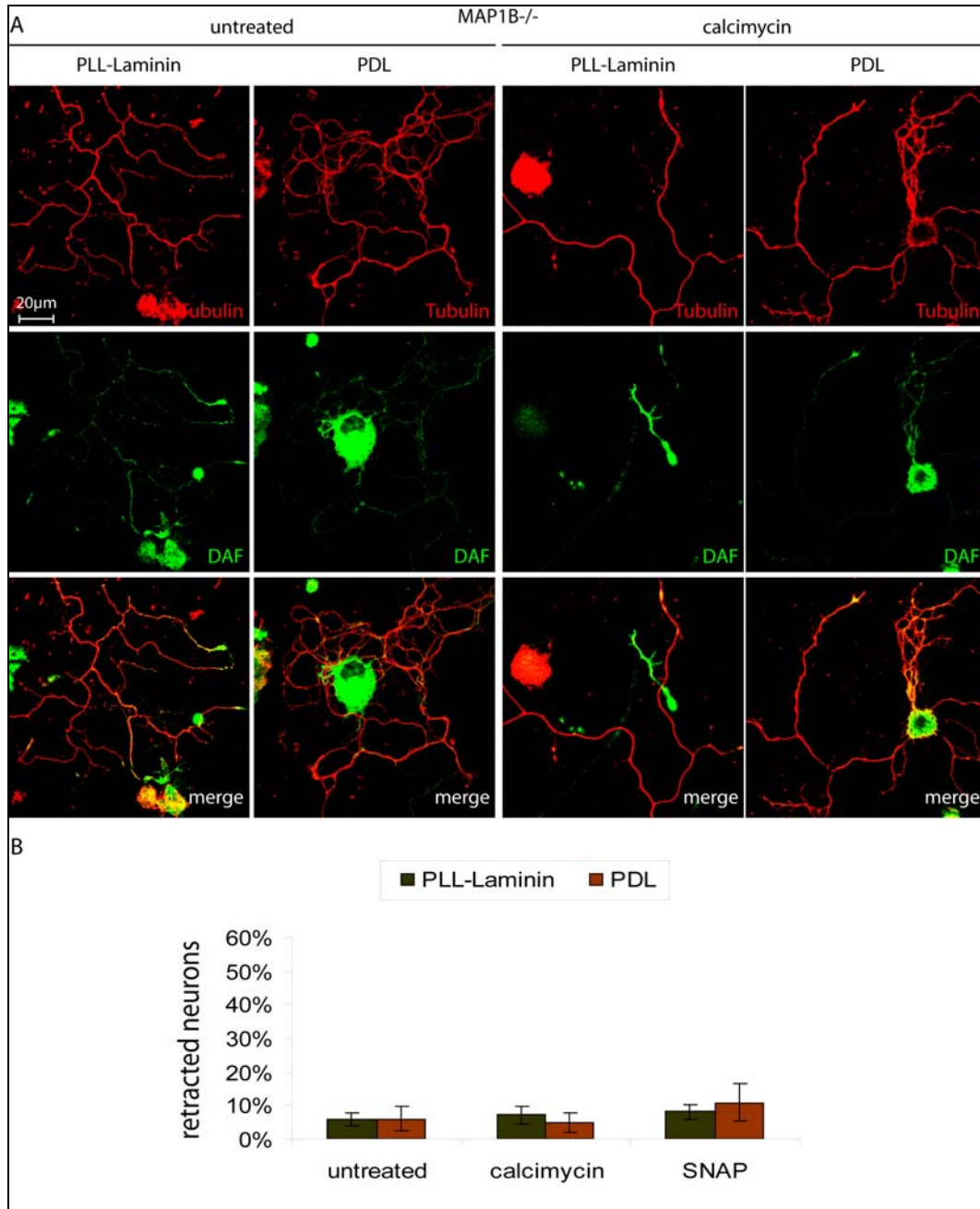


**Figure 12: Calcimycin and SNAP do not induce axon retraction in MAP1B<sup>-/-</sup> DRG neurons.**

Mouse DRG neurons were isolated from MAP1B<sup>-/-</sup> mice, cultured for 24hrs on PLL-laminin or PDL coated coverslips and were left untreated or were treated with 1 μM calcimycin for 15min or 100 μM SNAP for 1h, as indicated. A) Before fixation, cells were incubated with the cell permeable, photo-stable fluorescent indicator for intracellular NO-levels DAF-FM DA (5 μM) for 1h. Then cells were fixed and stained for tubulin. Untreated MAP1B<sup>-/-</sup> DRG neurons showed basic NO-levels revealed by the very weak

DAF-FM T fluorescent signal on both coatings, but calcimycin treatment did not lead to an increase in NO production. B) For the quantitative analysis, approximately 100 cells in each of 3 independent experiments were assessed for microtubule configuration. DRG neurons with one axon exhibiting features of retraction were considered as retracted. In untreated samples the amount of retracting neurons was in the range of 6 to 8%. After treatment with calcimycin or SNAP, MAP1B<sup>-/-</sup> cultures did not show an increased amount of retracted neurons. Error bars represent standard errors of the mean.

### **Netrin-1 induced retraction involves production of intracellular NO**

The repulsive netrin-1 signaling induced by the presence of laminin increases the intracellular cGMP concentration. This might require the activation of sGC which can be triggered by NO binding. In order to investigate whether NO production is involved in the repulsive netrin-1 signal transduction pathway, I visualized intracellular NO-levels with the fluorescent indicator DAF-FM DA. Wild-type and MAP1B<sup>-/-</sup> DRG neurons were cultured on PLL-laminin coated coverslips and incubated for 21hrs with netrin-1 and 1h with DAF-FM DA prior to fixation and staining for tubulin. Untreated cells showed a weak fluorescent signal in the cell body and some parts of their axons stemming from basal NO-levels in the cell (Figure 13). In contrast, after netrin-1 treatment, a striking increase in the strength of the fluorescent signal of DAF-FM T could be observed in wild-type and MAP1B<sup>-/-</sup> DRG neurons. The strongest signal and hence presumably the highest concentration of NO was seen in the collapsed growth cones of retracted axons. This might be observed because of the difference in the thickness of a growth cone compared to an axon. Nevertheless, this result suggests that the Ca<sup>2+</sup> influx induced by binding of netrin-1 to its receptors activates, among other enzymes, a nitric oxide synthase. However, up to now it remains elusive whether the activation of NOS leading to a visible increase of NO-levels is the main reason for eventual axon retraction or if NO is only a side product and nonrelevant for netrin-1 induced repulsion in the presence of laminin. In any case, the similarity between the responses of wild-type and MAP1B<sup>-/-</sup> DRG neurons to netrin-1 demonstrates that S-nitrosylation of MAP1B is not a necessary step in the repulsive netrin-1 signaling downstream of NOS activation even though it might occur in wild-type neurons.

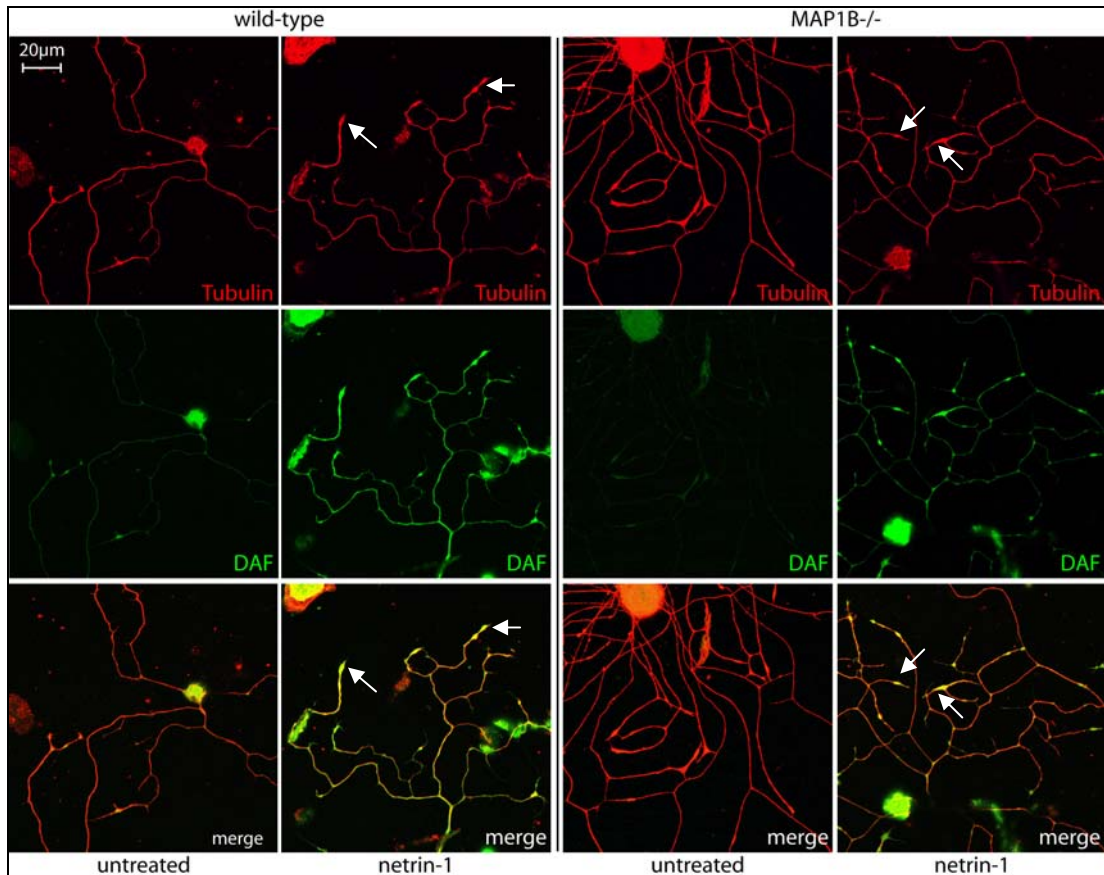


**Figure 13: NO production in netrin-treated wild-type and MAP1B<sup>-/-</sup> DRG neurons.**

Mouse DRG neurons were isolated from wild-type (left panel) and MAP1B<sup>-/-</sup> mice (right panel), cultured for 24hrs on PLL-laminin coated coverslips and were left untreated or were treated with 250ng/ml netrin-1 for 21hrs, as indicated. Before fixation, cells were incubated with the cell permeable, photo-stable fluorescent indicator for intracellular NO-levels DAF-FM DA (5µM) for 1h. Then cells were fixed and stained for tubulin. Untreated wild-type or MAP1B<sup>-/-</sup> DRG neurons showed basic NO-levels revealed by the very weak DAF-FM T fluorescent signal. In contrast, wild-type and MAP1B<sup>-/-</sup> DRG neurons which were treated with netrin-1 exhibited a strong fluorescent signal stemming from the reaction of DAF-FM DA with high levels of intracellular NO. Especially in the collapsed growth cones of treated neurons a strong signal was observed (white arrows).

#### **Inhibition of nNOS reduces netrin-1 induced axon retraction in wild-type DRG neurons**

Whether the increase of intracellular NO-levels is crucial for induction of axon retraction after netrin-1 treatment of DRG neurons on laminin can be investigated by inhibiting NOS and the subsequent NO production. Wild-type and MAP1B<sup>-/-</sup> DRG neurons were treated with 250ng/ml netrin-1 for 21hrs, with the specific nNOS inhibitor NPA at a concentration of 300µM for 21hrs or treated with netrin-1 in the presence of NPA for 21hrs. Figure 14 shows the percentage of retracted neurons after these

treatments. Incubation of wild-type and MAP1B<sup>-/-</sup> DRG neurons with NPA served as control and did not induce any retraction. Compared to the retraction in samples treated with netrin-1, a significant reduction was observed in samples treated with netrin-1 in the presence of NPA. This effect occurred in both wild-type and MAP1B<sup>-/-</sup> DRG neurons. The percentage of retracted wild-type DRG neurons was reduced from 34% to 19% and in MAP1B<sup>-/-</sup> DRG neurons it was reduced from 40% to 29%. Although the differences in percentages of retraction were significant in both genotypes, the effect of nNOS inhibition in MAP1B<sup>-/-</sup> DRG neurons (11% difference in percentage points) was less dramatic than in the case of wild-type neurons (14% difference in percentage points).

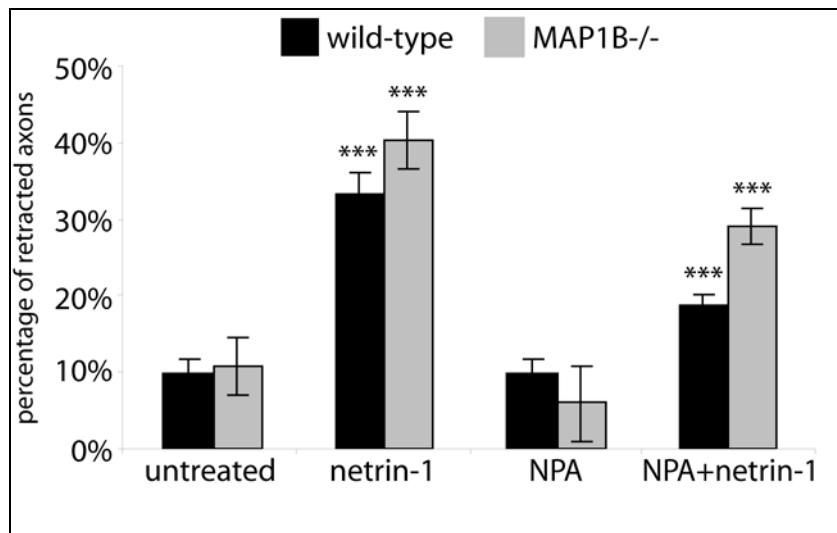


**Figure 14: Percentage of retracted wild-type and MAP1B<sup>-/-</sup> DRG neurons following treatment with netrin-1 and inhibition of nNOS with NPA.**

Mouse DRG neurons were isolated from wild-type and MAP1B<sup>-/-</sup> mice. Cells were cultured for 24hrs on PLL-laminin coated coverslips, were left untreated or were treated with 250ng/ml netrin-1 for 21hrs, with 300μM NPA for 21hrs, or with 250ng/ml netrin-1 in the presence of 300μM NPA for 21hrs, as indicated, fixed and stained for tubulin. For quantitative analysis, approximately 100 cells in each of 3 independent experiments were assessed for microtubule configuration. DRG neurons with one axon exhibiting features of retraction were considered as retracted. In untreated or NPA-treated samples the amount of retracting neurons was in the range of 6 to 11%. After netrin-1 treatment wild-type cultures showed 34% and MAP1B<sup>-/-</sup> DRG cultures showed 40% of retracted neurons. NPA treatment reduced the netrin-1-induced retraction to 19% in wild-type and to 29% in MAP1B<sup>-/-</sup> DRG neurons. Error bars represent standard errors of the mean. Asterisks indicate that the values for cells treated with netrin-1 were significantly different from corresponding values of untreated cells and the values for cells treated with netrin-1 in the presence of NPA were significantly different from corresponding values of cells treated with netrin-1 alone (\*\*\*,  $p < 0.001$ ).



In order to confirm the importance of NOS activation during repulsive netrin-1 signal transduction, I visualized NO production in neurons after these treatments. Figure 15 shows the level of intracellular NO in wild-type DRG neurons. In correlation with the determined percentage of retracted neurons, the NO-levels in untreated samples remained very low. In contrast, neurons treated with 250ng/ml netrin-1 for 21hrs showed again a strong fluorescent signal stemming from the reaction of DAF-FM DA with NO. Interestingly, in neurons treated with netrin-1 in the presence of 300 $\mu$ M NPA the fluorescent signal was observed only in growth cones but not along axons and was strikingly reduced. The level of intracellular NO after simultaneous treatment with netrin-1 and NPA was comparable to the NO level after NPA treatment alone. Although DRG neurons incubated with netrin-1 and NPA or NPA alone exhibit slightly higher NO-levels than untreated neurons, the NO production seemed to stay below the threshold concentration necessary to induce retraction. This result suggests that in wild-type DRG neurons repulsive netrin-1 signal transduction involves activation of nNOS and subsequent increase in NO-levels in the cells leading to axon retraction.

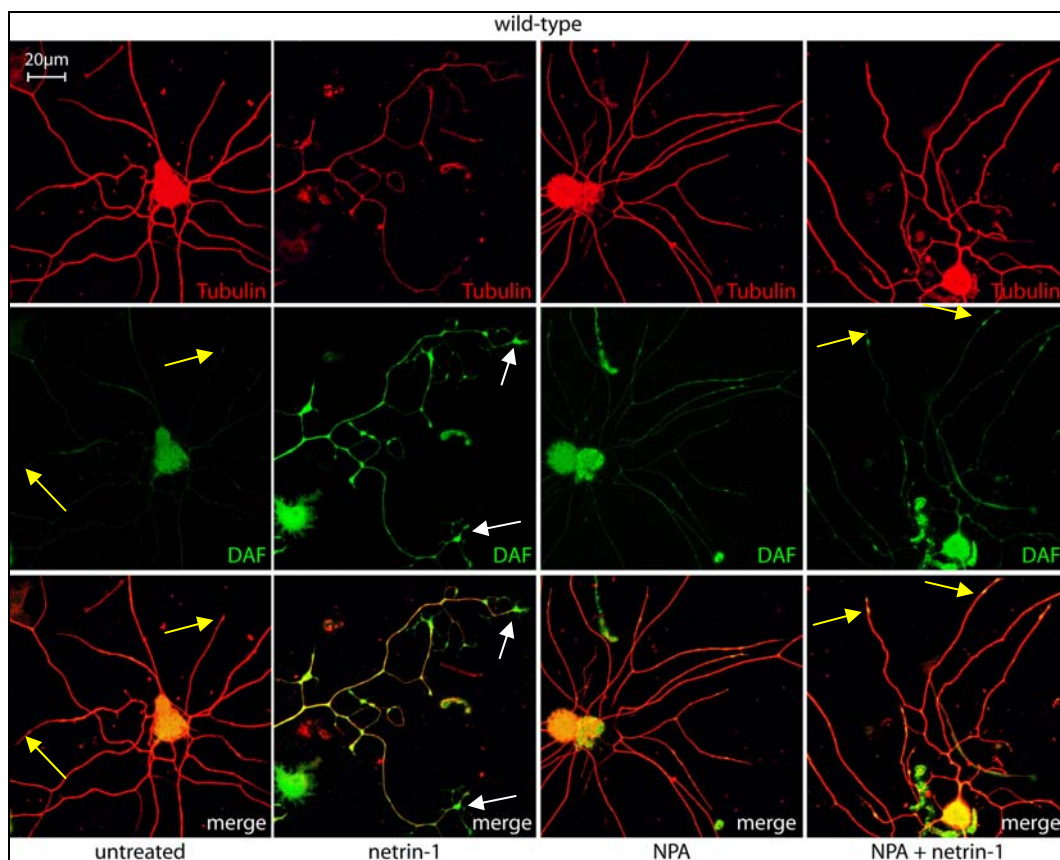


**Figure 15: NPA reduces NO production in wild-type DRG neurons during treatment with netrin-1.** DRG neurons were isolated from wild-type mice, cultured for 24hrs on PLL-laminin coated coverslips, were left untreated or were treated with 250ng/ml netrin-1 for 21hrs, with 300 $\mu$ M NPA for 21hrs, or with

250ng/ml netrin-1 in the presence of 300 $\mu$ M NPA for 21hrs, as indicated. Before fixation, cells were incubated with the cell permeable, photo-stable fluorescent indicator for intracellular NO-levels DAF-FM DA (5 $\mu$ M) for 1h. Then cells were fixed and stained for tubulin. Untreated and NPA treated wild-type DRG neurons showed basic NO-levels displayed by very weak DAF-FM T fluorescence. In contrast, DRG neurons which were treated with netrin-1 exhibited a strong fluorescent signal stemming from the reaction of DAF-FM DA with intracellular NO (white arrows). Neurons that were treated with 250ng/ml netrin-1 in the presence of 300 $\mu$ M NPA for 21hrs showed reduced levels of intracellular NO (yellow arrows) resembling those of neurons treated with NPA.

In contrast, in MAP1B<sup>-/-</sup> DRG neurons the intracellular NO level was not reduced as dramatically by the inhibition of nNOS as in wild-type neurons (Figure 16). A strong fluorescent signal was observed after netrin-1 treatment and this signal strength remained in the presence of NPA, especially in growth cones. This result correlated with the percentage of retracted neurons seen in figure 14 and it showed that nNOS is not the main producer of NO in the MAP1B<sup>-/-</sup> neurons after treatment with netrin-1 although it could play a role as NPA had an effect in preventing netrin-1 induced axon retraction, at least partially. However, the activation of a NOS enzyme was confirmed as NO production was switched on.



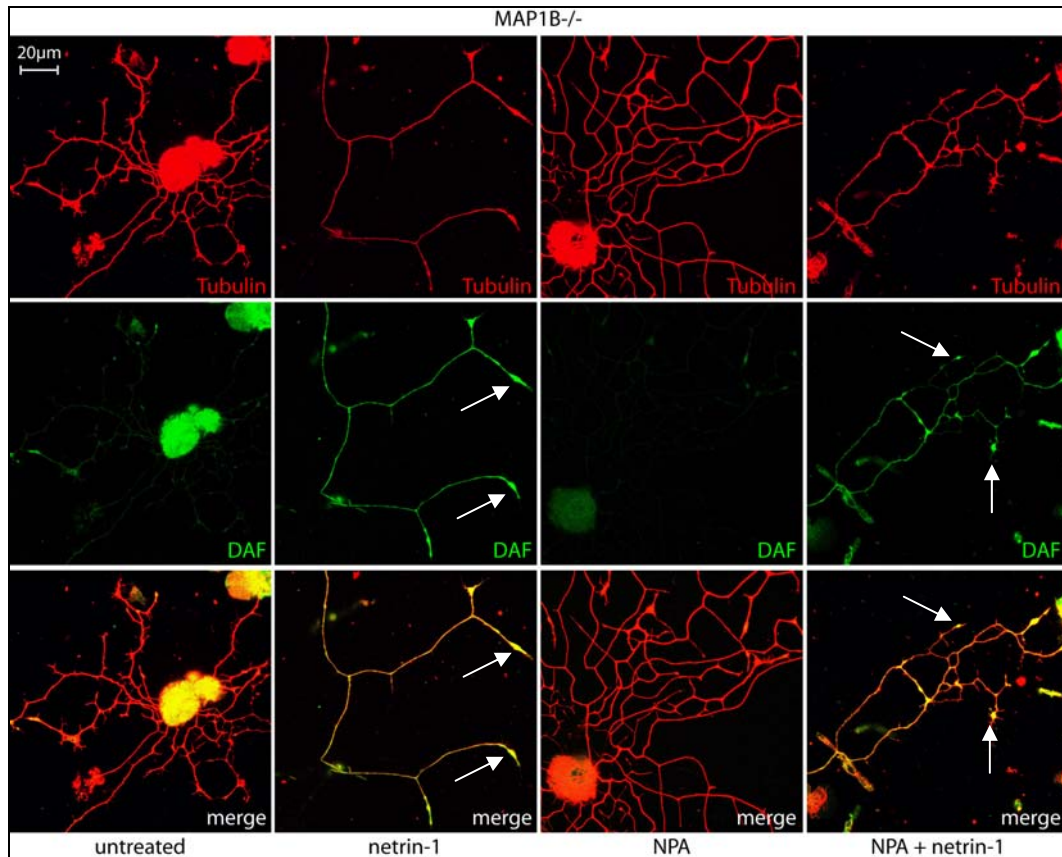


**Figure 16: NPA does not reduce NO production in MAP1B<sup>-/-</sup> DRG neurons during treatment with netrin-1.**

DRG neurons were isolated from MAP1B<sup>-/-</sup> mice, cultured for 24hrs on PLL-laminin coated coverslips, were left untreated or were treated with 250ng/ml netrin-1 for 21hrs, with 300μM NPA for 21hrs, or with 250ng/ml netrin-1 in the presence of 300μM NPA for 21hrs, as indicated. Before fixation, cells were incubated with the cell permeable, photo-stable fluorescent indicator for intracellular NO DAF-FM DA (5μM) for 1h. Then cells were fixed and stained for tubulin. Untreated and NPA treated MAP1B<sup>-/-</sup> DRG neurons showed basic NO-levels revealed by very weak DAF-FM DA fluorescence. In contrast, DRG neurons which were treated with netrin-1 exhibited a strong fluorescent signal indicative of increased intracellular NO-levels. Neurons that were treated with 250ng/ml netrin-1 in the presence of 300μM NPA for 21hrs showed only weak reduction of intracellular NO-levels compared to cells treated with netrin-1 only. Strong fluorescence could be seen most notably in the growth cones (white arrows) but also along axons.

**nNOS and eNOS expression and localization in wild-type and MAP1B<sup>-/-</sup> DRG neurons**

In order to determine why nNOS inhibition is less effective in prevention of netrin-1 induced axon retraction in MAP1B<sup>-/-</sup> DRG neurons than in wild-type neurons, I performed immunofluorescence and immunoblotting assays to detect and localize nNOS in wild-type and MAP1B<sup>-/-</sup> DRG neurons. Figure 17A shows the stainings of untreated DRG neurons for nNOS, actin and tubulin. In wild-type DRG neurons nNOS localized to the cell body, to axons and partially to growth cones, whereas in MAP1B<sup>-/-</sup> DRG neurons the expression of nNOS was strongly reduced. Only a faint staining in the cell body and in primary axons was observed. This difference in the expression level of nNOS between wild-type and MAP1B<sup>-/-</sup> DRG neurons was seen in four independent experiments. Other NOS enzymes probably being activated by netrin-1 are endothelial and inducible NOS. Since iNOS plays a role predominantly in immune and cardiovascular systems and its activation is not calcium dependent, the expression of eNOS was investigated in DRG neurons. As far as it can be deduced from immunofluorescence analyses, wild-type and MAP1B<sup>-/-</sup> DRG neurons exhibited the same expression pattern of eNOS (Figure 17B). In both cell types, the enzyme was localized in the cell bodies, along axons, where it co-localized with tubulin, and sometimes in growth cones, where it co-localized with actin. Although the expression level seemed to be lower than for nNOS, this cannot be ascertained since different antibodies were used to detect the respective enzyme.

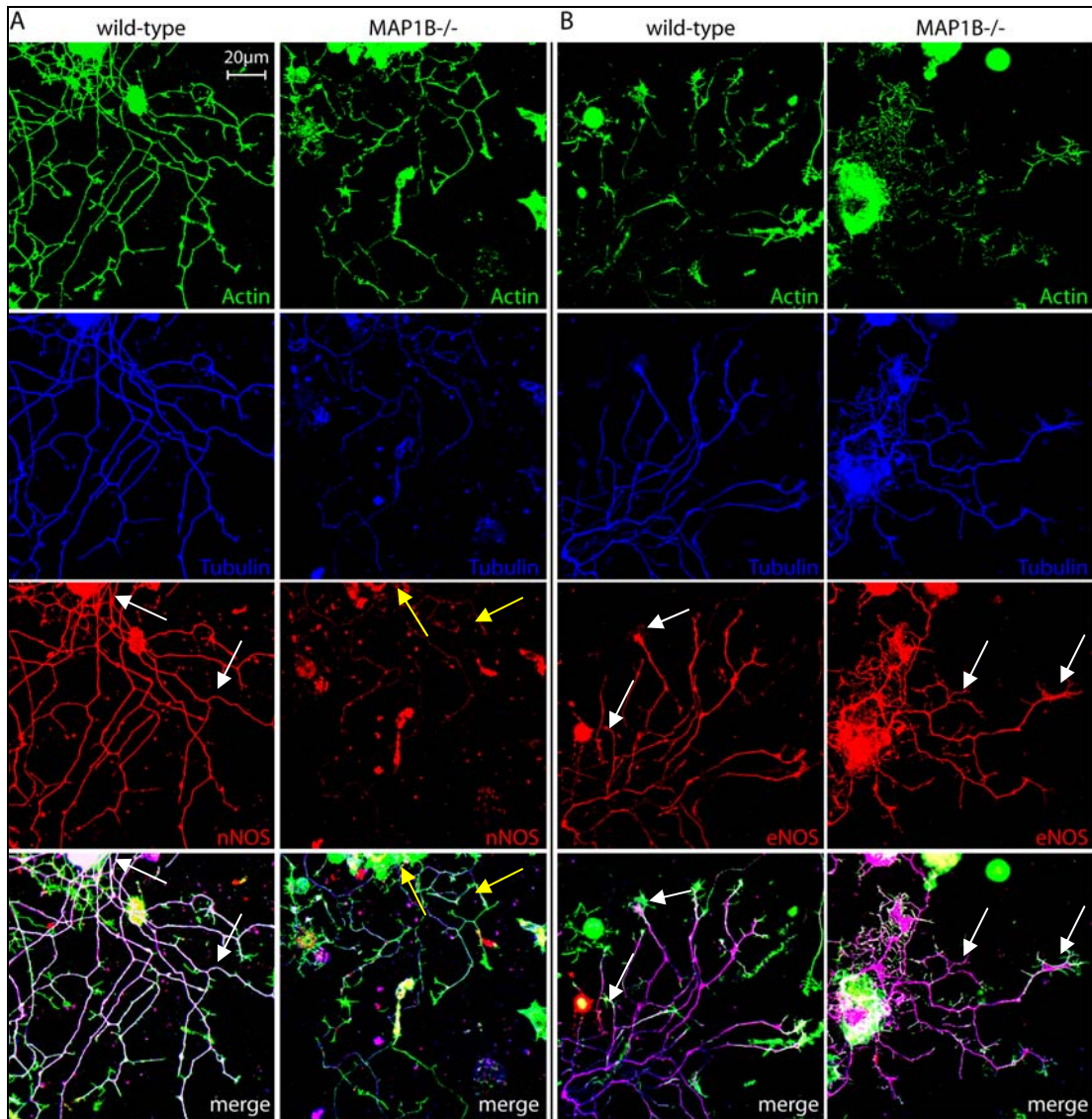


**Figure 17: Expression and localization of nNOS and eNOS in untreated DRG neurons of wild-type and MAP1B<sup>-/-</sup> mice.**

Mouse DRG neurons were isolated from wild-type and MAP1B<sup>-/-</sup> mice. Neurons were cultured for 24hrs on PLL-laminin coated coverslips, fixed and stained for tubulin, actin and nNOS (A) or eNOS (B). Wild-type DRG neurons expressed nNOS mainly in their cell bodies and in the axons where it co-localized with tubulin (white arrows). In the growth cones nNOS was found only sporadically. MAP1B<sup>-/-</sup> DRG neurons exhibited a much lower expression level of nNOS. Only a weak staining was observed in the cell body and the axons (yellow arrows). In contrast, eNOS was expressed at similar levels in wild-type and MAP1B<sup>-/-</sup> DRG neurons (white arrows). It co-localized with tubulin in the cell body and in axons and was also found in the growth cones.

The reduced nNOS expression in MAP1B<sup>-/-</sup> mice could also be confirmed by immunoblot assays (Figure 18). Dorsal root ganglia lysates and total brain lysates of adult or newborn wild-type and MAP1B<sup>-/-</sup> mice were examined. Actin or tubulin served as loading control. nNOS expression was almost not detectable in MAP1B<sup>-/-</sup> DRGs compared to wild-type DRGs and only very weak signals were obtained in extracts from brains of newborn or adult mice. In contrast, nNOS showed a relatively strong expression in wild-type brains, independent of the age of the mice. Concerning eNOS, the expression level was very low in all tissues that were investigated but no big difference could be observed between wild-type and MAP1B<sup>-/-</sup> mice.

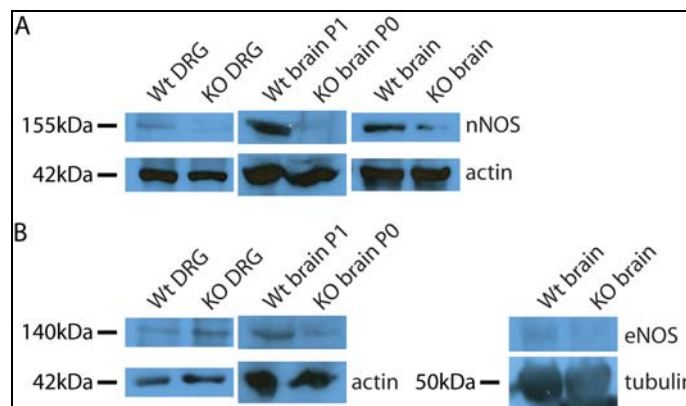


**Figure 18: Immunoblot analyses of wild-type and MAP1B<sup>-/-</sup> DRGs and brains of adult and newborn mice for nNOS and eNOS.**

Wild-type and MAP1B<sup>-/-</sup> lysates were prepared from DRGs and from brains of adult and newborn mice and loaded on a 10% PAA gel for detection of nNOS and eNOS. Actin or tubulin was used as loading control. (A) Immunoblotting showed that the expression of nNOS is strongly reduced in MAP1B<sup>-/-</sup> DRGs and brains compared to lysates of wild-type mice. In contrast, although weakly expressed, eNOS shows similar expression levels in both genotypes, independent of the tissue examined (B).

nNOS and NO production were shown to play an important role in the repulsive effect of netrin-1 on wild-type DRG neurons. Next I checked whether nNOS changes its localization upon activation during netrin-1 treatment. As the strongest fluorescent signal stemming from NO production was observed in the growth cone of retracting DRG neurons, one could expect nNOS to relocate from the cell body and axons of DRG neurons to their growth cones, at least partially. Therefore, wild-type DRG neurons were cultured as usual, treated with 250ng/ml netrin-1 or with netrin-1 in the presence of 300μM NPA for 21hrs, stained for tubulin, actin and nNOS and were compared to untreated neurons (Figure 19). When neurons were left untreated or treated with NPA, nNOS was almost never found in the growth cones of axons, only along

axons themselves. In contrast, when DRG neurons were incubated with netrin-1, nNOS was found more often in growth cones, although the relocation of nNOS did not occur in all examined cells. Additionally, in certain neurons a stronger fluorescent signal for nNOS was observed. Unfortunately, it was not feasible to perform immunoblot analysis of cultured DRG neurons because the yield of protein was too low to detect nNOS. The expression and localization of eNOS was also tested in wild-type DRG neurons but did not show any difference induced by netrin-1 treatment (data not shown).



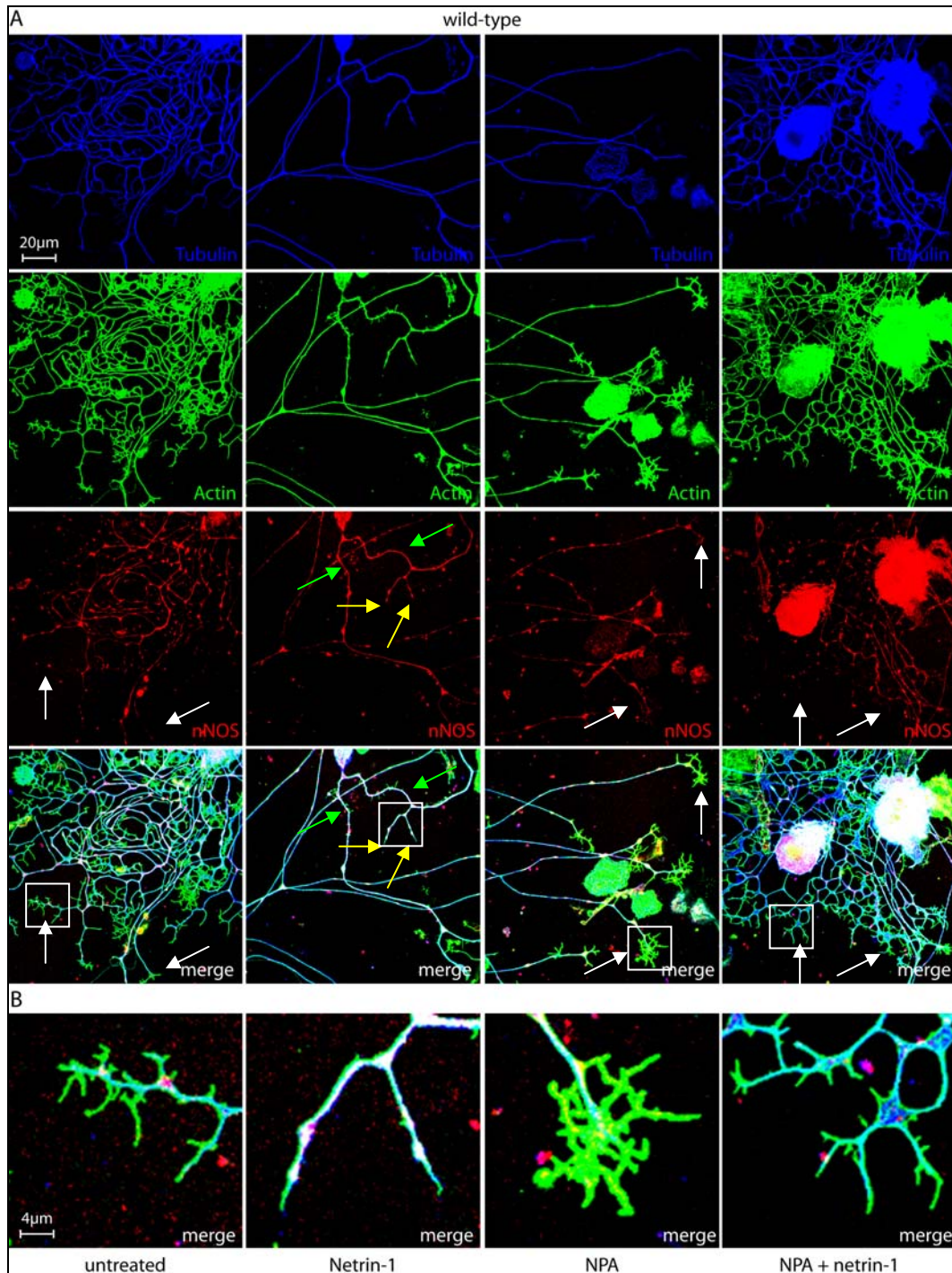


**Figure 19: Expression and localization of nNOS in wild-type DRG neurons after treatment with netrin-1 and/or NPA.**

Mouse DRG neurons were isolated from wild-type mice, were cultured for 24hrs on PLL-laminin coated coverslips, were left untreated, or were treated with 250ng/ml netrin-1 for 21hrs, with 300µM NPA for 21hrs, or with 250ng/ml netrin-1 in the presence of 300µM NPA for 21hrs, as indicated. Neurons were then fixed and stained for tubulin, actin and nNOS. A) Upon treatment with netrin-1, a fraction of wild-type DRG neurons showed a slight increase in nNOS fluorescent signal (green arrows). This could not be observed after NPA treatment or NPA + netrin-1 treatment, as far as it could be stated after immunofluorescences analysis. Additionally, a change in nNOS localization to the growth cones of DRG neurons occurred after treatment with netrin-1 (yellow arrows) which could not be observed without

treatment or after treatment with netrin-1 in the presence of NPA (white arrows). White boxes indicate the area shown at higher magnification in the lowest panel (B).

### Inhibition of eNOS reduces netrin-1 induced retraction in MAP1B<sup>-/-</sup> DRG neurons

In MAP1B<sup>-/-</sup> DRG neurons nNOS expression was shown to be lower than in wild-type DRG neurons and inhibition of nNOS with NPA did not have the same strong effect in inhibiting netrin-1 induced retraction of axons. In contrast, eNOS was shown to be expressed at a similar level as in wild-type cells. Thus, the next step in the investigation of signaling molecules downstream of netrin-1 in MAP1B<sup>-/-</sup> neurons was to inhibit eNOS specifically during incubation with netrin-1. The specific inhibitor for eNOS is L-NIO which was used at a concentration of 10 $\mu$ M. The graph in Figure 20 shows the reaction of wild-type and MAP1B<sup>-/-</sup> DRG neurons to netrin-1 treatment in the presence of L-NIO. L-NIO itself led to a relatively high percentage of retraction, but it was still far below the percentage of retracted cells after netrin-1 treatment. Simultaneous incubation of DRG neurons with netrin-1 and L-NIO did almost not affect the reaction of wild-type DRG neurons to netrin-1; the percentage of retracted neurons remained at 28%. In MAP1B<sup>-/-</sup> DRG neurons, L-NIO had a much stronger effect on the retraction. L-NIO reduced the amount of retracted neurons significantly by 26 percentage points to 14%. This result suggests that eNOS activity is not essential for repulsive netrin-1 signaling in wild-type DRG neurons but might play an important role in MAP1B<sup>-/-</sup> DRG neurons, in contrast to nNOS.

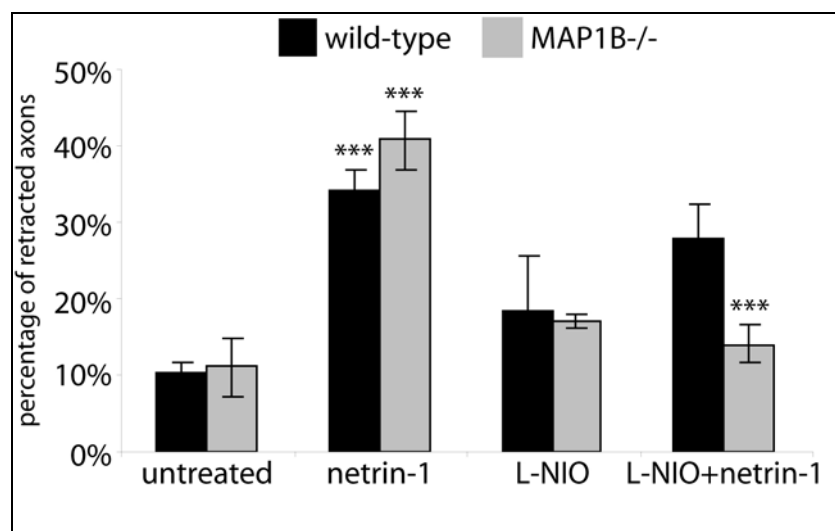


**Figure 20: L-NIO reduces netrin-1 induced retraction in MAP1B<sup>-/-</sup> DRG neurons.**

Mouse DRG neurons were isolated from wild-type and MAP1B<sup>-/-</sup> mice. Cells were cultured for 24hrs on PLL-laminin coated coverslips, were left untreated or were treated with 250ng/ml netrin-1 for 21hrs, with 10μM L-NIO for 21hrs, or with 250ng/ml netrin-1 in the presence of 10μM L-NIO for 21hrs, as indicated, fixed, and stained for tubulin. For quantitative analysis, approximately 100 cells in each of 3 independent experiments were assessed for microtubule configuration. DRG neurons with one axon exhibiting features of retraction were considered as retracted. In untreated samples the amount of retracting neurons was in the range of 10 to 11%. After L-NIO treatment, the percentage of retracted neurons reached 17 to 19%. After netrin-1 treatment, wild-type cultures showed 34% and MAP1B<sup>-/-</sup> DRG cultures showed 40% of retracted neurons. L-NIO treatment reduced the netrin-1-induced retraction to 28% in wild-type and to 14% in MAP1B<sup>-/-</sup> DRG neurons. Error bars represent standard error of the mean. Asterisks indicate that the values for cells treated with netrin-1 were significantly different from corresponding values of untreated cells and that the values for cells treated with netrin-1 in the presence of L-NIO were significantly different from corresponding values of cells treated with netrin-1 only (\*\*\*, p<0.001).

Seeing that NO production by eNOS might not play a role in induction of retraction by netrin-1 in wild-type DRG neurons, the inhibition of eNOS should not lead to reduced intracellular NO-levels after netrin-1 treatment in these cells. In order to confirm this hypothesis, DRG neurons of wild-type mice were cultured and treated as before and stained for tubulin. Additionally, the NO-levels were visualized with DAF-FM DA. Incubation of wild-type DRG neurons with L-NIO led to a weak increase of NO production in axons. Moreover, inhibition of eNOS was not efficient in reducing netrin-1 induced NO production. A strong increase in DAF-FM T signal could be observed after incubation with netrin-1 and L-NIO which was comparable to the NO-levels after treatment with netrin-1 alone (Figure 21).



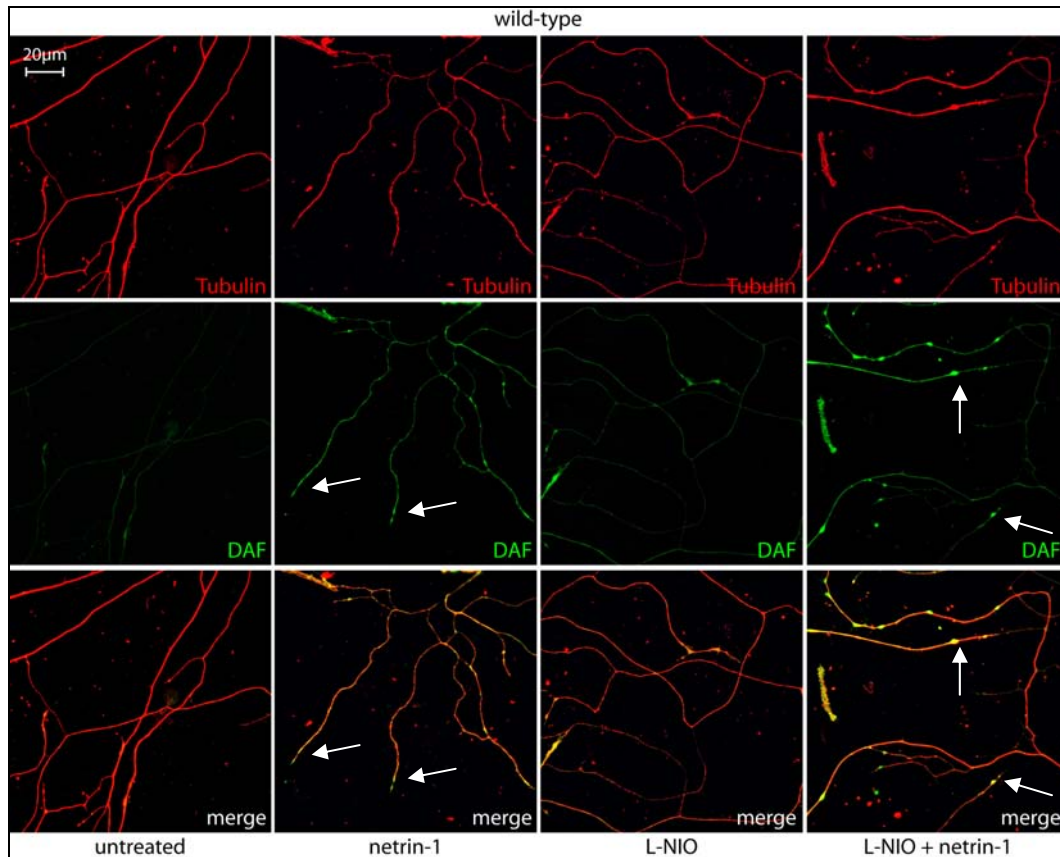


**Figure 21: NO production in wild-type DRG neurons after treatment with netrin-1 and L-NIO.**

DRG neurons were isolated from wild-type mice, cultured for 24hrs on PLL-laminin coated coverslips, were left untreated or were treated with 250ng/ml netrin-1 for 21hrs, with 10µM L-NIO for 21hrs, or with 250ng/ml netrin-1 in the presence of 10µM L-NIO for 21hrs, as indicated. Before fixation, cells were incubated with the cell permeable, photo-stable fluorescent indicator for intracellular NO-levels DAF-FM DA (5µM) for 1h. Then cells were fixed and stained for tubulin. Untreated and L-NIO treated wild-type DRG neurons showed basic NO-levels as revealed by very weak DAF-FM DA fluorescence. In contrast, DRG neurons which were treated with netrin-1 exhibited a strong fluorescent signal stemming from the reaction of DAF-FM DA with intracellular NO. Neurons that were treated with 250ng/ml netrin-1 in the presence of 10µM L-NIO for 21hrs showed intracellular NO-levels comparable to neurons treated with netrin-1 only. Strong fluorescence could be seen most notably in the growth cones showing retraction or collapse (white arrows).

In contrast to wild-type DRG neurons, the NO production of MAP1B<sup>-/-</sup> DRG neurons during netrin-1 treatment could be impeded successfully by L-NIO. Compared to netrin-1 treated cells, the fluorescent signal of neurons treated with netrin-1 and L-NIO was reduced dramatically (Figure 22). This correlates with the percentage of retraction assessed in Figure 20 and confirms the idea that eNOS seems to be more important for MAP1B<sup>-/-</sup> DRG neurons reacting to the repulsive netrin-1 signal than for wild-type neurons.

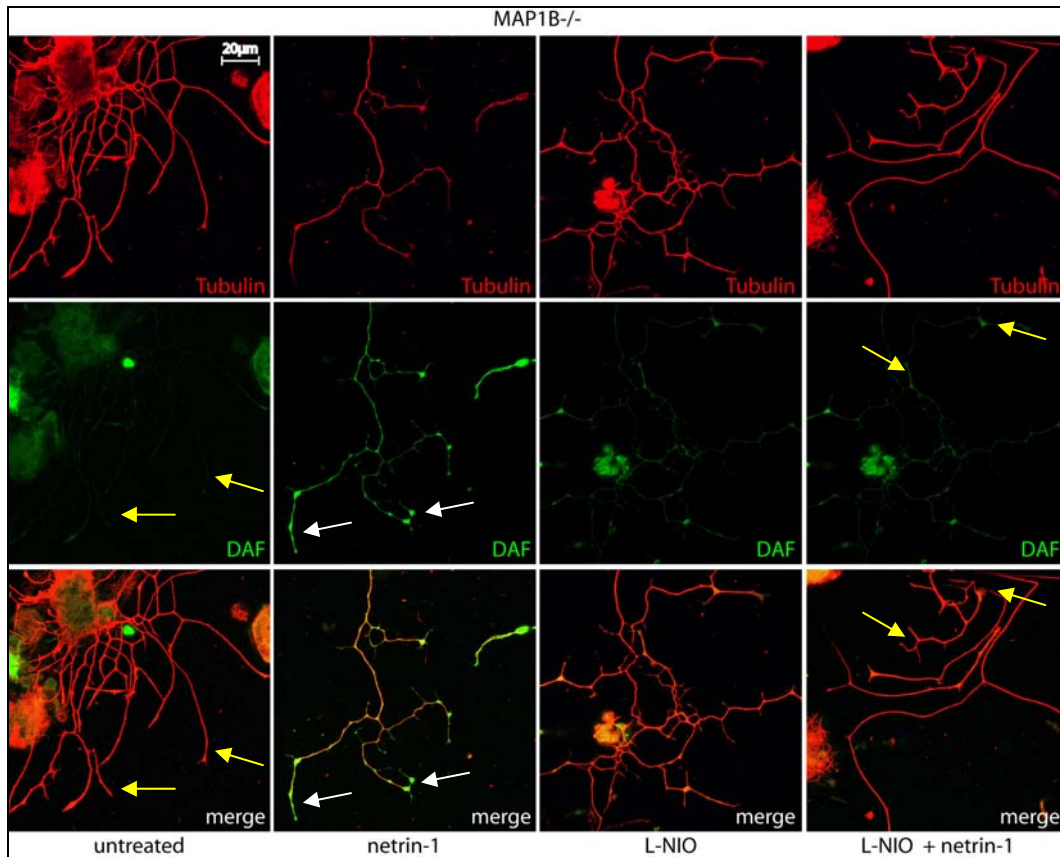


**Figure 22: NO production in MAP1B<sup>-/-</sup> DRG neurons after treatment with netrin-1 and L-NIO.**

DRG neurons were isolated from MAP1B<sup>-/-</sup> mice, cultured for 24hrs on PLL-laminin coated coverslips, were left untreated or were treated with 250ng/ml netrin-1 for 21hrs, with 10µM L-NIO for 21hrs, or with 250ng/ml netrin-1 in the presence of 10µM L-NIO for 21hrs, as indicated. Before fixation, cells were incubated with the cell permeable, photo-stable fluorescent indicator for intracellular NO-levels DAF-FM DA (5µM) for 1h. Then cells were fixed and stained for tubulin. Untreated and L-NIO treated MAP1B<sup>-/-</sup> DRG neurons showed basic NO-levels as revealed by very weak DAF-FM T fluorescence. In contrast, DRG neurons which were treated with netrin-1 exhibited a strong fluorescent signal stemming from the reaction of DAF-FM DA with intracellular NO (white arrows). Presence of L-NIO during netrin-1 treatment inhibited NO production and led to NO-levels comparable to untreated neurons (yellow arrows).

Binding of netrin-1 to its receptor was suggested to have an influence on the localization and activity of nNOS in wild-type DRG neurons. Since in MAP1B<sup>-/-</sup> DRG neurons eNOS seems to be more important, the question arose whether the localization of eNOS changes as well upon netrin-1 signaling. Therefore MAP1B<sup>-/-</sup> DRG neurons were cultured as usual, treated with 250ng/ml netrin-1, or with netrin-1 in the presence of 10µM L-NIO for 21hrs, stained for tubulin, actin and eNOS and the localization and expression levels of the enzyme in treated cells was compared to the one in untreated neurons (Figure 23). Only a small number of DRG neurons showed relocation of

eNOS following the netrin-1 treatment. However, no change in localization could be observed in untreated samples compared to DRG neurons treated with netrin-1, L-NIO or both. In these samples, some growth cones were found to show an eNOS signal.

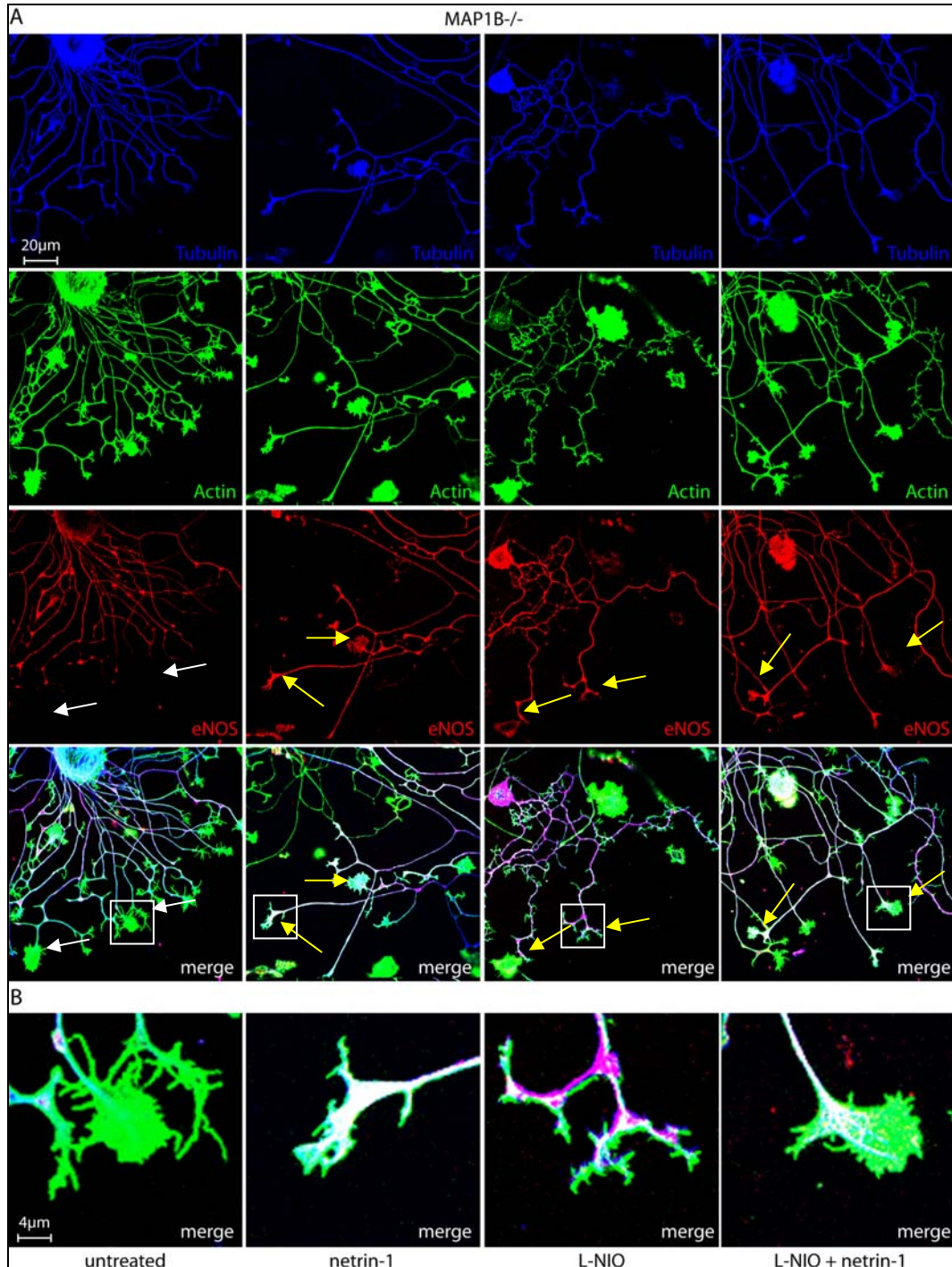


**Figure 23: Localization of eNOS in MAP1B<sup>-/-</sup> DRG neurons after treatment with netrin-1 and L-NIO.**

Mouse DRG neurons were isolated from MAP1B<sup>-/-</sup> mice, were cultured for 24hrs on PLL-laminin coated coverslips, were left untreated or were treated with 250ng/ml netrin-1 for 21hrs, with 10µM L-NIO for 21hrs, or with 250ng/ml netrin-1 in the presence of 10µM L-NIO for 21hrs, as indicated, fixed and

stained for tubulin, actin and eNOS. In untreated neurons, eNOS was predominantly found in the cell body and along axons but not in growth cones (white arrows), whereas after netrin-1 and/or L-NIO treatment, eNOS staining revealed a partial relocalization of eNOS to growth cones (yellow arrows). White boxes indicate the area shown at higher magnification in the lowest panel (B).

### **Soluble guanylyl cyclase as downstream target of netrin-1 induced NO synthesis**

There are two possible signaling mechanisms that might be initiated by NO production: first, S-nitrosylation of proteins and second, activation of soluble guanylyl cyclase (sGC) by binding of NO. MAP1B was shown not to be necessary for the repulsive netrin-1 signaling pathway; therefore, its nitrosylation might not be essential either. Other potential targets of protein S-nitrosylation have not been investigated due to the impossibility of a biotin switch on DRG neurons which do not provide enough material for this assay. Whether sGC is activated during the process of netrin-1 induced repulsion was tested by inhibiting the enzyme with its specific inhibitor LY83583. Another more prominent inhibitor of sGC, ODQ, was already tested by a former PhD student and was found to induce retraction on its own (Trancikova, PhD Thesis 2007). Due to this result, I performed experiments where I inhibited sGC specifically with LY83583. DRG neurons of wild-type and MAP1B<sup>-/-</sup> mice were grown on PLL-laminin coated coverslips, left untreated or were treated with 250ng/ml netrin-1, or with netrin-1 in the presence of 1μM LY83583. LY83583 *per se* caused a significantly high percentage of wild-type DRG neurons to retract (Figure 24). It has also been observed for ODQ that the inhibition of sGC did not have this strong effect in MAP1B<sup>-/-</sup> DRG neurons. They exhibited an insignificant increase in retraction by 7%. When applied additionally to netrin-1 treated DRG neurons, LY83583 even increased the amount of retracted axons. This effect could be observed in both wild-type and MAP1B<sup>-/-</sup> DRG neurons.

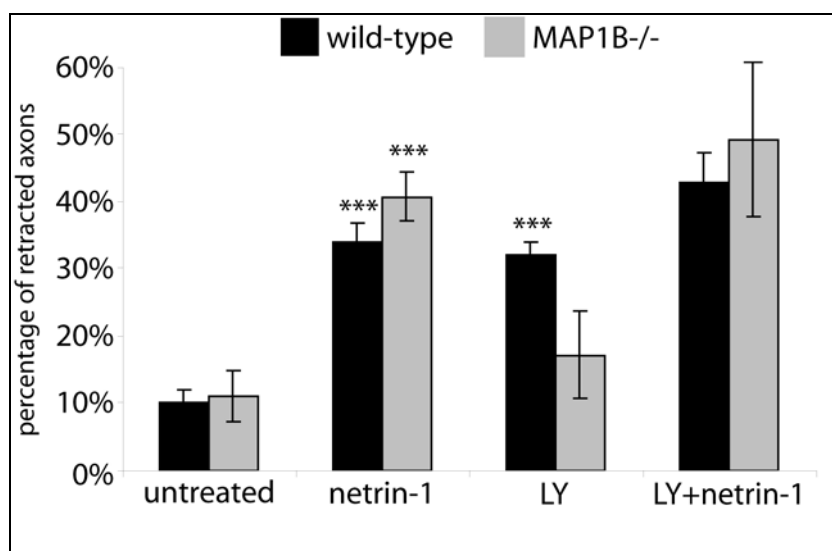


**Figure 24: LY induces axon retraction in wild-type DRG neurons.**

Mouse DRG neurons were isolated from wild-type and MAP1B<sup>-/-</sup> mice. Cells were cultured for 24hrs on PLL-laminin coated coverslips, were left untreated or were treated with 250ng/ml netrin-1 for 21hrs, with 1μM LY83583 for 21hrs (LY), or with 250ng/ml netrin-1 in the presence of 1μM LY83583 for 21hrs, as indicated, fixed and stained for tubulin. For quantitative analysis, approximately 100 cells in each of 2 independent experiments were assessed for microtubule configuration. DRG neurons with one axon exhibiting features of retraction were considered as retracted. In untreated treated samples the amount of retracting neurons was in the range of 10 to 11%. After netrin-1 treatment, wild-type cultures showed 34% and MAP1B<sup>-/-</sup> DRG cultures showed 40% of retracted neurons. After LY83583 treatment, the percentage of retracted wild-type neurons was 32% and the percentage of retracted MAP1B<sup>-/-</sup> DRG neurons was 17%. LY83583 treatment increased the netrin-1-induced retraction to 43% in wild-type and to 49% in MAP1B<sup>-/-</sup> DRG neurons. Error bars represent standard errors of the mean. Asterisks indicate that the values for cells treated with netrin-1 or LY83583 were significantly different from corresponding values of untreated cells (\*\*\*,  $p < 0.001$ ).

Direct comparison of the levels of retraction induced by treatment with 1μM LY83583 for 1h or with 10μM ODQ for 30min confirmed the previous results of Trancikova, PhD Thesis 2007, especially in wild-type DRG cultures. In these neurons both inhibitors of sGC led to a significant increase in the percentage of retracted cells compared to retraction observed in untreated samples, although the incubation time was reduced dramatically from 21hrs to 1h. Moreover, the experiments showed that MAP1B<sup>-/-</sup> DRG neurons did not respond as wild-type DRG neurons to inhibition of the cGMP pathway, no matter which inhibitor was used (Figure 25). The possible explanation for the retraction induced by inhibition of sGC lies in a negative feedback mechanism in which cGMP dependent protein kinase, PKG, plays an essential role. After the production of cGMP due to activation of sGC by NO, PKG becomes



activated. One target of PKG is nNOS, which is phosphorylated by the kinase on a specific cysteine resulting in the inactivation of nNOS<sup>5</sup>. This mechanism assures that nNOS is not capable of producing excessive amounts of NO which could be toxic to the cell. It is also important to be capable of switching off a signal in order to respond to another one. With the inhibition of sGC by ODQ or LY83583, this negative feedback mechanism is shut down, thus, nNOS is not inactivated by phosphorylation by PKG and produces continuously NO, probably resulting in axon retraction. This hypothesis also explains the weak response in MAP1B<sup>-/-</sup> DRG neurons which were shown to lack nNOS at least partially. Moreover, MAP1B<sup>-/-</sup> DRG neurons do not respond to the NO-donor SNAP either<sup>1</sup>, thus, it might be the lack of MAP1B which led to this result. However, in order to substantiate this theory, the simultaneous inhibition of nNOS during treatment with either ODQ or LY83583 should prevent axon retraction. Indeed, the presence of NPA during treatment of wild-type DRG neurons with the sGC inhibitors caused a significant reduction in levels of retracted neurons. The percentage of retracted neurons following treatment with LY83583 or ODQ in the presence of NPA was reduced by 25 percentage points (Figure 25). These results show that short time incubation of wild-type DRG neurons with inhibitors of sGC led to retraction as it was the case for long time incubation. Moreover, the feedback mechanism involving PKG activation by cGMP resulting in nNOS inactivation was confirmed.

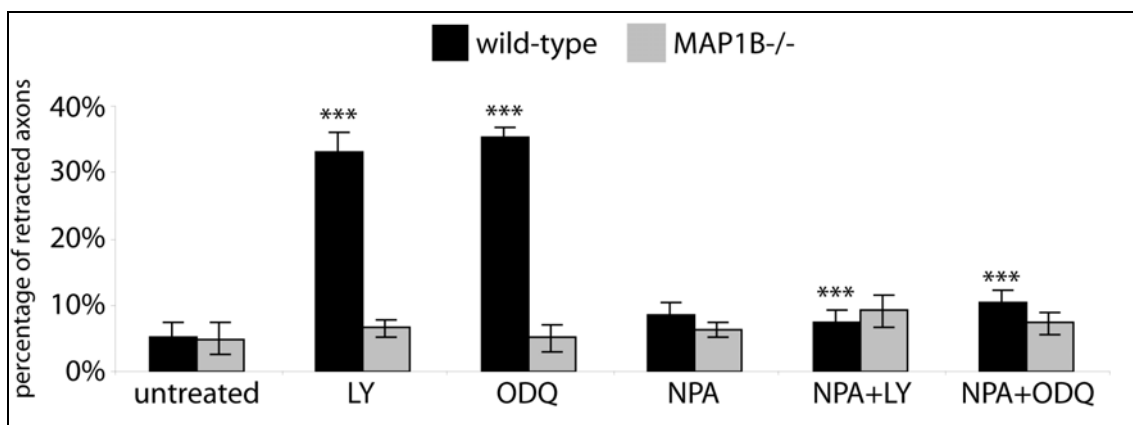


**Figure 25: Percentage of retracted DRG neurons after treatment with LY, ODQ and NPA.**

Mouse DRG neurons were isolated from wild-type and MAP1B<sup>-/-</sup> mice. Cells were cultured for 24hrs on PLL-laminin coated coverslips, were left untreated or were treated with 1 $\mu$ M LY83583 for 1h, with 10 $\mu$ M ODQ for 30min, with 300 $\mu$ M NPA for 1h, or with 1 $\mu$ M LY83583 in the presence of 300 $\mu$ M NPA for 1h, or with 10 $\mu$ M ODQ in the presence of 300 $\mu$ M NPA, as indicated, fixed and stained for tubulin. For quantitative analysis, approximately 100 cells in each of 3 or more independent experiments were assessed for microtubule configuration. DRG neurons with one axon exhibiting features of retraction were considered as retracted. In untreated samples the amount of retracting neurons was in the range of

4%. Treatment with LY83583 or ODQ resulted in wild-type cultures to 33% and 35% of retracted neurons, respectively. In MAP1B<sup>-/-</sup> DRG cultures, LY83583 did not have such a striking effect, only 7% of the neurons were retracted. MAP1B<sup>-/-</sup> DRG neurons did not react to ODQ treatment; the amount of retracted neurons was similar to untreated samples (5%). In wild-type DRG neurons, the presence of NPA during treatment with LY83583 or ODQ prevented retraction of neurons significantly. The percentage of retraction induced by LY83583 or ODQ was reduced by NPA by 25 percentage points. Error bars represent standard errors of the mean. Asterisks indicate that the values for cells treated with LY83583 or ODQ were significantly different from corresponding values of untreated cells and that the values for cells treated with LY83583 or ODQ in the presence of NPA were significantly different from corresponding values of cells treated with LY83583 or ODQ only (\*\*\*,  $p < 0.001$ ).

When the negative feedback mechanism via PKG is disabled due to inhibition of sGC, the levels of intracellular NO should increase. Indeed, the amount of retracted DRG neurons after inhibition of sGC correlated with the observed increase in intracellular NO-levels visualized with DAF-FM DA. Wild-type DRG neurons were cultured on PLL-laminin coated coverslips and treated as before with 1  $\mu$ M LY83583 for 1h or with LY83583 in the presence of 300  $\mu$ M NPA (Figure 26). The same assay was performed with the sGC inhibitor ODQ in presence or not of NPA (Figure 27). Both experiments showed a clear increase in fluorescence stemming from reaction of DAF-FM DA with intracellular NO after inhibition of sGC, no matter which sGC inhibitor was used. Apparently, inhibition of sGC ruptured the signal cascade which is negatively regulating nNOS activity. Therefore, nNOS was still capable of synthesizing NO, but in the presence of NPA the levels of intracellular NO production were reduced drastically.

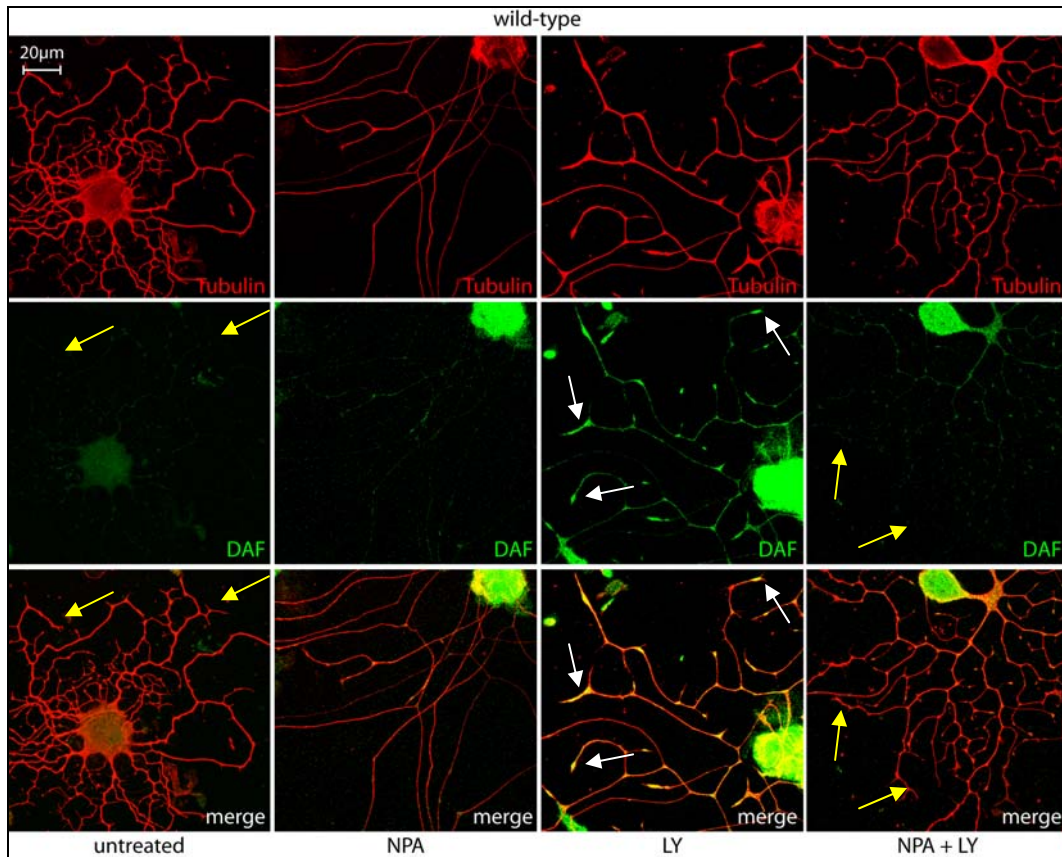


**Figure 26: NO production in wild-type DRG neurons after treatment with LY83583 and NPA.**

DRG neurons were isolated from wild-type mice, cultured for 24hrs on PLL-laminin coated coverslips, were left untreated or were treated with 1µM LY83583 for 1h, with 300µM NPA for 1h or with 1µM LY83583 in the presence of 300µM NPA for 1h, as indicated. Before fixation, cells were incubated with the cell permeable, photo-stable fluorescent indicator for intracellular NO-levels DAF-FM DA (5µM) for 1h. Then cells were fixed and stained for tubulin. Untreated and NPA treated DRG neurons showed basic NO-levels displayed by very weak DAF-FM DA fluorescence. In contrast, DRG neurons which were treated with LY83583 exhibited a strong fluorescent signal stemming from the reaction of DAF-FM DA with intracellular NO (white arrows). The presence of NPA during LY83583 treatment inhibited NO production and led to NO-levels comparable to untreated neurons (yellow arrows).



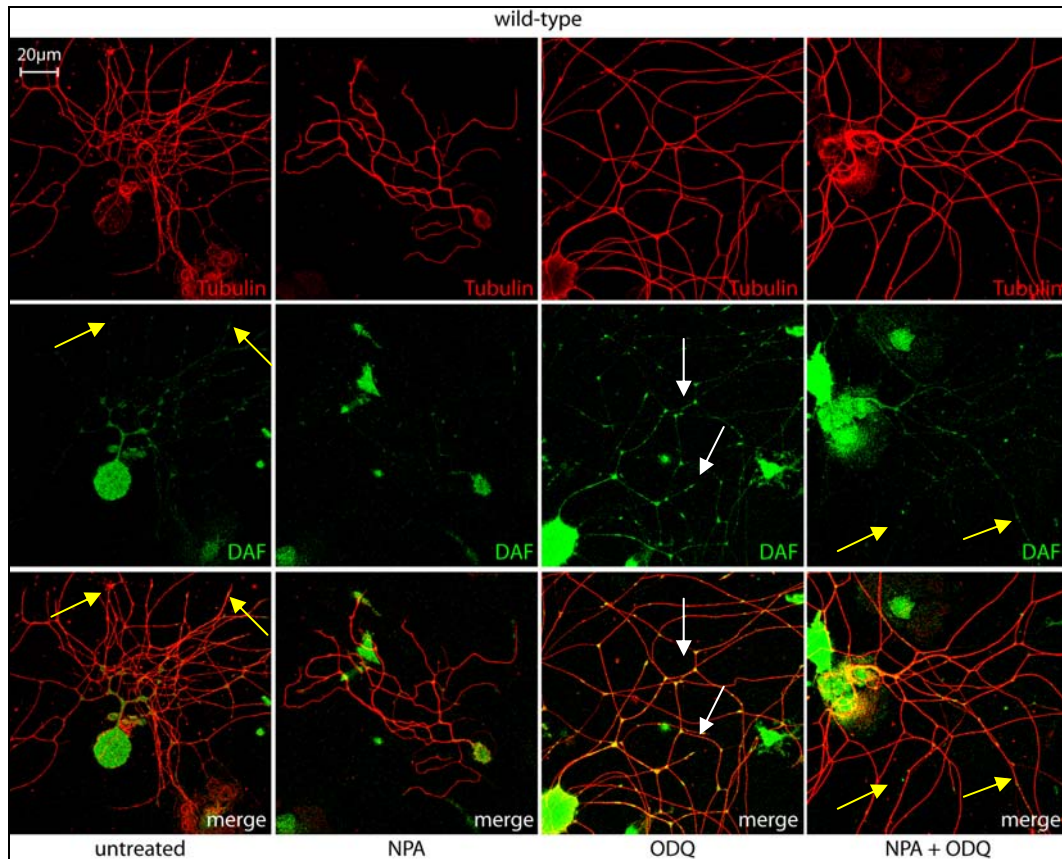


**Figure 27: NO production in wild-type DRG neurons after treatment with ODQ and NPA.**

DRG neurons were isolated from wild-type mice, cultured for 24hrs on PLL-laminin coated coverslips, were left untreated or were treated with 1µM ODQ for 30min, with 300µM NPA for 1h or with 1µM ODQ in the presence of NPA, as indicated. Before fixation, cells were incubated with the cell permeable, photo-stable fluorescent indicator for intracellular NO-levels DAF-FM DA (5µM) for 1h. Then cells were fixed and stained for tubulin. Untreated and NPA treated DRG neurons showed basic NO-levels displayed by very weak DAF-FM DA fluorescence. In contrast, DRG neurons which were treated with ODQ exhibited a fluorescent signal stemming from the reaction of DAF-FM DA with intracellular NO (white arrows). The presence of NPA during ODQ treatment inhibited NO production and led to NO-levels comparable to untreated neurons (yellow arrows).

Compared to wild-type DRG neurons which showed a much higher percentage of retraction and a correspondingly high level of intracellular NO-levels following inhibition of sGC, MAP1B<sup>-/-</sup> DRG neurons exhibited only a weak fluorescent signal stemming from DAF-FM DA reaction with NO after sGC inhibition with LY83583 (Figure 28) or ODQ (Figure 29). This result correlates with the lack of retraction in MAP1B<sup>-/-</sup> DRG neurons and the lower expression level of nNOS.

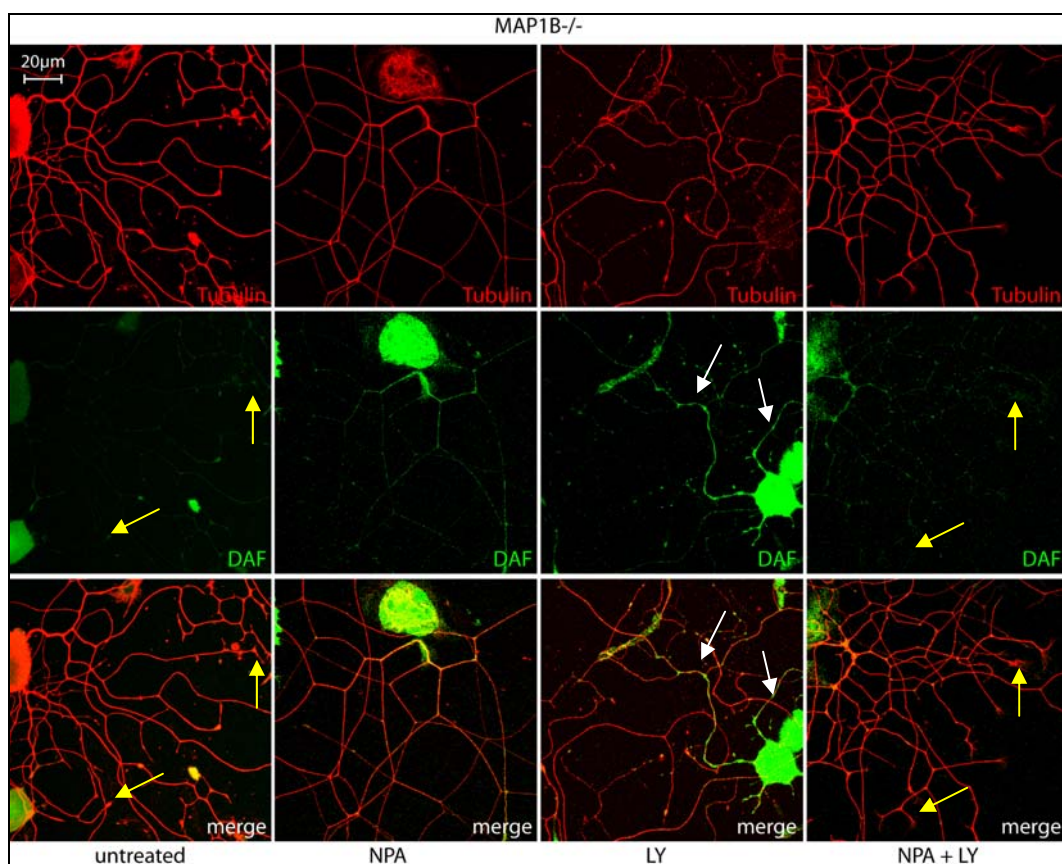


**Figure 28: NO production in MAP1B<sup>-/-</sup> DRG neurons after treatment with LY83583 and NPA.**

DRG neurons were isolated from MAP1B<sup>-/-</sup> mice, cultured for 24hrs on PLL-laminin coated coverslips, were left untreated or were treated with 1µM LY83583 for 1h, with 300µM NPA for 1h or with 1µM LY83583 in the presence of 300µM NPA for 1h, as indicated. Before fixation, cells were incubated with the cell permeable, photo-stable fluorescent indicator for intracellular NO-levels DAF-FM DA (5µM) for 1h. Then cells were fixed and stained for tubulin. Untreated and NPA treated DRG neurons showed basic NO-levels displayed by very weak DAF-FM DA fluorescence. In contrast, some MAP1B<sup>-/-</sup> DRG neurons which were treated with LY83583 exhibited a weak fluorescent signal stemming from the reaction of DAF-FM DA with intracellular NO (white arrows). The presence of NPA during netrin-1 treatment inhibited the little NO production and led to NO-levels comparable to untreated neurons (yellow arrows).

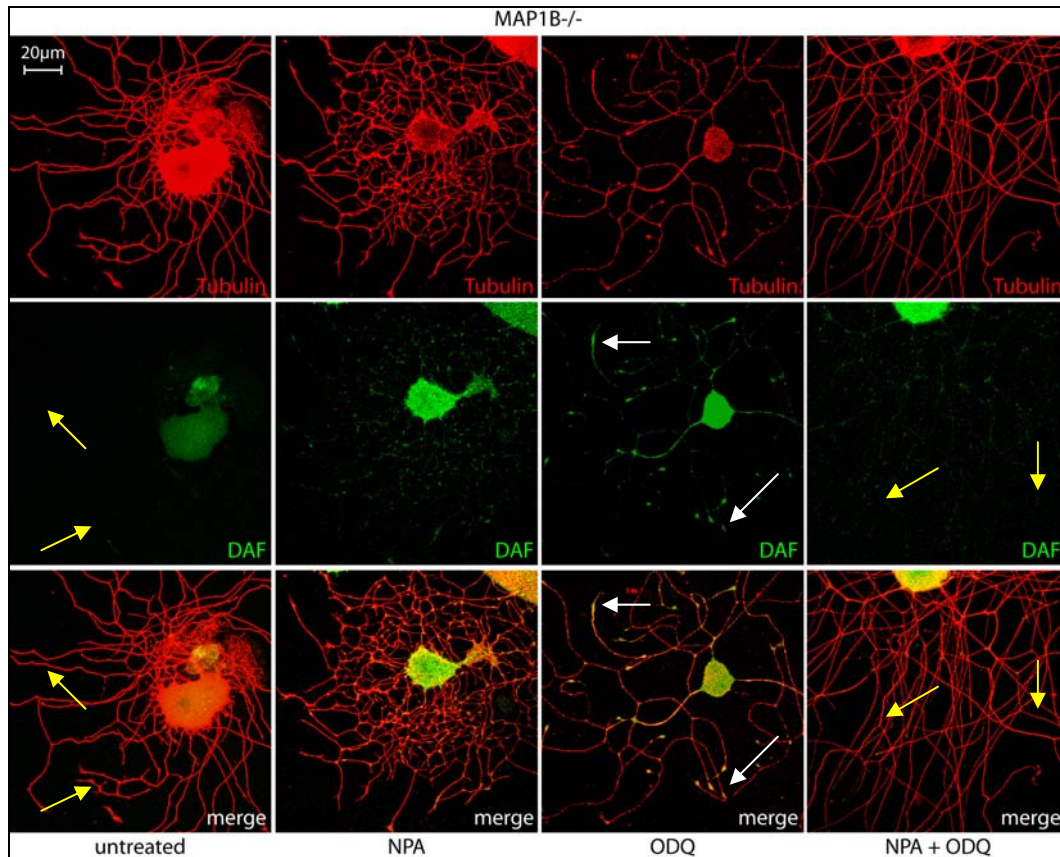


**Figure 29: NO production in MAP1B<sup>-/-</sup> DRG neurons after treatment with ODQ and NPA.**

DRG neurons were isolated from MAP1B<sup>-/-</sup> mice, cultured for 24hrs on PLL-laminin coated coverslips, were left untreated or were treated with 1µM ODQ for 30min, with 300µM NPA for 1h or with 1µM ODQ in the presence of 300µM NPA, as indicated. Before fixation, cells were incubated with the cell permeable, photo-stable fluorescent indicator for intracellular NO-levels DAF-FM DA (5µM) for 1h. Then cells were fixed and stained for tubulin. Untreated and NPA treated DRG neurons showed basic NO-levels displayed by almost invisible DAF-FM T fluorescence. In contrast, DRG neurons which were treated with ODQ exhibited a slightly increased fluorescent signal stemming from the reaction of DAF-FM DA with intracellular NO (white arrows). The presence of NPA during ODQ treatment inhibited any NO production and led to NO-levels comparable to untreated neurons (yellow arrows).

### The role of NOS in the Sema3A signaling pathway

Sema3A acts mainly as repellent guidance cue and induces axon retraction and growth cone collapse. Moreover, Sema3A induced growth cone collapse involves Rho-GTPases, cyclic nucleotides<sup>151</sup>, PKA and PKG<sup>302</sup>, and several other kinases such as MAPK, Cdk5 and GSK3-β<sup>203</sup>. All these features make of Sema3A a guidance cue which is especially interesting concerning the question whether NOS might be involved in one of the pathways leading to growth inhibitory effects. Therefore I wanted to investigate

how different kinds of explants react to the guidance cue when applied in the medium. The first experiments were performed with hippocampal explants from newborn wild-type and MAP1B<sup>-/-</sup> mice. For these experiments hippocampi of P0 to P1 mice were dissected, cut into 3 to 4 pieces and were directly transferred into Matrigel<sup>TM</sup>. The Matrigel<sup>TM</sup> was allowed to dry for 1 hour and then growth medium for hippocampal neurons was added to each well. This medium was supplemented with the nNOS inhibitors, NPA or L-NAME, or with Sema3A at concentrations 50ng/ml or 100ng/ml, or the combination of a nNOS inhibitor with Sema3A. The neurites were allowed to grow out of the explants for 2 to 3 days. After this period, explants were analyzed by phase contrast microscopy and the lengths of neurites were measured. Then, the relative outgrowth of neurites was calculated by comparing the average lengths of neurites grown in differently supplemented growth medium to the lengths of neurites grown in normal growth medium without any supplement. Figure 30 shows the results of 7 independent experiments with wild-type hippocampal explants and 4 independent experiments performed with MAP1B<sup>-/-</sup> mice. Hippocampal explants of wild-type mice showed increased outgrowth when cultured in media supplemented with nNOS inhibitors. This effect could not be observed for hippocampal explants of MAP1B<sup>-/-</sup> mice. Concerning the growth inhibitory effect of Sema3A, wild-type hippocampal explants showed a significant reduction in neurite length after growth in medium supplemented with 100ng/ml Sema3A but not when medium was supplemented with 50ng/ml Sema3A only. However, inhibition of nNOS had again a significant effect on the outgrowth of neurites. Addition of NPA or L-NAME led to a significant increase in neurite length compared to corresponding values of neurites grown in media supplemented with 50ng/ml or 100ng/ml Sema3A. In general, neurite outgrowth of MAP1B<sup>-/-</sup> hippocampal explants was largely unaffected by any of the treatments. The visualization of intracellular NO-levels with DAF-FM DA was not possible with explant cultures and therefore dissociated hippocampal neurons were cultured and treated with the guidance cue and inhibitors. Unfortunately, dissociated neurons from hippocampi of newborn mice did not react to Sema3A treatments. No signs of axon retraction or growth cone collapse could be found after treatment with Sema3A. In addition, no indication of intracellular NO production was seen in these neurons.



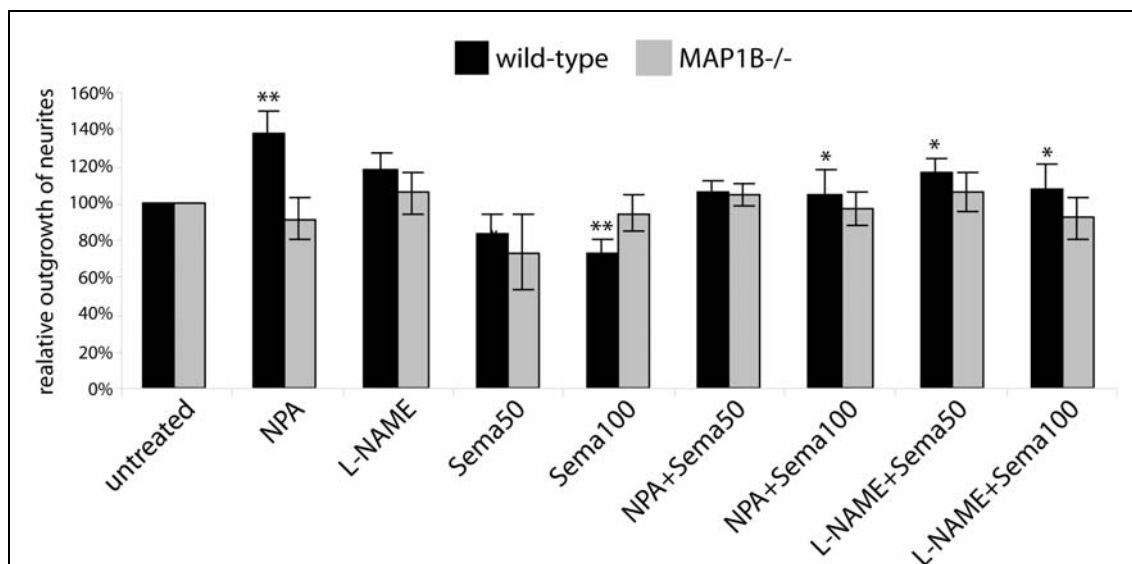


**Figure 30: Relative outgrowth of neurites from hippocampal explants of newborn wild-type and MAP1B<sup>-/-</sup> mice.**

Hippocampal explants were isolated from newborn wild-type and MAP1B<sup>-/-</sup> mice and cultured in Matrigel<sup>TM</sup>. The medium was left unchanged or was supplemented with 300μM NPA, 300μM L-NAME, 50ng/ml or 100ng/ml Sema3A, with 50ng/ml or 100ng/ml Sema3A in the presence of 300μM NPA or 300μM L-NAME. The neurites were allowed to grow out for 2-3 days without changing the medium. Hippocampal explants were analysed by phase contrast microscopy of living cells and neurite length was assessed with appropriate software (AxioVision Rel. 4.7, Zeiss). From each of 7 wild-type and 4 MAP1B<sup>-/-</sup> experiments the lengths of 5 to 10 neurites per hippocampal explant were measured and the relative outgrowth compared to the outgrowth of untreated explants was calculated. Error bars represent standard errors of the mean. Asterisks indicate that the values for explants treated with Sema3A were significantly different from corresponding values of untreated explants and that the values for explants treated with Sema3A in the presence of NPA or L-NAME were significantly different from corresponding values of explants treated with Sema3A only (\*,  $p < 0.05$ ; \*\*,  $p < 0.005$ ).

Similar experiments were performed with DRG explants of adult wild-type and MAP1B<sup>-/-</sup> mice. In total 8 independent experiments with wild-type DRG explants and 5 independent experiments with MAP1B<sup>-/-</sup> DRG explants were taken into account. The experiments including studies of L-NIO effects were performed only 3 times. DRGs were dissected as usual from adult mice and directly transferred into Matrigel<sup>TM</sup>. After 1 hour incubation, DRG growth medium supplemented with the nNOS inhibitors, NPA or L-NAME, with the eNOS inhibitor L-NIO, or with Sema3A, at concentrations 50ng/ml or 100ng/ml, or with the combination of a NOS inhibitor with Sema3A was added. The neurites were then allowed to grow out of the explants for 2 to 3 days. After this period, explants were analyzed by phase contrast microscopy and the lengths of 5 to 10 neurites per ganglion were measured. Then, the relative outgrowth of neurites was calculated by

comparing the average lengths of neurites obtained in differently supplemented DRG growth medium to neurites obtained in normal DRG growth medium without any supplement (Figure 31). In case of wild-type DRG explants, the inhibition of NOS enzymes generally led to an increase in neurite length suggesting that inhibition of NO production acts in favor of outgrowth. In contrast to NOS inhibition, treatment with 50ng/ml or 100ng/ml Sema3A led to significant reduction in neurite lengths, whereby the concentration of Sema3A was not critical. The simultaneous bath application of nNOS inhibitors and Sema3A increased the length of neurites significantly compared to neurites of explants grown in Sema3A-supplemented medium. Here, the nature of the inhibitor did not play a role as NPA and L-NAME were both successfully rescuing the growth inhibitory effect of Sema3A treatment. However, compared to the inhibition of nNOS, the inhibition of eNOS by L-NIO did not have such a striking effect in preventing the Sema3A dependent reduction of outgrowth in wild-type DRG explants.

In contrast, DRG explants from MAP1B<sup>-/-</sup> mice did not show any comparable reaction. Their outgrowth did not increase during growth in medium supplemented with nNOS inhibitors, only slightly in the presence of L-NIO. This is plausible since the role of nNOS in MAP1B<sup>-/-</sup> DRG neurons was already shown to be negligible. Moreover, MAP1B<sup>-/-</sup> DRG explants exhibited a reduced response to Sema3A compared to wild-type DRG explants. Their neurites were not significantly inhibited in their outgrowth and even additional inhibition of nNOS did not help to overcome the weak effect of Sema3A. In contrast, L-NIO abolished the weak negative effect of Sema3A on neurite outgrowth.

These results show that in wild-type DRG explants, indeed, nNOS seems to play a role in the growth inhibitory signaling pathway activated by Sema3A and this effect can be abrogated by inhibiting nNOS. Unfortunately, the visualization of intracellular NO-levels with DAF-FM DA was not possible with explant cultures and therefore dissociated DRG neurons were cultured and treated with the guidance cue and NOS inhibitors. This experiment has been performed twice but no reaction to Sema3A leading to retraction or growth cone collapse could be observed in these neurons (data not shown). Moreover, no increase in NO-levels was detected. Probably the dissociated DRG neurons of adult mice do not respond to treatment with Sema3A.

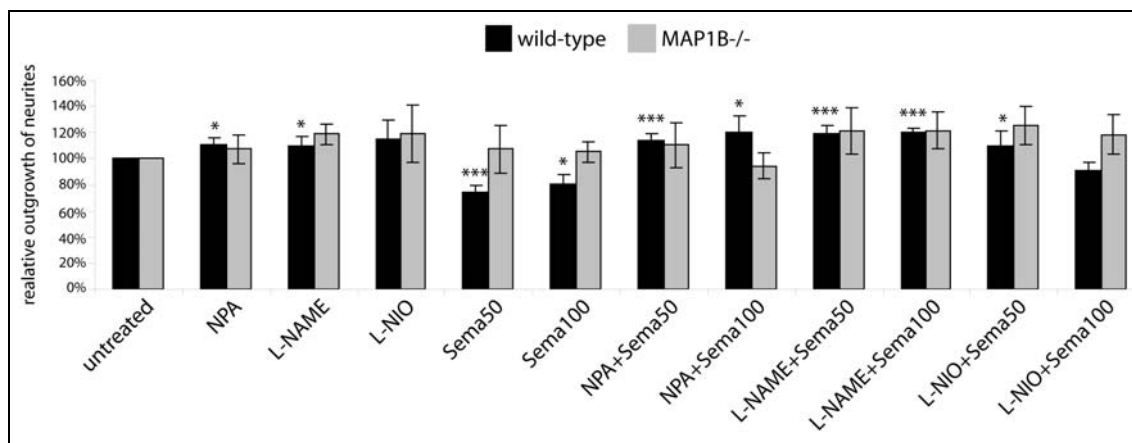


**Figure 31: Relative outgrowth of neurites from DRG explants of adult wild-type and MAP1B<sup>-/-</sup> mice.**

DRG explants were isolated from adult wild-type and MAP1B<sup>-/-</sup> mice and cultured in Matrigel<sup>TM</sup>. The medium was left unchanged or was supplemented with 300 $\mu$ M NPA, 300 $\mu$ M L-NAME, 10 $\mu$ M L-NIO, 50ng/ml or 100ng/ml Sema3A, or with 50ng/ml or 100ng/ml Sema3A in the presence of 300 $\mu$ M NPA, 300 $\mu$ M L-NAME or 10 $\mu$ M L-NIO. The neurites were allowed to grow out for 2-3 days without changing the medium. DRG explants were analyzed by phase contrast microscopy of living cells and neurite length was assessed with appropriate software (AxioVision Rel. 4.7, Zeiss). From each of 8 wild-type and 5 MAP1B<sup>-/-</sup> experiments the lengths of 8 to 10 neurites per ganglion were measured and the relative outgrowth compared to the outgrowth of untreated neurites was calculated. Experiments including L-NIO treatment were performed 3 times. Error bars represent standard errors of the mean. Asterisks indicate that the values for neurites treated with NPA were significantly different from corresponding values of untreated neurites, that the values for neurites treated with Sema3A were significantly different from corresponding values of untreated neurites and that the values for neurites treated with Sema3A in the presence of NPA or L-NAME were significantly different from corresponding values of neurites treated with Sema3A (\*,  $p < 0.05$ ; \*\*\*,  $p < 0.001$ ).

However, these results confirm the data obtained for hippocampal explants and emphasize the role of nNOS in the response to Sema3A of neurites growing out of wild-type explants. Similar effects of Sema3A and nNOS inhibition could be observed independent of the age of mice used for these experiments which suggests that Sema3A acts in a comparable manner in the nervous system of newborn and adult mice. Moreover, my results demonstrate the importance of NOS and MAP1B in Sema3A signaling.





## PART I DISCUSSION

Many axon guidance cues can act either as attractive or repulsive signals. This is also true for netrin-1. The Tessier-Lavigne laboratory demonstrated that the chemoattractive guidance receptor for netrin-1 is DCC, the mammalian orthologue for Unc40<sup>152</sup>, whereas the family of Unc5 receptors mediates repulsive netrin-1 signaling<sup>106</sup>. In contrast to short range signaling, long range signaling requires a netrin-1 gradient which is stabilized through interactions with components of the extracellular matrix, such as laminin. Activation of DCC triggers activation of Rac1 and Cdc42 promoting lamellipodium and filopodium extension, respectively<sup>159</sup>. The mechanism underlying the attractive signaling was studied by many groups. One of them, Del Rio et al., was able to show that MAP1B phosphorylation by GSK3- $\beta$  and CDK5 occurs during netrin-1 signal transduction and that the lack of MAP1B impairs netrin-1 mediated chemoattraction *in vitro* and *in vivo*. They suggested that MAP1B might be an essential downstream effector of the attractive netrin-1 signaling pathway<sup>3</sup>. In addition, the phenotypes of MAP1B<sup>-/-</sup> mice<sup>4</sup> and netrin-1<sup>-/-</sup> mice<sup>49</sup> share some similarities, although the lack of netrin-1 causes much more severe effects. Both mutants exhibit defects in forebrain commissures such as the generation of corpus callosum or hippocampal commissure suggesting that both proteins are essential for proper axon guidance during brain development.

Much less work has been done regarding chemorepulsive netrin-1 signaling. The repulsive response to netrin-1 is mediated by Unc5-dependent RhoA activation and a decrease in the ratio of cAMP to cGMP. Growth cones respond to a repulsive guidance cue secreted from a local source by turning away from this source. If the repulsive factor surrounds the growing neuron, as it is the case for bath application, the growth cone collapses and the axon retracts. One mechanism of axon retraction was shown to involve S-nitrosylation of MAP1B as an essential part of the signal transduction pathway<sup>1</sup>. Calcium influx leading to the activation of nNOS and subsequent MAP1B S-nitrosylation eventually results in axon retraction in wild-type but not in MAP1B<sup>-/-</sup> DRG neurons.

Netrin-1 has been shown to act as a repulsive signal for growth cones when neurons are grown on substrates containing laminin<sup>2</sup>. Since the established protocol for culturing mouse DRG neurons utilizes PLL-laminin coated glass coverslips, I expected the neurons to retract when treated with netrin-1. Indeed, I observed a significant

increase in retracting axons in netrin-1 treated samples. The binding of netrin-1 to its receptors leads to an increase in intracellular calcium levels.  $\text{Ca}^{2+}$  signaling is extremely important in controlling growth cone steering, although the precise role of  $\text{Ca}^{2+}$  signals in directional sensing and steering of the growth cone is unclear<sup>135</sup>. A small local  $\text{Ca}^{2+}$  was found to mediate repulsion, whereas a modest elevation of  $\text{Ca}^{2+}$  results in attraction<sup>303</sup>. Cyclic nucleotide signaling directly modulates the activity of L-type  $\text{Ca}^{2+}$  channels (LCCs) in the axonal growth cones. Moreover, cGMP suppresses LCC activity triggered by netrin-1 and is required for growth cone repulsion mediated by the DCC-Unc5 receptor complex<sup>146</sup>.

I wondered whether the expected change in calcium concentration after netrin-1 binding would induce nNOS activation. As consequence of nNOS activation, the increased NO synthesis could result in MAP1B S-nitrosylation and MAP1B-dependent axon retraction. Moreover, in the presence of laminin, the response to netrin-1 includes a decrease in the ratio of cAMP and cGMP concentrations, suggesting that sGC becomes activated. sGC is a target of NO and is activated by its binding. Thus, it appeared plausible that nNOS is the signaling molecule linking the calcium influx and the presence of laminin to the repulsion mediated by netrin-1.

Additionally, phosphorylation of MAP1B might also be a critical step during repulsive netrin-1 signaling in the presence of laminin. Phosphorylation of MAP1B by Cdk5 occurs after activation of the kinase by laminin<sup>53</sup>. Since the presence of laminin switches the neuronal response to netrin-1 from attraction to repulsion the question arose whether MAP1B and its phosphorylation play a role in the chemorepellent netrin-1 signaling pathway.

In order to test the hypothesis that MAP1B is involved in repulsive netrin-1 signaling as well, DRG neurons of wild-type and MAP1B<sup>-/-</sup> mice were cultured on PLL-laminin coated coverslips. After bath application of netrin-1 for 21hrs the response of axons was analyzed. As expected, the presence of laminin led to a repulsive effect of netrin-1 resulting in typical axon retraction including all three characteristics: sinusoidal microtubule bundles along the axon shaft, a collapsed growth cone and a trailing remnant. Interestingly, the axons of wild-type and MAP1B<sup>-/-</sup> DRG neurons showed a similar reaction to the treatment. Both cell types exhibited comparable percentages of retracted neurons suggesting that the lack of MAP1B did not impair the signal transduction downstream of netrin-1. This result showed that, in contrast to the attractive netrin-1 signaling, MAP1B is not necessary for the correct signal transduction

of the repulsive netrin-1 signaling. Consequently, neither S-nitrosylation nor phosphorylation of MAP1B appear to be relevant for this signaling pathway. However, these modifications might have occurred in presence of MAP1B.

Since MAP1B is dispensable for repulsive netrin-1 signaling, it seems that a completely different mechanism can be activated by netrin-1 in the presence of laminin compared to attractive signaling. Probably not only the ratio between cAMP to cGMP is important but many other factors too, that are not needed for attraction. Another possible explanation for the difference between the results obtained for the attractive versus repulsive netrin-1 pathway is that different cells were used for the studies. Del Rio worked mainly with embryonic tissues and cells. They isolated hippocampal and spinal explants or dissociated neurons from cortex or the lower rhombic lip whereas I used DRG neurons of adult mice. Thus, not only the source of the cells but also the developmental stage might play a role in the responses to the guidance cue.

However, the irrelevance of MAP1B does not eliminate the possible involvement of nNOS in this pathway. The activation of nNOS was investigated with the cell permeable fluorescent indicator for intracellular NO, DAF-FM DA. In the presence of oxygen, DAF-FM DA reacts with NO yielding the fluorescent dye DAF-FM T. The incubation of netrin-1 treated cells with this dye revealed a clear increase in intracellular NO following activation of the netrin-1 signaling pathway. In wild-type and MAP1B<sup>-/-</sup> DRG neurons high levels of NO were observed along axons and especially in collapsed growth cones. Once more, the response of the neurons was not MAP1B dependent. This shows that, first, a NOS was activated downstream of netrin-1. Since netrin-1 binding to its receptors induces changes in the intracellular Ca<sup>2+</sup> levels, it is likely that this change is responsible for the activation of NOS. Secondly, S-nitrosylation of MAP1B was not essential for the mechanism although it might have occurred in wild-type DRG neurons, what has not been tested.

In order to confirm the activation of a NOS downstream of netrin-1 and its importance in mediating axon retraction by producing high levels of NO, the specific nNOS inhibitor NPA was used. DRG neurons from wild-type and MAP1B<sup>-/-</sup> mice were cultured and treated with netrin-1 or with netrin-1 in the presence of NPA, and the percentage of retracted axons was quantified. Compared to neurons exposed to netrin-1 alone, those treated with netrin-1 and NPA showed a significant reduction in retracted axons. The level of retraction in wild-type DRG neurons could be reduced to the level observed in untreated samples, whereas MAP1B<sup>-/-</sup> DRG neurons responded in a less

striking manner. In correlation with the assessed retraction, the DAF-FM T signal in wild-type DRG neurons was abolished by NPA whereas in MAP1B<sup>-/-</sup> DRG neurons only a weak reduction of the fluorescence could be seen. I concluded from these results that in wild-type DRG neurons, indeed, nNOS is involved in the repulsive netrin-1 signaling pathway and that the increase of NO is a crucial step in induction of axon retraction. In contrast, nNOS is of minor importance in MAP1B<sup>-/-</sup> DRG neurons. In these neurons another NOS might play a role since NO production comparable to that observed in wild-type neurons was observed.

To find out why nNOS inhibition was less effective in preventing axon retraction in MAP1B<sup>-/-</sup> DRG neurons than in wild-type DRG neurons, I tested wild-type and MAP1B<sup>-/-</sup> DRG neurons for expression of nNOS and eNOS. eNOS is found mainly in endothelial cells but it is also expressed in neurons and glia cells. It is, like nNOS, a constitutively expressed NOS and its activation is Ca<sup>2+</sup> dependent. Immunofluorescence analysis clearly revealed a difference in expression level of nNOS between the two cell types. In MAP1B<sup>-/-</sup> DRG neurons nNOS expression was reduced dramatically, whereas the levels of eNOS expression seemed to be comparable between wild-type and MAP1B<sup>-/-</sup> DRG neurons. These results were confirmed by western blot analysis of lysates of DRGs and brains from adult or newborn mice.

Acute control of nNOS activity is mediated by allosteric enzyme regulation, by posttranslational modification and by subcellular targeting of the enzyme. However, in case of MAP1B<sup>-/-</sup> neurons I observed changes in nNOS expression levels. How the lack of MAP1B influences the expression level of nNOS still remains elusive. However, direct interactions of a variety of proteins bearing a PDZ domain with the PDZ domain of nNOS have been shown to influence the subcellular distribution and activity of the enzyme, such as PSD-95 or PSD-93<sup>304</sup>. MAP1B for instance was shown to bind the PDZ domain of nNOS. The interaction between the two proteins does not occur exclusively through this domain, though (Trancikova, PhD Thesis 2007). This interaction might have an influence on the stability of the enzyme.

Another possible reason for the reduced nNOS expression could be at the level of mRNA. The mRNA of nNOS is structurally diverse as a consequence of alternative promoters and alternative splicing<sup>305</sup>. The expression of nNOS in MAP1B<sup>-/-</sup> DRG neurons was principally reduced to the cell body and primary axons and not always completely absent. MAP1B has been shown to colocalize with staufen1-containing RNP complexes in DRG neurons<sup>306</sup> (Steffel, PhD Thesis 2007). Thus, MAP1B might also

play a role in the stabilization or transport of mRNA. At least for eNOS it has been suggested that RNA binding proteins are involved in regulation of eNOS transcription. A similar mechanism could be assumed for nNOS mRNA stability, transport and following transcription. One could investigate whether the transcription of nNOS is impaired in cells lacking MAP1B by performing quantitative RT PCR. In addition, a pulse chase experiment could be performed with a neuronal cell line transfected with siRNA against MAP1B in order to follow nNOS protein-synthesis. Moreover, transfecting MAP1B<sup>-/-</sup> DRG neurons with full length MAP1B or MAP1B-LC1 should provide an indication of the role of MAP1B in the stability of nNOS at the mRNA and protein level. Another explanation for the reduced signal from antibodies against nNOS in MAP1B<sup>-/-</sup> mice is the regulation of the enzyme through alternative transcripts. It is known that the isoforms nNOS- $\beta$  and nNOS- $\gamma$  lack the PDZ domain which is responsible for targeting nNOS to synaptic membranes<sup>228</sup>. Moreover, all our antibodies against nNOS detect the PDZ domain of the enzyme, and thus, would not recognize the different isoform which might be expressed in MAP1B<sup>-/-</sup> DRG neurons.

In any case, it was important to clarify whether eNOS could substitute for nNOS. The first approach was to inhibit eNOS with the specific inhibitor L-NIO during treatment with netrin-1 and to evaluate axon retraction under these conditions. Additionally, the level of intracellular NO production was analyzed with DAF-FM DA. In wild-type DRG neurons L-NIO was not successful in preventing retraction induced by netrin-1. Moreover, the level of NO synthesis was not reduced in netrin-1 treated DRG neurons. In contrast, MAP1B<sup>-/-</sup> DRG neurons showed a much better response to L-NIO. Inhibition of eNOS reduced the amount of retracted axons after netrin-1 treatment to the levels of retraction seen in untreated DRG neurons and the fluorescent signal from DAF-FM T was almost abolished. Hence, in MAP1B<sup>-/-</sup> DRG neurons netrin-1 signaling involves NO production, but the main responsible enzyme here is eNOS.

Thus, NO production seems to be a key event mediating netrin-1 induced axon retraction in wild-type and in MAP1B<sup>-/-</sup> DRG neurons. Whether nNOS is available is not the most important fact. Since the expression level of eNOS in MAP1B<sup>-/-</sup> DRGs or brains is quite similar to that in wild-type DRGs or brains, it is not an upregulation of eNOS expression which provides relief. There might be a feedback mechanism which activates eNOS if nNOS is not expressed or stable enough. Interestingly, eNOS is not taking over from nNOS when nNOS is inhibited, only when the expression or

stabilization of nNOS is impaired. Otherwise a specific inhibition of nNOS alone would not have been that effective and simultaneous inhibition of eNOS would have been necessary to see a decrease in retraction. Why eNOS becomes only more important when nNOS expression is reduced and not when nNOS is simply inhibited remains elusive. A plausible cause could be the availability of  $\text{Ca}^{2+}/\text{CaM}$ . Activation of both enzymes, nNOS and eNOS, is dependent on increase in intracellular  $\text{Ca}^{2+}$  which leads to the binding of  $\text{Ca}^{2+}/\text{CaM}$  to the NOS. nNOS and eNOS translocate upon  $\text{Ca}^{2+}/\text{CaM}$  binding from membrane associated PSD95 and caveolin, respectively, to the cytoplasm where they produce  $\text{NO}$ <sup>305, 307</sup>. Perhaps the concentration of  $\text{Ca}^{2+}/\text{CaM}$  is a rate limiting factor and nNOS might have a higher affinity to  $\text{Ca}^{2+}/\text{CaM}$  than eNOS. Inhibition of nNOS by NPA might not interfere with the binding of  $\text{Ca}^{2+}/\text{CaM}$  to nNOS and therefore no  $\text{Ca}^{2+}/\text{CaM}$  is free to bind eNOS and induce its translocation from caveolin to the cytoplasm. The suggestion that eNOS adopts the role of nNOS in tissues with reduced nNOS expression would also help to explain the phenotype observed in nNOS mutant mice. These mice did not show any histopathological abnormalities in neuronal tissues and other enzymes were suggested to generate NO in their brains<sup>308</sup>. In contrast to the weak phenotypic changes in single knockout mice for nNOS or eNOS, the mice mutant for both enzymes showed a significantly reduced long term potentiation suggesting that neuronal and endothelial isoforms can compensate for each other<sup>236</sup>.

Obviously, laminin does not only play a role in giving support to neuronal migration but it is also essential for the correct interpretation of the guidance signals according to the environmental situation of the neuron. On the one hand, I could show that the production of NO is a necessary event during the transduction of the repulsive netrin-1 signaling pathway and on the other hand, the repulsion does not occur when laminin is not available. A similar effect has been observed in DRG neurons that were submitted to high NO concentrations. Wild-type DRG neurons cultured on PLL-laminin retract their axons extensively when exposed to the NO-donor SNAP or to the ionophor calcimycin which activates nNOS<sup>1</sup>. By contrast, wild-type DRG neurons do not show any response to these treatments when they were grown on PLL only. Thus, laminin might be essential for transduction of NO-mediated signaling. Moreover, the differential branching observed between wild-type and MAP1B<sup>-/-</sup> DRG neurons is abolished by the lack of laminin suggesting that some functions of MAP1B are laminin-dependent (Krupa, PhD Thesis 2009). The NO production downstream of netrin-1 signaling in the presence of laminin might be an important feature of neurons when they are at risk to be

misdirected into inappropriate zones. These zones might provide an environment with higher concentration of laminin than those where netrin-1 attracted neurons should extend. Thereby the response to netrin-1 switches from attraction to repulsion. It would be interesting to find out in which zones of the developing nervous system laminin surrounds neurons supposed to respond to netrin-1 signaling. Probably these neurons are repelled and produce increased amounts of NO.

Since NO production seemed to be essential for the repulsive netrin-1 signaling I wondered what could be the downstream effectors of NO. There are two possibilities in which NO can act as signaling molecule: posttranslational modification of proteins by protein-S-nitrosylation and activation of sGC. Protein-S-nitrosylation of MAP1B might not play an essential role since the responses of DRG neurons to netrin-1 were independent of the MAP1B. Other proteins have not been tested for S-nitrosylation because the only way to detect this posttranslational modification is to perform a biotin switch. For this experiment one would need large amounts of proteins and the yield of proteins from DRG neurons is simply too small. Thus, protein-S-nitrosylation downstream of netrin-1 has not been investigated in more detail. The other target of NO is sGC which becomes activated by binding of NO. Subsequently, the amount of intracellular cGMP increases and the ratio between cAMP and cGMP is altered. This change could lead to the switch from attraction to repulsion mediated by laminin<sup>2</sup>.

In order to analyse whether the activation of sGC and the subsequent increase in cGMP formation are the crucial events leading to axon retraction, I inhibited sGC with the specific inhibitors ODQ or LY83583 during treatment with netrin-1. Surprisingly, in wild-type DRG neurons treatment with netrin-1 and ODQ or netrin-1 and LY83583 led to a significant increase in axon retraction. The observed dramatic increase in axon retraction following this double treatment was in the first moment an indication that sGC cannot be the main downstream target of NO in the repulsive netrin-1 signaling pathway. However, even treatment with ODQ or LY83583 *per se* led to a rapid, MAP1B dependent axon retraction and at the same time to a MAP1B dependent increase in intracellular NO synthesis. These results indicate that the inhibition of sGC interferes probably with a feedback mechanism working via cGMP dependent protein kinase, PKG. PKG is activated by cGMP and one of its targets is nNOS, which becomes inactivated when phosphorylated by PKG<sup>5</sup>. When sGC is inhibited by ODQ or LY83583, this negative feedback is switched off and nNOS remains active and will continue to produce NO which eventually results in axon retraction. The axon retraction

following sGC inhibition was observed to be MAP1B dependent, as MAP1B<sup>-/-</sup> DRG neurons showed greatly reduced response to treatment with ODQ or LY83583. Hence, S-nitrosylation of MAP1B might be relevant for the induction of axon retraction when cGMP production is reduced. Another explanation for the MAP1B dependence would be that PKG does not act on eNOS and another mechanism is responsible for the proper inactivation of eNOS, which is not affected by ODQ or LY83583.

Netrin-1 signaling might not be the only axon guidance cue which involves NO production during signal transduction. Other well characterized repellent axon guidance cues are for instance the semaphorins. Sema3A activity was shown to be regulated by NGF through TrkA<sup>309</sup>. NGF was shown to reduce the expression of nNOS<sup>310</sup>. In addition, NGF and NO interact during embryonic development and assure survival of neurons<sup>311</sup>. A probable mechanism underlying Sema3A regulation by NGF could be the prevention of NO synthesis which provides the second messenger molecule mediating repulsive signals.

In the first attempt to investigate whether NOS and NO play a role in the Sema3A signaling I cultured DRG neurons from adult mice and hippocampal neurons from newborn mice on PLL or on PLL-laminin coated coverslips. The neurons were incubated with different concentrations of Sema3A. None of the neurons showed reaction (data not shown). Perhaps the length of the incubation or the concentrations of Sema3A were not optimal to induce retraction or growth cone collapse in DRG or hippocampal neurons. It was shown previously that embryonic mouse DRG neurons are less sensitive to Sema3A-induced growth cone collapse than to axon outgrowth inhibition<sup>309</sup>. Thus, I cultured explants of DRGs and hippocampus from adult and newborn mice, respectively. In agreement with the previous findings, I observed a significant reduction in the lengths of neurites when the explants were grown in media supplemented with Sema3A. The presence of NGF generally enhanced growth dramatically and helped thereby to abrogate the growth inhibitory effect of Sema3A (data not shown). A similar effect was observed when nNOS was inhibited during explant culture. Explants from wild-type DRGs or hippocampus exhibited a significant increase in neurite length when exposed to NPA, suggesting that NO production might negatively affect neurite outgrowth. Moreover, a significant change was observed in explants cultured in medium containing Sema3A and NPA compared to explants grown in medium supplemented with Sema3A only. This difference could be due to the effects of nNOS inhibition promoting axon elongation. On the other hand, Sema3A could have



induced NO production by nNOS resulting in the observed decrease of neurite length, which was overridden by its inhibition. The lack of clarity after these results demands investigation of intracellular NO production after Sema3A treatments. For this purpose, dissociated neurons that react to the repulsive cue would be required. The establishment of Sema3A-sensitive neuronal cultures will make it feasible to investigate intracellular NO production in response to the guidance cue with DAF-FM DA. Since semaphorins are important for axon guidance during development of the nervous system, embryonic neurons could be advantageous.

Regarding the role of MAP1B in signal transduction downstream of semaphorins, Sema3A was especially interesting for me because Cdk5 and GSK3- $\beta$  are involved in Sema3A induced growth cone collapse<sup>219</sup> and these kinases also phosphorylate MAP1B<sup>53, 312</sup>. An additional hint suggesting MAP1B to be important for Sema3A signaling was the finding of Good et al. who observed co-localization of Sema3A and phosphorylated MAP1B in hippocampus of Alzheimer's disease (AD) patients<sup>313</sup>. Moreover, hippocampal immunolabeling of Sema3A and phosphorylated MAP1B increases in intensity with the progressive severity of AD and hyper-phosphorylation of MAP1B is observed during the progression of AD<sup>314</sup>. In correlation with this finding, very recent data show that Sema3A-stimulation of embryonic hippocampal neurons causes a dramatic increase in MAP1B protein levels within distal axons<sup>315</sup>. Moreover, the Sema3A induced growth cone collapse might be partially dependent on FMRP, the protein whose mutation is the main cause for fragile X syndrome, and which is binding to the MAP1B mRNA in neuronal processes<sup>316</sup>. The diminished response of MAP1B<sup>-/-</sup> explants to Sema3A in neurite outgrowth suggests that, indeed, MAP1B might be involved in the downstream signaling of Sema3A. The MAP1B<sup>-/-</sup> explants did not show any significant increase in length in the presence of nNOS inhibitors and no decrease when Sema3A was supplied. This correlates with the results obtained for nNOS expression in MAP1B<sup>-/-</sup> mice and it suggests that Sema3A might mediate some of its effects through MAP1B phosphorylation. Further work will be required to elucidate a potential MAP1B-mediated mechanism in Sema3A regulated neurite outgrowth.



## **PART II RESULTS:**

### **The role of MAP1B and nitric oxide in oligodendrocytes**



In consideration of the facts that MAP1B is expressed in glial cells and that these cells are sensitive to nitric oxide, the question arose if S-nitrosylation of MAP1B LC1 might play a role in nitric oxide toxicity and whether this posttranslational modification might affect oligodendrocyte function. I wanted to investigate whether the lack of MAP1B influences the cellular morphology, their ability to differentiate and to maintain myelination. Moreover, I was interested in whether the S-nitrosylation of MAP1B LC1 is involved in the pathways leading to NO-induced cell death and if the lack of MAP1B might therefore help the cells to resist the toxic effect of NO.

## **Morphology and differentiation of oligodendrocytes**

### **Expression of MAP1B in oligodendrocytes and OLN93 cells**

Oligodendrocytes were isolated from newborn wild-type and MAP1B<sup>-/-</sup> mouse brains. After the initial enrichment procedure, they were cultured for two to five days in differentiation medium. The duration varied depending on the desired stage of differentiation. After two days in culture, oligodendrocytes had attained the oligodendrocyte precursor (OPC) stage where no myelin proteins are expressed yet. In order to reach the stage of terminal differentiation where cells express myelin specific proteins such as MBP and MAG, they had to be cultured for at least 5 days in the differentiation medium. However, every culture of oligodendrocytes is very heterogenous and not all cells show the same level of differentiation when they are fixed. Some cells exhibit first branches already after one night in culture whereas others are still bipolar and migrate or proliferate. Oligodendrocytes from wild-type mice were all positively stained for MAP1B, independent of their stage of differentiation. Figure 32 shows that MAP1B is expressed throughout the cell body and overlaps with tubulin staining (in green) except at the tips of the processes where MAP1B does not seem to be expressed. At first glance, the staining of MAP1B<sup>-/-</sup> oligodendrocytes shows that the morphology of these cells is not disturbed by the lack of MAP1B. The difference in appearance between wild-type and MAP1B<sup>-/-</sup> cells in the picture stems from the fact that the wild-type cell in the picture is slightly delayed in the differentiation process compared to the MAP1B<sup>-/-</sup> cell. This can be seen at the shape of the processes. In case of the wild-type cell, the processes exhibit a straight, less branched appearance (white arrowheads) whereas in the MAP1B<sup>-/-</sup> oligodendrocyte processes start to approach

others and look more curved, especially at the tips, where they are already in touch with other processes from the same cell (white arrows). In later differentiation stages the myelin sheath will be generated at these sites.

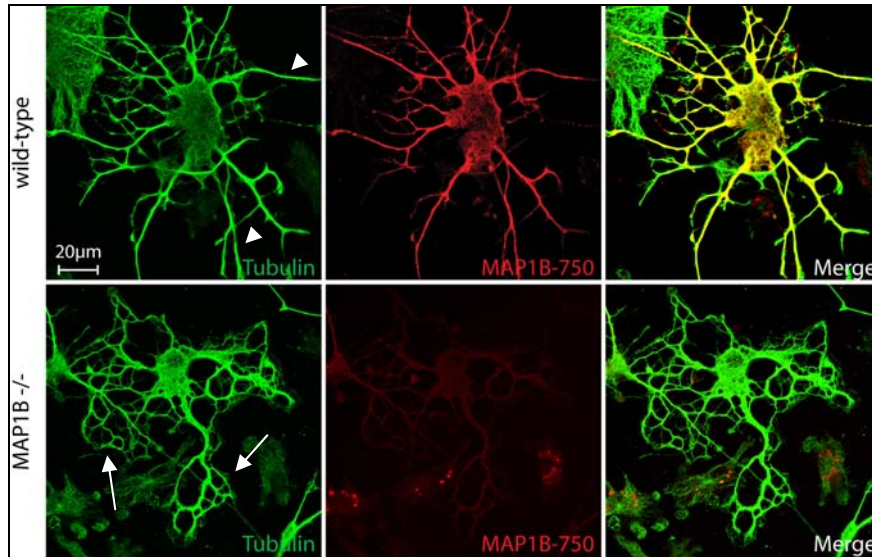


**Figure 32: Expression of MAP1B in oligodendrocytes.**

Wild-type and MAP1B<sup>-/-</sup> oligodendrocytes were cultured for five days in differentiation medium on poly-D-lysine coated coverslips, fixed and stained for tubulin in green and MAP1B-750 in red. The upper panel shows a wild-type oligodendrocyte which was fixed in an earlier differentiation stage than the MAP1B<sup>-/-</sup> oligodendrocyte showed beneath. This is visible on the straightness of the processes (white arrowheads). MAP1B is expressed in the cell body and in major processes. The lower panel shows a MAP1B<sup>-/-</sup> oligodendrocyte with only background staining of MAP1B-750. The arrows indicate the typical morphology of the process tips when oligodendrocytes are on the verge of myelin production. Tips of processes contact with other tips of the same cell and build a network of microtubules which will provide the cytoskeletal frame for the myelin sheath.

As alternative to primary oligodendrocytes, a cell line (OLN93) derived from rat oligodendrocytes was generated by Richter-Landsberg et al<sup>317</sup>. Since the yield of primary oligodendrocytes is always very low, I performed several experiments with this cell line. In the undifferentiated stage, OLN93 cells look quite similar to elongated fibroblasts with one or two processes. They are not yet branched and express already MAP1B. When the cells are cultured on poly-L-lysine (PLL) coated coverslips in differentiation medium they start to differentiate. Thus, they develop processes and, eventually, express all myelin specific proteins, such as MBP or MAG. The expression of MAP1B persists at all stages of differentiation (Figure 33 A), similar to primary wild-type oligodendrocytes. MAP1B is expressed throughout the cell and co-localizes with tubulin. In the level of expression undifferentiated OLN93 do not differ from

differentiated ones. Lysates of differentiated and undifferentiated OLN93 cells were analysed by western blot for the expression of MAP1B with antibodies against MAP1B LC1 (Figure 33 B). Tubulin was used as loading control. Before cell lysis, the medium was supplemented for the last 4 days with 3 different NOS inhibitors NPA, L-NAME or L-NIO. The long term inhibition of NOS did not change the appearance of the culture (not shown) and had no effect on the expression of MAP1B LC1. Additionally, whether the cells were allowed to differentiate or not did not change expression level of LC1. Thus, MAP1B expression in OLN93 could be confirmed by western blot. OLN93 cells therefore can be used for experiments investigating some properties of LC1 in oligodendrocytes.

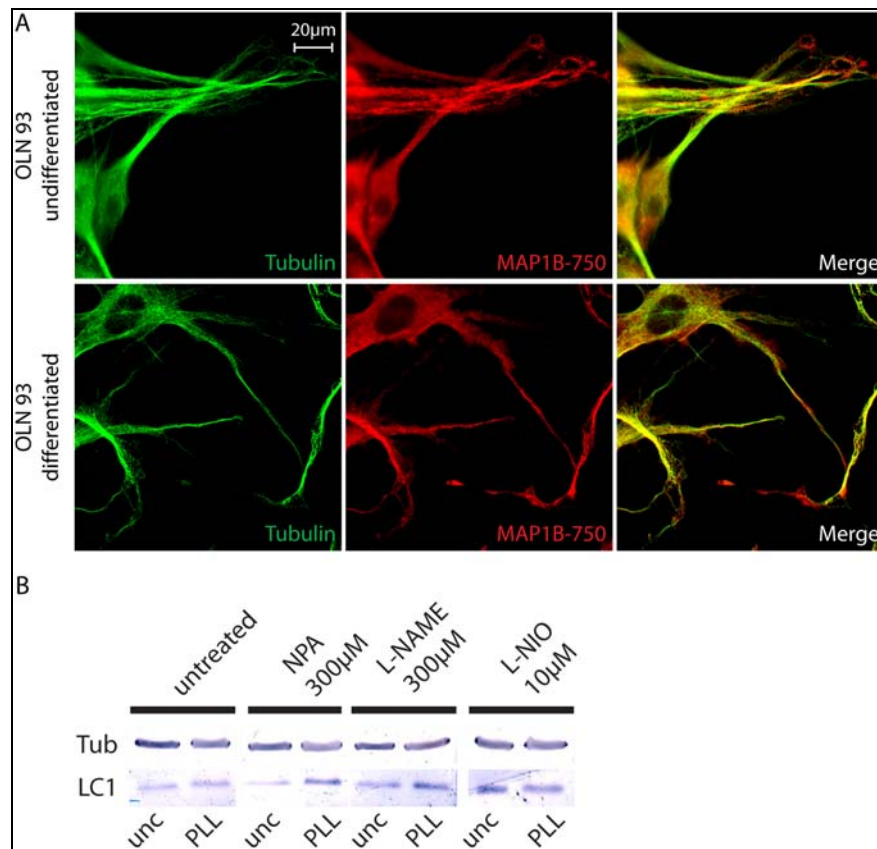


**Figure 33: Expression of MAP1B in the oligodendrocyte cell line OLN93.**

A) The rat oligodendrocyte cell line OLN93 was cultured in normal growth medium on uncoated glass coverslips (upper panel) or in differentiation medium on poly-L-lysine (PLL)-coated coverslips (lower panel) and stained for  $\alpha$ 1-tubulin (green) and MAP1B-750 (red). The cells express MAP1B independent of the stage of differentiation in the cell body and in processes. MAP1B co-localizes with tubulin. B) The western blot analysis shows the expression of MAP1B LC1 in OLN93. Cells grown on uncoated dishes (unc) were not differentiated in contrast to cells grown on PLL. In differentiated cells, the expression level of LC1 is slightly increased compared undifferentiated cells grown on uncoated coverslips. Treatments with the indicated NOS inhibitors for 4 days did not change LC1 levels.

### **Expression of nitric oxide synthases in oligodendrocytes**

In oligodendrocytes only inducible and endothelial nitric oxide synthases have been found to be expressed<sup>7</sup>. As nNOS plays an essential role in DRG neurons during axon elongation, axon retraction and growth cone response to different guidance cues, I wanted to check nNOS expression in oligodendrocytes once more. Therefore, I performed immunofluorescence on primary oligodendrocytes (Figure 34 A). Unlike previous data, I found that primary cells express nNOS. A weak staining was observed in the cell body and in the primary and secondary processes. In contrast to DRG neurons, no difference in the expression level of nNOS between wild-type and MAP1B<sup>-/-</sup> oligodendrocytes could be detected. Nevertheless, even a weakly expressed nNOS might be involved in process elongation or retraction, as it is the case for DRG neurons. Regarding the discrepancy between former analyses and my results, one could argue that the antibody reacted unspecifically. Unfortunately, no nNOS-lacking cells were available for control experiments. Moreover, nNOS has seldomly been investigated in oligodendrocytes since initially they were not found in oligodendrocytes in guinea pig optic nerve<sup>318</sup>, but one has to mention that this group did not find eNOS either which was later shown to be expressed (Boullerne 2005, unpublished data, Descovich, PhD Thesis 2009).

Regarding eNOS, the expression is relatively strong in oligodendrocytes. The synthase is located in the cell body, in major processes and also in thinner ones, like it is the case for MAP1B expression (Figure 34 B). In terms of expression level, MAP1B<sup>-/-</sup> cells show a slightly stronger staining than wild-type cells, especially in the cell body. Comparing expression levels of eNOS and nNOS based on the strength of the staining is not possible. However, the strong expression of eNOS suggests that eNOS might be an important NO producer in oligodendrocytes, particularly in MAP1B<sup>-/-</sup> cells.



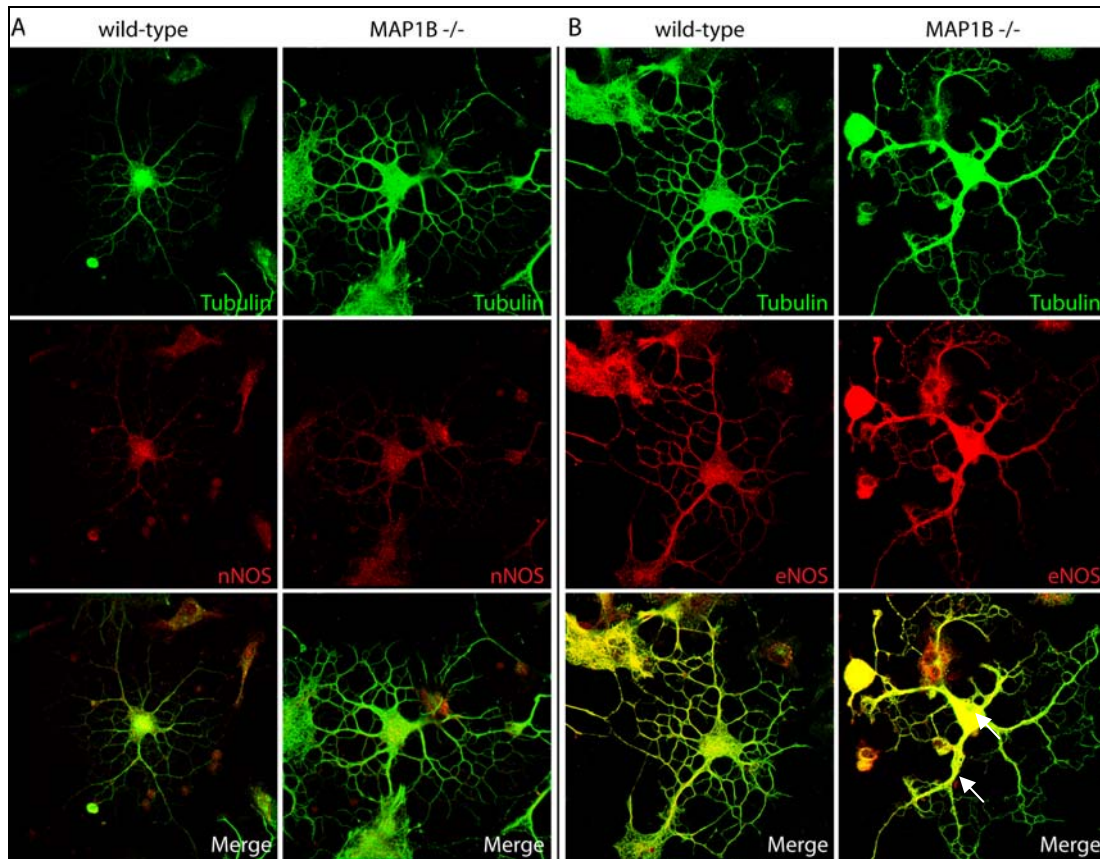


**Figure 34: Expression and localization of nNOS and eNOS in wild-type and MAP1B<sup>-/-</sup> primary oligodendrocytes.**

Wild-type and MAP1B<sup>-/-</sup> oligodendrocytes were cultured for five days in differentiation medium on poly-D-lysine coated coverslips, fixed and stained for tubulin and nNOS or eNOS. A) nNOS is expressed weakly in both wild-type and MAP1B<sup>-/-</sup> oligodendrocytes, mainly in the cell body and in primary processes. No differences in the expression level or localization could be observed between the two genotypes. B) The staining for eNOS shows expression in the cell body and in all processes of both wild-type and MAP1B<sup>-/-</sup> oligodendrocytes. The signal looks stronger in MAP1B<sup>-/-</sup> cells (arrow) suggesting a higher expression level of eNOS in MAP1B<sup>-/-</sup> oligodendrocytes.

In order to investigate nNOS expression levels in OLN93, these cells were cultured in normal growth medium on uncoated coverslips or in differentiation medium on PLL-coated coverslips. Immunofluorescence and western blot analysis were performed (Figure 35). As it is the case in primary wild-type oligodendrocytes, nNOS is only weakly expressed, independent of the stage of differentiation. nNOS is mainly expressed in the cell body and primary processes. Strong eNOS expression is visible throughout the whole cells including all processes of differentiated OLN93.

For the western blot analysis (Figure 36), OLN93 were cultured on uncoated coverslips in normal growth medium or on PLL-coated ones in differentiation medium. 4 days before cell lysis, cells were left untreated or the medium was supplemented with

different NOS inhibitors. None of the treatments did alter the expression of nNOS. This confirms the hypothesis that NOS inhibitors do not have an influence on the expression of the enzyme but only act on its activity. Moreover, the weak expression of nNOS in OLN93 seen in immunofluorescences was confirmed. Unfortunately, the antibodies against eNOS were not working properly on western blot and it was not possible to investigate the dependence of the eNOS expression levels on MAP1B since no MAP1B negative OLN93 cells were available.

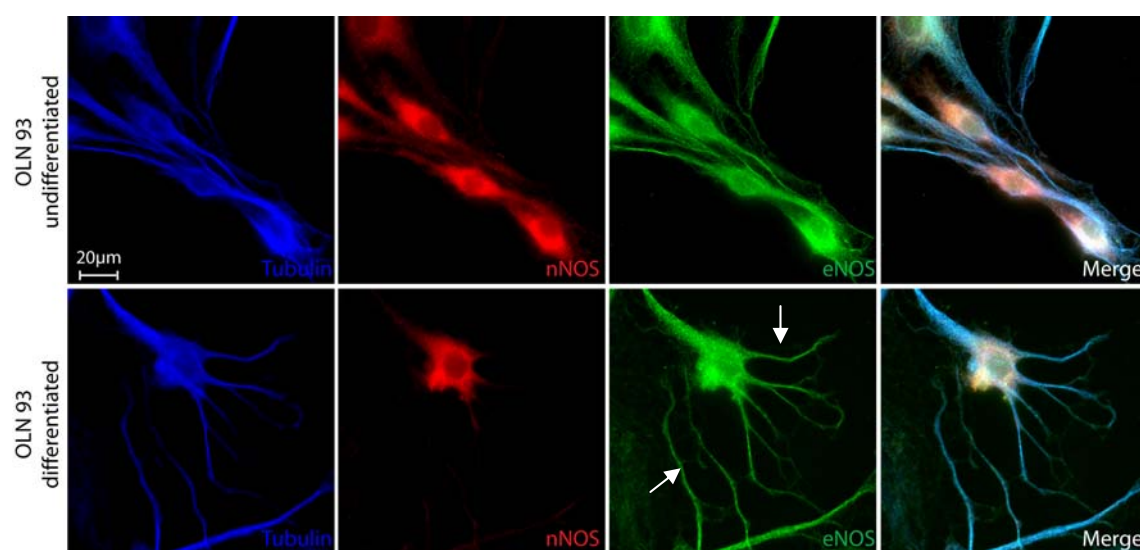


**Figure 35: Expression of nNOS and eNOS in OLN93.**

OLN93 cells were cultured in normal growth medium on uncoated coverslips (undifferentiated, upper panel) or in differentiation medium on PLL-coated coverslips (differentiated, lower panel) for 3 days. Then, cells were fixed and stained for tubulin, nNOS and eNOS. The oligodendrocyte cell line expresses in undifferentiated and differentiated stages nNOS and eNOS. The level of nNOS expression seems rather low and restricted to the cell body, whereas eNOS is strongly expressed throughout the cell, is found in cellular processes of differentiated cells (arrows) and co-localizes with tubulin.

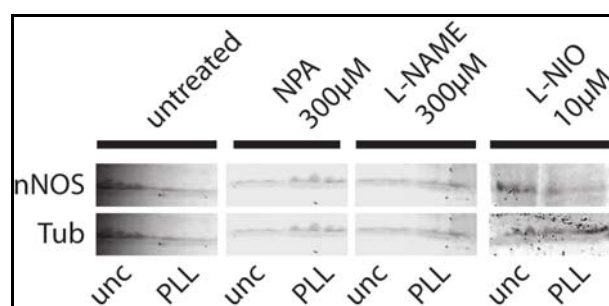


**Figure 36: Western blot analysis of the expression of nNOS in OLN93.**

Western blot analyses were performed of OLN93 cells cultured for 4 days in normal growth medium on uncoated dishes (unc, undifferentiated) or cells grown in differentiation medium on PLL-coated dishes (PLL, differentiated). The cell line shows weak expression of nNOS, unaffected by the coating. 4 days

before cell lysis, OLN93 were left untreated or the medium was supplemented with different NOS-inhibitors. The level of nNOS-expression did not change upon these treatments. Expression of eNOS could not be analysed due to lack of satisfying antibodies against eNOS.

Taken together, these results show that both mouse primary oligodendrocytes and the rat cell line OLN93 express MAP1B from early to late stages of differentiation. Additionally, both cell types express comparable amounts of NOS enzymes what makes OLN93 a useful model for primary oligodendrocytes regarding effects of NOS activating reagents.

### **Localization of peroxisomes and mitochondria in oligodendrocytes**

In cells bearing processes, such as neurons or glia like oligodendrocytes, organelles like peroxisomes or mitochondria need to be transported along microtubules in order to reach parts distant from the cell body. Peroxisomes are responsible for removing toxic products in the cell and play a role in many metabolic pathways. Their localization and function might be affected by microtubule associated proteins. The lack of MAP1B could influence the velocity of their anterograde or retrograde transport and thereby modify the localization. In order to address this question, wild-type and MAP1B<sup>-/-</sup> oligodendrocytes were stained for peroxisomes after 5 days of differentiation (Figure 37A). Peroxisomes localized primarily to the cell body of oligodendrocytes. In addition, many peroxisomes were found along the processes, especially at the branch points. No role for MAP1B in peroxisomes transport could be found by immunofluorescence as wild-type and MAP1B<sup>-/-</sup> cells show the same distribution of these organelles.

MAP1B has been shown to influence the retrograde transport of mitochondria in neurons<sup>27</sup>. Since mitochondria are the main energy provider for a cell, it is essential for these organelles to be located correctly in order to function in a proper way. A reagent called mitotracker is a way to stain mitochondria in the living cell in order to analyse their motility using time lapse microscopy. I wanted to investigate mitochondria movement in wild-type and MAP1B<sup>-/-</sup> oligodendrocytes and the effect of increased NO-levels on their motility. Unfortunately, staining of mitochondria in live cells turned out to be very toxic for oligodendrocytes. Thus, I was not able to follow the mitochondrial movement in living cells. However, the localization of these organelles could be

investigated by the use of antibodies against ATP-synthase (Figure 37B). Mitochondria were localized mainly in the cell body and in the primary processes of oligodendrocytes and in smaller processes they were found too. There is no special enrichment at the tips although this is the site of local protein synthesis for the generation of the myelin sheath which requires much energy. Wild-type and MAP1B<sup>-/-</sup> oligodendrocytes displayed a similar number and localization of mitochondria. Thus, the MAP1B-dependent increase of retrograde mitochondrial motility, which can be seen in neurons, does not appear to take place in oligodendrocytes. Otherwise, an enrichment of mitochondria would have been seen in the cell body.

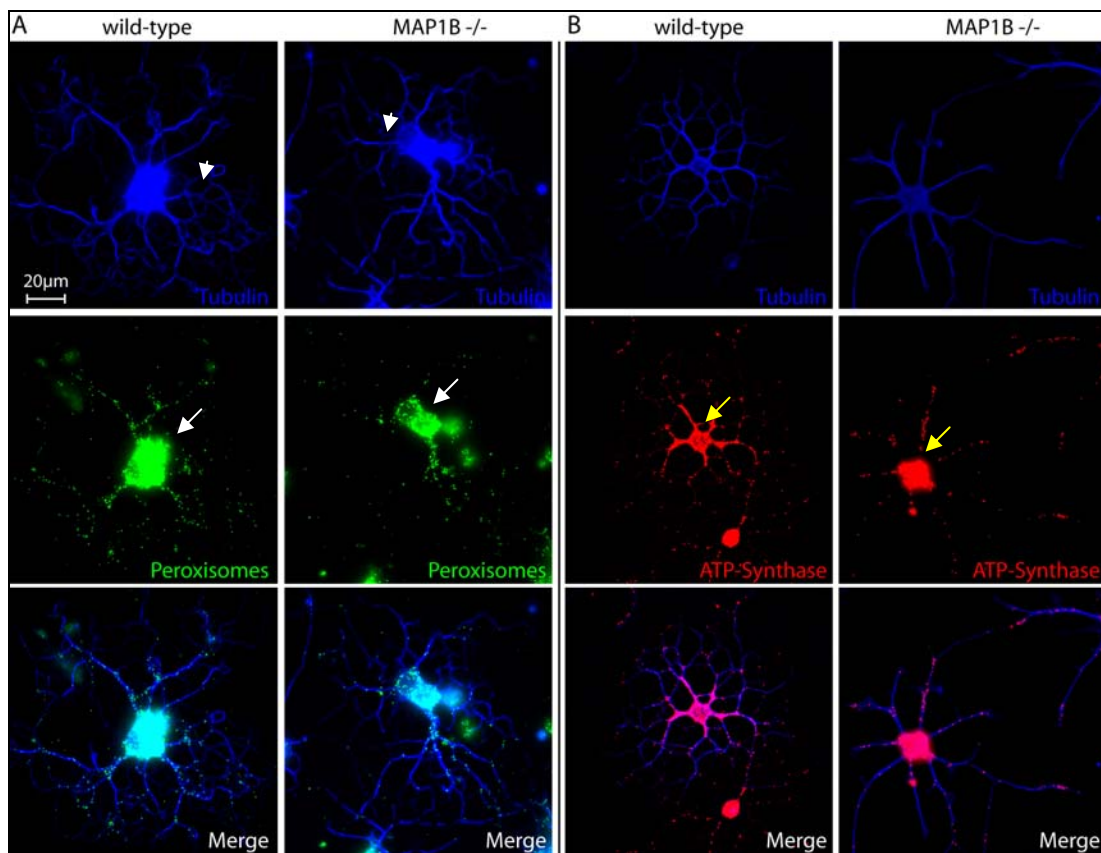


**Figure 37: Localization of peroxisomes and mitochondria in wild-type and MAP1B<sup>-/-</sup> oligodendrocytes.**

Wild-type and MAP1B<sup>-/-</sup> oligodendrocytes were cultured for five days in differentiation medium on poly-D-lysine coated coverslips and fixed. A) Wild-type and MAP1B<sup>-/-</sup> oligodendrocytes were stained for peroxisomes and tubulin. No difference between wild-type and MAP1B<sup>-/-</sup> oligodendrocytes was observed concerning the distribution of peroxisomes. They were found distributed mainly in the cell body (white arrows) and at branch points (white arrowheads), but also along all processes. B) Wild-type and MAP1B<sup>-/-</sup> oligodendrocytes were stained for tubulin and mitochondria. Mitochondria were stained with antibodies against ATP-synthase. Wild-type and MAP1B<sup>-/-</sup> oligodendrocytes do not show any difference

in the localization of mitochondria. The organelles are found mainly in the cell body (yellow arrows) and are distributed uniformly along the processes.

### **Expression and localization of EF1 $\alpha$ in OPCs**

An important factor for protein synthesis is the elongation factor 1 alpha (EF1 $\alpha$ ). EF1 $\alpha$  is required for polypeptide elongation during protein synthesis. It has been shown that MAP1B, EF1 $\alpha$  and staufen1 co-localize in ribonucleoprotein (RNP) granules (Steffel, PhD Thesis 2007). In MAP1B<sup>-/-</sup> DRG neurons EF1 $\alpha$  and staufen1 expression are reduced as well as the number of RNPs which suggests that MAP1B plays a role in generation of RNPs and/or their transport. The localization and expression level of EF1 $\alpha$  were tested in wild-type and MAP1B<sup>-/-</sup> OPCs by immunofluorescence (Figure 38). Wild-type and MAP1B<sup>-/-</sup> OPCs were cultured in differentiation medium, fixed and stained with antibodies against EF1 $\alpha$ . In both cell types EF1 $\alpha$  is expressed in the cell body and faintly in primary processes. EF1 $\alpha$  was found in some branch points along the processes but not at the end of any process where it could have played a role in local synthesis of myelin specific proteins like MBP, MAG or galactocerebroside (GalC). A possible reason for that could be the early differentiation stage of the cells analysed. Perhaps EF1 $\alpha$  is transported to the tips of processes right before the cell achieves terminal differentiation. It was not found in RNP-resembling structures and, in contrast to DRG neurons, no difference between wild-type and MAP1B<sup>-/-</sup> OPCs could be observed in the level of expression.

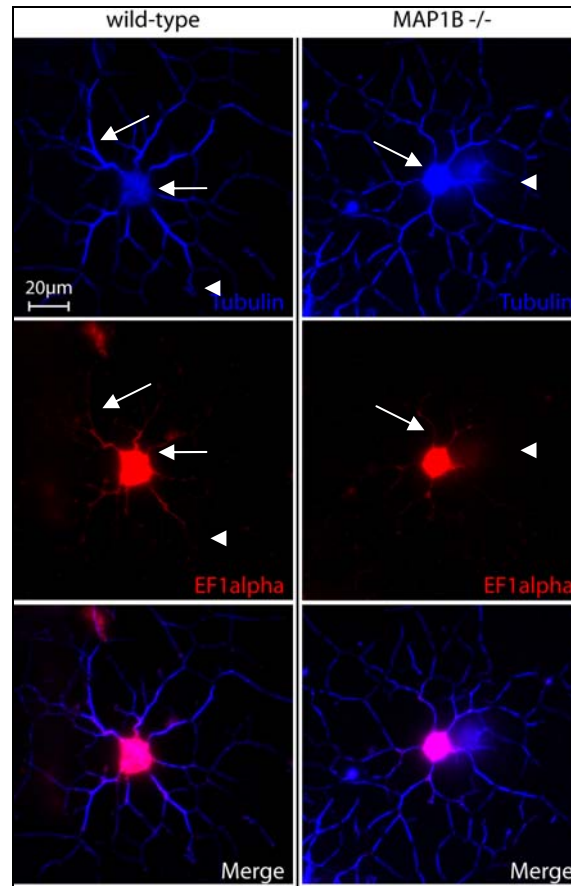


**Figure 38: Expression and localization of EF1 $\alpha$  in wild-type and MAP1B<sup>-/-</sup> OPCs.**

Wild-type and MAP1B<sup>-/-</sup> OPCs were cultured for 2 days in differentiation medium, fixed and stained for EF1 $\alpha$  in red and tubulin in blue. EF1 $\alpha$  is expressed weakly in the cell body (arrows), in primary processes and at some branch points. No EF1 $\alpha$  could be found for instance at the tips of the processes (arrowheads) where it might play a role for local protein synthesis. The lack of MAP1B does not change the expression level or the localization of EF1 $\alpha$  in the OPCs.

#### **Differentiation of wild-type and MAP1B<sup>-/-</sup> oligodendrocytes**

Previous experiments showed that the lack of MAP1B does not change the general morphology of oligodendrocytes at early stages of differentiation (Figure 32). However, the most important feature of these cells is the generation and maintenance of several myelin sheaths in order to protect nerve cell process and to allow rapid nerve conduction velocity. Oligodendrocyte precursor cells (OPC) are easy to distinguish from mature oligodendrocytes by their morphology. At early stages, OPCs exhibit straight processes with a few branches. Their processes can be very long and thin. Myelin specific proteins are not yet expressed or co-localize still with tubulin. In contrast, in terminally differentiated oligodendrocytes, the processes look completely



different. Primary processes become much thicker and the branching is enhanced. Nevertheless, the tips of the processes are very thin and interact with each other in order to form the characteristic shape of myelin bearing oligodendrocytes which can be seen in Figure 39. The microtubule scaffold of myelin sheaths is often hard to detect because of the delicate nature of the tubulin structures. At this stage, the cells express the myelin specific proteins mainly in the peripheral sheaths. Nevertheless, the co-localization with tubulin remains. During the differentiation, not only growth and branching take place but a complete rearrangement of the cytoskeleton is necessary to afford these remarkable morphological changes. Transport of ribosomes and mRNA encoding MBP, MAG and other proteins along microtubules is very important for the correct synthesis of myelin. Microtubule associated proteins and their ability to influence the stability of microtubules might play an important role in the mechanism of myelination and its maintenance. I compared the differentiation efficiency of wild-type and MAP1B<sup>-/-</sup> oligodendrocytes. To this end, oligodendrocytes were cultured for several days in differentiation medium until myelin sheaths became visible. Oligodendrocytes were then stained with antibodies against different markers for terminal differentiation. Such markers are GalC, MBP and MAG, which are essential components of myelin. Unfortunately, GalC antibodies did not work properly, thus, only MBP and MAG staining could be analysed. In culture, oligodendrocytes need 5-7 days to differentiate. However, the culture remains always very heterogenous and not all cells show the same stage of differentiation. Wild-type and MAP1B<sup>-/-</sup> oligodendrocytes both differentiated well in culture. At the beginning of the differentiation process, they showed the typical co-localization of tubulin and myelin specific proteins (not shown) and, at later stages, normal generation of myelin sheaths could be observed. Figure 39 shows terminally differentiated wild-type and MAP1B<sup>-/-</sup> oligodendrocytes stained in blue for tubulin, in red for MAG and in green for MBP. MAG and MBP are expressed at similar levels and show typical localization in flat myelin sheaths regardless of the presence or absence of MAP1B.

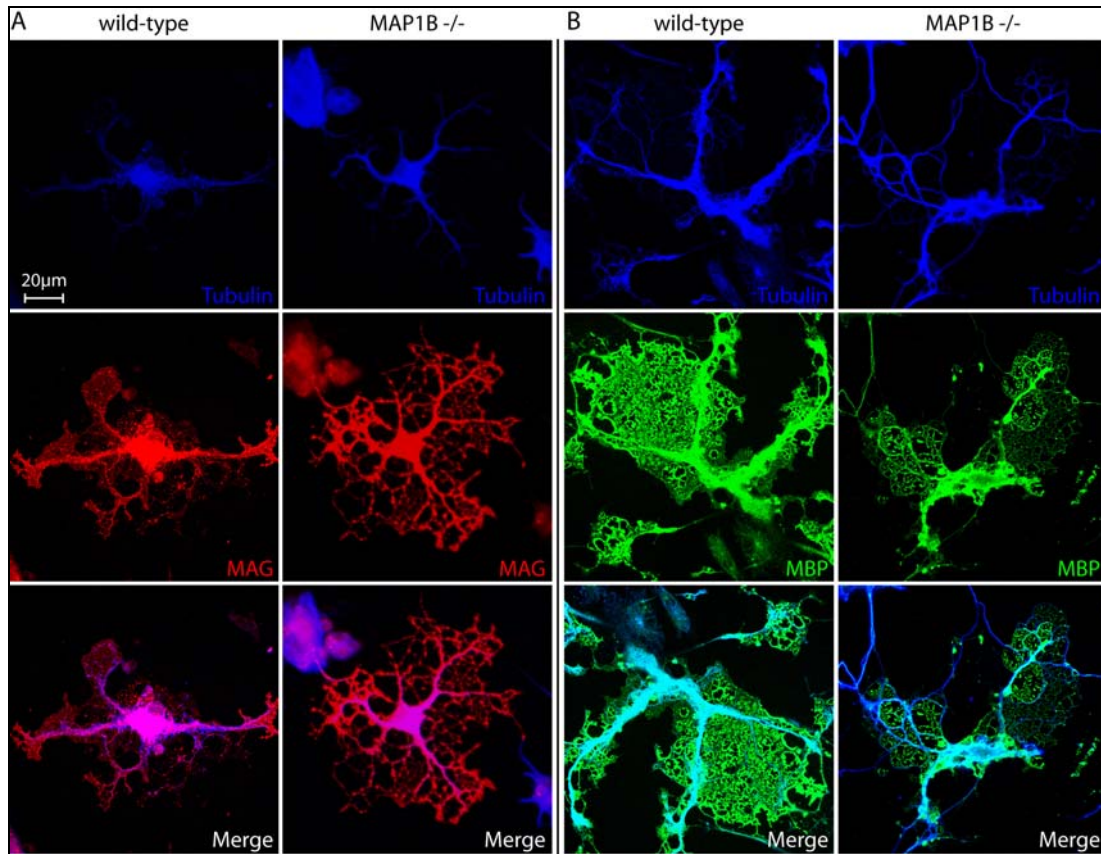


**Figure 39: Differentiated wild-type and MAP1B<sup>-/-</sup> oligodendrocytes.**

Wild-type and MAP1B<sup>-/-</sup> oligodendrocytes were cultured for 5 days in differentiation medium until they reached terminal differentiation. Cells were fixed and stained for tubulin and MAG (A) or MBP (B). Wild-type and MAP1B<sup>-/-</sup> oligodendrocytes did not differ in morphology of myelin sheaths. MAG and MBP were expressed and correctly localized. Both cell types showed all characteristics of a myelin producing oligodendrocyte. Thus, MAP1B<sup>-/-</sup> oligodendrocytes did not seem to be impaired in differentiation.

Next, I assessed the percentage of terminally differentiated oligodendrocytes compared to undifferentiated cells in wild-type and MAP1B<sup>-/-</sup> cultures (Figure 40). There was a difference in the number of MBP-expressing cells in wild-type and MAP1B<sup>-/-</sup> oligodendrocytes (7% in wild-type compared to 3% in MAP1B<sup>-/-</sup> oligodendrocytes). Likewise, I could observe that MAP1B<sup>-/-</sup> oligodendrocytes showed a higher ratio of differentiated cells expressing MAG than wild-type cells (6% in wild-type cultures compared to 25% in MAP1B<sup>-/-</sup> cultures). A possible explanation is that generally, MAP1B<sup>-/-</sup> oligodendrocytes survived slightly better than their wild-type counterparts. Thus, there were always more MAP1B<sup>-/-</sup> cells that had the chance to differentiate than wild-type cells. However, the exact reason for this observation was not investigated in more detail.



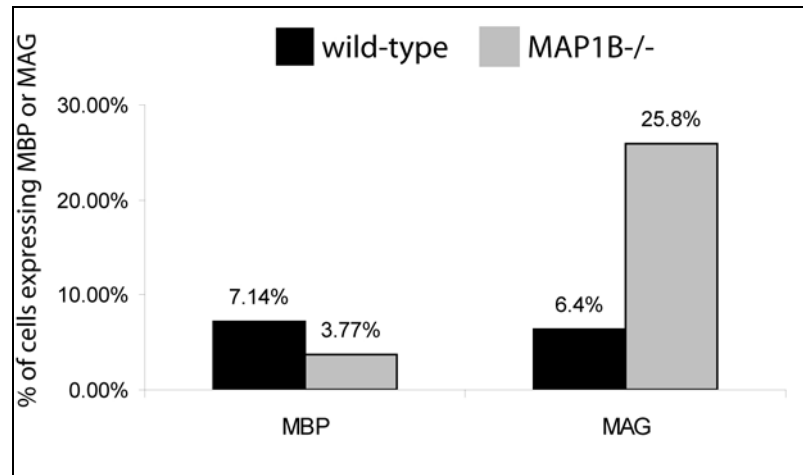


**Figure 40: Percentage of oligodendrocytes expressing MBP or MAG after 7 days of differentiation.**

Wild-type and MAP1B<sup>-/-</sup> oligodendrocytes were cultured for 7 days in differentiation medium until they reached terminal differentiation. Cells were fixed and stained for tubulin and MAG or MBP. The graph shows the percentage of MBP or MAG positive wild-type and MAP1B<sup>-/-</sup> oligodendrocytes. For quantitative analysis, approximately 100 cells were assessed for protein expression. Cells were considered expressing MBP or MAG when the protein was found in sheaths and was not colocalizing with tubulin only, as it is the case in early differentiation stages. There was a striking difference in the percentage of MBP expressing cells: in wild-type cultures 7% of the cells showed MBP expression after 7 days in culture in differentiation medium compared to 3% of MAP1B<sup>-/-</sup> oligodendrocytes. Regarding MAG expression, MAP1B<sup>-/-</sup> oligodendrocytes appear to differentiate better than wild-type cells: 6% of wild-type cells express MAG after the same culture period, whereas in MAP1B<sup>-/-</sup> oligodendrocyte cultures, 25% of the cells are MAG positive after 7 days.

## Effect of increased NO concentration on OPCs and oligodendrocytes

### Reaction of undifferentiated wild-type and MAP1B<sup>-/-</sup> OPCs to the NO-donor SNAP

High concentrations of nitric oxide lead to MAP1B dependent axon retraction in mouse DRG neurons. Oligodendrocytes were also shown to be sensitive to increased NO-levels<sup>7</sup>. This raised the question whether S-nitrosylation of MAP1B mediates the toxic effect of NO in oligodendrocytes. In neurons S-nitrosylation of MAP1B leads to increased microtubule binding of the protein which finally leads to retraction of axons. There could be a related mechanism taking place in oligodendrocytes resulting in withdrawal of myelin bearing processes from neurites, including degeneration of myelin sheaths. Eventually, this would render nerve conduction impossible and cause neurodegenerative diseases. I used two different ways to increase the intracellular NO concentration: the first method is the treatment of cells with the NO-donor SNAP

(S-nitroso-N-acetylpenicillamine) and the second one is the treatment with calcimycin. Calcimycin induces calcium influx and thereby activates many different calcium-dependent pathways in the cell. One of the targets is nNOS which becomes activated and produces NO.

OPCs were cultured for 2 days in differentiation medium. At this stage they do not yet express myelin specific proteins. These undifferentiated OPCs should react stronger to high NO concentrations than differentiated oligodendrocytes<sup>7</sup>. I tried different incubation times and concentrations of SNAP. I started with 100µM for 1h, as it was used for DRG neurons. None of the oligodendrocytes reacted to this treatment (not shown). The cells looked completely unaffected and had long processes with an unchanged cytoskeletal morphology. Thus, I increased the concentration up to 1mM and the incubation time to 5hrs (Figure 41 left panel). Unexpectedly, still no effect could be observed. The microtubules showed a straight shape and no sign of depolymerization of microtubules or retraction. The cells were indistinguishable from untreated ones. The same was observed in SNAP treated OLN93 cells (data not shown). Similarly, EF1α did not exhibit any change in expression or intracellular localization. EF1α was still mainly found in the cell body and only in major processes. Regarding peroxisomes, also no difference occurred. Their distribution in the cell was not altered. Moreover, MAP1B<sup>-/-</sup> OPCs ignored the high NO-levels in the same way as wild-type cells and SNAP-treated MAP1B<sup>-/-</sup> OPCs did not differ at all from the untreated MAP1B<sup>-/-</sup> OPCs (Figure 41, right panel).

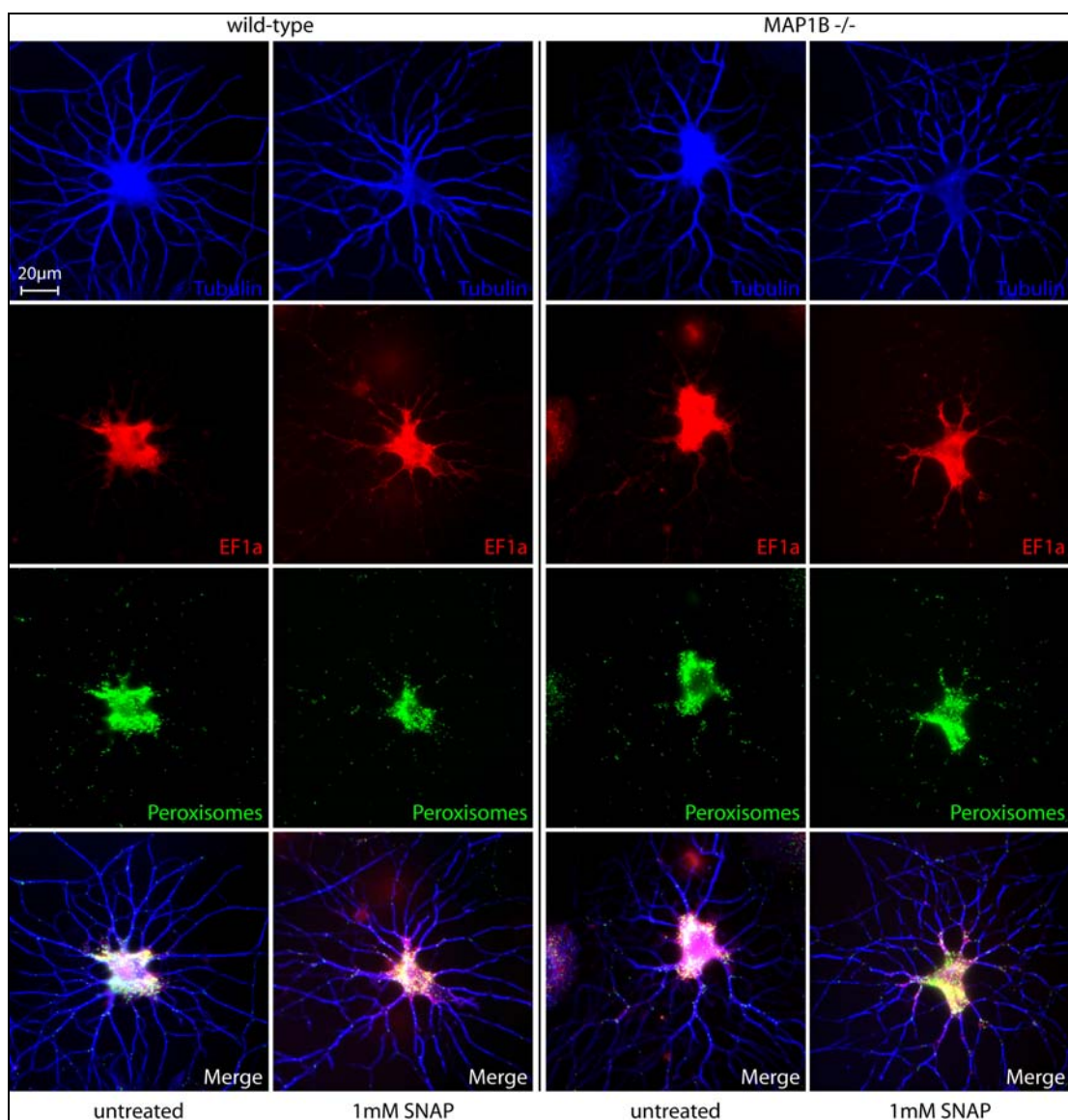


**Figure 41: Localization of EF1 $\alpha$  and peroxisomes after treatment with 1mM SNAP for 5hrs in undifferentiated OPCs.**

Wild-type and MAP1B<sup>-/-</sup> OPCs were cultured for 2 days in differentiation medium, were left untreated or were treated with 1mM SNAP for 5hrs, fixed and stained for tubulin, EF1 $\alpha$  and peroxisomes. They did not show any difference in the microtubule organization or in the expression level and the localization of EF1 $\alpha$  after the treatment with SNAP. Similarly, the distribution of peroxisomes remained unchanged at high NO-levels.

Mitochondria have been shown to be damaged in different ways by NO. One example is the impairment of their motility in cortical neurons<sup>262</sup>. As already mentioned above, life cell imaging of mitochondria was not feasible in oligodendrocytes. Thus, whether SNAP affects movements of mitochondria could not be analysed. In order to investigate the influence of NO on mitochondrial localization in OPCs I stained the cells with antibodies against ATP-synthase and tubulin and compared the localization of

mitochondria in wild-type and MAP1B<sup>-/-</sup> cells untreated or treated with 1mM SNAP for 5hrs (Figure 42). Regarding the localization of mitochondria, no difference between untreated and treated cells could be seen. Mitochondria were distributed in a normal way all over wild-type and MAP1B<sup>-/-</sup> OPCs after the SNAP treatment.

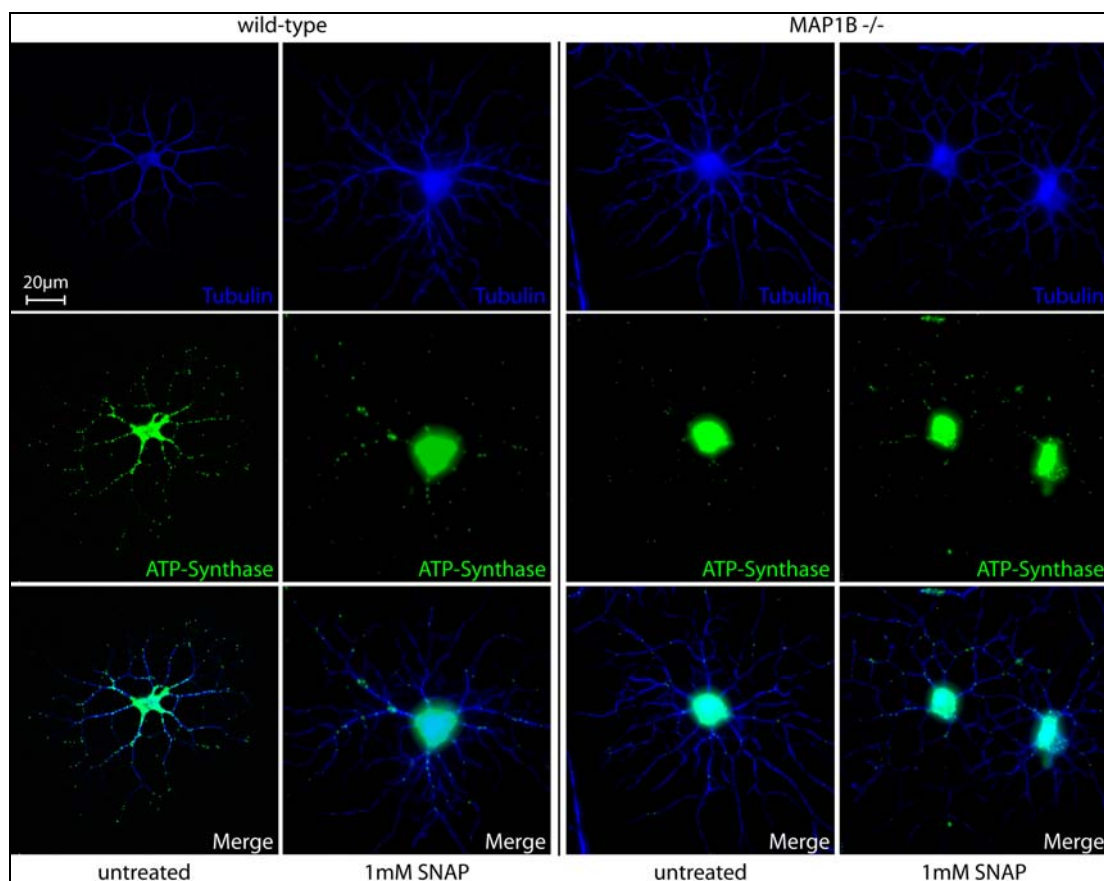


**Figure 42: Localization of mitochondria in wild-type and MAP1B<sup>-/-</sup> OPCs after treatment with 1mM SNAP.**

Wild-type and MAP1B<sup>-/-</sup> OPCs were cultured for 2 days in differentiation medium, were left untreated or were treated with 1mM SNAP for 5hrs, fixed and stained for tubulin and mitochondria. Mitochondria were stained with an antibody against ATP-synthase. Treatment with SNAP did not have any effect on the localization of mitochondria in wild-type or MAP1B<sup>-/-</sup> oligodendrocytes. Wild-type and MAP1B<sup>-/-</sup> cells also showed similar distribution of mitochondria.

Hence, the elevated NO-levels induced by the NO-donor SNAP did not appear to have an impact on anterograde or retrograde transport of peroxisomes and mitochondria. Moreover, their essential function for the survival of the oligodendrocytes might not be harmed either since the immunofluorescences analyses did not reveal any cellular damage of OPCs. However, tests for mitochondrial or peroxisomal functionality have not been performed.

### Reaction of differentiated wild-type and MAP1B<sup>-/-</sup> oligodendrocytes to the NO-donor SNAP

Despite the prevailing view that undifferentiated oligodendrocytes are more sensitive to elevated NO-levels than differentiated cells, I treated more differentiated oligodendrocytes, which were cultured for 4 to 5 days in differentiation medium, with 1mM SNAP for 5hrs before fixation and staining. However, the same complacency about SNAP treatment was observed in those cells (Figure 43). The microtubules remained unchanged in wild-type and MAP1B<sup>-/-</sup> oligodendrocytes. And once more, EF1 $\alpha$  and peroxisomes localization was the same as in untreated cells. They were again found mainly in the cell body and in proximal parts of the cells.

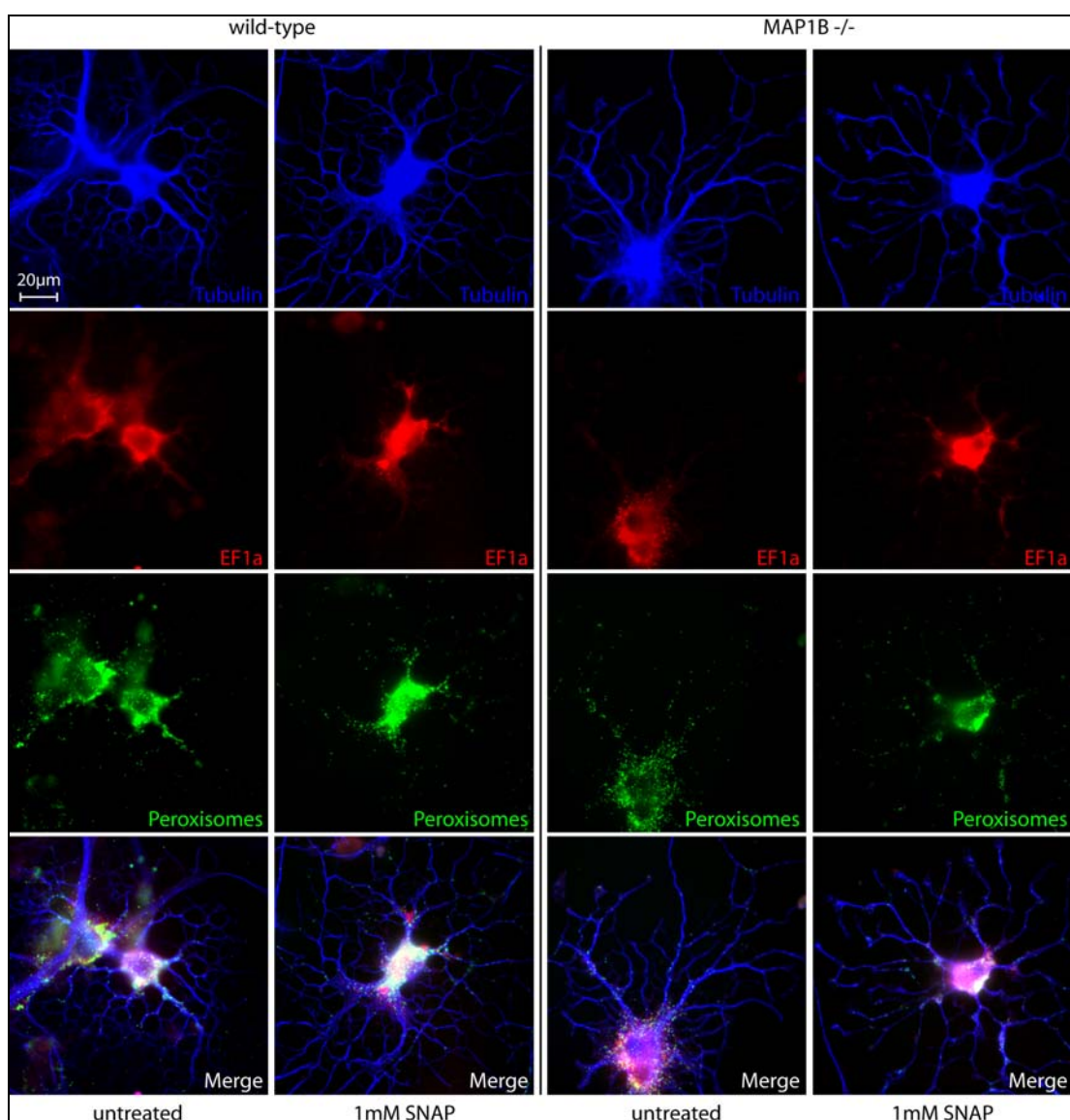


**Figure 43:** Localization of EF1 $\alpha$  and peroxisomes after treatment with 1mM SNAP for 5hrs in early differentiated oligodendrocytes.

Wild-type and MAP1B<sup>-/-</sup> oligodendrocytes were allowed to differentiate for 4 days in culture and were left untreated or were treated with 1mM SNAP for 5hrs. The cells were stained for tubulin, EF1 $\alpha$  and peroxisomes. The tubulin staining did not show any change or sign of retraction and the cells do not show any difference in the localization of EF1 $\alpha$  and peroxisomes after the treatment. EF1 $\alpha$  and peroxisomes show normal expression and localization respectively. Likewise, no difference was observed between untreated wild-type and MAP1B<sup>-/-</sup> oligodendrocytes.

In diverse neurodegenerative diseases elevated NO-levels have been found at sites of damaged nervous tissue. As I could show in previous experiments, MAP1B does obviously not play any role in the development of oligodendrocytes including the differentiation and generation of myelin *in vitro*. Nevertheless, the question remains whether the lack of MAP1B delays or enhances any reaction of myelinating oligodendrocytes to high NO-levels. Moreover, the possible role of MAP1B in the mechanism of demyelination was an interesting topic for this thesis. In order to investigate whether high intracellular NO-levels lead to destruction of myelin in a MAP1B-dependent way, I treated terminally differentiated oligodendrocytes with SNAP and stained them for tubulin and MAG (Figure 44). Despite the expected toxicity of the highly concentrated SNAP, the myelin sheaths of both wild-type and MAP1B<sup>-/-</sup> oligodendrocytes were not affected at all by this treatment. MAG-staining revealed spreadout myelin sheaths in wild-type and MAP1B<sup>-/-</sup> oligodendrocytes before and after SNAP treatment. Similarly, microtubules did not show any difference and oligodendroglial processes did neither retract nor collapse. These results show that, although high NO-levels in oligodendrocytes were suggested to be toxic for these cells, treatment with 1mM SNAP *in vitro* does not harm oligodendrocytes. Perhaps a longer treatment would have been necessary to see an effect of the drug on microtubules, organelle behavior or myelin sheaths.



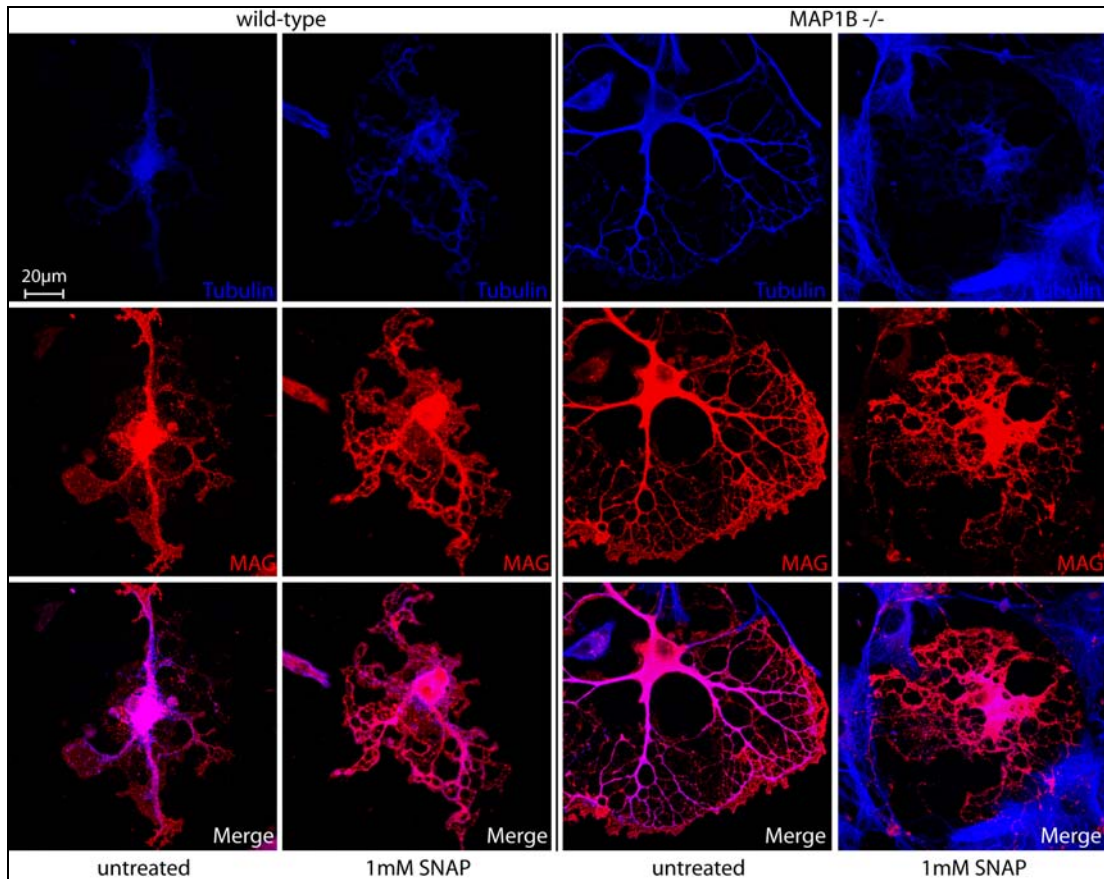


**Figure 44: Expression and localization of MAG in terminally differentiated wild-type and MAP1B<sup>-/-</sup> oligodendrocytes after a treatment with 1mM SNAP for 5hrs.**

Wild-type and MAP1B<sup>-/-</sup> oligodendrocytes were cultured for 5 days in differentiation medium until they reached terminal differentiation. Cells were left untreated or were treated with 1mM SNAP for 5hrs, fixed and stained for tubulin and MAG. Localization and expression level of MAG did not differ in wild-type or MAP1B<sup>-/-</sup> cells. Terminally differentiated oligodendrocytes did not show any reaction to the treatment with SNAP. The myelin sheaths remained undamaged and the tubulin network did not show any sign of retraction or collapse.

#### **Effect of calcium influx and subsequent NOS activation in oligodendrocytes**

The second way to increase the NO concentration is the addition of the ionophor calcimycin to the cells. This causes an influx of calcium which activates, among other things, nNOS and eNOS. In mouse DRG neurons calcimycin induces activation of nNOS and subsequently results in MAP1B-dependent axon retraction which can be prevented by inhibition of nNOS. I showed that oligodendrocytes express nNOS and eNOS, thus, calcimycin might lead also in these cells to increased NO-production and process retraction. Wild-type and MAP1B<sup>-/-</sup> oligodendrocytes were cultured 5 days in differentiation medium. 15min before fixation calcimycin was added to the medium.

Then oligodendrocytes were stained for tubulin and MBP in order to investigate the effect on the cytoskeleton and the myelin sheaths. Incubation with calcimycin led in most wild-type cells to complete lysis (Figure 45). The microtubule network collapsed completely, and the myelin sheaths were also destroyed. Only a few oligodendrocytes did not react that strongly (see figure 48 and 49). The calcimycin-induced calcium influx is a potential activator of several signaling pathways. In order to distinguish the effects of NOS activation by calcimycin from other  $\text{Ca}^{2+}$  dependent signaling pathways, cells were pretreated for one hour with the inhibitors of different NO-synthases. NPA (300 $\mu\text{M}$ ) was used to specifically inhibit nNOS, L-NAME (300 $\mu\text{M}$ ) for NOS inhibition (unspecific nNOS and eNOS inhibition) and L-NIO (10 $\mu\text{M}$ ) for specific inhibition of eNOS. Control samples were left untreated or were treated with NOS inhibitor only. Those cells did not differ from untreated ones (not shown). Wild-type cells were pretreated with NPA or L-NAME before addition of calcimycin appeared to be protected against the toxicity of calcimycin. More cells were found undamaged in the culture than in the sample with calcimycin only. These cells exhibited mostly normal microtubule morphology and had even kept their myelin sheaths. In contrast, inhibition of eNOS with L-NIO did not prevent calcimycin induced cell collapse in wild-type oligodendrocytes. Whether these oligodendrocytes underwent apoptosis or necrosis was not tested. These results suggest that in wild-type oligodendrocytes, the toxicity of calcimycin is mediated by the activation of nNOS and increased NO production and this effect can be prevented by the inhibition of nNOS with NPA or L-NAME.



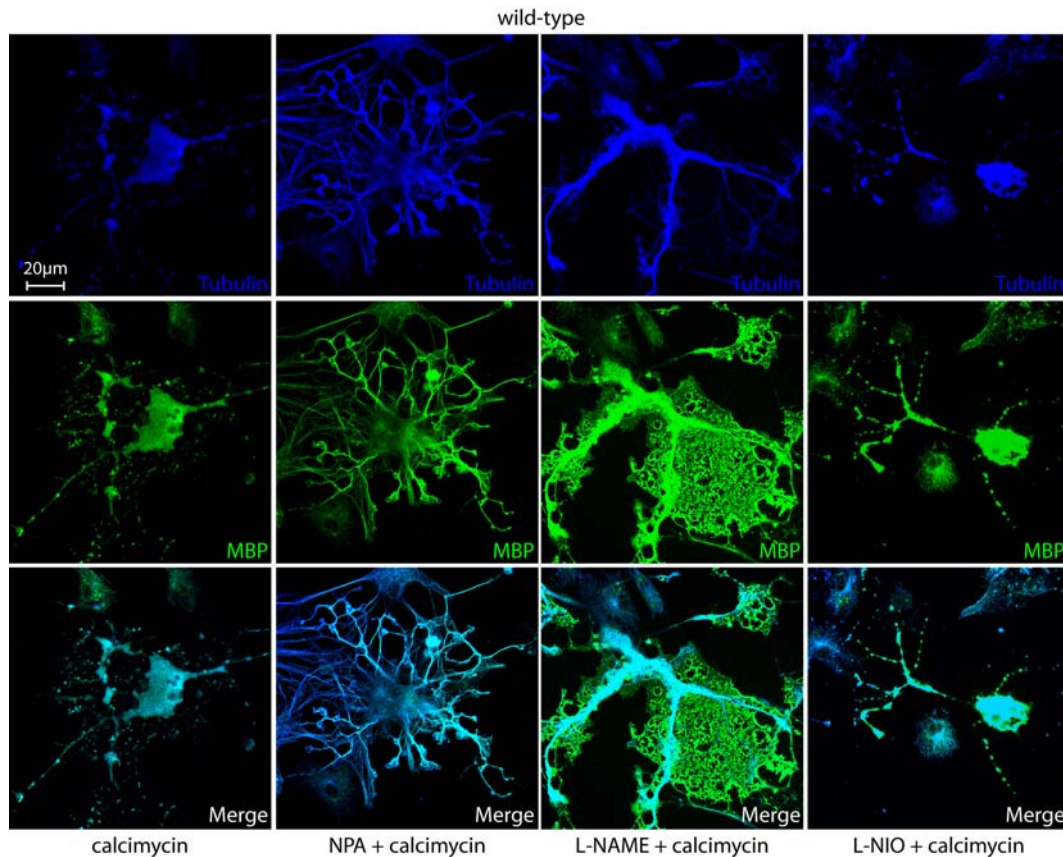


**Figure 45: Inhibition of nNOS but not eNOS prevents calcimycin toxicity in wild-type oligodendrocytes.**

Wild-type oligodendrocytes were cultured for 5 days in differentiation medium. Terminally differentiated cells were treated with 1µM calcimycin for 15min or with NOS inhibitors NPA (300µM), L-NAME (300µM) or L-NIO (10µM) for 1h followed by treatment with 1µM calcimycin for 15min, as indicated. Control samples were left untreated or were treated with a NOS inhibitor only. These cells did not show any remarkable change compared to untreated samples (not shown). In contrast, oligodendrocytes reacted to the treatment with 1µM calcimycin for 15min with collapsed myelin sheaths and tubulin network. Inhibition of nNOS by NPA or L-NAME could prevent this striking effect, whereas inhibition of eNOS with L-NIO did not help to protect cells against the toxic calcium influx induced by calcimycin.

The same assay was performed with MAP1B<sup>-/-</sup> oligodendrocytes which were shown to express nNOS at the same level as wild-type oligodendrocytes, in contrast to eNOS expression, which might be slightly enhanced. Similar to wild-type cells, MAP1B<sup>-/-</sup> oligodendrocytes reacted to calcimycin by a complete collapse of the cytoskeleton including the myelin sheaths (Figure 46). Almost no cells survived in the calcimycin treated samples. Thus, MAP1B does not seem to be essential in the mechanisms activated by calcimycin that lead to collapse of oligodendrocytes. In contrast to wild-type oligodendrocytes, inhibition of nNOS by NPA did not prevent calcimycin-induced cell death. The same phenotype as in cells which were not

pretreated with a nNOS inhibitor was observed. Most of the cells showed complete collapse and only cell remnants could be found in the culture. However, L-NIO and L-NAME, which is also inhibiting eNOS, could rescue MAP1B<sup>-/-</sup> oligodendrocytes from cell death induced by calcimycin. This suggests that in MAP1B<sup>-/-</sup> oligodendrocytes, only inhibition of eNOS prevents collapse and cell death, and that eNOS and not nNOS is the most important NO producer in these cells.

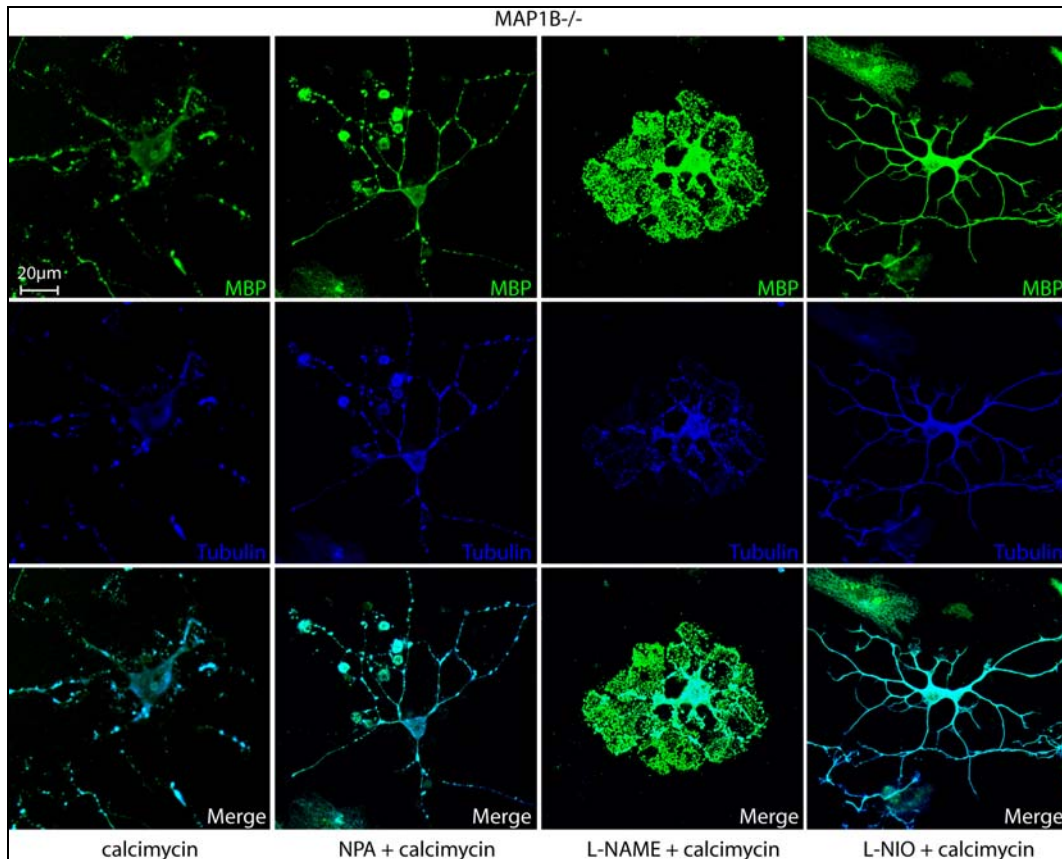


**Figure 46: Inhibition of eNOS but not nNOS prevents calcimycin toxicity in MAP1B<sup>-/-</sup> oligodendrocytes.**

MAP1B<sup>-/-</sup> oligodendrocytes were cultured for 5 days in differentiation medium. Terminally differentiated cells were treated with 1µM calcimycin for 15min or with NOS inhibitors NPA (300µM), L-NAME (300µM) or L-NIO (10µM) for 1h followed by treatment with 1µM calcimycin for 15min, as indicated. Control samples were left untreated or were treated with a NOS inhibitor only. These cells did not show any remarkable change compared to untreated samples (not shown). In contrast, MAP1B<sup>-/-</sup> oligodendrocytes reacted to the treatment with 1µM calcimycin for 15min with collapsed myelin sheaths and tubulin network, as it was the case for wild-type cells. Inhibition of nNOS by NPA could not prevent this striking effect, whereas inhibition of eNOS with L-NIO or L-NAME, a NOS inhibitor with similar potency for nNOS and eNOS, protected cells against the toxic calcium influx induced by calcimycin.

Taken together, these results indicate that in oligodendrocytes calcimycin leads to NOS activation resulting in oligodendrocyte cell death. Interestingly, in wild-type oligodendrocytes nNOS seems to play a more important role than in MAP1B<sup>-/-</sup> oligodendrocytes where mainly eNOS activity and its downstream targets damage the cells. How the lack of MAP1B leads to enhanced importance of eNOS in these cells remains elusive.

In order to confirm the previous results, I treated OLN93 cells with calcimycin (Figure 47). They reacted in the same way as wild-type oligodendrocytes and showed collapsed microtubules independent of the cellular differentiation stage. Again, inhibition of nNOS by NPA prevented calcimycin induced cell death. In those cells, the tubulin network did not show any sign of retraction and the processes remained elongated. Thus, in OLN93, the harmful effect of calcimycin is mediated via nNOS activation.

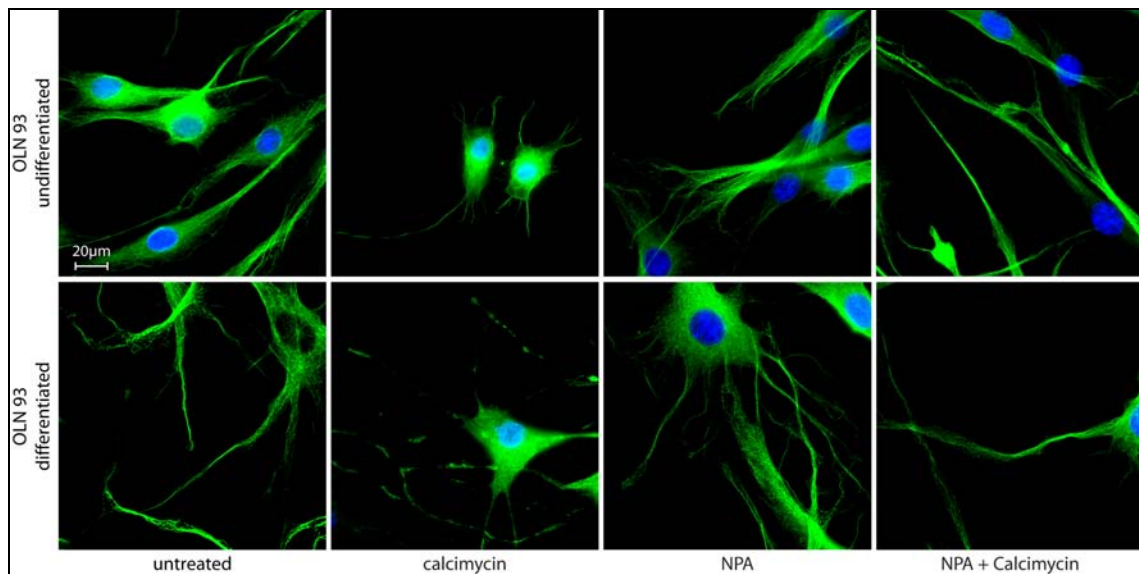


**Figure 47: Inhibition of nNOS prevents calcimycin toxicity in OLN93.**

OLN93 cells were cultured in normal growth medium on uncoated coverslips (undifferentiated, upper panel) or in differentiation medium on PLL-coated coverslips (differentiated, lower panel) for 3 days. Cells were left untreated or were treated with 1µM calcimycin for 15min, with 300µM NPA for 1h, or with 300µM NPA for 1h followed by treatment with 1µM calcimycin for 15min, as indicated, fixed and stained for tubulin and Hoechst. As in the case of wild-type oligodendrocytes, calcimycin lead to cell collapse and inhibition of nNOS by NPA helped to prevent this effect, independent of the stage of differentiation.

Some oligodendrocytes in the samples did not show a strong reaction to calcimycin treatment. In these cells, the analysis of the localization of EF1α and

peroxisomes was still possible (Figure 48). Once more wild-type and MAP1B<sup>-/-</sup> oligodendrocytes were treated with 1 $\mu$ M calcimycin for 15 minutes. In wild-type cells, EF1 $\alpha$  and peroxisome localization was not disturbed by the treatment. Both showed the same distribution as in untreated oligodendrocytes (Figure 37A and Figure 38). In samples that were treated with L-NAME and calcimycin I observed also no change in EF1 $\alpha$  or peroxisome distribution. The same was observed in MAP1B<sup>-/-</sup> oligodendrocytes (Figure 49).

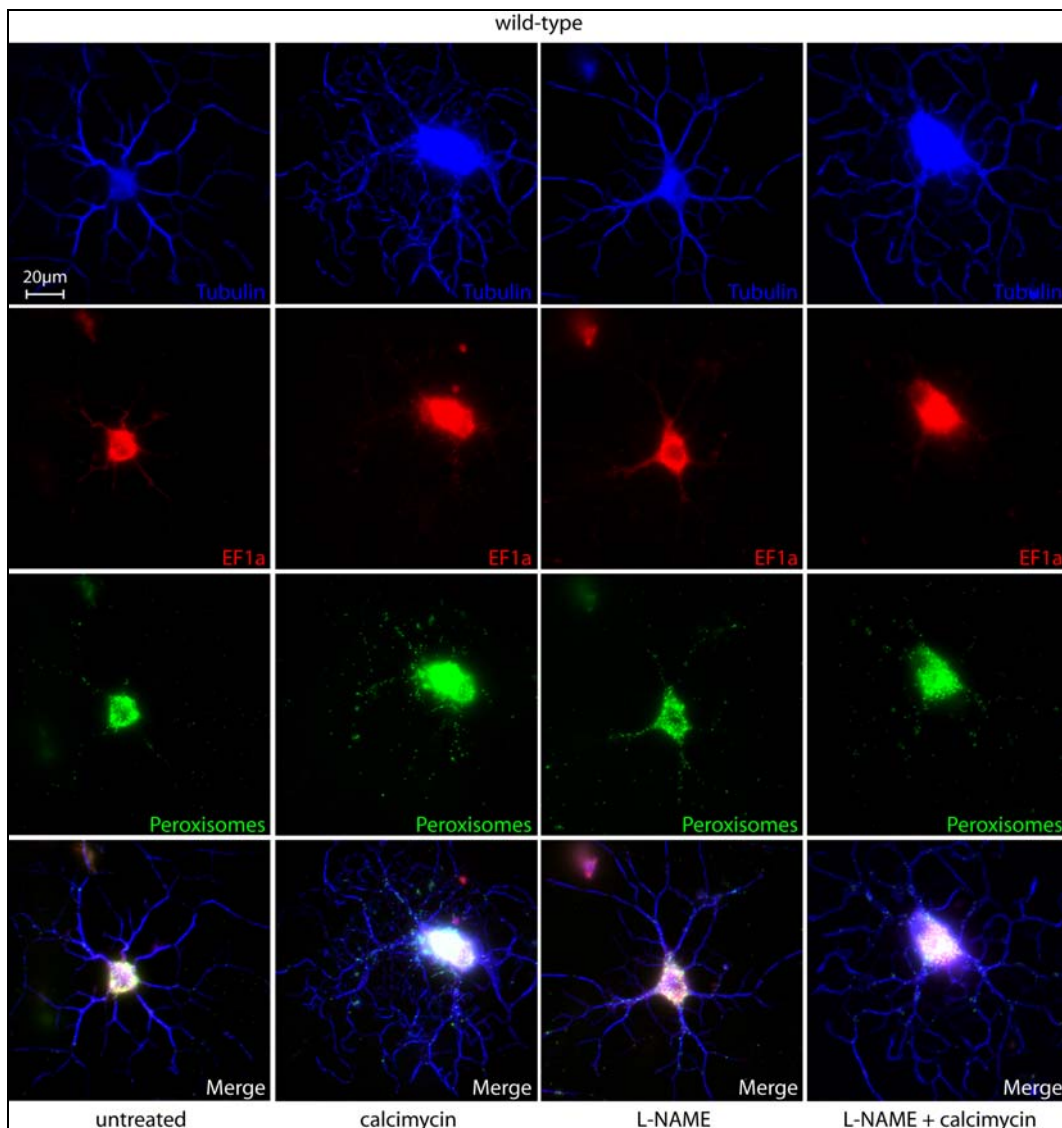


**Figure 48: EF1 $\alpha$  and peroxisome localization was not disturbed by the calcimycin treatment in wild-type oligodendrocytes.**

Wild-type oligodendrocytes were cultured for 5 days in differentiation medium. Terminally differentiated cells were left untreated, were treated with 1 $\mu$ M calcimycin for 15min, with 300 $\mu$ M L-NAME for 1h, or with 300 $\mu$ M L-NAME for 1h followed by a treatment with 1 $\mu$ M calcimycin for 15min, as indicated. A small fraction of wild-type oligodendrocytes treated with 1 $\mu$ M calcimycin for 15min showed only slightly



collapsed morphology. In these cells, the expression level of EF1 $\alpha$  and its localization as well as peroxisomes distribution remained unchanged.

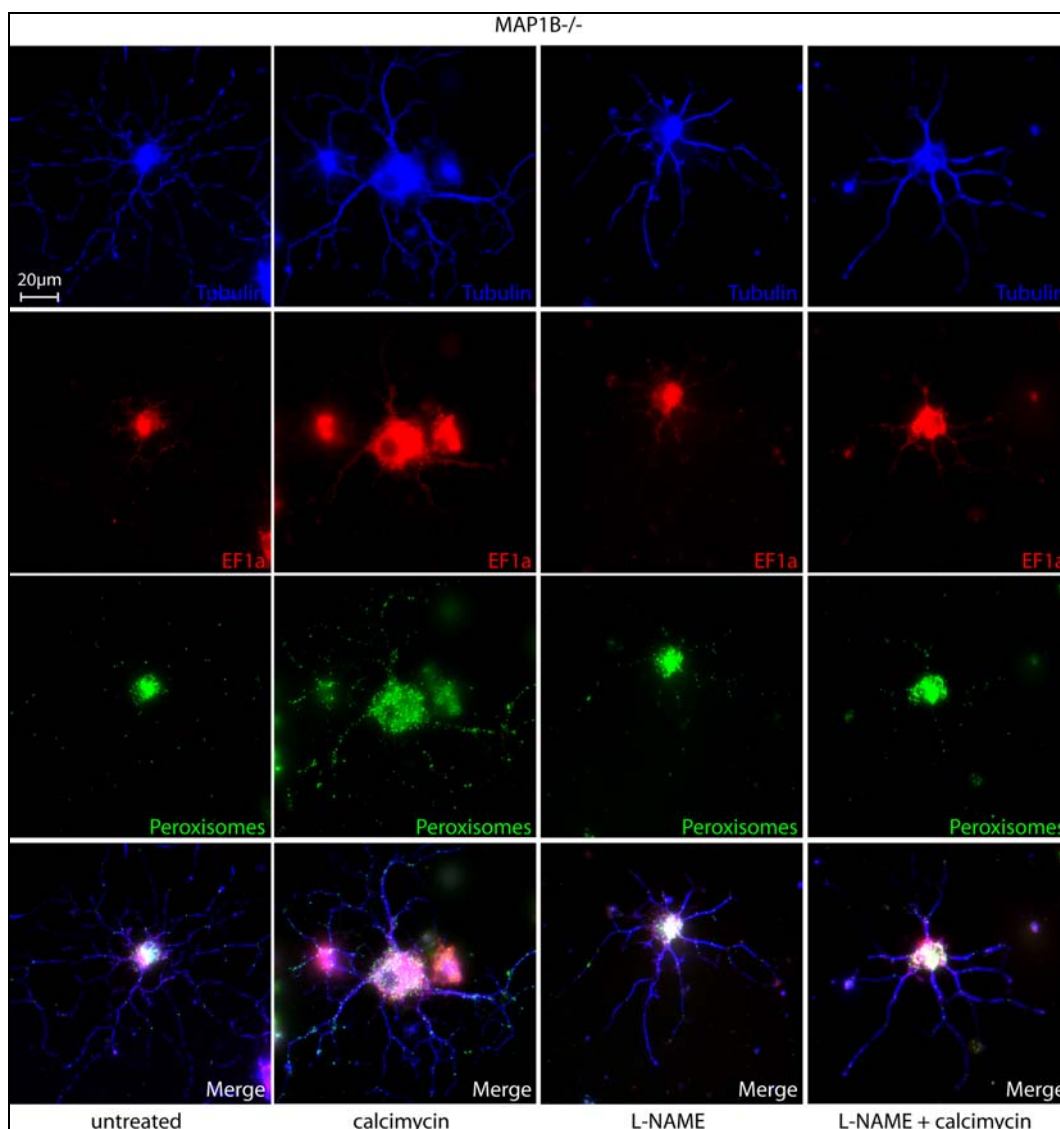


**Figure 49: EF1 $\alpha$  and peroxisome localization was not disturbed by the calcimycin treatment in MAP1B<sup>-/-</sup> oligodendrocytes.**

MAP1B<sup>-/-</sup> oligodendrocytes were cultured for 5 days in differentiation medium. Terminally differentiated cells were left untreated, were treated with 1μM calcimycin for 15min, with 300μM L-NAME for 1h, or with 300μM L-NAME for 1h followed by a treatment with 1μM calcimycin for 15min, as indicated. A small fraction of wild-type oligodendrocytes treated with 1μM calcimycin for 15min showed only slightly collapsed morphology. In these cells, the expression level of EF1 $\alpha$  and its localization as well as peroxisomes distribution remained unchanged.

### Inhibition of NOS leads to process elongation

In experiments with DRG-explants and hippocampal explants, I could show that long term inhibition of NOS leads to enhanced axon elongation. When oligodendrocytes were incubated for several hours in the NOS inhibitor L-NAME several cells started to elongate dramatically their processes. Figure 50 shows wild-type and MAP1B<sup>-/-</sup> oligodendrocytes stained for tubulin and peroxisomes after such a treatment. In both cases, oligodendrocytes display one or two extremely long processes whereas the other processes remain at a normal length. It seems that NOS activation does not only mediate retraction of processes but that its inhibition enables the cells to elongate special processes. In what these processes differ from others which do not elongate is unclear. However, tubulin staining and localization of peroxisomes is similar to the short processes.

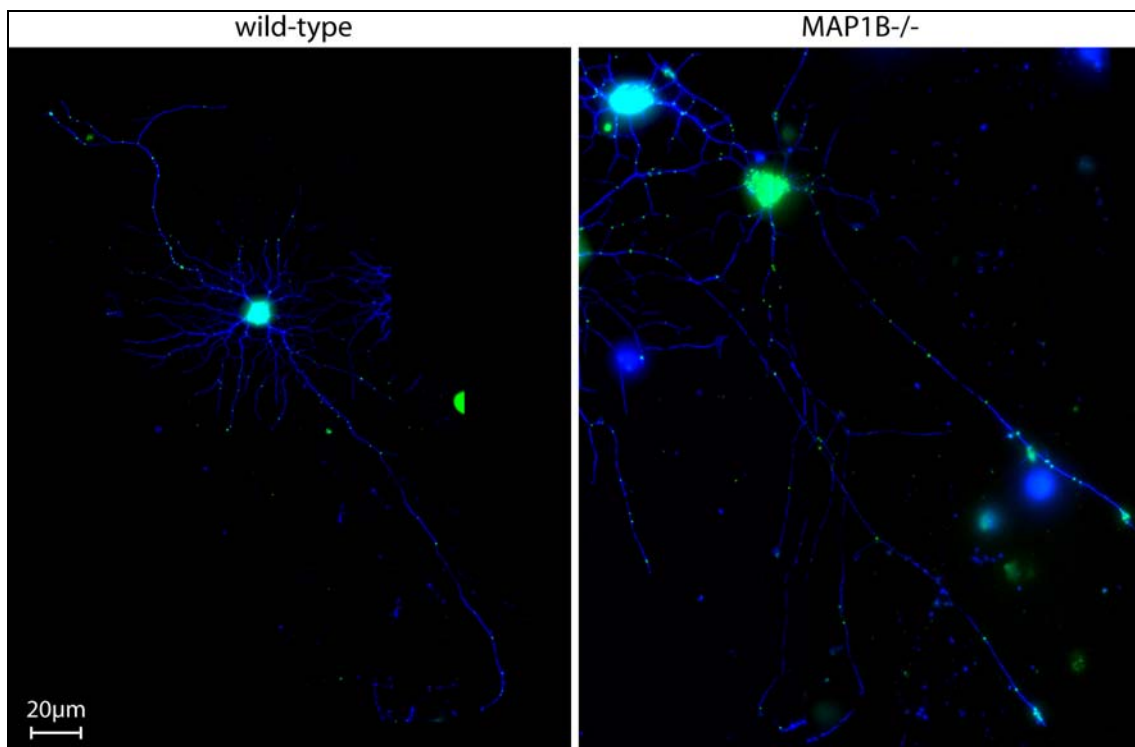


**Figure 50: Excessive process elongation after treatment with NOS inhibitor L-NAME for 4hrs.**

Wild-type and MAP1B<sup>-/-</sup> OPCs were cultured for 2 days in differentiation medium. After incubation with 300µM L-NAME for 4hrs, they were fixed and stained for tubulin and peroxisomes. This treatment induced the formation of a few very long processes in each cells, whereas the general appearance of the cells including the distribution of peroxisomes seemed not to be changed.

### Presence of MAP1B reduces the effect of a microtubule destabilizing reagent on oligodendrocytes

The lack of MAP1B does not seem to influence the reaction of oligodendrocytes to elevated NO-levels as I showed in several experiments. Nevertheless, MAP1B is known to stabilize microtubules. Thus, I investigated the response of wild-type and MAP1B<sup>-/-</sup> oligodendrocytes to the microtubule depolymerizing effect of nocodazole. The cells were incubated for 30 minutes with two different concentrations of nocodazole, 0.2mM and 0.5mM, fixed and stained for tubulin (Figure 51). Both wild-type and MAP1B<sup>-/-</sup> oligodendrocytes reacted in a strong way to the treatment with nocodazole. The cells showed a collapsed microtubule network which assumed the appearance of dots along the processes. However, a difference in the strength of the reaction is visible. At 0.2mM nocodazole, MAP1B<sup>-/-</sup> oligodendrocytes reacted similar to the wild-type cells to 0.5mM nocodazole. Besides, at 0.5mM nocodazole MAP1B<sup>-/-</sup> oligodendrocytes showed complete destruction of the microtubule network, whereas microtubules in wild-type cells appeared to resist complete depolymerization. This difference could also be seen in mouse DRG neurons (data not shown). Thus, MAP1B<sup>-/-</sup> cells are more sensitive to microtubule depolymerization than wild-type cells, which confirms once more the microtubule stabilizing role of MAP1B.

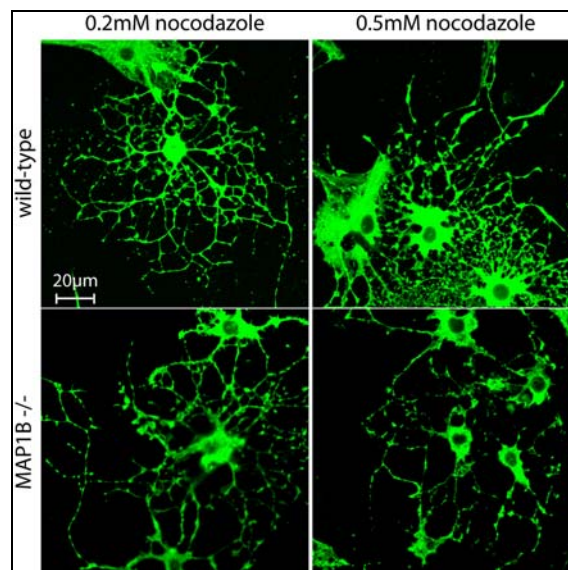


**Figure 51: MAP1B<sup>-/-</sup> oligodendrocytes show a stronger reaction to nocodazole than wild-type cells.**

Wild-type and MAP1B<sup>-/-</sup> OPCs were cultured for 2 days in differentiation medium. The cells were treated with two different concentrations of nocodazole, 0.2mM and 0.5mM. At both concentrations I observed a strong effect on the cytoskeleton of the wild-type and MAP1B<sup>-/-</sup> oligodendrocytes. However, MAP1B<sup>-/-</sup>

cells displayed higher sensitivity to the microtubule-depolymerizing effect of the drug than wild-type cells. The level of cell collapse seemed stronger in MAP1B<sup>-/-</sup> oligodendrocytes at 0.2mM nocodazole than in wild-type cells at 0.5mM nocodazole.



## PART II DISCUSSION

The importance of MAP1B in neurons regarding dynamics of cytoskeletal components and axon growth and retraction is undisputed. In addition, a potential role of MAP1B has been proposed in myelinating glia cells<sup>4, 6, 45, 280</sup>. The protein is expressed in Schwann cells and oligodendrocytes and co-localizes with microtubules. MAP1B deficiency results, apart from axon guidance defects, in alternations of central<sup>45</sup> and peripheral<sup>4</sup> myelination. In addition, MAP1B has been implicated in mRNA transport in neuronal processes<sup>306</sup> (Steffel, PhD Thesis 2007). In oligodendrocytes, cells with long processes, the proper transport of mRNA, proteins and organelles to the tips of the myelin-bearing process or sites of local translation is essential for survival of the cells and their ability to build and maintain myelin sheaths. To investigate a potential role of MAP1B in these cells, wild-type and MAP1B<sup>-/-</sup> oligodendrocytes were compared concerning their ability to differentiate and the expression and localization of diverse proteins or organelles. I confirmed the expression of MAP1B and its co-localization with microtubules at different stages of differentiation in primary oligodendrocytes and in the oligodendrocyte cell line OLN93. Regarding the differentiation of oligodendrocytes, markers for differentiation, such as MBP or MAG, were used to distinguish OPCs from terminally differentiated oligodendrocytes bearing myelin sheaths at the end of the processes. In early differentiation stages, these markers are not expressed and do not co-localize with tubulin. Although this co-localization never disappeared, an obvious change in the localization of these proteins was observed when oligodendrocytes differentiated. The myelin sheaths became visible as flat structures at the end of processes. However, oligodendrocyte differentiation seemed not to depend on the presence of MAP1B since MAP1B<sup>-/-</sup> cells differentiated normally and did not show any obvious difference in their morphology compared to wild-type oligodendrocytes. As it was already observed in several knockout studies, related proteins could have taken over for MAP1B. For instance tau<sup>319</sup> and MAP2<sup>319, 320</sup> were shown to be expressed in oligodendrocytes, although not continuously. The possible overlapping functions would have to be investigated in more detail using these knock-out mice. On the other hand, in order to avoid studies of double knock-out mice, one could think about making use of siRNA. However, I doubt that transfection of primary oligodendrocytes would be easy to perform as the culture and differentiation of these cells is very unreliable. The cells are very sensitive to many environmental factors and might not tolerate transfection.

Regarding the differentiation, the only difference which I could observe was that the number of differentiated cells was increased in MAP1B<sup>-/-</sup> cultures. Surprisingly, MAP1B<sup>-/-</sup> oligodendrocytes were generally easier to cultivate than the wild-type cells in terms of their survival. Wild-type oligodendrocytes that survived differentiated as fast as MAP1B<sup>-/-</sup> cells, but since they were fewer, they gave the false impression to be impaired in their ability to differentiate. Whether the lack of MAP1B causes an anti-apoptotic effect was not investigated. The difference in differentiation could simply be due to variations in the genetic background as the wild-type mice used for dissection were not optimal controls for the appropriate MAP1B<sup>-/-</sup> mice. I observed for instance several times that the culture of oligodendrocytes from Black 6 mice was almost impossible with the protocol I used, although it worked pretty well for the 5B22 mouse line.

The role of MAP1B in transport of organelles was also analyzed. In order to visualize mitochondria, oligodendrocytes were incubated with MitoTracker®, a mitochondrion-selective stain which diffuses across the plasma membrane and accumulates in mitochondria. In contrast to many other cell types studied, this treatment turned out to be toxic for oligodendrocytes. Time lapse microscopy could only be performed for a short interval where no difference in motility of mitochondria could be detected. Mitochondria were generally hardly mobile at all, in both wild-type and MAP1B<sup>-/-</sup> oligodendrocytes. This lack of movement could be due to the bad condition in which the cells had been during the image acquisition caused by incubation with the MitoTracker®. Thus, mitochondria motility could not be investigated in more detail. Alternatively, the localization of mitochondria was visualized in fixed cells using antibodies against ATP-synthase. This staining did not reveal any difference between wild-type and MAP1B<sup>-/-</sup> oligodendrocytes in the localization of the organelles. They were not accumulated in the cell body, which would have been reminiscent of the observed increase in retrograde mitochondrial movement in MAP1B<sup>-/-</sup> neurons shown by Jimenez-Mateos<sup>27</sup>. Likewise, peroxisomes were stained but their localization was not altered in MAP1B<sup>-/-</sup> oligodendrocytes either. Thus, either MAP1B does not play a role for organelle transport in oligodendrocytes or, as already mentioned, another MAP substituted MAP1B.

The expression and localization of the elongation factor EF1α was also tested. EF1α is an important factor for protein synthesis and has been shown to co-localize with staufen1 and MAP1B in RNP granules. Interestingly, its expression was found to be

reduced in MAP1B<sup>-/-</sup> DRG neurons (Steffel, PhD Thesis 2007). The staining of OPCs for EF1 $\alpha$  did not show any alteration in strength or localization between wild-type and MAP1B<sup>-/-</sup> cells. EF1 $\alpha$  was localized in wild-type and MAP1B<sup>-/-</sup> oligodendrocytes in and close to the cell body and sometimes in branching points. Obviously, it is not possible to compare neurons with glia cells, but it would have been striking to see a cell type overlapping phenotype in MAP1B<sup>-/-</sup> cells. Moreover, the age of mice, wherefrom the cells have been isolated, differs, as DRG neurons were isolated from adult mice whereas OPCs have been taken from newborn mice. It remains unclear whether the terminal differentiated oligodendrocytes would have exhibited any difference in EF1 $\alpha$  staining, but, since the process of differentiation was not impaired in MAP1B<sup>-/-</sup> cells, I would not expect to see a difference in such an experiment.

In diverse neurodegenerative diseases, such as Alzheimer's disease, multiple sclerosis or Parkinson's disease, the NO-levels in brain around plaques were found to be increased, suggesting that NO is involved in cellular damage leading to these plaques<sup>254, 321</sup>. The elevated NO-levels could stem from invading macrophages<sup>296</sup> which are responsible for the degradation and removal of cell debris. It is still unclear wherefrom NO stems and whether NO is leading to cellular damage in these diseases or if it is a side product of the ongoing inflammation. However, physiologic concentrations in brain under normal conditions are around 1nM NO and 1 $\mu$ M nitrite. During pathologic conditions, NO level can reach up to 1 $\mu$ M while nitrite levels are around 100 $\mu$ M<sup>7</sup>. Increase of NO concentration leads in neurons to cytoskeletal changes resulting in axon retraction and growth cone collapse. Apparently, mature mouse oligodendrocytes are as sensitive to elevated NO-levels as neurons<sup>7</sup>. Damage of oligodendrocytes would be expected to lead to a reduction in neuronal signal transduction velocity, which is dependent on an intact myelin sheath, and to damage to neurons, further leading to neurodegenerative diseases. In studies investigating the toxic effect of NO to oligodendrocytes, groups were mainly assessing oligodendrocyte cell death induced by NO<sup>291, 322</sup> and not morphological changes which might occur before apoptosis or necrosis. I wondered whether oligodendrocytes would react to NO in a similar way as neurons do, by retraction or growth cone collapse. The retraction observed in neurons following increased NO-levels, either obtained with NO-donors or via activation of nNOS, is mediated by MAP1B-S-nitrosylation. MAP1B is expressed in oligodendrocytes prior to terminal differentiation. In contrast, nNOS or eNOS have not been detected *per se* in oligodendrocytes<sup>7</sup>. Nevertheless, NO stemming from

extracellular sources, such as macrophages or NO-donors, should be as toxic as intracellularly produced NO.

In order to investigate whether MAP1B is one mediator of NO-toxicity in oligodendrocytes, I cultured primary mouse oligodendrocytes of wild-type and MAP1B<sup>-/-</sup> newborn mice. Then, the response of these cells to increased NO-levels was analyzed by observing the morphological changes in their processes upon treatment with the NO-donor SNAP. I stained the cells after treatment with SNAP for microtubules and analyzed whether any sign of retraction occurred. Unfortunately, I did not find any response of the microtubules to increased NO-levels. Wild-type and MAP1B<sup>-/-</sup> oligodendrocytes remained completely unaffected when they were treated with 100μM SNAP, a concentration which caused up to 50% of DRG neurons to retract. Even to higher SNAP concentrations, such as 0.5mM or 1mM, oligodendrocytes did not respond. Also the possible effect of NO on the localization of mitochondria and peroxisomes and the expression and localization of EF1α were investigated by immunofluorescence. Both did not show any alteration after SNAP-treatment. This tolerance of increased NO-levels was observed in OPCs and in terminally differentiated oligodendrocytes. Finally, the incubation times for SNAP were changed from 1h to 5hrs, but the cells did not react either. Considering incubation times of 12-24hrs used by the groups investigating cell death<sup>291, 322</sup>, one could think about increasing the duration of the treatment, but I think the most efficient way would be to perform time-lapse experiments in order to find the moment in which oligodendrocytes start to respond to their environment. Such experiments might be the best way to find the right moment for fixation after a treatment. For DRG neurons 1h is enough, but oligodendrocytes might need much longer for a cytoskeletal change than neurons. Since the physiological duty of a glia cell is to protect neurons from environmental changes it might be expected that they are not as sensitive to certain factors as neurons. Moreover, increasing concentrations of NO-donors might not anymore be physiologically relevant because such NO-levels would never be reached in the brain, not even under pathological conditions. Thus, a role of MAP1B and its nitrosylation in oligodendrocyte reaction to NO remains doubtful.

The other possibility to increase NO-levels is by activation of a NOS-enzyme with the calcium-ionophore calcimycin. Since eNOS and nNOS have never been detected in oligodendrocytes, I first wanted to check the expression of these enzymes in primary cells and in OLN93. In contrast to previous reports, I found nNOS and eNOS

expression in primary oligodendrocytes and in the OLN93 cell line. Although the immunofluorescence signal from nNOS was very weak in primary cells and in OLN93, western blot analysis revealed a clear expression in the cell line. In contrast to DRG neurons, I could not find a difference in the strength of the immunofluorescent signal in the nNOS staining between wild-type and MAP1B<sup>-/-</sup> oligodendrocytes. The eNOS staining also did not reveal any difference between the two genotypes, suggesting that in oligodendrocytes MAP1B might not be involved in the regulation of expression or stability of either enzyme.

The treatment with calcimycin leads to a calcium influx and subsequent activation of NOS. In contrast to the treatment with the NO-donor SNAP, oligodendrocytes were extremely sensitive to calcimycin treatment. The treatment with calcimycin was performed according to the protocol used for DRG neurons with 1  $\mu$ M calcimycin for 15min. Most of the oligodendrocytes showed severe collapse of the cytoskeleton and myelin sheaths or even complete cell lysis. Still, the presumed activation of NOS had to be confirmed, since calcium influx could have led to activation of several signaling pathways. This was done by inhibition of nNOS or eNOS with the appropriate inhibitor NPA or L-NIO, respectively. The inhibition of nNOS in wild-type oligodendrocytes and OLN93 could partially prevent the calcimycin-induced collapse, and the inhibition of eNOS was reducing MAP1B<sup>-/-</sup> oligodendrocyte cell death. In contrast, NPA did not have an effect in MAP1B<sup>-/-</sup> oligodendrocytes and L-NIO did not help wild-type cells to overcome the calcimycin treatment. Due to the fact that oligodendrocytes were only partially protected by NOS-inhibition, other signaling pathways might have become activated by calcimycin-induced calcium influx. Clear roles have been demonstrated for neurotransmitter-mediated calcium signaling in oligodendrocytes, for instance via glutamate or ATP released from axons or astrocytes<sup>323</sup>. Oligodendrocytes are highly vulnerable to perturbations in intracellular calcium and, like in neurons, dysregulation of calcium channels can be deleterious for glia cells and leads to apoptosis<sup>324</sup>.

A further indication for the importance of NOS in oligodendrocytes was the observation that incubation of oligodendrocytes with the nonspecific NOS inhibitor L-NAME for several hours led to excessive process elongation in wild-type and MAP1B<sup>-/-</sup> cells. Surprisingly, only few but not all processes of one cell were affected. The morphology of the treated oligodendrocytes looked completely normal, except two

or three processes that were extremely long. In what these special processes differed from others has not been clarified yet.

Despite the fact that NOS-inhibition could not impede calcimycin-induced collapse completely, I suggest that NOS enzymes are activated in oligodendrocytes by calcium influx. Since these cells react in a more drastic way than DRG neurons, the concentration or incubation time of calcimycin should be optimized in order to avoid extreme reactions such as cell death. In the treated samples there were no cells exhibiting a weak reaction or signs of retraction. Either cells looked unchanged or they were completely collapsed. Moreover, with a lower dose of calcimycin, perhaps a different response of wild-type and MAP1B<sup>-/-</sup> oligodendrocytes would be observed. In addition, it could be investigated whether the coating of the coverslips, on which the oligodendrocytes grew, is affecting the glial response. For instance the additional coating with laminin might influence the reaction to SNAP, as it was shown for DRG neurons. However, the fact that eNOS-inhibition does and nNOS-inhibition does not help MAP1B<sup>-/-</sup> oligodendrocytes to overcome the calcimycin toxicity is reminiscent of the findings in DRG neurons discussed in the first part of my PhD thesis. I could show that eNOS plays a special role in MAP1B<sup>-/-</sup> DRG neurons during the repulsive netrin-1 pathway. Although nNOS seemed to be expressed to the same extend in wild-type and MAP1B<sup>-/-</sup> oligodendrocytes, in MAP1B<sup>-/-</sup> oligodendrocytes eNOS might be more important in the signaling downstream of calcium than nNOS. This raises again the matter how the lack of MAP1B could influence the activity of nNOS. This question remains unanswered and might be easier to solve by the use of a cell line and tools to knock down MAP1B.

Despite some ambiguities, I could show that MAP1B might play a minor role in oligodendrocytes and that these cells are perhaps not that sensitive to elevated NO-levels as previously claimed. However, the presence of NOS enzymes was found and NO might be relevant for process elongation during development. The question of NO involvement in oligodendrocyte pathology is not yet resolved and should be investigated in more detail.

## **MATERIALS AND METHODS**

### **Tissue culture**

#### **Culture of cell lines**

The cell line OLN93 was cultured at 37°C in 8.5% CO<sub>2</sub> in growth medium (Dulbeccos MEM supplemented with 10% FCS, 50U/ml Penicillin and 50µg/ml Streptomycin, Fungizone and L-Glutamine). The cells were fed every second day with preheated media, split every week. Therefore cells were first washed with PBS to remove all FCS-containing medium, then incubated with 2ml Trypsin 0.25%; EDTA 0.5M. To stop the trypsin digestion 8ml medium were added and the cell suspension was centrifuged for 3min at 300g. The cell pellet was resuspended in an appropriate volume of fresh medium and redistributed on 2-5 new petri dishes. For freezing, the cells were resuspended in FCS 10% DMSO to prevent crystallization and stored at -80°C in Styrofoam boxes and for long term storage in liquid nitrogen.

#### **Preparation of glass coverslips**

13mm coverslips were washed with acetone and twice with 96% EtOH, dried and autoclaved. Coverslips were coated with 10µg/ml poly-L-lysine in H<sub>2</sub>O for 1h or longer at 37°C, washed 2-3 times with H<sub>2</sub>O and dried. Additionally, PLL-coated coverslips could be coated with 10µg/ml laminin for at least 3h at 37°C, washed 3 times with H<sub>2</sub>O. PLL-laminin coated coverslips should not dry before cells are plated on them. Alternatively, coverslips were coated with poly-L-ornithine (Sigma P6282) 1h and fibronectin (Sigma F0895, 1µg/ml) 1h.

#### **Cultivation of dissociated adult DRG neurons**

Cultivation of mouse DRG neurons was performed following the protocol described by Tonge<sup>325</sup>. Mice were anesthetized with IsoFluoran (Abbott, Rungis, France) and killed by decapitation. DRG neurons were harvested in DMEM F-12 medium and enzymatically dissociated by collagenase (4000U/ml, Sigma, St. Louis, MO) for 90min

at 37°C followed by 0.125% Trypsin/EDTA (Invitrogen) and DNaseI (50µg/ml; Sigma) treatment for 12min at 37°C. DRG neurons were finally triturated several times with two fire-polished Pasteur pipettes of different size. After harvesting cells by centrifugation at 150 g for 5min, cells were resuspended in fresh DMEM-F-12 medium and washed further two times. Finally cells were resuspended in DRG growth medium (DMEM-F-12 medium supplemented with 20% horse serum, 0.7% glucose, 50 U/ml penicillin, 50µg/ml streptomycin<sup>326</sup>, and supplemented with N3<sup>327</sup>) and plated at a density of approximately 100 cells/cm<sup>2</sup> on poly-L-Lysine and laminin-1 coated glass coverslips and incubated at 37°C, 5% CO<sub>2</sub> for 24hrs. For analysis, mouse DRG neurons were treated with different reagents and fixed for immunofluorescences. For time lapse microscopy, medium was supplemented with 20mM Hepes, pH 7.4.

**Table 1: N3 components**

<b>Chemical</b>	<b>Stock concentration</b>	<b>Volume for 10ml N3</b>	<b>Concentration</b>	<b>Company</b>
HBSS -Ca,-Mg		5.9ml		Invitrogen
BSA	10mg/ml in HBSS	1ml	17.5µg/ml	Sigma, A4261
Apo- transferrin	500mg/ml in Hanks	2ml	175µg/ml	Sigma, T1147
Na-Selenite	100µg/ml in HBSS	100µl	17.5ng/ml	Sigma, S9133
Putrescine	80mg/ml in HBSS	400µl	56.1µg/ml	Sigma, P5780
Progesterone	125µg/ml in EtOH	100µl	21.9ng/ml	Sigma, P6149
Corticosterone	2mg/ml in EtOH	20µl	70.1ng/ml	Sigma, C2505
Tri- iodothyronine	200µg/ml in 0.01N NaOH	100µl	35ng/ml	Sigma, T6397
Insuline	25mg/ml in 20mM HCl	400µl	17.5µg/ml	Sigma, I6634

### **Cultivation of dissociated embryonic DRG neurons**

Mouse embryos were isolated from the mother at embryonic day 13.5. Embryos were placed into cold L15 medium, the vertebra was isolated and removed from the spinal cord. DRGs were dissected from the spinal cord and transferred into an eppendorf tube with cold DMEM-F12 medium. After a quick centrifugation step of 2min at 1000rpm, the supernatant was removed and the DRGs were incubated in 0.125% Trypsin/EDTA (Invitrogen) treatment for 30min at 37°C. The digestion was



stopped with DMEM containing 10% FCS and the suspension was centrifuged for 5min at 2000rpm. The supernatant was removed and 500µl NLA medium (Neurobasal medium, 2% B27 supplement (GIBCO), 10ng/ml NGF) was added to the DRGs. After that, the DRGs were dissociated mechanically with a 1ml tip until all large fragments had disappeared. The cells were then spotted in the middle of a dried PLL-coated coverslip and kept for at least 30min at 37°C. Finally, 300-500µl NLA medium were added to each well. The DRGs from 1 embryo were cultured on 6-12 coverslips (13mM).

### **Cultivation of adult and embryonic DRG explants**

DRGs were isolated from mice as for regular culture of DRG neurons and transferred into cold DMEM-F12 medium. A 5-10µl drop of matrigel (BD Biosciences, 356230) was placed on uncoated coverslips, and then the ganglia were placed on it and covered with 10µl matrigel. After drying for 1h in the incubator, 500µl DRG growth medium was added to each well. For the outgrowth studies, reagents were added immediately and explants were cultured for 2-4 days without changing the medium.

### **Cultivation of hippocampal neurons from newborn mice**

Hippocampi were dissected from P0 to P4 mice and placed in ice cold DMEM and washed three times with DMEM. The explants were then incubated in 5ml DMEM + 5U/ml Papain (Sigma P4762) + 8.3µg/ml DNase I for 15min at 37°C to dissociate cells.

After the dissociation the cells still form large aggregates and are washed 3x with hippocampi culture medium (Neurobasal medium, B27 supplement (Gibco 17504-044), N2, Penicillin, Streptomycin and L-Glutamine).

The cells were resuspended in culture medium (approximately 1ml per 2 hippocampi); tissue was dissociated first with the blue tip until solution got homogenous, then with the yellow tip. Transfection with Amaxa electroporation kit can be done directly before plating the neurons on coverslips; transfection with Lipofectamine 2000 could be done after 24hrs of cultivation but was not successful.

Cells were seeded on poly-L-ornithine (Sigma P6282) and fibronectin (Sigma F0895, 1µg/ml) coated coverslips at a density of 100-200 cells per cm<sup>2</sup>. After 1 day in culture hippocampi began to show a polarized morphology.

**Table 2: N2 components**

Chemical	Stock concentration	Volume for 10ml N3	Concentration	Company
HBSS,-Ca,-Mg		6.23ml		Invitrogen
Apo-transferrin	50mg/ml in Hanks	2ml	10mg/ml	Sigma, T1147
Na-Selenite	5µg/ml in HBSS	1.04ml	0.52µg/ml	Sigma, S9133
Putrescine	16.1mg/ml in HBSS	1ml	1.61mg/ml	Sigma, P5780
Progesterone	125µg/ml in EtOH	50µl	0.63µg/ml	Sigma, P6149
Insuline	25mg/ml in 20mM HCl	200µl	500µg/ml	Sigma, I6634

### Cultivation and staining of hippocampal explants

Hippocampi were dissected from P0 to P4 mice and placed in ice cold DMEM and washed three times with DMEM. A drop of approximately 5µl matrigel (BD Biosciences, 356230) was pipetted on a coverslip. Hippocampi were each cut into 3-4 pieces, placed on the gel and covered with 10µl matrigel. After 1 h drying of the matrigel in the incubator, 500µl hippocampal growth medium was added to each well. The explants were kept in culture 2-4 days without changing the medium. For phase contrast microscopy, the explants were not fixed. For immunofluorescence explants were fixed with 4% PFA for 20min, blocked with 2% BSA in PBS and stained with primary antibodies for 3 h and secondary antibodies for 2h. Then the cultures were mounted in 50µl mowiol.

### Cultivation of oligodendrocytes from newborn mice

Cultivation of mouse oligodendrocytes was performed following the protocol described by Holly Colognato. Mixed glial cultures were obtained from cerebrum of P0 to P3 mice. The hemispheres were separated from the meninx, homogenized in

HEPES/MEM and digested for 25min in 0.3U/ml Papain (Sigma P4762) and 0.24mg/ml L-cystein (Sigma C7352) + 40µg/ml DNase at 37°C. The digestion was stopped with DMEM + 10% FCS, the suspension was pipetted up and down to obtain a homogeneous cell solution and centrifuged 5min at 300g. The cell pellet was resuspended in DMEM + 10% FCS and cultured on 10µg/ml poly-D-lysine (Sigma P6407) coated tissue-culture flasks for up to 10 days at 37°C and 8.5% CO<sub>2</sub>. To assess differences in oligodendrocyte differentiation, oligodendrocyte precursors were obtained by differential shaking. The mixed cultures were shaken 12-24hrs at 200rpm at 37°C and 8.5% CO<sub>2</sub>. Immediately after shaking, oligodendrocyte progenitors, which are less adherent than fibroblasts and consequently in suspension, were centrifuged at 300g for 5min, the pellet was resuspended in 10ml DMEM 10% FCS. Cells are plated for 2hrs on normal uncoated tissue culture dishes in order to let settle down fibroblasts, while oligodendrocyte progenitors stay in suspension. These cells were then centrifuged and plated on 100µg/ml poly-D-lysine coated glass coverslips at a density of approximately 100-200 cells/cm<sup>2</sup> in differentiation medium (DMEM supplemented with 2% FCS, 25µg/ml insuline, 130ng/ml progesterone, 100mM putrescine, 50µg/ml apo-transferrin, 5ng/ml sodium-selenite, 2mM sodium-pyruvate, 20ng/ml tri-iodothyronine, 10ng/ml D-biotin). Cells were kept in culture for up to 9 days in order to reach terminal differentiation.

### **Time lapse microscopy and local application of reagents**

Primary neurons were cultured as described above on coated 3 cm coverslips (for time lapse in a 6 well plate) or on coverslips fixed with paraffine on a 6 cm petridish (for time lapse in the incubation chamber). After incubation of the cells for 24h, 20mM hepes, pH 7.4, cultures were placed in a chamber maintained at 37°C of an inverted microscope equipped with phase contrast and a Plan Apo 100x/0.7 numerical aperture lens. Acquisition and illumination devices were driven by MetaMorph software (Universal Imaging, West Chester, PA) or Axiophot (Zeiss). Pictures of cells were taken at different frequencies depending on the cell type and the treatment.

For local application of guidance cues, a stock solution of netrin-1 (25µg/ml) or semaphoring (10µg/ml) was locally applied through a 0.5µM pipette attached to an Eppendorf microinjection system. The pipette was positioned close to the growth cone of an axon and was ejected continuously from the tip every with the pressure of 100hPa

for up to 8hrs. In order to determine the effect of NOS inhibition, the appropriate NOS inhibitor was added previously to the medium.

### Treatment of cells with different inhibitors or other reagents

Primary cells were all treated according to the list in table 3 by simply adding the appropriate amount of the reagent to the growth medium. After the indicated incubation time, cells were fixed as usual. Cultured dissociated neurons or glia cells were incubated with inhibitors for 1h, whereas explants were allowed to grow for several days in the reagents. Concerning guidance cues, netrin-1 was added 2-3hrs after plating of the cells and kept in the medium until fixation, whereas Sema3A was added only 30min before fixation of dissociated cells. For treatment of explants, both guidance cues were added with the growth medium and not removed until microscopy.

**Table 3: List of inhibitors and chemicals for treatments of primary cells**

<b>Inhibitor</b>	<b>Function</b>	<b>Concentration</b>	<b>Incubation</b>	<b>Company</b>
NPA	Inhibition of nNOS	300µM	1-72 h	Tocris Biosciences Cat.No:1200
L-NAME	Inhibition of NOSs	300µM	1-72 h	Cayman Cat.No: 80210
L-NIO	Inhibition of eNOS	10µM	1-72 h	Calbiochem Cat.No:400600
LY83583	Inhibition of sGC	1µM	1 h	Calbiochem Cat.No:440205
ODQ	Inhibition of sGC	10µM	30min	Sigma Cat.No:O3636
<b>Reagent</b>				
SNAP	NO-Donor	100µM-1mM	4 h	Invitrogen Cat.No:N7927
Calcimycin	Activator of nNOS	1µM	15min	Sigma Cat.No:C7522
DAF-FM-DA	Fluorescent indicator for NO	10µM	1 h	Calbiochem Cat.No:D23842
<b>Guidance cue</b>				
Netrin-1	Attraction or repulsion	250ng/ml	21-72 h	Alexis Cat.No:ALX522100
Semaphorin 3A	Repulsion	0.05-1µg/ml	0.5-1h	R&D Systems Cat.No:1250-S3

## Immunological Assays

### Immunofluorescence of primary neurons and glia cells

The cells were fixed by adding gently 8% paraformaldehyde in PBS to the medium in order to obtain a final PFA concentration of 4%, washed 3 times with PBS. Alternatively, depending on the antibody used, cells were fixed for 5-10min in MetOH at -20°C. In case of PFA-fixation, the cell membranes were broken with 0.3% Triton-X-100 in PBS. Unspecific binding sites were blocked with 5% BSA in PBS for 1h. Then the cells were incubated with the first antibodies diluted in 5% BSA (and 0.15% Triton-X-100 in case of PFA-fixed cells) for 3hrs and, after washing with PBS, incubated with labeled secondary antibodies diluted in PBS for 2hrs in the dark. For immunofluorescences of cell lines like OLN93, the incubation time of primary and secondary antibodies was reduced to 1h each. For the nuclear staining the cells were incubated with Hoechst diluted 1:3000 for 10min in the dark. Then cells were washed 3x with PBS and once with H<sub>2</sub>O, finally the coverslips were mounted with mowiol. The coverslips were analysed by confocal microscopy and LSM software (Zeiss).

### **Incubation of DRG neurons with the fluorescent NO indicator DAF-FM DA**

One hour before fixation, DRG neurons were treated with 5µM DAF-FM DA (Calbiochem, 251520). This cell permeable, photo-stable nitric oxide fluorescent indicator releases DAF-FM by the action of intracellular esterases. It reacts with NO, in the presence of oxygen, resulting in the formation of a triazolo-fluorescein analog DAF-FM T with an excitation max.: 500nm and emission max.: 515nm.

### **Immunohistochemistry on cryosections**

The cryosections were stored at -80°C. For staining, the slices were dried, and the areas with tissue were lined with Daco-pen. In a humidified chamber, the slices were first incubated with 0.3% Triton-X-100 in OXPBS; then unspecific binding sites were blocked with 10% normal goat serum (NGS) in OXPBS. The primary antibodies were diluted in 5% NGS in OXPBS and incubated over night at RT. The next day slices were rinsed three times with 5% NGS in OXPBS and the secondary antibodies were applied and incubated 1-1.5hrs at RT in the dark. After 10min of DAPI incubation, slices were washed intensely and mounted in mowiol.

Table 4: List of primary antibodies

Antigen	Name/clone	Company	IF/IHC	WB
mouse ATP-Synthase		Lilli Winter	1:400	
mouse EF1 $\alpha$		Sigma	1:100	
mouse eNOS	hum eNOS	Bioscience	1:50	1:1000(0)
rabbit iNOS	AB5382 p rb IgG	Chemicon	1:1000/"	1:5000
rabbit Laminin	L9393	Sigma	1:100	
mouse MAG	513	Chemicon	1:200	1:1000
rabbit MAP1B LC1a	LC1A	M. Tögel	1:200	1:1000
rabbit MAP1B 750	MAP1B-750	F. Nothias	1:3000	
rat MBP	bov. MBP	Chemicon	1:1000	
rabbit nNOS	R-20, sc-648	Santa Cruz	1:500	1:2000
rabbit Peroxisome	pmp70	Kunze	1:1000	
Phalloidin-TR or -488		invitrogen	1:100	
mouse Syntrophin	1351	Sigma	1:100	1:10.000
rat $\alpha$ 1-tubulin	YL1/2	Acris	1:300	
mouse $\alpha$ 1-tubulin	B512	sigma	1:1000	1:5000
mouse b tub class III tuj	MMS435P0250	covance	1:2000	1:10.000
rabbit b tub class III tuj1	T-2200	sigma	1:100	1:2000

Table 5: List of secondary antibodies

Antigen	Conjugated to	Company	IF	WB
<b>anti Rabbit</b>				
goat $\alpha$ rabbit	Alexa 488	Mol. Probes	1:1000	
goat $\alpha$ rabbit	Texas Red	Mol. Probes	1:1000	
goat $\alpha$ rabbit	Amca	Jackson Lab	1:50	
goat $\alpha$ rabbit	Cy5	Jackson Lab	1:1000	
goat $\alpha$ rabbit	HRPO	Jackson Lab		1:10000
goat $\alpha$ rabbit	AP	Jackson Lab		1:5000
<b>anti Mouse</b>				
goat $\alpha$ mouse	Alexa 488	Jackson Lab	1:1000	
donkey $\alpha$ mouse	Rhodamine Red	Jackson Lab	1:1000	
$\alpha$ mouse-IgM	Rhodamine Red	Jackson Lab	1:1000	
donkey $\alpha$ mouse	Cy 5	Jackson Lab	1:1000	
goat $\alpha$ mouse	Amca	Jackson Lab	1:50	
goat $\alpha$ mouse	HRPO	Jackson Lab		1:10000
goat $\alpha$ mouse	AP	Jackson Lab		1:5000
<b>anti Rat</b>				
goat $\alpha$ rat	FITC	Jackson Lab	1:1000	
goat $\alpha$ rat	Texas Red	Jackson Lab	1:1000	
goat $\alpha$ rat	Amca	Jackson Lab	1:800	
donkey $\alpha$ rat	Cy 5	Jackson Lab	1:500	
DAPI		Sigma	1:30000	

## Western blot analysis

The cells were grown until confluence, washed, scraped in Lysis buffer with Dnase and Rnase (5mM Hepes/HCl pH 7.0; 0.5mM MgCl<sub>2</sub>; 0.1mM EGTA; 10mM NaCl; 0.5% Triton-X-100; 100nM DTT; 0.5mg Dnase; 0.2ng Rnase; 5% Proteaseinhibitormix) and incubated 10minutes at RT. After adding 3x Sample buffer they were boiled at 95°C for 10 minutes and stored at -20°C

Lysates were loaded on a 8-12.5% SDS-PAGE gel, transferred on a Nitrocellulose membrane, blocked in 2% BSA in PBST (0.005% Tween in PBS) at RT and incubated at RT with the primary antibody, diluted in 2% BSA/PBST and 0.2% Sodium acid; after incubation with the secondary antibody conjugated with Horse Reddish Peroxidase, the membrane was developed with Pierce Supersignal West Pico Chemiluminescent Substrate or using reaction with Alkaline Phosphatase.

**Table 6: Components of Acrylamid gel for SDS-PAGE**

<b>Separating gel</b>	<b>8%</b>	<b>10%</b>	<b>12,5%</b>	<b>Stacking gel</b>	<b>2 gels</b>	<b>4 gels</b>
Acrylamide	2,7ml	6ml	7.5ml	Acrylamide	1,3ml	2,6ml
ddH <sub>2</sub> O	4,7ml	7.5ml	6ml	ddH <sub>2</sub> O	6,1ml	12,2ml
1,5M Tris/Cl pH 8,8 - SDS	2,6ml	4.5ml	4.5ml	1,5M Tris/Cl pH 6,8 - SDS	2,6ml	5,2ml
APS	100μl	120μl	120μl	APS	100μl	200μl
TEMED	5μl	12μl	12μl	TEMED	10μl	20μl

### Solutions:

10% Acetic acid

#### Ponceau solution

0.2% Ponceau-S

3% Trichloroacetic acid

#### Amidoblack solution

0.1% Amidoblack

45% Ethanol

Phosphate buffered saline (PBS), pH

7.4

137mM NaCl

2.6mM KCl

8mM Na<sub>2</sub>HPO<sub>4</sub>

1.5mM KH<sub>2</sub>PO

AP-Buffer

100mM Tris/HCl pH 9.5

100mM NaCl

5mM MgCl<sub>2</sub>

NBT-solution

0.5g Nitro blue tetrazolium (NBT)

10ml 70% DMF, stored at -20°C

BCIP-solution

0.5g Bromchloroindolyl phosphate  
(BCIP)

10ml 100% DMF, stored at -20°C



## ANNEX

### Table of figures and tables

Figure 1: The family of microtubule associated proteins 1 with its members MAP1A, MAP1B, MAP1S, and Futsch.....	19
Figure 2: A retracting axon.....	22
Figure 3: The structure of the growth cone.....	25
Figure 4: The homology between different netrins and the structure of netrin.....	32
Figure 5: Attractive or repulsive signaling by netrin-1.....	35
Figure 6: Protein structures of the semaphorin family.....	38
Figure 7: The three nitric oxide synthases.....	41
Figure 8: Activation of nNOS and downstream targets of NO.....	43
Figure 9: Ensheathment of an axon by an oligodendrocyte.....	47
Figure 10: Expression of MAP1B in mouse DRG neurons and netrin-1 induced retraction.....	56
Figure 11: Calcimycin and SNAP induce axon retraction only in wild-type DRG neurons in the presence of laminin.....	58
Figure 12: Calcimycin and SNAP do not induce axon retraction in MAP1B <sup>-/-</sup> DRG neurons.....	59
Figure 13: NO production in netrin-treated wild-type and MAP1B <sup>-/-</sup> DRG neurons.....	61
Figure 14: Percentage of retracted wild-type and MAP1B <sup>-/-</sup> DRG neurons following treatment with netrin-1 and inhibition of nNOS with NPA.....	62
Figure 15: NPA reduces NO production in wild-type DRG neurons during treatment with netrin-1.....	63
Figure 16: NPA does not reduce NO production in MAP1B <sup>-/-</sup> DRG neurons during treatment with netrin-1.....	65
Figure 17: Expression and localization of nNOS and eNOS in untreated DRG neurons of wild-type and MAP1B <sup>-/-</sup> mice.....	67
Figure 18: Immunoblot analyses of wild-type and MAP1B <sup>-/-</sup> DRGs and brains of adult and newborn mice for nNOS and eNOS.....	68
Figure 19: Expression and localization of nNOS in wild-type DRG neurons after treatment with netrin-1 and/or NPA.....	70
Figure 20: L-NIO reduces netrin-1 induced retraction in MAP1B <sup>-/-</sup> DRG neurons.....	71

Figure 21: NO production in wild-type DRG neurons after treatment with netrin-1 and L-NIO. ....	73
Figure 22: NO production in MAP1B <sup>-/-</sup> DRG neurons after treatment with netrin-1 and L-NIO. ....	74
Figure 23: Localization of eNOS in MAP1B <sup>-/-</sup> DRG neurons after treatment with netrin-1 and L-NIO. ....	75
Figure 24: LY induces axon retraction in wild-type DRG neurons. ....	77
Figure 25: Percentage of retracted DRG neurons after treatment with LY, ODQ and NPA. ....	78
Figure 26: NO production in wild-type DRG neurons after treatment with LY83583 and NPA. ....	80
Figure 27: NO production in wild-type DRG neurons after treatment with ODQ and NPA. ....	81
Figure 28: NO production in MAP1B <sup>-/-</sup> DRG neurons after treatment with LY83583 and NPA. ....	82
Figure 29: NO production in MAP1B <sup>-/-</sup> DRG neurons after treatment with ODQ and NPA. ....	83
Figure 30: Relative outgrowth of neurites from hippocampal explants of newborn wild-type and MAP1B <sup>-/-</sup> mice. ....	85
Figure 31: Relative outgrowth of neurites from DRG explants of adult wild-type and MAP1B <sup>-/-</sup> mice. ....	87
Figure 32: Expression of MAP1B in oligodendrocytes. ....	102
Figure 33: Expression of MAP1B in the oligodendrocyte cell line OLN93. ....	103
Figure 34: Expression and localization of nNOS and eNOS in wild-type and MAP1B <sup>-/-</sup> primary oligodendrocytes. ....	105
Figure 35: Expression of nNOS and eNOS in OLN93. ....	106
Figure 36: Western blot analysis of the expression of nNOS in OLN93. ....	106
Figure 37: Localization of peroxisomes and mitochondria in wild-type and MAP1B <sup>-/-</sup> oligodendrocytes. ....	108
Figure 38: Expression and localization of EF1 $\alpha$ in wild-type and MAP1B <sup>-/-</sup> OPCs. ....	110
Figure 39: Differentiated wild-type and MAP1B <sup>-/-</sup> oligodendrocytes. ....	112
Figure 40: Percentage of oligodendrocytes expressing MBP or MAG after 7 days of differentiation. ....	113

Figure 41: Localization of EF1 $\alpha$ and peroxisomes after treatment with 1mM SNAP for 5hrs in undifferentiated OPCs.....	115
Figure 42: Localization of mitochondria in wild-type and MAP1B <sup>-/-</sup> OPCs after treatment with 1mM SNAP. ....	116
Figure 43: Localization of EF1 $\alpha$ and peroxisomes after treatment with 1mM SNAP for 5hrs in early differentiated oligodendrocytes. ....	117
Figure 44: Expression and localization of MAG in terminally differentiated wild-type and MAP1B <sup>-/-</sup> oligodendrocytes after a treatment with 1mM SNAP for 5hrs. ....	119
Figure 45: Inhibition of nNOS but not eNOS prevents calcimycin toxicity in wild-type oligodendrocytes.....	121
Figure 46: Inhibition of eNOS but not nNOS prevents calcimycin toxicity in MAP1B <sup>-/-</sup> oligodendrocytes.....	122
Figure 47: Inhibition of nNOS prevents calcimycin toxicity in OLN93. ....	123
Figure 48: EF1 $\alpha$ and peroxisome localization was not disturbed by the calcimycin treatment in wild-type oligodendrocytes. ....	124
Figure 49: EF1 $\alpha$ and peroxisome localization was not disturbed by the calcimycin treatment in MAP1B <sup>-/-</sup> oligodendrocytes.....	125
Figure 50: Excessive process elongation after treatment with NOS inhibitor L-NAME for 4hrs.....	126
Figure 51: MAP1B <sup>-/-</sup> oligodendrocytes show a stronger reaction to nocodazole than wild-type cells.....	127
 Table 1: N3 components.....	 136
Table 2: N2 components.....	138
Table 3: List of inhibitors and chemicals for treatments of primary cells.....	140
Table 4: List of primary antibodies.....	142
Table 5: List of secondary antibodies.....	142
Table 6: Components of Acrylamid gel for SDS-PAGE.....	143



## References

1. Stroissnigg, H. et al. S-nitrosylation of microtubule-associated protein 1B mediates nitric-oxide-induced axon retraction. *Nat Cell Biol* 9, 1035-45 (2007).
2. Höpker, V. H., Shewan, D., Tessier-Lavigne, M., Poo, M. & Holt, C. Growth-cone attraction to netrin-1 is converted to repulsion by laminin-1. *Nature* 401, 69-73 (1999).
3. Del Rio, J. A. et al. MAP1B is required for Netrin 1 signaling in neuronal migration and axonal guidance. *Curr Biol* 14, 840-50 (2004).
4. Meixner, A. et al. MAP1B is required for axon guidance and is involved in the development of the central and peripheral nervous system. *J Cell Biol* 151, 1169-78 (2000).
5. Dinerman, J. L., Steiner, J. P., Dawson, T. M., Dawson, V. & Snyder, S. H. Cyclic nucleotide dependent phosphorylation of neuronal nitric oxide synthase inhibits catalytic activity. *Neuropharmacology* 33, 1245-51 (1994).
6. Vouyiouklis, D. A. & Brophy, P. J. Microtubule-associated protein MAP1B expression precedes the morphological differentiation of oligodendrocytes. *J Neurosci Res* 35, 257-67 (1993).
7. Boullerne, A. I. & Benjamins, J. A. Nitric oxide synthase expression and nitric oxide toxicity in oligodendrocytes. *Antioxid Redox Signal* 8, 967-80 (2006).
8. Mingorance-Le Meur, A. & O'Connor, T. P. Neurite consolidation is an active process requiring constant repression of protrusive activity. *Embo J* 28, 248-60 (2009).
9. Luduena, R. F. Multiple forms of tubulin: different gene products and covalent modifications. *Int Rev Cytol* 178, 207-75 (1998).
10. Tanaka, E. & Sabry, J. Making the connection: cytoskeletal rearrangements during growth cone guidance. *Cell* 83, 171-6 (1995).
11. Luo, L. Actin cytoskeleton regulation in neuronal morphogenesis and structural plasticity. *Annu Rev Cell Dev Biol* 18, 601-35 (2002).
12. Pollard, T. D. & Borisy, G. G. Cellular motility driven by assembly and disassembly of actin filaments. *Cell* 112, 453-65 (2003).
13. Gungabissoon, R. A. & Bamberg, J. R. Regulation of growth cone actin dynamics by ADF/cofilin. *J Histochem Cytochem* 51, 411-20 (2003).
14. Bixby, J. L. & Bookman, R. J. Intracellular mechanisms of axon growth induction by CAMs and integrins: some unresolved issues. *Perspect Dev Neurobiol* 4, 147-56 (1996).
15. Lin, W. & Szaro, B. G. Neurofilaments help maintain normal morphologies and support elongation of neurites in *Xenopus laevis* cultured embryonic spinal cord neurons. *J Neurosci* 15, 8331-44 (1995).
16. Dehmelt, L. & Halpain, S. Actin and microtubules in neurite initiation: are MAPs the missing link? *J Neurobiol* 58, 18-33 (2004).
17. Schoenfeld, T. A. & Obar, R. A. Diverse distribution and function of fibrous microtubule-associated proteins in the nervous system. *Int Rev Cytol* 151, 67-137 (1994).
18. Sanchez, C., Perez, M. & Avila, J. GSK3 $\beta$ -mediated phosphorylation of the microtubule-associated protein 2C (MAP2C) prevents microtubule bundling. *Eur J Cell Biol* 79, 252-60 (2000).

19. Teng, J. et al. Synergistic effects of MAP2 and MAP1B knockout in neuronal migration, dendritic outgrowth, and microtubule organization. *J Cell Biol* 155, 65-76 (2001).
20. Tögel, M., Wiche, G. & Propst, F. Novel features of the light chain of microtubule-associated protein MAP1B: microtubule stabilization, self interaction, actin filament binding, and regulation by the heavy chain. *J Cell Biol* 143, 695-707 (1998).
21. Takei, Y., Teng, J., Harada, A. & Hirokawa, N. Defects in axonal elongation and neuronal migration in mice with disrupted tau and map1b genes. *J Cell Biol* 150, 989-1000 (2000).
22. Gordon-Weeks, P. R. & Fischer, I. MAP1B expression and microtubule stability in growing and regenerating axons. *Microsc Res Tech* 48, 63-74 (2000).
23. Avila, J., Dominguez, J. & Diaz-Nido, J. Regulation of microtubule dynamics by microtubule-associated protein expression and phosphorylation during neuronal development. *Int J Dev Biol* 38, 13-25 (1994).
24. Baas, P. W. & Qiang, L. Neuronal microtubules: when the MAP is the roadblock. *Trends Cell Biol* 15, 183-7 (2005).
25. Seitz, A. et al. Single-molecule investigation of the interference between kinesin, tau and MAP2c. *Embo J* 21, 4896-905 (2002).
26. Stamer, K., Vogel, R., Thies, E., Mandelkow, E. & Mandelkow, E. M. Tau blocks traffic of organelles, neurofilaments, and APP vesicles in neurons and enhances oxidative stress. *J Cell Biol* 156, 1051-63 (2002).
27. Jimenez-Mateos, E. M., Gonzalez-Billault, C., Dawson, H. N., Vitek, M. P. & Avila, J. Role of MAP1B in axonal retrograde transport of mitochondria. *Biochem J* 397, 53-9 (2006).
28. Fink, J. K., Jones, S. M., Esposito, C. & Wilkowski, J. Human microtubule-associated protein 1a (MAP1A) gene: genomic organization, cDNA sequence, and developmental- and tissue-specific expression. *Genomics* 35, 577-85 (1996).
29. Orban-Nemeth, Z., Simader, H., Badurek, S., Trancikova, A. & Propst, F. Microtubule-associated protein 1S, a short and ubiquitously expressed member of the microtubule-associated protein 1 family. *J Biol Chem* 280, 2257-65 (2005).
30. Zou, B., Yan, H., Kawasaki, F. & Ordway, R. W. MAP1 structural organization in *Drosophila*: in vivo analysis of FUTSCH reveals heavy- and light-chain subunits generated by proteolytic processing at a conserved cleavage site. *Biochem J* 414, 63-71 (2008).
31. Noiges, R. et al. Microtubule-associated protein 1A (MAP1A) and MAP1B: light chains determine distinct functional properties. *J Neurosci* 22, 2106-14 (2002).
32. Ma, D., Chow, S., Obrocka, M., Connors, T. & Fischer, I. Induction of microtubule-associated protein 1B expression in Schwann cells during nerve regeneration. *Brain Res* 823, 141-53 (1999).
33. Longhurst, D. M., Watanabe, M., Rothstein, J. D. & Jackson, M. Interaction of PDZRhoGEF with microtubule-associated protein 1 light chains: link between microtubules, actin cytoskeleton, and neuronal polarity. *J Biol Chem* 281, 12030-40 (2006).
34. Halpain, S. & Dehmelt, L. The MAP1 family of microtubule-associated proteins. *Genome Biol* 7, 224 (2006).
35. Ulloa, L., Avila, J. & Diaz-Nido, J. Heterogeneity in the phosphorylation of microtubule-associated protein MAP1B during rat brain development. *J Neurochem* 61, 961-72 (1993).

36. Ramon-Cueto, A. & Avila, J. Two modes of microtubule-associated protein 1B phosphorylation are differentially regulated during peripheral nerve regeneration. *Brain Res* 815, 213-26 (1999).
37. Trivedi, N., Marsh, P., Goold, R. G., Wood-Kaczmar, A. & Gordon-Weeks, P. R. Glycogen synthase kinase-3 $\beta$  phosphorylation of MAP1B at Ser1260 and Thr1265 is spatially restricted to growing axons. *J Cell Sci* 118, 993-1005 (2005).
38. Hahn, C. M. et al. Role of cyclin-dependent kinase 5 and its activator P35 in local axon and growth cone stabilization. *Neuroscience* 134, 449-65 (2005).
39. Jimenez-Mateos, E. M., Wandosell, F., Reiner, O., Avila, J. & Gonzalez-Billault, C. Binding of microtubule-associated protein 1B to LIS1 affects the interaction between dynein and LIS1. *Biochem J* 389, 333-41 (2005).
40. Bouquet, C. et al. Microtubule-associated protein 1B controls directionality of growth cone migration and axonal branching in regeneration of adult dorsal root ganglia neurons. *J Neurosci* 24, 7204-13 (2004).
41. Kitamura, C., Shirai, K., Inoue, M. & Tashiro, T. Changes in the subcellular distribution of microtubule-associated protein 1B during synaptogenesis of cultured rat cortical neurons. *Cell Mol Neurobiol* 27, 57-73 (2007).
42. Tanner, S. L., Franzen, R., Jaffe, H. & Quarles, R. H. Evidence for expression of some microtubule-associated protein 1B in neurons as a plasma membrane glycoprotein. *J Neurochem* 75, 553-62 (2000).
43. Edelmann, W. et al. Neuronal abnormalities in microtubule-associated protein 1B mutant mice. *Proc Natl Acad Sci U S A* 93, 1270-5 (1996).
44. Gonzalez-Billault, C. et al. Perinatal lethality of microtubule-associated protein 1B-deficient mice expressing alternative isoforms of the protein at low levels. *Mol Cell Neurosci* 16, 408-21 (2000).
45. Takei, Y. et al. Delayed development of nervous system in mice homozygous for disrupted microtubule-associated protein 1B (MAP1B) gene. *J Cell Biol* 137, 1615-26 (1997).
46. Hummel, T., Krukkert, K., Roos, J., Davis, G. & Klambt, C. *Drosophila* Futsch/22C10 is a MAP1B-like protein required for dendritic and axonal development. *Neuron* 26, 357-70 (2000).
47. Roos, J., Hummel, T., Ng, N., Klambt, C. & Davis, G. W. *Drosophila* Futsch regulates synaptic microtubule organization and is necessary for synaptic growth. *Neuron* 26, 371-82 (2000).
48. Bettencourt da Cruz, A. et al. Disruption of the MAP1B-related protein FUTSCH leads to changes in the neuronal cytoskeleton, axonal transport defects, and progressive neurodegeneration in *Drosophila*. *Mol Biol Cell* 16, 2433-42 (2005).
49. Serafini, T. et al. Netrin-1 is required for commissural axon guidance in the developing vertebrate nervous system. *Cell* 87, 1001-14 (1996).
50. Fazeli, A. et al. Phenotype of mice lacking functional Deleted in colorectal cancer (Dcc) gene. *Nature* 386, 796-804 (1997).
51. Lanier, L. M. et al. Mena is required for neurulation and commissure formation. *Neuron* 22, 313-25 (1999).
52. Kwon, Y. T., Tsai, L. H. & Crandall, J. E. Callosal axon guidance defects in p35(-/-) mice. *J Comp Neurol* 415, 218-29 (1999).
53. Paglini, G. et al. Evidence for the participation of the neuron-specific CDK5 activator P35 during laminin-enhanced axonal growth. *J Neurosci* 18, 9858-69 (1998).

54. Kalil, K. & Dent, E. W. Touch and go: guidance cues signal to the growth cone cytoskeleton. *Curr Opin Neurobiol* 15, 521-6 (2005).
55. Fukata, M., Nakagawa, M. & Kaibuchi, K. Roles of Rho-family GTPases in cell polarisation and directional migration. *Curr Opin Cell Biol* 15, 590-7 (2003).
56. Lehmann, M. et al. Inactivation of Rho signaling pathway promotes CNS axon regeneration. *J Neurosci* 19, 7537-47 (1999).
57. Ridley, A. J. & Hall, A. Distinct patterns of actin organization regulated by the small GTP-binding proteins Rac and Rho. *Cold Spring Harb Symp Quant Biol* 57, 661-71 (1992).
58. Kozma, R., Ahmed, S., Best, A. & Lim, L. The Ras-related protein Cdc42Hs and bradykinin promote formation of peripheral actin microspikes and filopodia in Swiss 3T3 fibroblasts. *Mol Cell Biol* 15, 1942-52 (1995).
59. Dickson, B. J. Rho GTPases in growth cone guidance. *Curr Opin Neurobiol* 11, 103-10 (2001).
60. Koh, C. G. Rho GTPases and their regulators in neuronal functions and development. *Neurosignals* 15, 228-37 (2006).
61. Mattson, M. P. Calcium as sculptor and destroyer of neural circuitry. *Exp Gerontol* 27, 29-49 (1992).
62. Kater, S. B. & Mills, L. R. Regulation of growth cone behavior by calcium. *J Neurosci* 11, 891-9 (1991).
63. Mattson, M. P. Establishment and plasticity of neuronal polarity. *J Neurosci Res* 57, 577-89 (1999).
64. Gomez, T. M. & Zheng, J. Q. The molecular basis for calcium-dependent axon pathfinding. *Nat Rev Neurosci* 7, 115-25 (2006).
65. Aspenstrom, P., Fransson, A. & Saras, J. Rho GTPases have diverse effects on the organization of the actin filament system. *Biochem J* 377, 327-37 (2004).
66. Luo, L. & O'Leary, D. D. Axon retraction and degeneration in development and disease. *Annu Rev Neurosci* 28, 127-56 (2005).
67. Ahmad, F. J., Echeverri, C. J., Vallee, R. B. & Baas, P. W. Cytoplasmic dynein and dynactin are required for the transport of microtubules into the axon. *J Cell Biol* 140, 391-401 (1998).
68. Ahmad, F. J. et al. Effects of dynactin disruption and dynein depletion on axonal microtubules. *Traffic* 7, 524-37 (2006).
69. Bito, H. et al. A critical role for a Rho-associated kinase, p160ROCK, in determining axon outgrowth in mammalian CNS neurons. *Neuron* 26, 431-41 (2000).
70. Kozma, R., Sarner, S., Ahmed, S. & Lim, L. Rho family GTPases and neuronal growth cone remodelling: relationship between increased complexity induced by Cdc42Hs, Rac1, and acetylcholine and collapse induced by RhoA and lysophosphatidic acid. *Mol Cell Biol* 17, 1201-11 (1997).
71. Li, Z., Van Aelst, L. & Cline, H. T. Rho GTPases regulate distinct aspects of dendritic arbor growth in *Xenopus* central neurons in vivo. *Nat Neurosci* 3, 217-25 (2000).
72. He, Z. & Koprivica, V. The Nogo signaling pathway for regeneration block. *Annu Rev Neurosci* 27, 341-68 (2004).
73. Hutchins, B. I. & Kalil, K. Differential outgrowth of axons and their branches is regulated by localized calcium transients. *J Neurosci* 28, 143-53 (2008).
74. Guzik, B. W. & Goldstein, L. S. Microtubule-dependent transport in neurons: steps towards an understanding of regulation, function and dysfunction. *Curr Opin Cell Biol* 16, 443-50 (2004).



75. Gunawardena, S. & Goldstein, L. S. Cargo-carrying motor vehicles on the neuronal highway: transport pathways and neurodegenerative disease. *J Neurobiol* 58, 258-71 (2004).
76. Hollenbeck, P. J. & Saxton, W. M. The axonal transport of mitochondria. *J Cell Sci* 118, 5411-9 (2005).
77. Mattson, M. P. & Partin, J. Evidence for mitochondrial control of neuronal polarity. *J Neurosci Res* 56, 8-20 (1999).
78. Miller, K. E. & Sheetz, M. P. Axonal mitochondrial transport and potential are correlated. *J Cell Sci* 117, 2791-804 (2004).
79. Chada, S. R. & Hollenbeck, P. J. Nerve growth factor signaling regulates motility and docking of axonal mitochondria. *Curr Biol* 14, 1272-6 (2004).
80. Hollenbeck, P. J. The pattern and mechanism of mitochondrial transport in axons. *Front Biosci* 1, d91-102 (1996).
81. Bridgman, P. C. Myosin-dependent transport in neurons. *J Neurobiol* 58, 164-74 (2004).
82. Rapp, S. et al. Microtubule-based peroxisome movement. *J Cell Sci* 109 (Pt 4), 837-49 (1996).
83. Wiemer, E. A., Wenzel, T., Deerinck, T. J., Ellisman, M. H. & Subramani, S. Visualization of the peroxisomal compartment in living mammalian cells: dynamic behavior and association with microtubules. *J Cell Biol* 136, 71-80 (1997).
84. Thiemann, M., Schrader, M., Volkl, A., Baumgart, E. & Fahimi, H. D. Interaction of peroxisomes with microtubules. In vitro studies using a novel peroxisome-microtubule binding assay. *Eur J Biochem* 267, 6264-75 (2000).
85. Schrader, M., King, S. J., Stroh, T. A. & Schroer, T. A. Real time imaging reveals a peroxisomal reticulum in living cells. *J Cell Sci* 113 (Pt 20), 3663-71 (2000).
86. Lowery, L. A. & Van Vactor, D. The trip of the tip: understanding the growth cone machinery. *Nat Rev Mol Cell Biol* 10, 332-43 (2009).
87. Kater, S. B., Davenport, R. W. & Guthrie, P. B. Filopodia as detectors of environmental cues: signal integration through changes in growth cone calcium levels. *Prog Brain Res* 102, 49-60 (1994).
88. Dent, E. W., Tang, F. & Kalil, K. Axon guidance by growth cones and branches: common cytoskeletal and signaling mechanisms. *Neuroscientist* 9, 343-53 (2003).
89. Rodriguez, O. C. et al. Conserved microtubule-actin interactions in cell movement and morphogenesis. *Nat Cell Biol* 5, 599-609 (2003).
90. Schaefer, A. W., Kabir, N. & Forscher, P. Filopodia and actin arcs guide the assembly and transport of two populations of microtubules with unique dynamic parameters in neuronal growth cones. *J Cell Biol* 158, 139-52 (2002).
91. Myers, K. A. et al. Antagonistic forces generated by cytoplasmic dynein and myosin-II during growth cone turning and axonal retraction. *Traffic* 7, 1333-51 (2006).
92. Baas, P. W. & Ahmad, F. J. Force generation by cytoskeletal motor proteins as a regulator of axonal elongation and retraction. *Trends Cell Biol* 11, 244-9 (2001).
93. Buck, K. B. & Zheng, J. Q. Growth cone turning induced by direct local modification of microtubule dynamics. *J Neurosci* 22, 9358-67 (2002).
94. Steward, O. & Schuman, E. M. Compartmentalized synthesis and degradation of proteins in neurons. *Neuron* 40, 347-59 (2003).

95. Campbell, D. S. & Holt, C. E. Chemotropic responses of retinal growth cones mediated by rapid local protein synthesis and degradation. *Neuron* 32, 1013-26 (2001).
96. Brittis, P. A., Lu, Q. & Flanagan, J. G. Axonal protein synthesis provides a mechanism for localized regulation at an intermediate target. *Cell* 110, 223-35 (2002).
97. Tessier-Lavigne, M. & Goodman, C. S. The molecular biology of axon guidance. *Science* 274, 1123-33 (1996).
98. Roche, F. K., Marsick, B. M. & Letourneau, P. C. Protein synthesis in distal axons is not required for growth cone responses to guidance cues. *J Neurosci* 29, 638-52 (2009).
99. Porcionatto, M. A. The extracellular matrix provides directional cues for neuronal migration during cerebellar development. *Braz J Med Biol Res* 39, 313-20 (2006).
100. Mecham, R. P. Laminin receptors. *Annu Rev Cell Biol* 7, 71-91 (1991).
101. Colognato, H., ffrench-Constant, C. & Feltri, M. L. Human diseases reveal novel roles for neural laminins. *Trends Neurosci* 28, 480-6 (2005).
102. Plantman, S. et al. Integrin-laminin interactions controlling neurite outgrowth from adult DRG neurons in vitro. *Mol Cell Neurosci* 39, 50-62 (2008).
103. Kuhn, T. B., Williams, C. V., Dou, P. & Kater, S. B. Laminin directs growth cone navigation via two temporally and functionally distinct calcium signals. *J Neurosci* 18, 184-94 (1998).
104. Baier, H. & Bonhoeffer, F. Axon guidance by gradients of a target-derived component. *Science* 255, 472-5 (1992).
105. Goodhill, G. J. & Urbach, J. S. Theoretical analysis of gradient detection by growth cones. *J Neurobiol* 41, 230-41 (1999).
106. Round, J. & Stein, E. Netrin signaling leading to directed growth cone steering. *Curr Opin Neurobiol* 17, 15-21 (2007).
107. Dickson, B. J. & Gilestro, G. F. Regulation of commissural axon pathfinding by slit and its Robo receptors. *Annu Rev Cell Dev Biol* 22, 651-75 (2006).
108. Kruger, R. P., Aurandt, J. & Guan, K. L. Semaphorins command cells to move. *Nat Rev Mol Cell Biol* 6, 789-800 (2005).
109. Flanagan, J. G. Neural map specification by gradients. *Curr Opin Neurobiol* 16, 59-66 (2006).
110. Endo, Y. & Rubin, J. S. Wnt signaling and neurite outgrowth: insights and questions. *Cancer Sci* 98, 1311-7 (2007).
111. Erskine, L. & Herrera, E. The retinal ganglion cell axon's journey: insights into molecular mechanisms of axon guidance. *Dev Biol* 308, 1-14 (2007).
112. Lindwall, C., Fothergill, T. & Richards, L. J. Commissure formation in the mammalian forebrain. *Curr Opin Neurobiol* 17, 3-14 (2007).
113. Chedotal, A., Kerjan, G. & Moreau-Fauvarque, C. The brain within the tumor: new roles for axon guidance molecules in cancers. *Cell Death Differ* 12, 1044-56 (2005).
114. Paul, L. K. et al. Agenesis of the corpus callosum: genetic, developmental and functional aspects of connectivity. *Nat Rev Neurosci* 8, 287-99 (2007).
115. Killeen, M. T. & Sybingco, S. S. Netrin, Slit and Wnt receptors allow axons to choose the axis of migration. *Dev Biol* 323, 143-51 (2008).
116. Dickson, B. J. Molecular mechanisms of axon guidance. *Science* 298, 1959-64 (2002).

117. Dent, E. W., Barnes, A. M., Tang, F. & Kalil, K. Netrin-1 and semaphorin 3A promote or inhibit cortical axon branching, respectively, by reorganization of the cytoskeleton. *J Neurosci* 24, 3002-12 (2004).
118. Fan, J., Mansfield, S. G., Redmond, T., Gordon-Weeks, P. R. & Raper, J. A. The organization of F-actin and microtubules in growth cones exposed to a brain-derived collapsing factor. *J Cell Biol* 121, 867-78 (1993).
119. Bagri, A. et al. Slit proteins prevent midline crossing and determine the dorsoventral position of major axonal pathways in the mammalian forebrain. *Neuron* 33, 233-48 (2002).
120. Kidd, T., Bland, K. S. & Goodman, C. S. Slit is the midline repellent for the robo receptor in *Drosophila*. *Cell* 96, 785-94 (1999).
121. Plump, A. S. et al. Slit1 and Slit2 cooperate to prevent premature midline crossing of retinal axons in the mouse visual system. *Neuron* 33, 219-32 (2002).
122. Wong, K. et al. Signal transduction in neuronal migration: roles of GTPase activating proteins and the small GTPase Cdc42 in the Slit-Robo pathway. *Cell* 107, 209-21 (2001).
123. Long, H. et al. Conserved roles for Slit and Robo proteins in midline commissural axon guidance. *Neuron* 42, 213-23 (2004).
124. Kim, T. H. et al. Netrin induces down-regulation of its receptor, Deleted in Colorectal Cancer, through the ubiquitin-proteasome pathway in the embryonic cortical neuron. *J Neurochem* 95, 1-8 (2005).
125. Stein, E. & Tessier-Lavigne, M. Hierarchical organization of guidance receptors: silencing of netrin attraction by slit through a Robo/DCC receptor complex. *Science* 291, 1928-38 (2001).
126. Kidd, T. et al. Roundabout controls axon crossing of the CNS midline and defines a novel subfamily of evolutionarily conserved guidance receptors. *Cell* 92, 205-15 (1998).
127. Li, H. S. et al. Vertebrate slit, a secreted ligand for the transmembrane protein roundabout, is a repellent for olfactory bulb axons. *Cell* 96, 807-18 (1999).
128. Conover, J. C. et al. Disruption of Eph/ephrin signaling affects migration and proliferation in the adult subventricular zone. *Nat Neurosci* 3, 1091-7 (2000).
129. Wilkinson, D. G. Multiple roles of EPH receptors and ephrins in neural development. *Nat Rev Neurosci* 2, 155-64 (2001).
130. Shamah, S. M. et al. EphA receptors regulate growth cone dynamics through the novel guanine nucleotide exchange factor ephexin. *Cell* 105, 233-44 (2001).
131. Huber, A. B., Kolodkin, A. L., Ginty, D. D. & Cloutier, J. F. Signaling at the growth cone: ligand-receptor complexes and the control of axon growth and guidance. *Annu Rev Neurosci* 26, 509-63 (2003).
132. Guan, K. L. & Rao, Y. Signalling mechanisms mediating neuronal responses to guidance cues. *Nat Rev Neurosci* 4, 941-56 (2003).
133. Islam, S. M. et al. Draxin, a repulsive guidance protein for spinal cord and forebrain commissures. *Science* 323, 388-93 (2009).
134. McFarlane, S. Attraction vs. repulsion: the growth cone decides. *Biochem Cell Biol* 78, 563-8 (2000).
135. Zheng, J. Q. Turning of nerve growth cones induced by localized increases in intracellular calcium ions. *Nature* 403, 89-93 (2000).
136. Hong, K., Nishiyama, M., Henley, J., Tessier-Lavigne, M. & Poo, M. Calcium signalling in the guidance of nerve growth by netrin-1. *Nature* 403, 93-8 (2000).
137. Culotti, J. G. & Merz, D. C. DCC and netrins. *Curr Opin Cell Biol* 10, 609-13 (1998).

138. Tang, F. & Kalil, K. Netrin-1 induces axon branching in developing cortical neurons by frequency-dependent calcium signaling pathways. *J Neurosci* 25, 6702-15 (2005).
139. Letourneau, P. C., Snow, D. M. & Gomez, T. M. Growth cone motility: substratum-bound molecules, cytoplasmic  $[Ca^{2+}]$  and  $Ca^{2+}$ -regulated proteins. *Prog Brain Res* 102, 35-48 (1994).
140. Griffith, L. C. Calcium/calmodulin-dependent protein kinase II: an unforgettable kinase. *J Neurosci* 24, 8391-3 (2004).
141. Graef, I. A. et al. Neurotrophins and netrins require calcineurin/NFAT signaling to stimulate outgrowth of embryonic axons. *Cell* 113, 657-70 (2003).
142. Price, L. S. et al. Calcium signaling regulates translocation and activation of Rac. *J Biol Chem* 278, 39413-21 (2003).
143. Cooper, D. M., Schell, M. J., Thorn, P. & Irvine, R. F. Regulation of adenylyl cyclase by membrane potential. *J Biol Chem* 273, 27703-7 (1998).
144. Bixby, J. L., Grunwald, G. B. & Bookman, R. J.  $Ca^{2+}$  influx and neurite growth in response to purified N-cadherin and laminin. *J Cell Biol* 127, 1461-75 (1994).
145. Gottmann, K. & Lux, H. D. Growth cone calcium ion channels: properties, clustering, and functional roles. *Perspect Dev Neurobiol* 2, 371-7 (1995).
146. Nishiyama, M. et al. Cyclic AMP/GMP-dependent modulation of  $Ca^{2+}$  channels sets the polarity of nerve growth-cone turning. *Nature* 423, 990-5 (2003).
147. Henley, J. & Poo, M. M. Guiding neuronal growth cones using  $Ca^{2+}$  signals. *Trends Cell Biol* 14, 320-30 (2004).
148. Song, H. J., Ming, G. L. & Poo, M. M. cAMP-induced switching in turning direction of nerve growth cones. *Nature* 388, 275-9 (1997).
149. Hong, K. et al. A ligand-gated association between cytoplasmic domains of UNC5 and DCC family receptors converts netrin-induced growth cone attraction to repulsion. *Cell* 97, 927-41 (1999).
150. Polleux, F., Morrow, T. & Ghosh, A. Semaphorin 3A is a chemoattractant for cortical apical dendrites. *Nature* 404, 567-73 (2000).
151. Song, H. et al. Conversion of neuronal growth cone responses from repulsion to attraction by cyclic nucleotides. *Science* 281, 1515-8 (1998).
152. Keino-Masu, K. et al. Deleted in Colorectal Cancer (DCC) encodes a netrin receptor. *Cell* 87, 175-85 (1996).
153. Leung-Hagesteijn, C. et al. UNC-5, a transmembrane protein with immunoglobulin and thrombospondin type 1 domains, guides cell and pioneer axon migrations in *C. elegans*. *Cell* 71, 289-99 (1992).
154. Hedgecock, E. M., Culotti, J. G. & Hall, D. H. The *unc-5*, *unc-6*, and *unc-40* genes guide circumferential migrations of pioneer axons and mesodermal cells on the epidermis in *C. elegans*. *Neuron* 4, 61-85 (1990).
155. Mitchell, K. J. et al. Genetic analysis of Netrin genes in *Drosophila*: Netrins guide CNS commissural axons and peripheral motor axons. *Neuron* 17, 203-15 (1996).
156. Ishii, N., Wadsworth, W. G., Stern, B. D., Culotti, J. G. & Hedgecock, E. M. UNC-6, a laminin-related protein, guides cell and pioneer axon migrations in *C. elegans*. *Neuron* 9, 873-81 (1992).
157. Serafini, T. et al. The netrins define a family of axon outgrowth-promoting proteins homologous to *C. elegans* UNC-6. *Cell* 78, 409-24 (1994).
158. Barallobre, M. J., Pascual, M., Del Rio, J. A. & Soriano, E. The Netrin family of guidance factors: emphasis on Netrin-1 signalling. *Brain Res Brain Res Rev* 49, 22-47 (2005).

159. Bradford, D., Cole, S. J. & Cooper, H. M. Netrin-1: Diversity in development. *Int J Biochem Cell Biol* (2008).
160. Püschel, A. W. Divergent properties of mouse netrins. *Mech Dev* 83, 65-75 (1999).
161. Kennedy, T. E., Wang, H., Marshall, W. & Tessier-Lavigne, M. Axon guidance by diffusible chemoattractants: a gradient of netrin protein in the developing spinal cord. *J Neurosci* 26, 8866-74 (2006).
162. Tessier-Lavigne, M., Placzek, M., Lumsden, A. G., Dodd, J. & Jessell, T. M. Chemotropic guidance of developing axons in the mammalian central nervous system. *Nature* 336, 775-8 (1988).
163. Placzek, M., Tessier-Lavigne, M., Jessell, T. & Dodd, J. Orientation of commissural axons in vitro in response to a floor plate-derived chemoattractant. *Development* 110, 19-30 (1990).
164. Murase, S. & Horwitz, A. F. Deleted in colorectal carcinoma and differentially expressed integrins mediate the directional migration of neural precursors in the rostral migratory stream. *J Neurosci* 22, 3568-79 (2002).
165. Yee, K. T., Simon, H. H., Tessier-Lavigne, M. & O'Leary, D. M. Extension of long leading processes and neuronal migration in the mammalian brain directed by the chemoattractant netrin-1. *Neuron* 24, 607-22 (1999).
166. Barallobre, M. J. et al. Aberrant development of hippocampal circuits and altered neural activity in netrin 1-deficient mice. *Development* 127, 4797-810 (2000).
167. Forsthoefel, D. J., Liebl, E. C., Kolodziej, P. A. & Seeger, M. A. The Abelson tyrosine kinase, the Trio GEF and Enabled interact with the Netrin receptor Frazzled in *Drosophila*. *Development* 132, 1983-94 (2005).
168. Shatzmiller, R. A. et al. Graded expression of netrin-1 by specific neuronal subtypes in the adult mammalian striatum. *Neuroscience* 157, 621-36 (2008).
169. Manitt, C. et al. Widespread expression of netrin-1 by neurons and oligodendrocytes in the adult mammalian spinal cord. *J Neurosci* 21, 3911-22 (2001).
170. Masuda, T. et al. Netrin-1 acts as a repulsive guidance cue for sensory axonal projections toward the spinal cord. *J Neurosci* 28, 10380-5 (2008).
171. Guan, W. & Condic, M. L. Characterization of Netrin-1, Neogenin and cUNC-5H3 expression during chick dorsal root ganglia development. *Gene Expr Patterns* 3, 369-73 (2003).
172. Ozaki, S. & Snider, W. D. Initial trajectories of sensory axons toward laminar targets in the developing mouse spinal cord. *J Comp Neurol* 380, 215-29 (1997).
173. Astic, L., Pellier-Monnin, V., Saucier, D., Charrier, C. & Mehlen, P. Expression of netrin-1 and netrin-1 receptor, DCC, in the rat olfactory nerve pathway during development and axonal regeneration. *Neuroscience* 109, 643-56 (2002).
174. de la Torre, J. R. et al. Turning of retinal growth cones in a netrin-1 gradient mediated by the netrin receptor DCC. *Neuron* 19, 1211-24 (1997).
175. Bloch-Gallego, E., Ezan, F., Tessier-Lavigne, M. & Sotelo, C. Floor plate and netrin-1 are involved in the migration and survival of inferior olivary neurons. *J Neurosci* 19, 4407-20 (1999).
176. Causeret, F., Danne, F., Ezan, F., Sotelo, C. & Bloch-Gallego, E. Slit antagonizes netrin-1 attractive effects during the migration of inferior olivary neurons. *Dev Biol* 246, 429-40 (2002).
177. Marin, O. & Rubenstein, J. L. Cell migration in the forebrain. *Annu Rev Neurosci* 26, 441-83 (2003).

178. Alcantara, S., Ruiz, M., De Castro, F., Soriano, E. & Sotelo, C. Netrin 1 acts as an attractive or as a repulsive cue for distinct migrating neurons during the development of the cerebellar system. *Development* 127, 1359-72 (2000).
179. Tsai, H. H., Macklin, W. B. & Miller, R. H. Netrin-1 is required for the normal development of spinal cord oligodendrocytes. *J Neurosci* 26, 1913-22 (2006).
180. Forcet, C. et al. Netrin-1-mediated axon outgrowth requires deleted in colorectal cancer-dependent MAPK activation. *Nature* 417, 443-7 (2002).
181. Bouchard, J. F. et al. Protein kinase A activation promotes plasma membrane insertion of DCC from an intracellular pool: A novel mechanism regulating commissural axon extension. *J Neurosci* 24, 3040-50 (2004).
182. Bouchard, J. F., Horn, K. E., Stroh, T. & Kennedy, T. E. Depolarization recruits DCC to the plasma membrane of embryonic cortical neurons and enhances axon extension in response to netrin-1. *J Neurochem* (2008).
183. Yebra, M. et al. Recognition of the neural chemoattractant Netrin-1 by integrins  $\alpha 6 \beta 4$  and  $\alpha 3 \beta 1$  regulates epithelial cell adhesion and migration. *Dev Cell* 5, 695-707 (2003).
184. Wen, Z., Guirland, C., Ming, G. L. & Zheng, J. Q. A CaMKII/calcineurin switch controls the direction of  $\text{Ca}^{2+}$ -dependent growth cone guidance. *Neuron* 43, 835-46 (2004).
185. Ming, G. L. et al. cAMP-dependent growth cone guidance by netrin-1. *Neuron* 19, 1225-35 (1997).
186. Ming, G. et al. Phospholipase C-gamma and phosphoinositide 3-kinase mediate cytoplasmic signaling in nerve growth cone guidance. *Neuron* 23, 139-48 (1999).
187. Moore, S. W. et al. Soluble adenylyl cyclase is not required for axon guidance to netrin-1. *J Neurosci* 28, 3920-4 (2008).
188. Li, X. et al. Netrin signal transduction and the guanine nucleotide exchange factor DOCK180 in attractive signaling. *Nat Neurosci* 11, 28-35 (2008).
189. Wittmann, T., Bokoch, G. M. & Waterman-Storer, C. M. Regulation of leading edge microtubule and actin dynamics downstream of Rac1. *J Cell Biol* 161, 845-51 (2003).
190. Shekarabi, M. et al. Deleted in colorectal cancer binding netrin-1 mediates cell substrate adhesion and recruits Cdc42, Rac1, Pak1, and N-WASP into an intracellular signaling complex that promotes growth cone expansion. *J Neurosci* 25, 3132-41 (2005).
191. Briancon-Marjollet, A. et al. Trio mediates netrin-1-induced Rac1 activation in axon outgrowth and guidance. *Mol Cell Biol* 28, 2314-23 (2008).
192. Moore, S. W. et al. Rho inhibition recruits DCC to the neuronal plasma membrane and enhances axon chemoattraction to netrin 1. *Development* 135, 2855-64 (2008).
193. Arimura, N., Menager, C., Fukata, Y. & Kaibuchi, K. Role of CRMP-2 in neuronal polarity. *J Neurobiol* 58, 34-47 (2004).
194. Bear, J. E. et al. Antagonism between Ena/VASP proteins and actin filament capping regulates fibroblast motility. *Cell* 109, 509-21 (2002).
195. Martinez-Lopez, M. J. et al. Mouse neuron navigator 1, a novel microtubule-associated protein involved in neuronal migration. *Mol Cell Neurosci* 28, 599-612 (2005).
196. Furne, C., Rama, N., Corset, V., Chedotal, A. & Mehlen, P. Netrin-1 is a survival factor during commissural neuron navigation. *Proc Natl Acad Sci U S A* 105, 14465-70 (2008).

197. Nguyen, A. & Cai, H. Netrin-1 induces angiogenesis via a DCC-dependent ERK1/2-eNOS feed-forward mechanism. *Proc Natl Acad Sci U S A* 103, 6530-5 (2006).
198. Kolodkin, A. L. et al. Fasciclin IV: sequence, expression, and function during growth cone guidance in the grasshopper embryo. *Neuron* 9, 831-45 (1992).
199. Williams, A. et al. Semaphorin 3A and 3F: key players in myelin repair in multiple sclerosis? *Brain* 130, 2554-65 (2007).
200. Holtmaat, A. J. et al. Transient downregulation of Sema3A mRNA in a rat model for temporal lobe epilepsy. A novel molecular event potentially contributing to mossy fiber sprouting. *Exp Neurol* 182, 142-50 (2003).
201. Hirsch, E. et al. Distribution of semaphorin IV in adult human brain. *Brain Res* 823, 67-79 (1999).
202. Yazdani, U. & Terman, J. R. The semaphorins. *Genome Biol* 7, 211 (2006).
203. Roth, L. et al. The many faces of semaphorins: from development to pathology. *Cell Mol Life Sci* 66, 649-66 (2009).
204. Nakamura, F., Kalb, R. G. & Strittmatter, S. M. Molecular basis of semaphorin-mediated axon guidance. *J Neurobiol* 44, 219-29 (2000).
205. Koncina, E., Roth, L., Gonthier, B. & Bagnard, D. Role of semaphorins during axon growth and guidance. *Adv Exp Med Biol* 621, 50-64 (2007).
206. Pasterkamp, R. J. R-Ras fills another GAP in semaphorin signalling. *Trends Cell Biol* 15, 61-4 (2005).
207. Chedotal, A. et al. Semaphorins III and IV repel hippocampal axons via two distinct receptors. *Development* 125, 4313-23 (1998).
208. Raper, J. A. Semaphorins and their receptors in vertebrates and invertebrates. *Curr Opin Neurobiol* 10, 88-94 (2000).
209. Cheng, H. J. et al. Plexin-A3 mediates semaphorin signaling and regulates the development of hippocampal axonal projections. *Neuron* 32, 249-63 (2001).
210. Gallo, G. & Letourneau, P. C. Regulation of growth cone actin filaments by guidance cues. *J Neurobiol* 58, 92-102 (2004).
211. Halloran, M. C. & Wolman, M. A. Repulsion or adhesion: receptors make the call. *Curr Opin Cell Biol* 18, 533-40 (2006).
212. Tang, X. Q., Tanelian, D. L. & Smith, G. M. Semaphorin3A inhibits nerve growth factor-induced sprouting of nociceptive afferents in adult rat spinal cord. *J Neurosci* 24, 819-27 (2004).
213. De Winter, F. et al. Injury-induced class 3 semaphorin expression in the rat spinal cord. *Exp Neurol* 175, 61-75 (2002).
214. Moreau-Fauvarque, C. et al. The transmembrane semaphorin Sema4D/CD100, an inhibitor of axonal growth, is expressed on oligodendrocytes and upregulated after CNS lesion. *J Neurosci* 23, 9229-39 (2003).
215. Pellet-Many, C., Frankel, P., Jia, H. & Zachary, I. Neuropilins: structure, function and role in disease. *Biochem J* 411, 211-26 (2008).
216. Kolodkin, A. L., Matthes, D. J. & Goodman, C. S. The semaphorin genes encode a family of transmembrane and secreted growth cone guidance molecules. *Cell* 75, 1389-99 (1993).
217. Lerman, O., Ben-Zvi, A., Yagil, Z. & Behar, O. Semaphorin3A accelerates neuronal polarity in vitro and in its absence the orientation of DRG neuronal polarity in vivo is distorted. *Mol Cell Neurosci* 36, 222-34 (2007).
218. Behar, O., Golden, J. A., Mashimo, H., Schoen, F. J. & Fishman, M. C. Semaphorin III is needed for normal patterning and growth of nerves, bones and heart. *Nature* 383, 525-8 (1996).

219. Uchida, Y. et al. Semaphorin3A signalling is mediated via sequential Cdk5 and GSK3 $\beta$  phosphorylation of CRMP2: implication of common phosphorylating mechanism underlying axon guidance and Alzheimer's disease. *Genes Cells* 10, 165-79 (2005).
220. Yoshimura, T. et al. GSK-3 $\beta$  regulates phosphorylation of CRMP-2 and neuronal polarity. *Cell* 120, 137-49 (2005).
221. Eickholt, B. J., Walsh, F. S. & Doherty, P. An inactive pool of GSK-3 at the leading edge of growth cones is implicated in Semaphorin 3A signaling. *J Cell Biol* 157, 211-7 (2002).
222. Kuhn, T. B. et al. Regulating actin dynamics in neuronal growth cones by ADF/cofilin and rho family GTPases. *J Neurobiol* 44, 126-44 (2000).
223. Chadborn, N. H. et al. PTEN couples Sema3A signalling to growth cone collapse. *J Cell Sci* 119, 951-7 (2006).
224. Orlova, I., Silver, L. & Gallo, G. Regulation of actomyosin contractility by PI3K in sensory axons. *Dev Neurobiol* 67, 1843-51 (2007).
225. Gallo, G., Yee, H. F., Jr. & Letourneau, P. C. Actin turnover is required to prevent axon retraction driven by endogenous actomyosin contractility. *J Cell Biol* 158, 1219-28 (2002).
226. Ueda, K., Murata-Hori, M., Tatsuka, M. & Hosoya, H. Rho-kinase contributes to diphosphorylation of myosin II regulatory light chain in nonmuscle cells. *Oncogene* 21, 5852-60 (2002).
227. Gallo, G. RhoA-kinase coordinates F-actin organization and myosin II activity during semaphorin-3A-induced axon retraction. *J Cell Sci* 119, 3413-23 (2006).
228. Alderton, W. K., Cooper, C. E. & Knowles, R. G. Nitric oxide synthases: structure, function and inhibition. *Biochem J* 357, 593-615 (2001).
229. Dimmeler, S. et al. Activation of nitric oxide synthase in endothelial cells by Akt-dependent phosphorylation. *Nature* 399, 601-5 (1999).
230. Komeima, K., Hayashi, Y., Naito, Y. & Watanabe, Y. Inhibition of neuronal nitric-oxide synthase by calcium/calmodulin-dependent protein kinase II $\alpha$  through Ser847 phosphorylation in NG108-15 neuronal cells. *J Biol Chem* 275, 28139-43 (2000).
231. Song, T. et al. Nitric oxide-mediated modulation of calcium/calmodulin-dependent protein kinase II. *Biochem J* 412, 223-31 (2008).
232. Nakane, M., Mitchell, J., Forstermann, U. & Murad, F. Phosphorylation by calcium calmodulin-dependent protein kinase II and protein kinase C modulates the activity of nitric oxide synthase. *Biochem Biophys Res Commun* 180, 1396-402 (1991).
233. Butt, E. et al. Endothelial nitric-oxide synthase (type III) is activated and becomes calcium independent upon phosphorylation by cyclic nucleotide-dependent protein kinases. *J Biol Chem* 275, 5179-87 (2000).
234. Keilhoff, G., Fansa, H. & Wolf, G. Nitric oxide synthase, an essential factor in peripheral nerve regeneration. *Cell Mol Biol (Noisy-le-grand)* 49, 885-97 (2003).
235. Garner, C. C., Nash, J. & Huganir, R. L. PDZ domains in synapse assembly and signalling. *Trends Cell Biol* 10, 274-80 (2000).
236. Son, H. et al. Long-term potentiation is reduced in mice that are doubly mutant in endothelial and neuronal nitric oxide synthase. *Cell* 87, 1015-23 (1996).
237. Rialas, C. M. et al. Nitric oxide mediates laminin-induced neurite outgrowth in PC12 cells. *Exp Cell Res* 260, 268-76 (2000).



238. Bredt, D. S. & Snyder, S. H. Transient nitric oxide synthase neurons in embryonic cerebral cortical plate, sensory ganglia, and olfactory epithelium. *Neuron* 13, 301-13 (1994).
239. Thippeswamy, T., Jain, R. K., Mumtaz, N. & Morris, R. Inhibition of neuronal nitric oxide synthase results in neurodegenerative changes in the axotomised dorsal root ganglion neurons: evidence for a neuroprotective role of nitric oxide in vivo. *Neurosci Res* 40, 37-44 (2001).
240. Sunico, C. R., Portillo, F., Gonzalez-Forero, D., Kasparov, S. & Moreno-Lopez, B. Evidence for a detrimental role of nitric oxide synthesized by endothelial nitric oxide synthase after peripheral nerve injury. *Neuroscience* 157, 40-51 (2008).
241. Dawson, T. M. & Snyder, S. H. Gases as biological messengers: nitric oxide and carbon monoxide in the brain. *J Neurosci* 14, 5147-59 (1994).
242. Lipton, S. A. et al. A redox-based mechanism for the neuroprotective and neurodestructive effects of nitric oxide and related nitroso-compounds. *Nature* 364, 626-32 (1993).
243. Melino, G. et al. S-nitrosylation regulates apoptosis. *Nature* 388, 432-3 (1997).
244. Patel, S., Robb-Gaspers, L. D., Stellato, K. A., Shon, M. & Thomas, A. P. Coordination of calcium signalling by endothelial-derived nitric oxide in the intact liver. *Nat Cell Biol* 1, 467-71 (1999).
245. Bellamy, T. C., Wood, J. & Garthwaite, J. On the activation of soluble guanylyl cyclase by nitric oxide. *Proc Natl Acad Sci U S A* 99, 507-10 (2002).
246. Zheng, J. Q. & Poo, M. M. Calcium signaling in neuronal motility. *Annu Rev Cell Dev Biol* 23, 375-404 (2007).
247. Mannick, J. B. et al. Fas-induced caspase denitrosylation. *Science* 284, 651-4 (1999).
248. Lipton, S. A. Neuronal protection and destruction by NO. *Cell Death Differ* 6, 943-51 (1999).
249. Lander, H. M. et al. A molecular redox switch on p21(ras). Structural basis for the nitric oxide-p21(ras) interaction. *J Biol Chem* 272, 4323-6 (1997).
250. Jia, L., Bonaventura, C., Bonaventura, J. & Stamler, J. S. S-nitrosohaemoglobin: a dynamic activity of blood involved in vascular control. *Nature* 380, 221-6 (1996).
251. Reynaert, N. L. et al. Nitric oxide represses inhibitory kappaB kinase through S-nitrosylation. *Proc Natl Acad Sci U S A* 101, 8945-50 (2004).
252. Stamler, J. S., Lamas, S. & Fang, F. C. Nitrosylation. the prototypic redox-based signaling mechanism. *Cell* 106, 675-83 (2001).
253. Hess, D. T., Matsumoto, A., Kim, S. O., Marshall, H. E. & Stamler, J. S. Protein S-nitrosylation: purview and parameters. *Nat Rev Mol Cell Biol* 6, 150-66 (2005).
254. Guix, F. X., Uribealago, I., Coma, M. & Munoz, F. J. The physiology and pathophysiology of nitric oxide in the brain. *Prog Neurobiol* 76, 126-52 (2005).
255. Rivier, C. Role of gaseous neurotransmitters in the hypothalamic-pituitary-adrenal axis. *Ann N Y Acad Sci* 933, 254-64 (2001).
256. Toda, N., Ayajiki, K. & Okamura, T. Nitric oxide and penile erectile function. *Pharmacol Ther* 106, 233-66 (2005).
257. Garthwaite, J. & Boulton, C. L. Nitric oxide signaling in the central nervous system. *Annu Rev Physiol* 57, 683-706 (1995).
258. Krumenacker, J. S., Hanafy, K. A. & Murad, F. Regulation of nitric oxide and soluble guanylyl cyclase. *Brain Res Bull* 62, 505-15 (2004).

259. Choi, Y. B. et al. Molecular basis of NMDA receptor-coupled ion channel modulation by S-nitrosylation. *Nat Neurosci* 3, 15-21 (2000).
260. Liu, L. & Stamler, J. S. NO: an inhibitor of cell death. *Cell Death Differ* 6, 937-42 (1999).
261. Brookes, P. S., Bolanos, J. P. & Heales, S. J. The assumption that nitric oxide inhibits mitochondrial ATP synthesis is correct. *FEBS Lett* 446, 261-3 (1999).
262. Zanelli, S. A., Trimmer, P. A. & Solenski, N. J. Nitric oxide impairs mitochondrial movement in cortical neurons during hypoxia. *J Neurochem* 97, 724-36 (2006).
263. Martinez-Ruiz, A. & Lamas, S. S-nitrosylation: a potential new paradigm in signal transduction. *Cardiovasc Res* 62, 43-52 (2004).
264. Gow, A. J. et al. Basal and stimulated protein S-nitrosylation in multiple cell types and tissues. *J Biol Chem* 277, 9637-40 (2002).
265. Perez-Mato, I., Castro, C., Ruiz, F. A., Corrales, F. J. & Mato, J. M. Methionine adenosyltransferase S-nitrosylation is regulated by the basic and acidic amino acids surrounding the target thiol. *J Biol Chem* 274, 17075-9 (1999).
266. Gaston, B. Nitric oxide and thiol groups. *Biochim Biophys Acta* 1411, 323-33 (1999).
267. Bredt, D. S. Nitric oxide signaling specificity--the heart of the problem. *J Cell Sci* 116, 9-15 (2003).
268. Jaffrey, S. R. & Snyder, S. H. The biotin switch method for the detection of S-nitrosylated proteins. *Sci STKE* 2001, PL1 (2001).
269. Semenza, G. L. HIF-1: mediator of physiological and pathophysiological responses to hypoxia. *J Appl Physiol* 88, 1474-80 (2000).
270. He, Y., Yu, W. & Baas, P. W. Microtubule reconfiguration during axonal retraction induced by nitric oxide. *J Neurosci* 22, 5982-91 (2002).
271. Miller, R. H. Regulation of oligodendrocyte development in the vertebrate CNS. *Prog Neurobiol* 67, 451-67 (2002).
272. Arroyo, E. J. & Scherer, S. S. On the molecular architecture of myelinated fibers. *Histochem Cell Biol* 113, 1-18 (2000).
273. Coman, I., Barbin, G., Charles, P., Zalc, B. & Lubetzki, C. Axonal signals in central nervous system myelination, demyelination and remyelination. *J Neurol Sci* 233, 67-71 (2005).
274. Hopkins, S. J. & Rothwell, N. J. Cytokines and the nervous system. I: Expression and recognition. *Trends Neurosci* 18, 83-8 (1995).
275. Johns, T. G. & Bernard, C. C. The structure and function of myelin oligodendrocyte glycoprotein. *J Neurochem* 72, 1-9 (1999).
276. Holz, A. et al. Molecular and developmental characterization of novel cDNAs of the myelin-associated/oligodendrocytic basic protein. *J Neurosci* 16, 467-77 (1996).
277. Lunn, K. F., Baas, P. W. & Duncan, I. D. Microtubule organization and stability in the oligodendrocyte. *J Neurosci* 17, 4921-32 (1997).
278. Benjamins, J. A. & Nedelkoska, L. Maintenance of membrane sheets by cultured oligodendrocytes requires continuous microtubule turnover and Golgi transport. *Neurochem Res* 19, 631-9 (1994).
279. Carson, J. H., Kwon, S. & Barbarese, E. RNA trafficking in myelinating cells. *Curr Opin Neurobiol* 8, 607-12 (1998).
280. Fischer, I., Konola, J. & Cochary, E. Microtubule associated protein (MAP1B) is present in cultured oligodendrocytes and co-localizes with tubulin. *J Neurosci Res* 27, 112-24 (1990).

281. Vouyiouklis, D. A. & Brophy, P. J. Microtubule-associated proteins in developing oligodendrocytes: transient expression of a MAP2c isoform in oligodendrocyte precursors. *J Neurosci Res* 42, 803-817 (1995).
282. Zhao, L. et al. QKI binds MAP1B mRNA and enhances MAP1B expression during oligodendrocyte development. *Mol Biol Cell* 17, 4179-86 (2006).
283. Wu, H. Y., Dawson, M. R., Reynolds, R. & Hardy, R. J. Expression of QKI proteins and MAP1B identifies actively myelinating oligodendrocytes in adult rat brain. *Mol Cell Neurosci* 17, 292-302 (2001).
284. Franzen, R. et al. Microtubule-associated protein 1B: a neuronal binding partner for myelin-associated glycoprotein. *J Cell Biol* 155, 893-8 (2001).
285. Steinman, L. & Zamvil, S. S. How to successfully apply animal studies in experimental allergic encephalomyelitis to research on multiple sclerosis. *Ann Neurol* 60, 12-21 (2006).
286. Hauser, S. L. & Oksenberg, J. R. The neurobiology of multiple sclerosis: genes, inflammation, and neurodegeneration. *Neuron* 52, 61-76 (2006).
287. Kornek, B. & Lassmann, H. Axonal pathology in multiple sclerosis. A historical note. *Brain Pathol* 9, 651-6 (1999).
288. Lovas, G., Szilagyi, N., Majtenyi, K., Palkovits, M. & Komoly, S. Axonal changes in chronic demyelinated cervical spinal cord plaques. *Brain* 123 (Pt 2), 308-17 (2000).
289. Grigoriadis, N., Ben-Hur, T., Karussis, D. & Milonas, I. Axonal damage in multiple sclerosis: a complex issue in a complex disease. *Clin Neurol Neurosurg* 106, 211-7 (2004).
290. Bhat, N. R. & Feinstein, D. L. NO and glial cell biology. *Antioxid Redox Signal* 8, 869-72 (2006).
291. Baud, O. et al. Nitric oxide-induced cell death in developing oligodendrocytes is associated with mitochondrial dysfunction and apoptosis-inducing factor translocation. *Eur J Neurosci* 20, 1713-26 (2004).
292. Cross, A. H., Manning, P. T., Keeling, R. M., Schmidt, R. E. & Misko, T. P. Peroxynitrite formation within the central nervous system in active multiple sclerosis. *J Neuroimmunol* 88, 45-56 (1998).
293. Cross, A. H., Manning, P. T., Stern, M. K. & Misko, T. P. Evidence for the production of peroxynitrite in inflammatory CNS demyelination. *J Neuroimmunol* 80, 121-30 (1997).
294. Bizzozero, O. A., DeJesus, G. & Howard, T. A. Exposure of rat optic nerves to nitric oxide causes protein S-nitrosation and myelin decompaction. *Neurochem Res* 29, 1675-85 (2004).
295. Druzhyna, N. M., Musiyenko, S. I., Wilson, G. L. & LeDoux, S. P. Cytokines induce nitric oxide-mediated mtDNA damage and apoptosis in oligodendrocytes. Protective role of targeting 8-oxoguanine glycosylase to mitochondria. *J Biol Chem* 280, 21673-9 (2005).
296. Oleszak, E. L. et al. Inducible nitric oxide synthase and nitrotyrosine are found in monocytes/macrophages and/or astrocytes in acute, but not in chronic, multiple sclerosis. *Clin Diagn Lab Immunol* 5, 438-45 (1998).
297. Okuda, Y. et al. Expression of the inducible isoform of nitric oxide synthase in the central nervous system of mice correlates with the severity of actively induced experimental allergic encephalomyelitis. *J Neuroimmunol* 62, 103-12 (1995).
298. Boullerne, A. I., Petry, K. G., Meynard, M. & Geffard, M. Indirect evidence for nitric oxide involvement in multiple sclerosis by characterization of circulating

- antibodies directed against conjugated S-nitrosocysteine. *J Neuroimmunol* 60, 117-24 (1995).
299. Boullerne, A. I. et al. Anti-S-nitrosocysteine antibodies are a predictive marker for demyelination in experimental autoimmune encephalomyelitis: implications for multiple sclerosis. *J Neurosci* 22, 123-32 (2002).
300. Danilov, A. I., Jagodic, M., Wiklund, N. P., Olsson, T. & Brundin, L. Effects of long term NOS inhibition on disease and the immune system in MOG induced EAE. *Nitric Oxide* 13, 188-95 (2005).
301. De Los Monteros, A. E., Zhao, P. M. & De Vellis, J. In vitro injury model for oligodendrocytes: development, injury, and recovery. *Microsc Res Tech* 52, 719-30 (2001).
302. Dontchev, V. D. & Letourneau, P. C. Nerve growth factor and semaphorin 3A signaling pathways interact in regulating sensory neuronal growth cone motility. *J Neurosci* 22, 6659-69 (2002).
303. Henley, J. R., Huang, K. H., Wang, D. & Poo, M. M. Calcium mediates bidirectional growth cone turning induced by myelin-associated glycoprotein. *Neuron* 44, 909-16 (2004).
304. Brenman, J. E. et al. Interaction of nitric oxide synthase with the postsynaptic density protein PSD-95 and alpha1-syntrophin mediated by PDZ domains. *Cell* 84, 757-67 (1996).
305. Wang, Y. & Marsden, P. A. Nitric oxide synthases: gene structure and regulation. *Adv Pharmacol* 34, 71-90 (1995).
306. Tretyakova, I. et al. Nuclear export factor family protein participates in cytoplasmic mRNA trafficking. *J Biol Chem* 280, 31981-90 (2005).
307. Ghosh, S. et al. Interaction between caveolin-1 and the reductase domain of endothelial nitric-oxide synthase. Consequences for catalysis. *J Biol Chem* 273, 22267-71 (1998).
308. Huang, P. L., Dawson, T. M., Bredt, D. S., Snyder, S. H. & Fishman, M. C. Targeted disruption of the neuronal nitric oxide synthase gene. *Cell* 75, 1273-86 (1993).
309. Ben-Zvi, A., Ben-Gigi, L., Yagil, Z., Lerman, O. & Behar, O. Semaphorin3A regulates axon growth independently of growth cone repulsion via modulation of TrkA signaling. *Cell Signal* 20, 467-79 (2008).
310. Thippeswamy, T. & Morris, R. Nerve growth factor inhibits the expression of nitric oxide synthase in neurones in dissociated cultures of rat dorsal root ganglia. *Neurosci Lett* 230, 9-12 (1997).
311. Thippeswamy, T., McKay, J. S., Quinn, J. & Morris, R. Either nitric oxide or nerve growth factor is required for dorsal root ganglion neurons to survive during embryonic and neonatal development. *Brain Res Dev Brain Res* 154, 153-64 (2005).
312. Goold, R. G., Owen, R. & Gordon-Weeks, P. R. Glycogen synthase kinase 3beta phosphorylation of microtubule-associated protein 1B regulates the stability of microtubules in growth cones. *J Cell Sci* 112 (Pt 19), 3373-84 (1999).
313. Good, P. F. et al. A role for semaphorin 3A signaling in the degeneration of hippocampal neurons during Alzheimer's disease. *J Neurochem* 91, 716-36 (2004).
314. Garcia, M. L. & Cleveland, D. W. Going new places using an old MAP: tau, microtubules and human neurodegenerative disease. *Curr Opin Cell Biol* 13, 41-8 (2001).

315. Li, C., Bassell, G. J. & Sasaki, Y. Fragile X Mental Retardation Protein is Involved in Protein Synthesis-Dependent Collapse of Growth Cones Induced by Semaphorin-3A. *Front Neural Circuits* 3, 11 (2009).
  316. Antar, L. N., Dichtenberg, J. B., Plociniak, M., Afroz, R. & Bassell, G. J. Localization of FMRP-associated mRNA granules and requirement of microtubules for activity-dependent trafficking in hippocampal neurons. *Genes Brain Behav* 4, 350-9 (2005).
  317. Richter-Landsberg, C. & Heinrich, M. OLN-93: a new permanent oligodendroglia cell line derived from primary rat brain glial cultures. *J Neurosci Res* 45, 161-73 (1996).
  318. Qi, X. & Guy, J. Localization of NADPH diaphorase/nitric oxide synthase in the optic nerve of the normal guinea pig: a light and electron microscopic study. *J Comp Neurol* 370, 396-404 (1996).
  319. Ksiezak-Reding, H., Farooq, M., Yang, L. S., Dickson, D. W. & LoPresti, P. Tau protein expression in adult bovine oligodendrocytes: functional and pathological significance. *Neurochem Res* 28, 1385-92 (2003).
  320. Suzuki, S. O. et al. MAP-2e, a novel MAP-2 isoform, is expressed in gliomas and delineates tumor architecture and patterns of infiltration. *J Neuropathol Exp Neurol* 61, 403-12 (2002).
  321. Encinas, J. M., Manganas, L. & Enikolopov, G. Nitric oxide and multiple sclerosis. *Curr Neurol Neurosci Rep* 5, 232-8 (2005).
  322. Boullerne, A. I., Nedelkoska, L. & Benjamins, J. A. Role of calcium in nitric oxide-induced cytotoxicity: EGTA protects mouse oligodendrocytes. *J Neurosci Res* 63, 124-35 (2001).
  323. Soliven, B. Calcium signalling in cells of oligodendroglial lineage. *Microsc Res Tech* 52, 672-9 (2001).
  324. Alberdi, E., Sanchez-Gomez, M. V. & Matute, C. Calcium and glial cell death. *Cell Calcium* 38, 417-25 (2005).
  325. Tonge, D. A., Golding, J. P. & Gordon-Weeks, P. R. Expression of a developmentally regulated, phosphorylated isoform of microtubule-associated protein 1B in sprouting and regenerating axons in vitro. *Neuroscience* 73, 541-51 (1996).
  326. Bottenstein, J. E. & Sato, G. H. Growth of a rat neuroblastoma cell line in serum-free supplemented medium. *Proc Natl Acad Sci U S A* 76, 514-7 (1979).
  327. Romijn, H. J., Habets, A. M., Mud, M. T. & Wolters, P. S. Nerve outgrowth, synaptogenesis and bioelectric activity in fetal rat cerebral cortex tissue cultured in serum-free, chemically defined medium. *Brain Res* 254, 583-9 (1981).
- Falconer, D. S. 1951: Two new mutants 'Trembler' and 'Reeler', with neurological actions in the house mouse. *Journal of Genetics* 50, 192–201.



## Curriculum Vitae

**Name:** Luise Descovich  
**Degree:** Mag. rer. nat  
**Date of Birth:** 11.12.1979  
**Address:** Liechtensteinstrasse 77/4  
 1090 Vienna, Austria  
**email:** luise.descovich@univie.ac.at



- |                          |   |
|--------------------------|---|
| September 2006 – present | PhD at Department of Molecular Cell Biology, Prof. Propst, Vienna Biocenter: <i>MAP1B and S-nitrosylation in axon guidance, glial function and neurodegeneration</i> . Estimated end in december 2009   |
| June 2008                | Internship at the University Pierre et Marie Curie, Paris, France in the laboratory of Prof. Fatiha Nothias   |
| March 2005 – Mai 2006:   | Diploma thesis at the Institute for Molecular Pathology, Prof. Hartmut Beug, Vienna Biocenter: <i>Novel functions of the transcription factor TCF8 cancer cell plasticity</i>   |
| January 2005:            | First Diploma exam Molecular Biology (cum laude)  |
| May-November 2004:       | Internships at the MFPL in the laboratories of Prof. Renée Schroeder, Prof. Rudolf Schweyen and Prof. Dr. Pavel Kovarik at the Department of Genetics, in the laboratory of Prof. Friedrich Propst at the Department of Biochemistry and Molecular Cell Biology and in the laboratory of Prof. Roland Foisner at the Department of Medical Biochemistry |
| 2002 – 2004:             | Undergraduate studies in Molecular Biology at the University of Vienna  |
| 1998-2002                | Undergraduate studies in Biology at the University of Natural Resources and Applied Life Sciences, Vienna, study of Biotechnology, first Diploma exam   |
| June 1998:               | Graduation from secondary school, Lycée Français de Vienne (cum laude)  |

### Technical experience:

#### Basic and advanced techniques of Molecular Biology, Cell Biology and Biochemistry:

Cloning techniques (including Gateway™ cloning), PCR; RT-PCR, yeast two-hybrid assay; protein chemistry (protein expression in *E. coli*, protein purification, co-immunoprecipitation, chromatin-immunoprecipitation, *in vitro* co-sedimentation assays, western blot analysis, overlay assays); cell culture (cultivation of different cell lines and primary cells; 3-dimensional organotypic cultures; transfections; constitutive or inducible (Tet-on) ectopic gene expression; cell fractionation); apoptosis assays; reporter assays; immunofluorescence microscopy studies; Confocal laser microscopy; FRET; Kinase assays; immunohistochemistry

**Teaching experience:**

Tutor at the University of Vienna for “Molekulare Biologie UE II, Teil A and Biochemisches Praktikum C (Proteinbiochemie) für Chemiker”

Assistant Professor at the University of Vienna for “Molekulare Biologie UE II, Teil A”

Supervision of undergraduate students in the context of their “Wahlbeispiel Molekulare Zellbiologie: Einzelunterweisung zur Anwendung moderner molekularbiologischer und zellbiologischer Techniken”

**Conferences:**

ELSO: Frontiers of Cellular, Developmental and Molecular Biology, Dresden, Germany, 1<sup>st</sup>-4<sup>th</sup> of September 2007, Poster

Axonal Connections: Molecular Cues for Development and Regeneration, Keystone, Colorado, USA, 12<sup>th</sup>-21<sup>st</sup> of February 2009, Poster

**Theoretical skills:**

General Biology: Human biology; zoology; botanic; ecology; developmental biology

Cell Biology: Mitosis; meiosis; cell structure of eukaryotic and prokaryotic cells; physiology of epithelial cells; epithelial polarity, development of the nervous system

Cancer Biology: Aetiology of cancer, cancer histology, molecular causes of cancer progression, cancer cell invasion and metastasis

Genetics: Gene expression in eukaryotes and prokaryotes; molecular biology of the cell cycle; genetic

engineering and biotechnology; human genetics; plant genetics; developmental genetics

Microbiology : Biology of microorganisms: metabolism, cell biology, cell chemistry, microbial growth, major microbial diseases, interactions of pathogens and hosts; bacterial systematics

Immunology: immune system; virology; immune genetics; molecular biology of vaccines

Biochemistry: Metabolism; membrane structure; structure of macromolecules; protein chemistry

Chemistry: organic and inorganic chemistry; analytical chemistry

**Language skills:**

Native German; fluent in written and spoken English and French

**IT skills:**

Microsoft Windows, Microsoft Office (MSWord, MExcel, MSPowerpoint); Imaging software (Adobe Photoshop and Illustrator, CorelDraw, LSM510, Axio Vision); Bioinformatic software (e.g. Clone manager, Align Plus, DNA Star); Internet, web based databases, EndNote, SPSS



## **Publications**

**The transcription factor ZEB1 (deltaEF1) represses Plakophilin 3 during human cancer progression.**

Aigner K, Descovich L, Mikula M, Sultan A, Dampier B, Bonn   S, van Roy F, Mikulits W, Schreiber M, Brabletz T, Sommergruber W, Schweifer N, Wernitznig A, Beug H, Foisner R, Eger A.

FEBS Letters 2007 Apr 17; 581(8): 1617-24. Epub 2007 Mar 21.

**The transcription factor ZEB1 (deltaEF1) promotes tumour cell dedifferentiation by repressing master regulators of epithelial polarity.**

Aigner K, Dampier B, Descovich L, Mikula M, Sultan A, Schreiber M, Mikulits W, Brabletz T, Strand D, Obrist P, Sommergruber W, Schweifer N, Wernitznig A, Beug H, Foisner R, Eger A.

Oncogene. 2007 Oct 25; 26(49): 6979-88. Epub 2007 May 7.

**S-nitrosylation of microtubule-associated protein 1B mediates nitric-oxide-induced axon retraction.**

Stroissnigg H, Tranc  kov   A, Descovich L, Fuhrmann J, Kutschera W, Kostan J, Meixner A, Nothias F, Propst F.

Nat Cell Biol. 2007 Sep 9 (9):1035-45. Epub 2007 Aug 19.